



MICAELA TAMARA VITOR

**“VEICULAÇÃO DE mRNA DE CÉLULAS TUMORAIS
EM LIPOSSOMAS CATIÔNICOS PARA
IMUNOTERAPIA DO CÂNCER”**

**CAMPINAS
2013**



**UNIVERSIDADE ESTADUAL DE CAMPINAS
FACULDADE DE ENGENHARIA QUÍMICA**

MICAELA TAMARA VITOR

**“VEICULAÇÃO DE mRNA DE CÉLULAS TUMORAIS EM
LIPOSSOMAS CATIÔNICOS PARA IMUNOTERAPIA DO
CÂNCER”**

Orientadora: Prof^a. Dr^a. Lucimara Gaziola de la Torre

Co-Orientador: Dr^a. Patrícia Cruz Bergami-Santos

Dissertação de mestrado apresentada ao Programa de Pós Graduação em Engenharia Química da Faculdade de Engenharia Química da Universidade Estadual de Campinas para obtenção do título de Mestre em Engenharia Química na área de concentração de Desenvolvimento de Processos Biotecnológicos.

**ESTE EXEMPLAR CORRESPONDE À VERSÃO FINAL DA TESE
DEFENDIDA PELA ALUNA MICAELA TAMARA VITOR
E ORIENTADA PELA PROFA. DRA. LUCIMARA GAZIOLA DE LA TORRE**

Assinatura do Orientador

A handwritten signature in black ink, appearing to read "Lucimara Gaziola", is written over a horizontal line.

**CAMPINAS
2013**

Ficha catalográfica
Universidade Estadual de Campinas
Biblioteca da Área de Engenharia e Arquitetura
Rose Meire da Silva - CRB 8/5974

V833v Vitor, Micaela Tamara, 1987-
Veiculação de mRNA de células tumorais em lipossomas catiônicos para
imunoterapia do câncer / Micaela Tamara Vitor. – Campinas, SP : [s.n.], 2013.

Orientador: Lucimara Gaziola de la Torre.
Coorientador: Patrícia Cruz Bergami-Santos.
Dissertação (mestrado) – Universidade Estadual de Campinas, Faculdade de
Engenharia Química.

1. Lipossoma. 2. Ácido ribonucleico. 3. Células dendríticas. 4. Câncer -
imunoterapia. I. Torre, Lucimara Gaziola de la, 1971-. II. Bergami-Santos, Patrícia
Cruz. III. Universidade Estadual de Campinas. Faculdade de Engenharia Química.
IV. Título.

Informações para Biblioteca Digital

Título em inglês: Cationic liposomes as carriers of mRNA from tumor cells for cancer
immunotherapy

Palavras-chave em inglês:

Liposome

Ribonucleic acid

Dendritic cells

Immunotherapy of cancer

Área de concentração: Desenvolvimento de Processos Biotecnológicos

Titulação: Mestra em Engenharia Química

Banca examinadora:

Lucimara Gaziola de la Torre [Orientador]

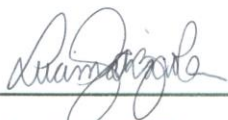
José Alexandre Marzagão Barbuto

Nelson Eduardo Durán Caballero

Data de defesa: 16-04-2013

Programa de Pós-Graduação: Engenharia Química

Dissertação de mestrado defendida por Micaela Tamara Vitor e aprovada no dia 16 de abril de 2013 pela banca examinadora constituída pelos seguintes doutores:



Profa. Dra. Lucimara Gaziola de la Torre – Orientadora



Dra. Patrícia Cruz Bergami-Santos – Co-orientadora



Prof. Dr. José Alexandre Marzagão Barbuto – Membro Titular



Prof. Dr. Nelson Eduardo Durán Caballero – Membro Titular

Dedico esta pesquisa à Deus, que me permitiu desenvolvê-la, aos meus familiares e amigos, pelo apoio e incentivo e ao Ricardo, pela compreensão e carinho.

AGRADECIMENTOS

O desenvolvimento desta pesquisa foi possível graças à colaboração de várias pessoas tanto da Universidade Estadual de Campinas (Unicamp) como da Universidade de São Paulo (USP). Agradeço à Profa. Dra. Lucimara Gaziola de la Torre, pela orientação e incentivo ao desenvolvimento da pesquisa. Agradeço também à Dra. Patrícia Cruz Bergami-Santos e ao Prof. Dr. José Alexandre Marzagão Barbuto pelo auxílio científico e pela disponibilização do laboratório para o desenvolvimento da parte biológica da pesquisa. Agradeço à Profa. Dra. Maria Helena Andrade Santana pela disponibilização do uso do seu laboratório para produção e caracterização dos lipossomas. Agradeço à Dra. Leide Cavalcanti Passos pelas análises de SAXS, à Ingrid Franco de Oliveira pelas análises de DSC, ao Prof. Dr. Niels Olsen Saraiva Câmara e à Marina Burgos da Silva pela disponibilização do uso do seu laboratório e auxílio na extração de RNA. Agradeço também à Fundação de Amparo à Pesquisa do Estado de São Paulo (FAPESP) pelo apoio financeiro.

Agradeço em especial ao técnico do Laboratório de Desenvolvimento de Processos Biotecnológicos, Gilson Barbosa Maia Jr., e à técnica do Laboratório de Imunologia de Tumores, Célia Regina Pinto Pizzo, pelo auxílio na parte experimental. Agradeço aos pesquisadores do Laboratório de Imunologia de Tumores, Bruna Zelante Barbosa, Cristiano Jacob de Moraes, Elizabeth Alexandra Borges Becerra, Graziela Gorete Romagnoli, Isabella Katz Migliorim, Karen Steponavicius Piedade Cruz, Mariana Pereira Pinho, Patrícia Argenta Toniolo, Rodrigo Nalio Ramos, pelo auxílio na parte biológica. Agradeço aos pesquisadores e colegas do Laboratório de Desenvolvimento de Processos Biotecnológicos e do Laboratório de Nano & Biotecnologia para Desenvolvimentos Avançados, Caroline Sipoli, Rafael Zômpero, Tiago Balbino, Gabriela de Sá, Susana Ossada, Aline Oliveira, Andréa Shimojo, Amanda Marcelino, Rafaela Bicudo, Fernanda Lopes, Renata Miliani, Mariana Beatriz, Patrícia Severino, Andressa Souza, Fernanda Isquierdo, Carolina Camerin, Felipe Ferrari, Rhelvis Oliveira, pelo apoio e incentivo.

*“Aprender é a única coisa de que a
mente nunca se cansa, nunca tem
medo e nunca se arrepende.”
Leonardo da Vinci*

RESUMO

Esta pesquisa teve como objetivo o desenvolvimento tecnológico de uma vacina lipossomal contendo RNA tumoral destinado à imunoterapia do câncer. Nesta estratégia, RNA total codificando o antígeno tumoral Her-2/*neu* extraído de linhagem de células de adenocarcinoma de mama humano SK-BR-3 foram incorporados em lipossomas catiônicos introduzidos *in vitro* em células dendríticas (DCs). A vacina de DCs tem a função de auxiliar o sistema imunológico a identificar antígenos tumorais para que as células cancerígenas sejam eliminadas. Porém uma das etapas críticas é a introdução (transfecção) de RNA nas DCs. Lipossomas catiônicos são uma alternativa promissora, pois além de ativarem as DCs, são capazes mediar a transfecção de ácidos nucleicos para células. A experiência prévia do grupo de pesquisa na área de lipossomas catiônicos mostrou a possibilidade da obtenção de lipossomas em larga escala para o desenvolvimento de vacina de DNA contra a tuberculose. Neste contexto, este trabalho avaliou os lipossomas catiônicos com a composição lipídica de fosfatidilcolina natural de ovo (EPC), 1,2-dioleoil-sn-glicero-3-fosfatidiletanolamina (DOTAP) e 1,2-dioleoil-3-trimetilamônio-propano (DOPE), na respectiva proporção molar de 50/25/25%. Metodologicamente, o trabalho foi dividido em quatro partes: na primeira parte foi apresentada uma visão geral do trabalho desenvolvido, demonstrando o potencial dos lipossomas catiônicos complexados com RNA na imunoterapia do câncer. Na segunda parte do trabalho investigou-se os efeitos dos lipossomas produzidos através do processo laboratorial na diferenciação/maturação das DCs *in vitro* e as DCs estimuladas por estes lipossomas, na indução da proliferação de linfócitos T, resultando em lipossomas catiônicos incorporados pelas DCs, com a capacidade de ativar as DCs *in vitro* e de induzir proliferação de linfócitos T. A terceira parte do trabalho teve como finalidade a otimização da produção dos lipossomas catiônicos obtidos através do método de injeção de etanol utilizando a ferramentas estatísticas, obtendo lipossomas com menor polidispersidade e tamanho, que demonstraram *in vitro* serem incorporadas e ativarem as DCs e induzirem a proliferação de linfócitos T. A última etapa refere-se ao estudo da incorporação do RNA nos lipossomas catiônicos produzidos através do processo escalonado otimizado e comparado com o laboratorial no intuito de serem internalizados pelas DCs, transfectar o RNA e induzir a proliferação de linfócitos T através das DCs. Os resultados demonstraram que os complexos foram internalizados pelas DCs e que estas são capazes de induzir a proliferação de linfócitos T, porém há necessidade de se obter a condição ótima de transfecção. Dessa forma, conclui-se que os lipossomas catiônicos em questão têm potencial para serem usados como ferramenta em futuras estratégias na imunoterapia do câncer.

Paravras-chave: Lipossomas catiônicos, RNA, células dendríticas, câncer, imunoterapia.

ABSTRACT

This research aimed at the technological development of a liposomal vaccine containing tumor RNA for cancer immunotherapy. In this strategy, total RNA encoding the Her-2/neu tumor antigen extracted from cell line of human breast adenocarcinoma SK-BR-3 were incorporated into cationic liposomes, which were introduced *in vitro* into dendritic cells (DCs). DCs vaccine has the function of helping the immune system to identify tumor antigens in order to eliminate cancerous cells. However, one of the critical steps is the introduction (transfection) of RNA in DCs. Cationic liposomes are a promising alternative, because besides activating DCs, they are able to mediate transfection of nucleic acids into cells. Previous work of our research group in the cationic liposomes field developed a liposomal nanostructure obtained by a scale up process containing DNA vaccine against tuberculosis. In this context, this work evaluated the cationic liposomes composed by egg phosphatidylcholine (EPC), 1,2-dioleoyl-3-trimethylammonium propane (DOTAP) and 1,2-dioleoylphosphatidylethanolamine (DOPE), at 50/25/25% molar proportion respectively. Methodologically, the present work was carried out in four main steps: in the first step, it was carried out an overview of all work, showing the relevancy of cationic liposomes complexed with RNA for cancer immunotherapy. The second part of this work investigated the effects of liposomes produced *via* laboratory process upon DCs differentiation/maturation *in vitro* and induction of T lymphocytes proliferation by DCs stimulated with these liposomes, resulting in cationic liposomes incorporated by DCs, capable to activate DCs *in vitro* and to induce proliferation of T lymphocytes. The third part of the work aimed at optimizing the production of cationic liposomes obtained *via* the ethanol injection method using statistical tools, obtaining liposomes with smaller size and polydispersity, which demonstrated to be incorporated and activate DCs *in vitro* and to induce T lymphocytes proliferation. The last step refers to the study of RNA incorporation in the cationic liposomes produced *via* optimized scalable process compared to the laboratory process in order to be internalized by DCs, transfected RNA and to induce T lymphocytes proliferation by DCs. The results showed that the complexes were internalized by DCs and they are able to induce T lymphocytes proliferation, however we still have to obtain the optimal transfection condition. In sum, we conclude that the cited cationic liposomes can be used as a potential tool in further strategies in cancer immunotherapy.

Keywords: cationic liposomes, RNA, dendritic cells, cancer, immunotherapy.

SUMÁRIO

AGRADECIMENTOS	ix
RESUMO	xiii
ABSTRACT	xv
SUMÁRIO	xvii
LISTA DE FIGURAS	xxiii
LISTA DE TABELAS	xxxI
NOMENCLATURA	xxxiii
Capítulo 1 - Introdução Geral	1
1. Introdução.....	1
2. Objetivos.....	5
3. Organização da dissertação em capítulos	6
4. Referências	9
Capítulo 2 - Revisão Bibliográfica - Cationic liposomes as non-viral vector for RNA delivery in cancer immunotherapy.....	13
Abstract	13
1. Introduction.....	15
2. Cancer: the need for improved treatment strategies and the place of immunotherapy	17
3. Nanotechnology as a tool for efficient RNA delivery	20
4. Liposomes as nanocarriers in cancer therapy	22
5. Cationic liposomes as a non-viral vector for nucleic acid delivery	26
6. Cationic liposomes as RNA delivery system: a promising strategy in cancer therapy	31
7. Current & Future Developments.....	33
8. Conflict of interest.....	34
9. Acknowledgement	35
10. References	35
Capítulo 3 - Dendritic Cells Stimulated by Cationic Liposomes	43
Abstract	43
1. Background	45
2. Methods.....	47
2.1. Liposomes preparation	47
2.2. Physico-chemical characterization.....	48
2.3. Biological evaluation of liposomal structures.....	50
3. Results.....	52

3.1.	Physico-chemical characterization of cationic liposomes production using thin film method followed by extrusion (ELs) and dehydration-rehydration method (DRVs)	52
3.2.	Biological evaluation of liposomal structures.....	57
4.	Discussion	60
5.	Acknowledgements	63
6.	References	63
7.	Supplementary materials.....	66
7.1.	Strategy of dendritic cells analysis	66
7.2.	Dendritic cells activation by liposomes.....	67
Capítulo 4 - Cationic Liposomes Produced <i>via</i> the Ethanol Injection Method Internalized by Dendritic Cells.....		69
	Abstract	69
1.	Introduction.....	71
2.	Materials and methods	75
2.1.	Materials	75
2.2.	Liposomes preparation using ethanol injection method, followed by high-pressure microfluidization.....	75
2.3.	Experimental design.....	76
2.4.	Physico-chemical characterisation	78
2.5.	Biological evaluation of liposomal structures.....	79
3.	Results and discussion.....	81
3.1.	Preliminary investigation of cationic liposome production using the ethanol injection method and high-pressure microfluidization	81
3.2.	Experimental design of cationic liposome production by the ethanol injection method.....	83
3.3.	Microfluidization for uniformity of size and polydispersity	95
3.4.	Physico-chemical characterisation of cationic liposomes produced using the ethanol injection method and high-pressure homogenisation.....	97
3.5.	Biological evaluation of liposomal structures.....	104
4.	Conclusion.....	108
5.	Acknowledgements	109
6.	References	109
7.	Supplementary data	112
7.1.	Strategy of dendritic cells analysis	112
7.2.	Dendritic cells activation by liposomes.....	112
Capítulo 5 - Cationic Liposomes incorporated with RNA from Human Breast Carcinoma (SK-BR-3) Internalized by Dendritic Cells.....		115

Abstract	115
1. Background	117
2. Methods	121
2.1. Liposomes preparation	121
2.1.1. Liposomes preparation using thin film method followed by extrusion	121
2.1.2. Liposomes preparation using ethanol injection method	122
2.2. SK-BR-3 cell line cultivation, isolation of RNA from SK-BR-3 and preparation of RNA/cationic liposomes complexes	122
2.3. Physico-chemical characterization of RNA/cationic liposomes complexes	123
2.4. Biological evaluation of liposomal structures incorporated with RNA	124
3. Results	126
3.1. Physico-chemical characterization of RNA/cationic liposomes complexes	126
3.2. Biological evaluation of liposomal structures	131
4. Discussion	138
5. Acknowledgements	145
6. References	145
7. Supplementary materials	149
7.1 Strategy of dendritic cells analysis	149
7.2 Strategy of dendritic cells molecule expression analysis	150
Capítulo 6 – Conclusões Finais	153
Capítulo 7 - Sugestões para trabalhos futuros	157
ANEXO I – Determinação da proporção apropriada de marcador fluorescente para os lipossomas	159
ANEXO II – Avaliação <i>in vitro</i> da proliferação de linfócitos T	165
ANEXO III – Curriculum Vitae e Histórico Escolar	171
CURRICULUM VITAE	171
ANEXO IV – Artigo apresentado no Capítulo 2 aceito para publicação na Recent Patents on Drug Delivery and Formulation	179

LISTA DE FIGURAS

Capítulo 2

Figure 2-1 - Schematic representation of liposome formation and self-assembly into a nano-structure. 23

Figure 2-2 – Schematic diagram describing the formation of a cationic liposome/RNA complex (lipoplex) and transfection of dendritic cells by this complex. 28

Figure 2-3 - Destabilization of the endosome membrane by cationic lipids of a lipoplex to escape from the endolysosomal vesicles and delivery nucleic acids. 30

Capítulo 3

Figure 3-1 - Schematic diagram of processes for cationic liposomes production. Adapted from.²⁵ 48

Figure 3-2 - Intensity-weighted distribution (A) and Number-weighted distribution (B) of extruded liposomes and DRV liposomes obtained under different conditions. The dotted, dashed and solid lines in each graph represent one independent size distribution (n=3). 53

Figure 3-3 – Negative-staining electron micrographs of extruded liposomes (EL) acquired at (A) 1000 nm (B) 200 nm and of DRV liposomes acquired at (C) 1000 nm (D) 200 nm. 55

Figure 3-4 – Thermograms of extruded liposomes (EL) at 16 mM and DRV liposomes at 64 mM. Samples were freeze-dried and heated at 10 °C/min. Note: These thermograms and the melting temperatures are for comparison only as the fast heating temperature (10 °C/min) would reduce accuracy. 56

Figure 3-5 - Histograms of CFSE (carboxyfluorescein diacetate succinimidyl ester) dilution representing proliferation of total T lymphocytes (A), CD4+ T lymphocytes (B) and CD8+ T lymphocytes (C), when co-cultured with allogeneic DCs stimulated by TNF- α (positive control) and when co-cultured with allogeneic DCs stimulated by extruded liposomes (ELs). 59

Figure 3-6 – Strategy of dendritic cells analysis. (A) Dot Plot graph of SSC (side scatter) by FSC (forward scatter) to delimit DCs gate. (B) Graph of CD11c versus HLA-DR to delimit Gate R1, corresponding to cells double-positive. 67

Figure 3-7 - Graphics CD86 *versus* liposomes' probe of dendritic cells (A) stimulated by TNF- α (positive control - mDC), or by (B) extruded liposomes (EL) or (C) DRV liposomes (DRV). 67

Capítulo 4

Figure 4-1 – Schematic process diagram of the investigated scalable processes for cationic liposome production. Note: the experimental setup used for liposome preparation using Ultra-Turrax®: 1) Glass syringe (Tomopal - Japan) with a 20 ml capacity containing the lipid dispersion in ethanol; 2) the syringe pump (KDSscientific, model KDS-200 - Holliston, Massachusetts, USA) with a capacity for two

syringes; 3) the reactor with four fins containing 150 mL of PBS buffer; 4) the Ultra-Turrax® Homogenizer (Ika Works, model IKA T25 digital – Staufen, Germany) with a S25N-10G small impeller (Wilmington, North Carolina, USA). Adapted from Trevisan, Cavalcanti, Oliveira, De La Torre and Santana [29]. 76

Figure 4-2 – Pareto’s graphics of the t value calculated for each variable, which represents the importance of variables on estimating particle size (A) and polydispersity (B). 85

Figure 4-3 – Response surface and contour curve for the Z-average as a function of (A) the stirring rate *versus* the lipid concentration, (B) the lipid concentration *versus* the injection flow and (C) the stirring rate *versus* the injection flow. 87

Figure 4-4 – Response surface and contour curve for polydispersity as a function (A) the stirring rate *versus* the lipid concentration, (B) the lipid concentration *versus* the injection flow and (C) the stirring rate *versus* the injection flow. 90

Figure 4-5 - Schematic diagram of the hypothesised mechanism for liposome formation using the ethanol injection method. The droplets injected into the tank mixture are composed of the lipid dispersion in ethanol. The Ultra-Turrax® mixes the droplets in the aqueous phase to form phospholipid bilayer fragments (PBF) that grow into vesicles to stabilise their hydrophobic PBF edges. The decrease in ethanol concentration destabilises the PBFs, which causes them to close into vesicles and thus form liposomes. 93

Figure 4-6 – Z-average and polydispersity profiles of SM-liposomes obtained after microfluidization at 850 bar as functions of the number of cycles. The lines are for visual reference only. 96

Figure 4-7 – Intensity-weighted and number-weighted size distributions of (A) ST-liposomes and (B) SM-liposomes before and after optimization. The dotted, dashed and solid lines in each graph represent one independent size distribution (n =3). 98

Figure 4-8 – Micrographs of ST-liposomes produced at 4.8 mM, 9,600 rpm and 50.0 mL/min (trial 5, Table 4-1) obtained via the negative staining technique using transmission electron microscopy. Bars indicate (A) 500 nm and (B) 200 nm. 99

Figure 4-9 - Micrographs of ST-liposomes after optimization produced at 2.0 mM, 11,000 rpm and 44.4 mL/min (Table 4-2) obtained via the negative staining technique using transmission electron microscopy. Bars indicate: (A) 500 nm, (B) 200 nm and (C) 100 nm. 99

Figure 4-10 - Micrographs of SM-liposomes after optimization produced at 2.0 mM, 11,000 rpm and 44.4 mL/min; these liposomes were later microfluidized at 850 bar for 1 cycle (Table 4-2) and were observed using the negative staining technique in conjunction with transmission electron microscopy. The presence of cylindrical structures, which are most likely formed due to the high pressure that is characteristic of this type of equipment, are indicated with arrows. Bars indicate (A) 500 nm, (B) 200 nm and (C) 100 nm. 101

Figure 4-11 - Thermogram of the liposomes produced via the ethanol injection method (ST-liposomes) and that of the liposomes subsequently subjected to microfluidization (SM-liposomes) before and after optimization. Samples were freeze-dried and heated at 10 °C/min. Note: These thermograms and the

melting temperatures are for comparison only because the fast heating temperature (10 °C/min) reduced their accuracy. 103

Figure 4-12 - Histograms of CFSE (carboxyfluorescein diacetate succinimidyl ester) dilution representing proliferation of total T lymphocytes (A), CD4+ T lymphocytes (B) and CD8+ T lymphocytes (C), when co-cultured with allogeneic DCs stimulated by TNF- α (positive control) and when co-cultured with allogeneic DCs stimulated by ST-liposomes after optimization (final lipid concentration of 2 mM, stirring rate of 11,000 rpm and injection flow of 44.4 mL/min) or by SM-liposomes after optimization (850 bar and 1 cycle passage). 107

Figure 4-13 – Strategy of dendritic cells analysis. (A) Dot Plot graph of SSC (side scatter) by FSC (forward scatter) to delimit DCs gate. (B) Graph of CD11c versus HLA-DR to delimit Gate R1, corresponding to cells double-positive. 112

Figure 4-14 - Graphics CD86 versus liposomes' probe of dendritic cells (A) stimulated by TNF- α (positive control - mDC), or by (B) ST-liposomes after optimization (final lipid concentration of 2 mM, stirring rate of 11,000 rpm and injection flow of 44.4 mL/min) or (C) SM-liposomes after optimization (850 bar and 1 cycle passage). 113

Capítulo 5

Figure 5-1 - Intensity and number-weighted size distribution of RNA/ELs complexes (A) and RNA/ST-liposomes complexes (B) at molar charge ratios ($R_{+/-}$) of 5, 7, 10 and 15. "Empty" cationic liposomes are presented for comparison. The lines in each size distribution represent the profile of three independent RNA/cationic liposome complexes. 128

Figure 5-2 - Negative staining electron micrographs (TEM) of RNA/ELs complexes at a molar charge ratio of $R_{+/-}=15$ (A and B) and RNA/ST-liposomes complexes at a molar charge ratio of $R_{+/-}=15$ (C and D). Scale bars indicate 300 nm in (A) and 100 nm in (B, C and D). 130

Figure 5-3 – Fluorescence images of dendritic cells stimulated by TNF- α (A), extruded liposomes (B), RNA/extruded liposomes complexes at a molar charge ratio of $R_{+/-}=15$ (C), ST-liposomes (D), RNA/ST-liposomes complexes at a molar charge ratio of $R_{+/-}=15$ (E); all cationic liposomes were labeled with lipid fluorescent probe (FITC). Scale bars indicate 100 μ m. 133

Figure 5-4 – Dot plot of Her-2/*neu* (A), CD11c (B), CD80 (C), CD86 (D), CD274 (E) and CD40 (F) versus liposomes' probe of Gate R1 dendritic cells stimulated by extruded liposomes (ELs), RNA/ELs complexes at a molar charge ratio of $R_{+/-}=15$, ST-liposomes and RNA/ST-liposomes complexes at a molar charge ratio of $R_{+/-}=15$ 135

Figure 5-5 - Histograms of CFSE (carboxyfluorescein diacetate succinimidyl ester) intensity representing proliferation of total T lymphocytes (A), CD4+ T lymphocytes (B) and CD8+ T lymphocytes (C), when co-cultured with allogeneic DCs stimulated by TNF- α (positive control) and when co-cultured with allogeneic DCs stimulated by RNA/extruded liposomes complexes at a molar charge ratio of $R_{+/-}=15$ and RNA/ST-liposomes complexes at a molar charge ratio of $R_{+/-}=15$ 137

Figure 5-6 – Strategy of dendritic cells analysis. (A) Dot Plot graph of SSC (side scatter) by FSC (forward scatter) to delimit DCs gate. (B) Histogram of HLA-DR fluorescence to delimit Gate R1, corresponding to cells presented in the fluorescent positive part of the histogram. 150

Figure 5-7 – Strategy of dendritic cells molecule expression analysis. (A) Dot Plot graph of FL1 (lipid fluorescent probe) by FL2 or FL3 (detectors in which FL1 interfered) to delimit the gate of DCs that expressed molecules whose fluorescence intensity is higher than the interference of FITC (B) Dot Plot graph of FITC (lipid fluorescent probe) by Her-2/*neu* or CD11c or CD80 or CD86 or CD274 or CD40 (molecules present in FL2 or FL3) to analyze the DCs expressing double-positive fluorescent molecules. 151

ANEXO I

Figura 1– Esquema de marcação das células dendríticas estimuladas por lipossomas laboratoriais e TNF- α analisadas no citômetro de fluxo.161

Figura 2 – Histogramas do fluorocromo FITC em função do número de DCs estimuladas com (A) lipossomas LE e (B) com DRV-LE contendo 0,1%, 0,01% e 0,001% de lipídio fluorescente.....162

ANEXO II

Figura 3 – Gráficos dot plot de CD25 versus SSC, para análise da molécula CD25 apresentada por linfócitos T quando colocados em co-cultura com DCs estimuladas por TNF- α (A), extruded liposomes (ELs) (B), ST-liposomes depois da otimização (C), SM-liposomes depois da otimização (D), complexos RNA/ELs (E) e complexos RNA/ST-liposomas (F).....167

Figura 4 – Gráficos dot plot de CD25 versus SSC, para análise da molécula CD25 apresentada por linfócitos T CD4⁺ quando colocados em co-cultura com DCs estimuladas por TNF- α (A), extruded liposomes (ELs) (B), ST-liposomes depois da otimização (C), SM-liposomes depois da otimização (D), complexos RNA/ELs (E) e complexos RNA/ST-liposomas (F).....168

Figura 5 - Gráficos dot plot de CD25 versus SSC, para análise da molécula CD25 apresentada por linfócitos T CD8⁺ quando colocados em co-cultura com DCs estimuladas por TNF- α (A), extruded liposomes (ELs) (B), ST-liposomes depois da otimização (C), SM-liposomes depois da otimização (D), complexos RNA/ELs (E) e complexos RNA/ST-liposomas (F).....169

LISTA DE TABELAS

Capítulo 2

Table 2-1- Summary of the Patents Invention.....	16
--	----

Capítulo 3

Table 3-1- Physico-chemical properties of cationic liposomes EL and DRV.	52
---	----

Table 3-2 – Median of liposomes' probe fluorescence and CD86 fluorescence expressed by dendritic cells stimulated by TNF- α (positive control - mDC), or by extruded liposomes (EL) or DRV liposomes (DRV), and the negative control (iDC).	57
---	----

Capítulo 4

Table 4-1– CCD matrix with the coded and real values for the factors (stirring rate, final lipid concentration, and injection flow) tested and the responses (particle size and polydispersity (Pdl)) obtained from the experimental design for liposome production using the ethanol injection method.77	
---	--

Table 4-2 - Physico-chemical properties of liposomes produced by the ethanol injection method (ST-liposomes) followed by microfluidization (SM-liposomes) before and after optimization.....	82
--	----

Table 4-3 - Analysis of variance and regression analyses for the response of the 2 ³ central composite design.	84
--	----

Table 4-4 - Melting temperature of the liposomes produced via the ethanol injection method (ST-liposomes) and that of the liposomes subsequently subjected to microfluidization (SM-liposomes) before and after optimization. Samples were freeze-dried and heated at 10 °C/min.	102
---	-----

Table 4-5 – Mean and median of liposomes' probe fluorescence and CD86 fluorescence expressed by dendritic cells stimulated by TNF- α (positive control - mDC), or by ST-liposomes after optimization (final lipid concentration of 2 mM, stirring rate of 11,000 rpm and injection flow of 44.4 mL/min), or SM-liposomes after optimization (850 bar and 1 cycle passage) and the negative control (iDC).	104
---	-----

Capítulo 5

Table 5-1 - Physico-chemical properties of RNA/ELs complexes and RNA/ST-liposomes complexes at different molar charge ratios ($R_{+/-}$).....	126
---	-----

Table 5-2 – Median of liposomes' probe fluorescence and SSC expressed by dendritic cells stimulated by TNF- α (positive control - mDC) or by extruded liposomes (ELs), RNA/ELs complexes at a molar charge ratio of $R_{+/-}=15$, ST-liposomes, RNA/ST-liposomes complexes at a molar charge ratio ($R_{+/-}$) of 15.....	131
---	-----

ANEXO I

Tabela 1– Nomenclatura utilizada para cada lipossomas com diferentes proporções de lipídio fluorescente.	159
---	-----

NOMENCLATURA

ANOVA:	analysis of variance;
CCD:	central composite design;
cmc:	critical micellar concentration;
CTL:	cytotoxic T lymphocytes;
DC-Chol:	3 β -[N-(N',N'-dimethylaminoethane)-carbamoil] cholesterol;
DCs:	dendritic cells;
DLS:	Dynamic Light Scattering;
DNA:	deoxyribonucleic acid;
DODAB:	dioctadecyldimethylammonium bromide;
DOPC:	1,2-dioleoyl- <i>sn</i> -glycero-3-phosphocholine;
DOPE:	1,2dioleoyl <i>sn</i> -glycero-3 phosphoethanolamine;
DOTAP:	1,2-dioleoyl-3-trimethylammonium-propane;
DOTMA:	N-[1-(2,3- dioleyloxy)propyl]-N,N,Ntrimethylammoniumchloride;
DRV:	liposomes prepared by thin film method, followed by extrusion and then dehydration-rehydration step;
DSC:	differential scanning calorimetry;
ELs:	liposomes prepared by thin film method, followed by extrusion;
EPC:	Egg phosphatidylcholine;
EPR:	enhanced penetration and retention;
FDA:	Food and Drug Administration;
FITC:	fluorescein fluorochrome, in this work the liposomes' probe is the fluorescent lipid 1,2-dioleoyl- <i>sn</i> -glycero-3-phosphoethanolamine-N-(carboxyfluorescein), which contains fluorescein fluorochrome;
FSC:	forward scatter - relative size of the cells;
HF:	hydrodynamic focusing;
HPHE:	high-pressure homogenization–extrusion;
Man-lipid:	β -D-mannopyranosyl-N-dodecylhexadecanamide;
MHC:	Major Histocompatibility Complex;
PBLs:	phospholipid bilayer fragments;

PBMCs:	Peripheral blood mononuclear cells;
PdI:	Polydispersity Index;
pDNA:	DNA plasmidial;
PEG:	polyethylene glycol;
PIC:	polyribocytidylic acid;
PSA:	prostate-specific antigen;
R_{+/-}:	cationic lipid:RNA molar charge ratios;
RNA/ELs:	Extruded liposomes incorporated with RNA;
RNA/ST-liposomes:	ST-liposomes incorporated with RNA;
RNA:	ribonucleic acid;
S.D.:	Standard Deviation;
SAXS:	small angle X-ray scattering;
SK-BR-3:	cell line derived from a human breast carcinoma;
SM-liposome:	liposomes prepared by scalable method of ethanol injection, followed by high pressure Microfluidization;
SSC:	side scatter - cells granularity (internal structure and complexity);
ST-liposome:	liposomes prepared by scalable method of ethanol injection;
TCRs:	T lymphocytes receptors;
TEM:	transmission electron microscopy;
T_m:	main phase transition;
Z-average:	cumulative mean hydrodynamic diameter.

Capítulo 1 - Introdução Geral

1. Introdução

Câncer é uma doença que aflige toda a humanidade e a perspectiva é de que de que as mortes causadas por ela continuem crescendo (WHO, 2011). Considerando a gravidade desta doença, uma alternativa para o seu tratamento é a imunoterapia, que se baseia em auxiliar o sistema imunológico a identificar antígenos tumorais, permitindo que o organismo inicie uma resposta imunológica apropriada, eliminando as células tumorais (PILCH, Y. H. *et al.*, 1976; PILCH, Y. H.; RAMMING, K. P.; DEKERNION, J. B., 1977; STEELE, G., JR. *et al.*, 1980).

O grande objetivo desta terapia é estabelecer condições para que o organismo perpetue a sua resposta imunológica específica contra os tumores. Porém, a vasta gama de antígenos tumorais decorrente das diferentes causas de câncer, sugere que a terapia dos pacientes deva ser individualizada para oferecer o melhor tratamento a cada paciente (COULIE, P. G. *et al.*, 1994; GREINER, J. *et al.*, 2002; WOLFEL, T. *et al.*, 1994).

Uma vez estabelecido os antígenos tumorais a serem usados na vacina, o próximo desafio é encontrar uma forma efetiva de oferecê-los, para fazer com que ativem o sistema imunológico e eliminem as células tumorais. Uma maneira é aplicá-los diretamente nos pacientes, outra pode ser combiná-lo conjuntamente com células dendríticas (DCs), as quais são consideradas potentes apresentadoras de antígenos para o sistema imunológico (STEINMAN, R. M.; WITMER, M. D., 1978).

FINN, O. J. (2003) sugeriu que quando o tumor atinge um determinado tamanho e causa prejuízo para o tecido adjacente, com a liberação de produtos ao microambiente, DCs locais são ativadas e subsequentemente alertam o sistema imunológico. Quando a DC incorpora e processa apropriadamente o antígeno, estas migram para os órgãos linfóides, onde apresentam o antígeno para os linfócitos T, induzindo respostas primárias para células B e T. Nestas condições, dependendo do tamanho e das características imunomoduladoras o organismo é

capaz de erradicar o câncer. Porém, em muitos casos o crescimento maligno é um processo lento e “silencioso”, falhando na sinalização para a ativação do sistema imune.

Dessa forma, faz-se necessária a ativação deste sistema imune de outra maneira, como por exemplo, com a utilização da vacina de DCs. Esta vacina baseia-se no “tratamento” *in vitro* destas células com os antígenos tumorais apropriados, visando “educar” ou ativar estas células. Uma vez que estas células respondam apropriadamente ao estímulo, elas podem ser administradas como vacinas para o paciente (GILBOA, E.; VIEWEG, J., 2004; SULLENGER, B. A.; GILBOA, E., 2002).

Estudos de vacinação envolvendo mRNA se mostram promissores, pois a partir de pequena quantidade de células tumorais é possível extrair RNA para gerar bibliotecas completas de cDNA do tumor e a partir de técnicas já consolidadas de biologia molecular, pode-se obter a quantidade necessária de mRNA para a vacinação (CARRALOT, J. P. *et al.*, 2005). Além disso, elas são consideradas seguras, por serem facilmente degradadas pelo organismo, não se integrarem ao genoma, como no caso dos plasmídeos (pDNA) (SCHEEL, B. *et al.*, 2006); há menos riscos de causarem efeitos colaterais, doenças auto-imunes ou gerar anticorpos anti-DNA. Apesar da viabilidade do emprego do RNA na imunoterapia, a perspectiva de se realizar este tratamento, requer a introdução destas biomoléculas no interior das DCs (processo de transfecção).

Apesar de ser possível a utilização de ácidos nucleicos na sua forma livre em vacinas, o processo de transfecção pode ser prejudicado, pois ácidos nucleicos administrados livremente (não veiculados) se tornam quimicamente instáveis quando em contato com vários componentes extracelulares (LASIC, D. D., 1997).

Nesse sentido, os veiculadores/vetores podem ser classificados em virais e não-virais. Os vetores virais baseiam-se na capacidade inata dos vírus de liberar seu material genético nas células infectadas, porém apresentam certas limitações tais como elevado custo, desenvolvimento de respostas imunogênicas, além de possíveis efeitos oncogênicos (PEDROSO DE LIMA, M. C. *et al.*, 2003). Já os vetores não-virais, utilizam moléculas ou polímeros de natureza catiônica para se ligarem eletrostaticamente aos ácidos nucleicos, cuja natureza é aniônica (REMAUT, K. *et*

al., 2007). Dentre os vetores não-virais, se destacam os lipossomas catiônicos (DE LA TORRE, L. G. *et al.*, 2009), que como sistema de carreamento de DNA pode ser administrado *in vitro* ou *in vivo* através de várias rotas, tais como a intramuscular e a intranasal.

Os lipossomas catiônicos apresentam-se promissores, pois permitem a proteção dos ácidos nucleicos e o acoplamento na sua superfície de compostos que aumentam a eficiência de transfecção. Além disso, a facilidade de interação com as células é uma característica intrínseca das estruturas lipídicas, devido à sua semelhança com a membrana celular (DE ROSA, G.; LA ROTONDA, M. I., 2009; LABAS, R. *et al.*, 2010).

Os primeiros estudos que realizaram a transfecção de RNA em células dendríticas utilizaram lipossomas compostos pelo lipídeo catiônico DOTAP (1,2-dioleoyl-3-trimethylammonium-propane) e mostraram a sua potencialidade (BOCZKOWSKI, D. *et al.*, 1996). Com experimentos nesta área, percebeu-se que outra grande vantagem de se utilizar os lipossomas é que além destes agregados supramoleculares estabilizarem este ácido nucleico, eles também ativam por si só as células do sistema imunológico, consolidando-se como adjuvantes (ESPUELAS, S. *et al.*, 2005; KORSHOLM, K. S. *et al.*, 2007).

Lipossomas catiônicos compostos pelos lipídios fosfatidilcolina de ovo (EPC), dioleoilfosfatidiletanolamina (DOPE) e 1,2-dioleoil 3-trimetilamonio propano (DOTAP) foram estudados pela primeira vez por (PERRIE, Y.; FREDERIK, P. M.; GREGORIADIS, G., 2001), demonstrando potencial utilização no tratamento contra Hepatite B. Posteriormente, nosso grupo de pesquisadores utilizou os lipossomas catiônicos compostos pelos lipídios EPC/DOTAP/DOPE na respectiva proporção molar 50/25/25% complexados com DNA-hsp65 para o desenvolvimento de vacina contra tuberculose, demonstrando baixa citotoxicidade e a potencialidade destas nanoestruturas para vacinação gênica pela rota intranasal (ROSADA, R. S. *et al.*, 2008; ROSADA, R. S. *et al.*, 2012).

Porém, o desenvolvimento de processos escalonados para a produção de lipossomas ainda é um grande obstáculo à comercialização deste produto (SORGI, F. L.; HUANG, L., 1996). Por isso, pesquisadores aumentaram o interesse no

desenvolvimento de processos industrializáveis, sugerindo o processo de injeção de éter/etanol (LASIC, D. D., 1993; NEW, R. R. C., 1994), sistemas microfluídicos (JAHN, A. *et al.*, 2007; JAHN, A. *et al.*, 2004; WAGNER, A. *et al.*, 2002), dentre outros.

Nestas circunstâncias, a perspectiva da utilização de lipossomas catiônicos na imunoterapia do câncer é obstruída pelo empecilho do escalonamento do processo. Logo, este trabalho visa a contribuir para o desenvolvimento de um processo escalonado para produção de lipossomas catiônicos que possam carrear mRNA para dentro de células dendríticas, conseqüentemente fornecendo mecanismos para a imunoterapia contra o câncer.

2. Objetivos

O objetivo da pesquisa foi contribuir nas áreas de nanobiotecnologia e imunoterapia do câncer, vislumbrando o desenvolvimento de nanoestrutura lipossomal capaz de veicular RNA tumoral total para células dendríticas *in vitro*. Neste contexto, o objetivo específico deste projeto foi determinar as melhores condições de transfecção *in vitro* de mRNA tumoral em células dendríticas, utilizando lipossomas catiônicos obtidos a partir de processo escalonável e a sua comparação com lipossomas obtidos em escala laboratorial.

Para alcançar este objetivo, a pesquisa foi estruturada a partir das três metas principais:

1) Avaliação do efeito da estimulação *in vitro* das DCs na presença de lipossomas catiônicos obtidos a partir de método escalonável e laboratorial: Os lipossomas (composição lipídica conforme ROSADA, R. S. *et al.* (2008)) obtidos a partir dos métodos laboratorial (DE LA TORRE, L. G. *et al.*, 2009) e escalonado foram avaliados quanto à diferenciação/maturação, incorporação, capacidade de ativação das DCs *in vitro* e as DCs estimuladas por estes lipossomas foram avaliadas quanto à indução da proliferação de linfócitos T. Esta investigação foi necessária uma vez que diferentes processos de obtenção dos lipossomas podem gerar partículas com propriedades estruturais diferentes. A associação entre

parâmetros estruturais dos lipossomas e a capacidade de ativação das células dendríticas foram avaliadas.

2) Incorporação de RNA tumoral total em lipossomas catiônicos: Estudo físico-químico da incorporação de RNA nos lipossomas catiônicos. Avaliação dos parâmetros razão molar de cargas ($R_{+/-}$) para completa incorporação do RNA na estrutura, diâmetro médio hidrodinâmico e distribuição de tamanhos, potencial zeta e morfologia.

3) Transfecção *in vitro* das nanopartículas lipossomais contendo RNA em células dendríticas: A partir do estudo físico-químico dos lipossomas contendo RNA, lipossomas produzidos por método escalonável e laboratorial com RNA em razão molar de carga determinada na etapa anterior foram comparados quanto à transfecção *in vitro* em células dendríticas. Também foram avaliadas a incorporação dos complexos pelas DCs, as moléculas expressas pelas DCs e a capacidade dessas DCs de induzirem proliferação de linfócitos T. Esta etapa visou estabelecer a melhor nanoestrutura que viabilizava a entrega do RNA nas DCs, estabelecendo os parâmetros físico-químicos apropriados.

3. Organização da dissertação em capítulos

A apresentação desta dissertação de mestrado foi organizada em capítulos, conforme descrito a seguir. Os resultados estão divididos na forma de artigos, que foi (capítulo 2) ou serão (capítulos 3, 4 e 5) submetidos a periódicos internacionais, selecionados de acordo com a afinidade do conteúdo abordado. Dessa forma, os itens introdução, metodologia, resultados, discussão e conclusões de cada etapa constam nos artigos em seus respectivos capítulos. É importante ressaltar que os artigos apresentados nos capítulos 3, 4 e 5 estão apresentados aqui numa primeira versão, posteriormente eles serão submetidos a uma rigorosa revisão da escrita em língua inglesa por uma empresa especializada, antes de serem enviadas às respectivas revistas.

Capítulo 1 – Introdução Geral

Capítulo 2 – Revisão Bibliográfica em forma de artigo de revisão: Cationic Liposomes as Non-viral Vector for RNA Delivery in Cancer Immunotherapy aceita para publicação na revista Recent Patents on Drug Delivery and Formulation

Neste capítulo é apresentado a utilização de lipossomas catiônicos como vetores não-virais para transfectar antígenos tumorais, mais especificamente codificados com RNA, em células dendríticas que ativarão linfócitos T de pacientes com câncer, desencadeando a chamada imunoterapia do câncer.

Capítulo 3 – Dendritic Cells Stimulated by Cationic Liposomes

Neste capítulo foram investigados os efeitos dos lipossomas catiônicos compostos por EPC/DOTAP/DOPE na respectiva proporção molar 50/25/25%, preparados pelo método do filme seco seguido por extrusão (ELs) e pelo método da desidratação-reidratação (DRV), na diferenciação/maturação de células dendríticas e na indução da proliferação de linfócitos T pelas DCs que incorporaram estes lipossomas, *in vitro*. A análise fenotípica das DCs e a determinação das subpopulações dos linfócitos T foram realizadas por citometria de fluxo e mostrou que ambos os lipossomas catiônicos foram incorporados e ativaram as DCs, e que as DCs que incorporaram os lipossomas extrudados induziram a proliferação de linfócitos T. Assim, os resultados demonstraram que os ELs têm grande potencial para serem utilizados na imunoterapia do câncer.

Capítulo 4 – Cationic Liposomes Produced via the Ethanol Injection Method Internalized by Dendritic Cells

Neste capítulo, foi realizada a otimização do processo de produção de lipossomas catiônicos através de planejamento experimental, utilizando o método de injeção de etanol (ST-liposomes), seguido de processamento em microfluidizador a alta pressão (SM-liposomes). Nesta investigação, objetivou-se a diminuição do tamanho e da polidispersidade dos lipossomas catiônicos compostos por EPC/DOTAP/DOPE (50/25/25% molar), para adequá-los para aplicações biológicas *in vitro* e *in vivo*. Estes lipossomas foram caracterizados quanto às propriedades

físico-químicas em termos de diâmetro hidrodinâmico médio, polidispersidade, potencial zeta, morfologia e temperatura de transição de fases. Os lipossomas obtidos após a otimização tinham tamanho aproximado de 100 nm e polidispersidade menor que 0,2 demonstrando homogeneidade e tamanho apropriado que viabilizam suas aplicações *in vivo* e *in vitro*. Posteriormente estes ST-liposomes e SM-liposomes otimizados foram avaliados biologicamente *in vitro* quanto à capacidade de diferenciação/maturação das DCs e na indução da proliferação de linfócitos T pelas DCs que incorporaram estes lipossomas, demonstrando serem incorporados e ativaram as DCs, e que as DCs que os incorporaram induziram a proliferação de linfócitos T.

Capítulo 5 – Cationic Liposomes Incorporated with RNA from Human Breast Carcinoma (SK-BR-3) Internalized by Dendritic Cells

Neste capítulo os lipossomas catiônicos compostos por EPC/DOTAP/DOPE na respectiva proporção molar 50/25/25%, preparados pelo método de injeção de etanol, após otimização apresentada no capítulo anterior, e os lipossomas preparados pelo método laboratorial do filme seco seguido por extrusão foram incorporados com RNA (RNA/ST-liposomes e RNA/ELs, respectivamente) em diversas proporções molares de carga ($R_{+/-}$), concluindo-se que a melhor para os ensaios biológicos estava na $R_{+/-}$ 15. Após, estes complexos foram comparados *in vitro* quanto ao efeito na diferenciação/maturação de células dendríticas, transfecção do RNA, e na indução da proliferação de linfócitos T pelas DCs que incorporaram estes lipossomas. Os resultados demonstraram que ambos os complexos foram incorporados pelas DCs, que as DCs que incorporaram os lipossomas expressaram moléculas co-estimuladoras (CD80, CD86 e CD40) e reguladoras (CD274) e também induziram a proliferação de linfócitos T. Porém a transfecção foi pequena (pouca expressão de Her-2/*neu* pelas DCs), indicando que as condições de transfecção também devem ser otimizadas. Assim, os resultados demonstraram que estes complexos RNA/ELs e RNA/ST-liposomes na $R_{+/-}$ 15 têm grande potencial para serem utilizados na imunoterapia do câncer.

Capítulo 6 – Conclusões Finais

Capítulo 7 – Sugestões para Trabalhos Futuros

ANEXO I - Determinação da proporção apropriada de marcador fluorescente para os lipossomas

Experimentos realizados com lipossomas produzidos pelos métodos laboratoriais extrudado e DRV contendo lipídio fluorescente nas concentrações 0,1%, 0,01% e 0,001% em relação à concentração total de lipídios, demonstraram que quando as DCs são estimuladas por lipossomas contendo 0,01% de lipídio fluorescente, a concentração de fluorocromo é detecta pelo citômetro sem extrapolar o histograma, sendo esta concentração a mais apropriada para os próximos estudos com lipossomas.

ANEXO II – Avaliação *in vitro* da proliferação de linfócitos T

Foi realizada a avaliação *in vitro* da proliferação de linfócitos T quando colocados em co-cultura com células dendríticas estimuladas por TNF- α e lipossomas laboratoriais extrudados e lipossomas produzidos por injeção de etanol. Os resultados indicaram que as DCs estimuladas por estes lipossomas são capazes de induzir a proliferação de linfócitos T alogénicos *in vitro*.

ANEXO III – Curriculum vitae e Histórico escolar

ANEXO IV – Artigo apresentado no Capítulo 2 aceito para publicação na Recent Patents on Drug Delivery and Formulation

4. Referências

- BOCZKOWSKI, D. *et al.* Dendritic cells pulsed with RNA are potent antigen-presenting cells in vitro and in vivo. **Journal of Experimental Medicine**, v. 184, n. 2, p. 465-472, 1996.
- CARRALOT, J. P. *et al.* Production and characterization of amplified tumor-derived cRNA libraries to be used as vaccines against metastatic melanomas. **Genet Vaccines Ther**, v. 3, p. 6, 2005.
- COULIE, P. G. *et al.* A new gene coding for a differentiation antigen recognized by autologous cytolytic T lymphocytes on HLA-A2 melanomas. **Journal of Experimental Medicine**, v. 180, n. 1, p. 35-42, 1994.

- DE LA TORRE, L. G. *et al.* The synergy between structural stability and DNA-binding controls the antibody production in EPC/DOTAP/DOPE liposomes and DOTAP/DOPE lipoplexes. **Colloids and Surfaces B: Biointerfaces**, v. 73, n. 2, p. 175-184, 2009.
- DE ROSA, G.; LA ROTONDA, M. I. Nano and microtechnologies for the delivery of oligonucleotides with gene silencing properties. **Molecules**, v. 14, n. 8, p. 2801-2823, 2009.
- ESPUELAS, S. *et al.* Effect of synthetic lipopeptides formulated in liposomes on the maturation of human dendritic cells. **Molecular Immunology**, v. 42, n. 6, p. 721-729, 2005.
- FINN, O. J. Cancer vaccines: between the idea and the reality. **Nat Rev Immunol**, v. 3, n. 8, p. 630-641, 2003.
- GILBOA, E.; VIEWEG, J. Cancer immunotherapy with mRNA-transfected dendritic cells. **Immunological Reviews**, v. 199, p. 251-263, 2004.
- GREINER, J. *et al.* Receptor for hyaluronan acid-mediated motility (RHAMM) is a new immunogenic leukemia-associated antigen in acute and chronic myeloid leukemia. **Experimental Hematology**, v. 30, n. 9, p. 1029-1035, 2002.
- JAHN, A. *et al.* Microfluidic Directed Formation of Liposomes of Controlled Size. **Langmuir**, v. 23, n. 11, p. 6289-6293, 2007.
- JAHN, A. *et al.* Controlled Vesicle Self-Assembly in Microfluidic Channels with Hydrodynamic Focusing. **Journal of the American Chemical Society**, v. 126, n. 9, p. 2674-2675, 2004.
- KORSCHOLM, K. S. *et al.* The adjuvant mechanism of cationic dimethyldioctadecylammonium liposomes. **Immunology**, v. 121, n. 2, p. 216-226, 2007.
- LABAS, R. *et al.* Nature as a source of inspiration for cationic lipid synthesis. **Genetica**, v. 138, n. 2, p. 153-168, 2010.
- LASIC, D. D. **Liposomes: From physics to applications**. Amsterdam: Elsevier Science Publishers B.V., 1993.
- LASIC, D. D. **Liposomes in Gene Delivery**. Boca Raton-Florida: CRC Press, 1997.
- NEW, R. R. C. **Liposomes: A practical approach**. Oxford University Press: IRL Press, 1994.
- PEDROSO DE LIMA, M. C. *et al.* Cationic liposomes for gene delivery: from biophysics to biological applications. **Current Medicinal Chemistry**, v. 10, n. 14, p. 1221-1231, 2003.
- PERRIE, Y.; FREDERIK, P. M.; GREGORIADIS, G. Liposome-mediated DNA vaccination: the effect of vesicle composition. **Vaccine**, v. 19, n. 23-24, p. 3301-3310, 2001.
- PILCH, Y. H. *et al.* Immunotherapy of cancer with "immune" RNA. A preliminary report. **American Journal of Surgery**, v. 132, n. 5, p. 631-637, 1976.
- PILCH, Y. H.; RAMMING, K. P.; DEKERNION, J. B. Preliminary studies of specific immunotherapy of cancer with immune RNA. **Cancer**, v. 40, n. 5 Suppl, p. 2747-2757, 1977.
- REMAUT, K. *et al.* Nucleic acid delivery: Where material sciences and bio-sciences meet. **Materials Science and Engineering: R: Reports**, v. 58, n. 3-5, p. 117-161, 2007.
- ROSADA, R. S. *et al.* Protection against tuberculosis by a single intranasal administration of DNA-hsp65 vaccine complexed with cationic liposomes. **BMC Immunol**, v. 9, p. 38, 2008.
- ROSADA, R. S. *et al.* Effectiveness, against tuberculosis, of pseudo-ternary complexes: peptide-DNA-cationic liposome. **Journal of Colloid and Interface Science**, v. 373, n. 1, p. 102-109, 2012.
- SCHEEL, B. *et al.* Therapeutic anti-tumor immunity triggered by injections of immunostimulating single-stranded RNA. **European Journal of Immunology**, v. 36, n. 10, p. 2807-2816, 2006.
- SORGI, F. L.; HUANG, L. Large scale production of DC-Chol cationic liposomes by microfluidization. **International Journal of Pharmaceutics**, v. 144, n. 2, p. 131-139, 1996.
- STEELE, G., JR. *et al.* In vivo effect and parallel in vitro lymphocyte-mediated tumor cytolysis after Phase I xenogeneic immune RNA treatment of patients with widespread melanoma or metastatic renal cell carcinoma. **Cancer Research**, v. 40, n. 7, p. 2377-2382, 1980.
- STEINMAN, R. M.; WITMER, M. D. Lymphoid dendritic cells are potent stimulators of the primary mixed leukocyte reaction in mice. **Proceedings of the National Academy of Sciences of the United States of America**, v. 75, n. 10, p. 5132-5136, 1978.
- SULLENGER, B. A.; GILBOA, E. Emerging clinical applications of RNA. **Nature**, v. 418, n. 6894, p. 252-258, 2002.
- WAGNER, A. *et al.* The crossflow injection technique: an improvement of the ethanol injection method. **J Liposome Res**, v. 12, n. 3, p. 259-270, 2002.

-
- WORLD HEALTH ORGANIZATION (WHO). **Are the number of cancer cases increasing or decreasing in the world?** Disponível em: < <http://www.who.int/features/qa/15/en/index.html> >. Acesso em: 16 de Julho de 2011.
- WOLFEL, T. *et al.* Two tyrosinase nonapeptides recognized on HLA-A2 melanomas by autologous cytolytic T lymphocytes. **European Journal of Immunology**, v. 24, n. 3, p. 759-764, 1994.

Capítulo 2 - Revisão Bibliográfica

Cationic liposomes as non-viral vector for RNA delivery in cancer immunotherapy

Vitor, M.T¹, Bergami-Santos, P.C², Barbuto, J.A.M³ and De La Torre, L.G^{4*}

¹School of Chemical Engineering, Department of Materials and Bioprocess Engineering, University of Campinas (Unicamp), Av. Albert Einstein, 500, Campinas, SP, 13083-852, Brazil; ²Institute of Biomedical Sciences, Department of Immunology, University of São Paulo (USP), Av. Prof. Lineu Prestes, 1730, São Paulo, SP, 05508-000, Brazil; ³Institute of Biomedical Sciences, Department of Immunology, University of São Paulo (USP), Av. Prof. Lineu Prestes, 1730, São Paulo, SP, 05508-000, Brazil; ⁴School of Chemical Engineering, Department of Materials and Bioprocess Engineering, University of Campinas (Unicamp), Av. Albert Einstein, 500, Campinas, SP, 13083-852, Brazil.

*Address correspondence to this author at the School of Chemical Engineering, Department of Materials and Bioprocess Engineering, University of Campinas (Unicamp), Av. Albert Einstein, 500, Campinas, SP, 13083-852, Brazil; Tel: + 55 19 3521-0397; Cell: + 55 19 9112-1145; E-mail: latorre@feq.unicamp.br

Accepted to publish by *Recent Patents on Drug Delivery and Formulation*

Received: September 27, 2012; Accepted: December 27, 2012; Revised: December 17, 2012

Reference this article as: Vitor MT, Bergami-Santos PC, Barbuto JA, De La Torre LG. Cationic liposomes as non-viral vector for RNA delivery in cancer immunotherapy. *Recent Pat Drug Deliv Formul*, 2013, *in press*. "Anexo IV" presents the article accepted to publish.

Abstract

This review presents the current status in the use of liposomes as non-viral vector for nucleic acid delivery in cancer immunotherapy. Currently, cancer treatment uses surgery, radiotherapy and/or chemotherapy. The search for new strategies to improve the efficiency of conventional treatments is a challenge, and biological therapy has emerged as a promising technique. Immunotherapy is a branch of biological therapy that uses the body's immune system to detect and destroy cancer cells. One immunotherapy approach is the activation of T lymphocytes from cancer patients by dendritic cells (DCs) loaded with tumor antigens. Among different antigens, mRNA coding the tumor antigens is advantageous due to its capability to be amplified from small amounts of tumor tissue, its safety because it is easily degraded without integrating into the host genome, and it does not need to cross the nuclear barrier to

exert its biological activity. Nanotechnology is an approach to deliver tumor antigens into DCs. Specially, we review the use of nanoliposomes is in the field of cancer therapy because cationic liposomes can be used as non-viral vectors for mRNA delivery. Aside from the promise of liposomes, the development of scalable processes and facilities to the use this individualized therapy is still a challenge. Thus, we also present the recent techniques used for liposome production. In this context, the integration between technological knowledge in the production of cationic liposomes and immunotherapy using mRNA may contribute to the development of new strategies for cancer therapy.

Keywords: cancer, dendritic cells, immunotherapy, liposomes, RNA, nanotechnology.

Short Running Title: Potentialities and perspectives from immunotherapy to technological development

1. Introduction

Nanotechnology provides medicine knowledge to produce several nanoparticles that can be used for the detection, analysis and treatment of diseases [1, 2]. Among such nanoparticles, cationic liposomes should be highlighted due to their enormous diversity of structure and compositions, which make them useful in biology, biochemistry and medicine [3]. Liposomes have an important role in cancer therapy, more specifically, in immunotherapy, as a nucleic acid carriers for dendritic cells (DCs) [4]. DCs are the main antigen-presenting cells in the immune system, capable of initiating an immune response against cancer, but the DCs must first be loaded with tumor antigens [5]. Additionally, for pre-clinical and clinical assays, technological processes by which liposomes are produced must be scalable to guarantee the reproducibility of the formulation [6]. In order to keep the same physico-chemical and biological properties of the prepared liposomes in laboratory and larger scales, an understanding of the phenomena involved, and the physico-chemical parameters of the liposomes are needed [6]. In this review, several recent US and world patents were used to develop an overview of these issues, and they are summarized in Table 2-1.

Table 2-1- Summary of the Patents Invention

Application	Summary of Invention	Document	References
Immunotherapy	Vaccine of T lymphocytes for cancer treatment.	US6406699	[7]
Immunotherapy	Dendritic cell loaded with tumor antigen protein.	US20110097346	[8]
Drug delivery	Polymeric micelle complexed with antitumor agents (anthracyclins drug) may improve specificity to cancer cells, decreasing adverse effect.	US20050208136	[9]
Imaging and drug delivery	Dendrimers and dendrons for diagnostic and therapeutic applications.	US7977452	[10]
Diagnosis, drug and gene delivery, imaging	Disulfide-containing dendritic polymers can be bound with proteins, oligonucleotides, peptides, hormones, other dendritic polymers, non-dendritic polymers, etc.	US6020457	[11]
Radiotherapy	Carbon nanotube X-ray for oral cancer therapy.	US7771117	[12]
Drug delivery	Carbon nanotubes as therapeutic agent carrier.	US20080193490	[13]
Radiotherapy	Gold nanoparticles for radiation therapy.	US20090154646	[14]
Imaging	Luminescence characterization of quantum dots conjugated with biomarkers for early cancer detection.	US20060003465	[15]
Imaging and monitoring	Multifunctional magnetic nanoparticles probe for intracellular molecular imaging and monitoring.	US20050130167	[16]
Gene and drug delivery	Fusogenic liposomes used to deliver drugs, peptide, proteins, RNA, DNA or other bioactive molecules to the target cells.	US5885613	[17]
Gene and drug delivery	A mixture of a liposome and a polypeptide lacking specificity for cellular receptors.	US6245427	[18]
Gene and drug delivery	Liposomes to treat various disorders, including bladder inflammation, infection, dysfunction and cancer.	US7063860	[19]
Drug delivery	Liposome-encapsulated vinca alkaloids and their use in combating tumors.	US4952408	[20]
Drug and gene delivery	Cationic liposomes as a system for the delivery to cells of agents or compounds, capable of silencing a target protein and enzyme substrates.	US20060159738	[21]
Liposomes production methods	Thin film method to produce large multilamellar lipid vesicles.	US4485054	[22]
Liposomes production methods	Liposomes prepared by reverse phase evaporation protect the enzyme glucose-6-phosphate against inactivation on preparation.	US4622294	[23]
Liposomes production methods	Multitubular system as an apparatus comprising an array of tubing or an inert packing which serves as a material support or a matrix surface for the deposition of lipids produced according to the thin film method.	US5980937	[24]
Liposomes production methods	Device for preparation of liposomes by emulsion method.	US20110163468	[25]
Drug delivery	Liposomes composition and method to encapsulate the anthracycline antibiotic doxorubicin.	US4898735	[26]
Drug delivery	Method of administrating liposomal encapsulated taxane.	US6461637	[27]
Drug delivery	Liposome encapsulated taxol and a method of using the same.	US5424073	[28]
Drug delivery	Liposome composed of saturated phospholipid and glycolip promotes a long time circulation of drug liposome-entrapped in blood.	US5000959	[29]
Liposomes production methods and composition	A solubilized cholesterol composition used to facilitate delivery of pharmaceutical agents.	US7709457	[30]
Gene delivery	Dehydrated-rehydrated cationic liposome EPC/DOTAP/DOPE for therapy and vaccination.	WO2009073941	[31]

2. Cancer: the need for improved treatment strategies and the place of immunotherapy

Cancer is a disease that afflicts mankind, with approximately 10 million new cases every year [32], and whose incidence and mortality are expected to increase over the next several decades [33]. This reflects, in part, the relative inefficiency of the usual treatment modalities (surgery, radiotherapy and chemotherapy) in dealing with advanced disease, a situation that is already common at the diagnosis of cancer. Indeed, it has been estimated that the overall contribution of chemotherapy to 5-year survival in adults with cancer is 2.1% in the USA and 2.3% in Australia [34]. This, accompanied by our deeper understanding of cancer biology, is furthering the development of new treatment approaches for cancer. Among these approaches, molecular-targeted therapies appear very promising because they are designed to act upon specific molecular targets present specifically in cancer cells [35]. Another group of strategies, the biologic therapies, aim to exploit the patient's physiological mechanisms to contain the growth of tumors, targeting those upon which tumors depend for their growth (e.g., the development of blood vessels [36, 37]) or to help the patient's body overcome the toxic effects of chemotherapy [38, 39].

It is noteworthy that with so many new and elaborate therapies that exploit the immune system's potential to control tumors [40], their origin can be traced back to the end of the nineteenth/beginning of the twentieth century [41]. Actually, one could argue that an immunotherapeutic approach for cancer is both a biologic and a molecular-targeted therapy. Because such an approach exploits the body's ability to eliminate the targets that the immune system identifies as potentially harmful, it is a biologic therapy, and because one of the hallmarks of an immune response is its molecular specificity, it would be, by definition, a molecular-targeted therapy.

The growing recognition of immunotherapy as potentially effective in advanced cancer comes from both a deeper understanding of the immune system's physiology [42] and from the ever-increasing possibility of interference with the immune response [43]. This is translated, clinically, in the many protocols that use genetically

engineered molecules, like cytokines [4], growth factors [44] and antibodies [45], or selected cell populations [7]. Among the latter, DCs occupy a place of increasing relevance.

The development of a tumor in an individual that is not immunodeficient requires that either the tumor carries no specific antigen that could distinguish it from healthy tissues or that, carrying such antigens, it escapes immune surveillance. Because tumor antigens are readily detectable [46], it is the second option that seems to be operative in cancer. In fact, the relationship between tumors and the immune system seems to evolve (in those individuals that do develop a clinically detectable tumor) from a stage of control or elimination to a stage of overt escape [47]. For this escape, the disruption of DC function constitutes an effective and general escape method. DCs are the main antigen-presenting cells in the immune system [48], and it is their job to detect tissue homeostatic imbalances and subsequently to present the antigens to T lymphocytes in the secondary lymphoid organs [49] as potential targets for elimination. By hampering DC maturation [50], a phenomenon required for their effective presentation of antigens [5], tumors create environments that are prone to induce tolerance to the antigens that they contain, thus avoiding the involvement of the immune system in their control. In contrast, the possibility to generate mature DCs *in vitro* [51] opened a way to many cancer therapeutic protocols exploiting these cells as a means to recruit the immune system to fight against tumor cells [52].

In these protocols, loading the DCs with the tumor antigen(s) is a crucial step [8, 53] because it will allow DCs to process these molecules into small peptides and associate them with molecules encoded by the Major Histocompatibility Complex (MHC) [5]. Once in the context of MHC molecules and presented on the surface of the antigen-presenting cell, antigenic peptides are recognizable by specific T cell receptors (TCRs), thus being able to induce T cell activation and the consequent immune response.

This loading of antigens into DCs faces some critical issues. First, the “right” antigen must be chosen. This means that the antigen has to ideally be present in all

tumor cells, or (at least) in such a proportion of these that their elimination significantly hampers the development of the tumor. The antigen should also be associated with a vital function in the tumor cell. Otherwise, it could be easily selected against by an ensuing immune response, and this might not impact tumor growth. The chosen antigen must be one that is “recognizable” by the immune system of the patient, a characteristic that will depend on the antigen itself and on the MHC molecules of the individual, providing to immunotherapy the possibility of individual treatment. Another issue to be considered is the availability of the antigen for loading the DCs, something that may be relatively easy if the antigen can be synthesized *in vitro*, which is not always the case. Finally, the antigen should be presented in the context of both class I and class II MHC molecules. While the presentation in the context of class II molecules is needed for the activation of CD4⁺ T cells, the orchestrators of the immune response, it is in the context of class I that the same antigens are presented in tumor cells, thus making it essential that the immune system is presented to them in this context by the DCs. Although DCs are able to perform “cross-presentation”, meaning that whatever pathway the antigen follows within the cell it may be presented in the context of both classes of MHC molecules [54], the usual source of peptides that are presented in the context of class I molecules are proteins that are synthesized by the cell itself [54].

In the face of these theoretical criteria, the use of messenger RNAs (mRNAs) extracted from tumor cells performs quite well. These mRNAs can be easily extracted from small tumor samples and, once extracted, can be expanded *in vitro*, thus providing a continuous source of antigens for therapy. They potentially represent the entire antigenic constitution of the cell, thus avoiding the danger of selecting the “wrong” antigens for treatment and leaving the selection job to the immune system of the patient. Finally, due to their translation within the cell, the antigens that the mRNAs encode will be preferentially presented in the context of MHC class I molecules, a phenomenon that facilitates the expansion of CD8⁺ T lymphocytes that should recognize the same antigens on the surface of the tumor cells.

In fact, DCs loaded with mRNA-encoding (tumor) antigens, isolated directly from tumor cells or synthesized *in vitro* from complementary DNA templates, induce CD8+T cell responses, as evaluated by the presence of potent cytotoxic T lymphocyte (CTL) responses and tumor immunity in mice [55-61]. Likewise, tumor mRNA from cancer patients loaded in DCs from healthy volunteers induces CTL responses in tissue culture [56, 60, 62-71].

In 1999, the Gilboa and Vieweg group initiated a series of clinical trials to explore the use of mRNA-transfected DCs in patients with renal and prostate cancer. The phase I clinical trials established the general safety of administering mRNA-transfected DCs to cancer patients, and the majority of the vaccinated patients exhibited an immunological response [53]. Additionally, Heiser *et al.* [72] performed a phase I clinical trial in patients with metastatic prostate cancer vaccinated with prostate-specific antigen (PSA) RNA-loaded DCs. Although in an advanced state of the disease, six out of seven available patients exhibited a statistically significant PSA-specific T-cell response, displaying an impact on the blood PSA levels. Due to the success with clinical trials, the Food and Drug Administration (FDA) approved a DC-based vaccine (Sipuleucel-T, Provenge®, Dendreon Corp.) in April 2010. In the phase III clinical trial, researchers cultured autologous DCs from advanced prostate cancer patients and then infused them back into patients. The results showed that the Sipuleucel-T group significantly extended the median survival of patients with metastatic prostate cancer by an average of 4.1 months longer than the placebo group [4].

However, efficient mRNA delivery to dendritic cells is still a challenge, and this is where the use of nanotechnology and, more specifically, liposomes can have a significant effect in the development of an individualized immunotherapy against cancer.

3. Nanotechnology as a tool for efficient RNA delivery

Nanotechnology is a multidisciplinary field that involves science and technology and that explores and designs structures, devices, and systems at the nanometer

scale [73]. Nanomedicine emerged as a branch of nanotechnology applied to the treatment, diagnosis, monitoring, and control of biological systems, incorporating a multitude of diverse and often unique nano-sized products, including new and/or improved therapeutic drugs, diagnostic/surgical devices, and targeted drug delivery systems [74]. The majority of nanotechnology-based systems that are useful for cancer therapeutics are defined as nanovectors, which are injectable nano-scale delivery systems [75, 76]. Nanovectors offer the promise of providing breakthrough solutions to the problem of optimizing the efficacy of therapeutic agents, while simultaneously diminishing the deleterious side-effects that commonly accompany the use of both single chemotherapeutic agents and multimodality therapeutic regimens [77].

In this field, nanotechnology has allowed the development of novel drug nanocarriers capable of targeting different cells in the body [78], increasing the availability of reactive groups on the particle surface. This effect is a consequence of the particle size decrease to the nano-scale level, which exponentially increases the surface area per unit mass [79]. There is ample evidence that size and surface characteristics can dramatically affect nanoparticle behavior in biological systems [80-83].

Administration of cytotoxic chemotherapy can be inconvenient for patients, since it involves unwanted exposure to non-cancerous cells, tissues and organ compartments not involved with the disease. Nanoparticles carrying chemotherapeutics can reduce the undesirable distribution of such compounds because they can be designed with specific targeting that makes it possible for drugs to only reach tumors [84].

The list of nanoparticle medicines approved and/or currently being developed is quite large, ranging from widespread forms of drug-encapsulation (e.g., liposomes and simple polymeric structures [85]) to more intricate multifunctional “nanoplatfoms” and diagnostics devices (e.g., polymeric micelles [9], dendrimers [10, 11], carbon nanotubes [12, 13], quantum dots [15], gold nanoparticles [14], and magnetic nanoparticles [16], to name a few [86]). Patents involving this issue are described in

Table 2-1. Due to their general capacity for multiple modifications and their inherent properties, the vast majority of these products can have multiple relevant functions to improve the early detection of cancer and/or to provide alternative clinical therapeutic approaches to fighting cancer. Thus, some of these products have been approved by the FDA for clinical use [87, 88].

Liposomes are often used as nanocarriers for the delivery and transfection of DNA, RNA, polypeptides, genes, proteins, drugs and biologically active agents to target cells of interest. For instance, fusogenic liposomes can be varied as required over a time scale to adopt a non-lamellar phase or assume a bilayer structure [17], cationic liposomes can be combined with a non-receptor-binding protein (serum albumin of the source animal of the cell to be transfected) [18] and antibody-coated liposomes can contain nerve growth factor antisense nucleic acids, which are used as a treatment for neurogenic bladder dysfunction [19].

Among the wide variety of nanoparticles that are being studied in cancer nanotechnology, liposomes are a potential vector for RNA delivery [53].

4. Liposomes as nanocarriers in cancer therapy

The first nanotechnology-based approach to be used as a means of delivering cancer chemotherapy was liposomes [89]. Liposomes are amphipathic lipid systems, similar to biological membranes, that self-assemble into spherical bilayers with an aqueous interior lumen in an excess of aqueous media (Figure 2-1). Depending on the lipid composition, they can be biodegradable and nontoxic [90-92]. Phospholipids are the main lipids used for liposomes, and depending on the composition and production system, liposomes can be classified as multilamellar vesicles, small unilamellar vesicles or large unilamellar vesicles [90, 92].

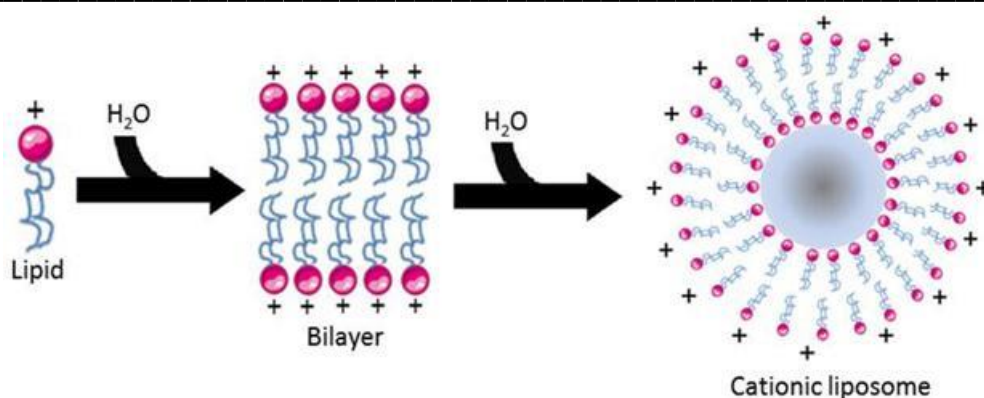


Figure 2-1 - Schematic representation of liposome formation and self-assembly into a nano-structure.

The liposome self-aggregation phenomena depends on a balance between the hydrophobic attraction of the hydrocarbon chains and the hydrophilic repulsion of the head groups of the lipids, leading one to define the critical packing parameter for the system, which in this case must be between 0.5 and 1, thus limiting the geometrically accessible forms available to the aggregate [93, 94].

The phospholipid's amphiphilic nature also allows the incorporation of molecules with different characteristics, such as vinca alkaloids (hydrophobic molecules) that display an improved antitumor effect when liposome-encapsulated [20]. Hydrophilic molecules can be loaded in the vesicle water core, while hydrophobic molecules can be incorporated within the bilayer. This is only possible because the lipophilic moieties of the phospholipids (hydrocarbon tails) can interact with hydrophobic molecules (e.g. poorly-soluble drugs), providing a stable incorporation of them into the lipid bilayer membranes of liposomes [95]. Amphiphilic molecules can be partially anchored to the bilayer, and if the phospholipid head group is charged, electrostatic interactions will retain the charged molecule, such as DNA and RNA incorporation for gene delivery [90]. Moreover, agents or compounds may electrostatically complex with cationic liposomes to inhibit the activity or apparent activity of a target protein in cells, providing a delivery system to cells [21].

Liposomes are considered thermodynamically metastable systems because bilayer structures usually adopt the lowest free energy aggregation state leading to

phase separation, but a bilayer is a kinetically trapped system. These metastable systems are well described by Evans and Wennerström [93]. As an advantage, the bilayer system is stable upon changes in the environment, e.g., dilutions [96]. Their colloidal stability can be improved through steric stabilization or electrostatic strategies [97]. For further information about liposome properties and their methods of production, see Lasic [98].

The first study to demonstrate the proof of principle that liposomes can be used as a nanovector for effective delivery of an active cancer therapeutic is based on the encapsulation of the anthracycline antibiotic doxorubicin [26], which is an effective and commonly used first line chemotherapeutic agent for both leukemia and solid tumors [77]. This liposome-encapsulated doxorubicin (Doxil[®]) is regulated by the FDA and has been clinically available for treatment since 1995. The use of doxorubicin is associated with dose-limiting cardiotoxicity, but the incorporation of this drug into liposomes improves drug solubility, enhances drug transfer into cells and tissues, facilitates organ avoidance, and modifies the drug release profiles, minimizing toxicity [99]. Doxorubicin encapsulated in liposomes has been clearly demonstrated to be clinically safe and efficacious for such malignancies as breast and ovarian cancer [100-102].

Indeed, liposomes are an effective means of delivering a diverse group of anti-tumor agents, such as doxorubicin and the poorly soluble drug paclitaxel [27], which is one of the most useful anticancer agents used for various cancers [103, 104]. Due to its poor aqueous solubility, the commercial product Taxol[®] combines paclitaxel with polyethoxylated castor oil and dehydrated ethanol [28]. However, some drawbacks, such as severe hypersensitivity reactions, neutropenia and neurotoxicity, have been reported during the clinical application of this formulation [105, 106]. To avoid these adverse effects and inconveniences, alternative formulations such as paclitaxel encapsulate in liposomes with polyethylene glycol (PEG) have been exploited. PEGylated liposomes are able to stabilize encapsulated paclitaxel in the blood, and in *in vivo* studies utilizing Colon-26 solid tumor-bearing mice, it was confirmed that PEG liposomes loaded with paclitaxel deliver large amounts of the

drug to tumor tissue. These results suggest that PEG liposomes can serve as a potent paclitaxel delivery vehicle for future cancer chemotherapy [107].

Liposomes can increase the amount of anti-cancer drugs delivered to solid tumors by passive targeting. The increase in fenestrations in tumor neovasculature allows the preferential concentration of liposome-encapsulated anti-tumor agents in close proximity to the local tumor site, a phenomenon defined as enhanced penetration and retention (EPR). In addition, tumors lack efficient lymphatic drainage, and consequently, clearance of extravasated liposomes is slow. Modifications of the liposomal surface by PEGylation or the attachment of antibodies or receptor ligands may improve their selective targeting and increase their circulation time [77, 108]. However, depending on the liposome composition, it is not necessary to add PEG to promote the stable circulation of liposome-entrapped drugs in blood for a long time after intravenous administration, as shown in [29].

Liposomes are considered promising potential carriers, but the FDA requires an effective scale-up and quality control measures, which have been the major drawbacks to the commercialization of liposomal dosage forms [109]. Therefore, researchers have increased their interest in developing industrial-scale processes for liposomal production. Initially, liposomes were produced by the thin film method, which essentially consists of producing a thin dried lipid film by evaporating an organic solvent and subsequent agitation in the presence of a liquid, providing film hydration and thus producing large multilamellar lipid vesicles [22]. Nevertheless, this method is not scalable. Among the various production methods, there is reverse phase evaporation [98, 110], which in the presence of an organic solvent and on storage as an aqueous suspension can protect enzymes against inactivation during preparation [23], the multitubular system [24, 111], detergent depletion or emulsion methods [25] and a method to reduce the size of nanoparticles by subjecting them to a microfluidizer (i.e., a high-pressure homogenizer) [112]. Patents involving these methods are described in Table 2-1.

Recently, ethanol injection has emerged as a potential technique to scale up the preparation of cationic liposomes, which is performed by the controlled addition of an ethanol/lipid solution in a reactor containing an aqueous phase under controlled agitation [6]. To further improve this method, it was modified by using a high lipid concentration in the alcohol phase, minimizing the concentration of ethanol in the liposome formulation [6]. More recently, a continuous liposome production process has emerged, in which lipids dissolved in alcohol are hydrodynamically focused between two aqueous streams in a microfluidic channel, thus forming a laminar flow in the microchannel that provides controlled diffusive mixing at the two liquid interfaces where the lipids self assemble [113].

5. Cationic liposomes as a non-viral vector for nucleic acid delivery

One of the immunotherapy strategies against cancer is the *in vitro* treatment of dendritic cells with mRNA. However, *in vitro* mRNA delivery inside dendritic cells requires special techniques.

There are different ways to delivery RNA into dendritic cells. Passive transfection, in which immature DCs absorb mRNA in medium as part of their function without external stimuli, was shown to work successfully and is sufficient to sensitize the DCs to stimulate a CTL response [65, 114]. Electroporation is also a highly efficient method to introduce mRNA into DCs because it does not require additional reagents and is compatible with clinical use [66, 70]. The application of an electrical pulse makes cells take up enough RNA for antigen presentation. However, electroporation makes DCs fragile, and special care is needed to recover the shocked cells [67, 115-122].

Another mRNA delivery method is transfection using cationic liposomes, which stimulates immune responses in mice when mRNA is transfected into DCs in the presence of a cationic lipid [57]. Cationic liposomes are normally composed of a cationic lipids (e.g., DOTAP (1,2-dioleoyl-3-trimethylammonium-propane) or DOTMA (N-[1-(2,3- dioleoyloxy)propyl]-N,N,N-trimethylammoniumchloride)), and a helper lipid (e.g., DOPE (1,2dioleoylsn-glycero-3 phosphoethanolamine) [123] or solubilized

cholesterol), which enhances transfection efficiency [30]. In the case of DOPE, the helper facilitates release of the nucleic acid within the cells after incorporating the cationic liposome complexes into the endosome [124].

However, the cationic characteristic of these lipids is known to be cytotoxic to cells, requiring careful optimization of the transfection protocol, and therefore, the molar ratio between the RNA and cationic lipids and the concentration used must be optimized [53, 125]. One strategy to overcome this cytotoxicity was studied by De La Torre *et al.* [126], who incorporated egg phosphatidilcholine into DOTAP/DOPE liposomes. The EPC/DOTAP/DOPE liposomes [31] were evaluated *in vivo* as a DNAhsp65 gene vaccine against tuberculosis [127] and transfected *in vitro* in HeLa cells [128].

The spontaneous formation of lipoplexes (cationic liposomes with negatively charged nucleic acid molecules) occurs through the electrostatic association between cationic lipids neutralizing the negative charges of nucleic acid, providing the complexes a net positive charge that allows their interaction with the negatively charged surface of cells (Figure 2-2) [129]. In addition to these electrostatic attractions, the cells must internalize the liposomes to deliver the nucleic acid into their cytoplasm. Understanding the cellular uptake mechanisms is very important to determine what and how the cells modulate signaling and, thus, the molecular response of the cells [130].

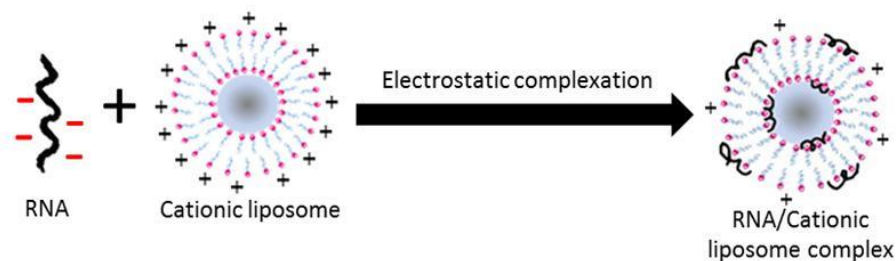
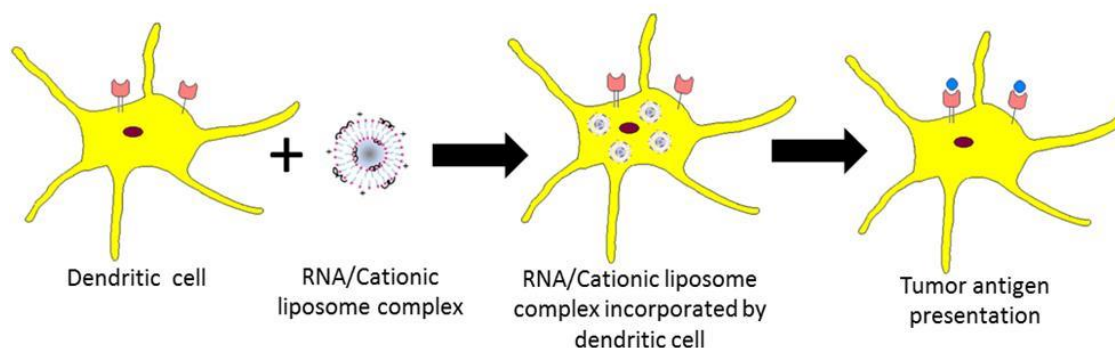
1st step: RNA/cationic liposome complexation2nd step: RNA transfection in dendritic cell

Figure 2-2 – Schematic diagram describing the formation of a cationic liposome/RNA complex (lipoplex) and transfection of dendritic cells by this complex.

Experiments using fluorescent lipids indicate that cationic liposomes composed of DOTMA:dioleoyl-PE complexed with DNA fuse with the cell membrane. This is indicated by the fluorescent probe diffusing throughout the intracellular membranes, beyond the intensity of cell-associated fluorescence, and increases with time [129]. The occurrence of membrane fusion allows nanoparticles to escape from the endosomes. Nanoparticles transported via endocytosis into cells do not have the capability to escape from the endosome and can be recycled and exocytosed out of the cell or trafficked to organelles, causing the transport of nanoparticles through cells without releasing the nucleic acid molecules. Furthermore, nanoparticles within endosomal vesicles undergo a rapid acidification due to the recruitment of degradative enzymes to digest the vesicular content, leading to possible lipoplex degradation [130].

Nevertheless, when a liposome membrane is composed of DOTMA:dioleoyl-PC complexed with DNA, fusion of the complex with the cell membrane is inhibited, and

only small points of fluorescence were observed, suggesting that the liposomes were either adsorbed or endocytosed by the cells [129]. Zhou and Huang [131] show by transmission electron microscopy that DNA/liposome complexes containing DOPE are taken up via endocytosis when after transfection into mouse L929 cells, and nucleic acid escapes into the cytosol by destabilizing the endosome membrane. Probably, the major mechanism for nucleic acid escape into the cytosol is the disruption of endosome, which depends on the interaction between the anionic lipids from endosome and cationic lipids from liposomes. The destabilizing process is increased by using “helper” lipids in the liposome composition, such as phosphatidylethanolamines [131, 132]. Phosphatidylethanolamines have a relatively small head-group areas as compared to the hydrocarbon chains (critical packing parameter > 1 for unsaturated phosphatidylethanolamine), which provides inverted hexagonal phase aggregation at acid pH. As example, if phosphatidylethanolamine is used in mass fraction between 0.41 to 0.85 with the cationic lipid DOTAP there is a coexistence of lamellar and inverted hexagonal phases [133] and liposomes composed by EPC/DOTAP/DOPE (2:1:1 molar) presents only lamellar phase [128]. Since cationic liposomes containing DOPE is used, this lipid enhances the endosome destabilization process, due its tendency to form inverse hexagonal phase, contributing to nucleic acid release into cytosol [94, 98, 132, 134]. Likewise, Xu and Szoka [124] propose the following mechanism of DNA release during transfection: 1) the complex is internalized into an endosome; 2) anionic phospholipids of the cytoplasmic face of the membrane flip-flop, resulting in destabilization of the endosome membrane; 3) the anionic lipids diffuse into the complex and form charge-neutral ion pairs with the liposomal cationic lipids; and 4) the DNA from the complex dissociates and is released into the cytosol. The destabilization of the endosome membrane by cationic lipids is a way that nanoparticles can escape from endolysosomal vesicles (Figure 2-3). The lipoplexes are extremely unstable against disintegration by cellular lipids and rapidly deliver DNA into the cytoplasm, avoiding degradation in the endosomal vesicles due to rapid acidification [135].

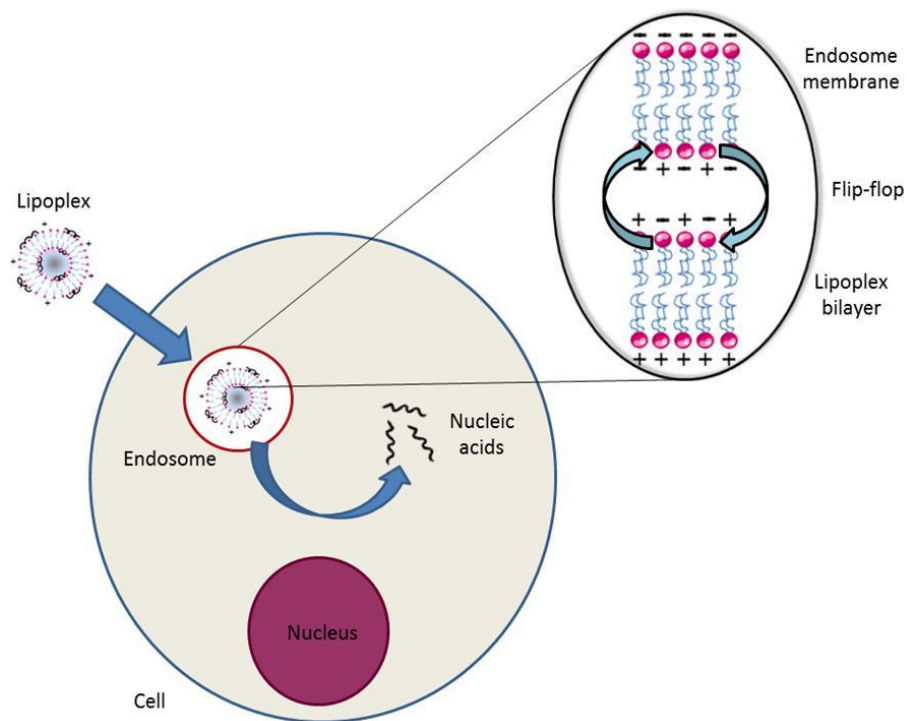


Figure 2-3 - Destabilization of the endosome membrane by cationic lipids of a lipoplex to escape from the endolysosomal vesicles and deliver nucleic acids.

In the case of RNA endosomal escape, the mechanism is not as highly studied as for DNA, likely due to the similarity between the molecules, thus inferring a similar mechanism for them. Nevertheless, the most widespread strategy for enhanced escape of liposome/siRNA complexes through the endosomal membrane (such that siRNA can reach the cytosol where all of the RNA machinery is present) is the membrane-fusion mechanism provided by the use of fusogenic peptides in the complex composition [136, 137]. In contrast, the use of commercially available cationic liposomes to transfect nucleic acids, such as Lipofectamine, demonstrates that it is possible to promote the escape of siRNA from the endosomes to a certain extent without additional helper molecules [137].

Another pathway for cationic liposomes to enter cells is via phagocytosis, but this only occurs with specific cells (e.g., macrophages, monocytes, neutrophils and DCs) whose main function is to clear off large particles or debris and large pathogens [130]. Immature dendritic cells possess a variety of ways to incorporate antigens. These

methods include phagocytosis for particles and microbes, macropinocytosis when they form large pinocytic vesicles with fluid and solutes inside, and receptor-mediated endocytosis [49, 125].

Roy *et al.* [138] and Ulmer *et al.* [139] proved that DNA vaccines, which are safe and stable, can induce antibody and T cell responses. In contrast to RNA and protein vaccines, naked DNA can be used to sustain the expression of antigens in cells for longer periods of time. However, oncogene DNA vaccines may transform normal cells, and DNA vaccines cannot amplify by themselves and have weak immunogenicity, making repeated vaccination and/or high dose administration necessary. Currently, DNA vaccine efficacy improvement requires the use of strategies to increase their immunogenicity (fused protein with cytokines or with calreticulum) and to protect them from degradation by encapsulation in nanoparticles, enhancing their half life in biological fluids and their uptake into cells [140-142]. These strategies are successful for increasing the immune response of DNA vaccines.

Recently, Hattori *et al.* [143] demonstrated that targeted delivery of a DNA vaccine using cationic liposomes as a nanovector is a potent method for DNA vaccine therapy. These researchers applied mannosylated liposomes, which are composed of Man-lipid (β -D-mannopyranosyl-N-dodecylhexadecanamide), to efficiently transfect the antigen encoded pDNA into dendritic cells, which express a large number of mannose receptors.

6. Cationic liposomes as RNA delivery system: a promising strategy in cancer therapy

The increasing attention toward using RNA molecules as therapeutic agents and their evaluation in clinical trials for the treatment of diseases is relatively new. Gene inhibitors, gene amenders, protein inhibitors and immunostimulatory RNAs are the therapeutic RNA agents that have received the most attention [5].

Researchers have used several techniques to load DCs with antigen: pulsing with peptides, incubating with proteins, transfecting with cDNA plasmids, transducing with vaccinia vectors and mRNA. They have found that mRNA-transfected dendritic

cells are invariably superior in stimulating the immune response [66, 67, 70, 71]. Additionally, a simple process can generate the mRNA encoding specific antigens.

The efficiency of mRNA transfection can be explained by several factors: 1) mRNA encodes antigens that after a translation process generates antigenic peptides for an extended amount of time (important for *in vivo* immunization), 2) the continuous supply of antigen translated from DCs transfected with mRNA can maintain a sufficient density of MHC–peptide until the DC has found its cognate T cell, and 3) mRNA transfection can induce or contribute (in some instances) to the DC maturation process [53, 71, 72, 144].

Mixtures of tumor antigens are remarkably effective in stimulating antitumor immunity, but for most cancer patients, it is not possible to obtain sufficient tumor tissue to attain the amount of antigens necessary for an effective and sustained immunization protocol. The use of mRNA is good way to solve this problem because it can be amplified from small amounts of tumor tissue (e.g., from frozen sections or from needle biopsies) by simple and straightforward PCR-based protocols. It is also possible to apply mRNA in the treatment of patients with recurring cancer, where sufficient RNA can be generated from a newly emerging antigen-loss tumor variant before it is too late. A virtually inexhaustible amount of antigen can be use in the treatment without the need to identify the potent tumor antigen on each patient [5, 53].

Aside from the easy access to large quantities of mRNA through its amplification by PCR, mRNA has other advantages as a vaccine. One of them is the safety of RNA molecules, which are easily degraded without integrating into the host genome, avoiding the induction of autoimmune diseases or anti-DNA antibodies [145]. Moreover, mRNA can be generated and characterized easier than protein, and the RNA template can be further modified to include sequences that may increase its stability and, consequently, the half life of the RNA [65].

Another advantage of RNA vaccines is that mRNA does not need to cross the nuclear barrier to exert its biological activity; for pDNA, the nuclear membrane remains a major barrier [123]. Rejman *et al.* [146] obtained data that support the

notion that the main barrier in cationic lipid-mediated delivery of pDNA is not the escape from the endosomal compartment but rather its delivery into the nucleus.

In fact, experiments in mice using mRNA-loaded DC vaccines demonstrate the development of protective and therapeutic antitumor responses [55, 57]. Perche *et al.* [147] tested four lipoplexes, imidazole/imidazolium binary liposomes complexed with mRNA and pDNA (LPR100, LPD100) and mannosylated liposomes complexed with mRNA and pDNA (Man₁₁-LPR100, Man₁₁-LPD100), against B16F10 melanoma in mice. The data show a greater inhibition of melanoma growth when mice are immunized with Man₁₁-LPR100, and this might suggest that mannosylated liposomes loaded with mRNA are more efficient than mannosylated liposomes loaded with pDNA to induce an anticancer immune response.

7. Current & Future Developments

In the future, the design and development of multifunctional nanoparticles will increase, targeting strategies for cancer detection, diagnosis and therapy based on the molecular tumor profile of each individual. It is not clear how the increase of complexity of the nanocarriers will influence the commercial scale-up of these products, but this is an important issue because nanotechnology development should be permanently established in both academia and industry. Since nanoparticles have several unique properties that provide numerous applications in various fields of science and technology, such as drug delivery systems, medical diagnostics, transfection vectors, to name a few [98]; the efforts in understanding the effects involved in nanotechnology-based products will allow rational design of nanoparticles, improving their selectivity, efficacy and safety for oncology [1, 148, 149].

Indeed, there is no doubt that multiple types of nanoparticles will be used in cancer treatment, but speaking specifically of liposomes as nanocarriers, we have an excellent perspective because they were one of the first to be employed for this purpose. There are many ways to engineer liposomes (changing their production system, ligands or the phospholipids that compose them) to find the best way to

employ them in cancer therapy. Among nucleic acid carriers, cationic liposomes are a promising strategy due to safety, scale up and capacity for multiple modifications.

Soon, oncologists will choose specific nanocarrier/targeting molecules combined with other drug strategies that may be personalized to optimize treatment regimens, improving therapeutic outcomes and reducing costs [148]. In brief, many nanotechnological platforms for drug delivery will emerge, changing the very foundations of cancer diagnosis, treatment and prevention [150].

The wide range of tumor antigens due to the different causes of cancer generates great difficulties in establishing a single formulation for every cancer patients, thus requiring individualized therapy. However, this runs counter to the pre-established structure used by industries. So, initially, a generalized scalable process should be established to later achieve an individualized and targeted product. After this, aspects of transfection, in the case of immunotherapeutic strategy based on the dendritic cells vaccine as illustrated in Figure 2-2, the constitution of nanocarriers and the incorporation of nucleic acids in nanocarriers should be investigated to obtain optimum conditions required for an individualized therapy. Some aspects of transfection that should be analyzed are the molar ratio between the nanoparticles and nucleic acids, the rate between nanoparticles/cell and the mechanism of nanoparticles transport to cells, which can be probed with the aid of microfluidic systems, e.g.

We believe that the development of clever nanoparticles for cancer therapies requires interdisciplinary research, including scientists from multiple fields such as medical professionals, engineers and the basic sciences (e.g., biology, chemistry and even physics). Joining forces in different areas will allow the development of new strategies to combat and prevent cancer.

8. Conflict of interest

The authors confirm that this article content has no conflicts of interest.

9. Acknowledgement

The study was financially supported by the Fundação de Amparo à Pesquisa do Estado de São Paulo (FAPESP).

10. References

- [1] Misra R, Acharya S, Sahoo SK. Cancer nanotechnology: application of nanotechnology in cancer therapy. *Drug Discov Today* 2010; 15(19, 20): 842-50.
- [2] Susa M, Milane L, Amiji M, Hornicek F, Duan Z. Nanoparticles: a promising modality in the treatment of sarcomas. *Pharm Res* 2011; 28(2): 260-72.
- [3] Bangham AD, Standish MM, Watkins JC. Diffusion of univalent ions across the lamellae of swollen phospholipids. *J Mol Biol* 1965; 13(1): 238-52.
- [4] Sheng WY, Huang L. Cancer immunotherapy and nanomedicine. *Pharm Res* 2011; 28(2): 200-14.
- [5] Sullenger BA, Gilboa E. Emerging clinical applications of RNA. *Nature* 2002; 418(6894): 252-8.
- [6] Trevisan JE, Cavalcanti LP, Oliveira CLP, De La Torre LG, Santana MHA. Technological aspects of scalable processes for the production of functional liposomes for gene therapy. In: Yuan X-b, Eds. *Non-Viral Gene Therapy*. InTech 2011: 267-92.
- [7] Wood, G.W. Composition and method of cancer antigen immunotherapy. US6406699 (2002).
- [8] Rubiolo, C. Dendritic Cells. US20110097346 (2011).
- [9] Maeda, H., Greish, K. Antitumor agent and process for producing the same. US20050208136 (2005).
- [10] Tomalia, D.A., Pulgam, V.R., Swanson, D.R., Huang, B. Janus dendrimers and dendrons. US7977452 (2011).
- [11] Klimash, J.W., Brothers II, H.M., Swanson, D.R., Yin, R., Spindler, R., Tomalia, D.A., *et al.* Disulfide-containing dendritic polymers. US6020457 (2000).
- [12] Kim, J.U., Choi, H.Y. X-ray system for dental diagnosis and oral cancer therapy based on nano-material and method thereof. US7771117 (2010).
- [13] Hirsch, A., Sagman, U., Wilson, S.R., Rosenblum, M.G., Wilson, L.J. Use of Carbon Nanotube for Drug Delivery. US20080193490 (2008).
- [14] Carol, M.P., Heanue, J.A. Delivery system for radiation therapy US20090154646 (2009).
- [15] Zhukov, T.A., Ostapenko, S., Sutphen, R., Lancaster, J., Sellers, T.A., Zhang, J.Z. Luminescence Characterization of Quantum Dots Conjugated with Biomarkers for Early Cancer Detection. US20060003465 (2006).
- [16] Bao, G., Nie, S., Nitin, N., La Conte, L. Multifunctional magnetic nanoparticle probes for intracellular molecular imaging and monitoring. US20050130167 (2005).
- [17] Holland, J.W., Madden, T.D., Cullis, P.R. Bilayer stabilizing components and their use in forming programmable fusogenic liposomes. US5885613 (1999).
- [18] Duzgunes, N., Simoes, S., Slepishkin, V., De Lima, M.C.P. Non-ligand polypeptide and liposome complexes as intracellular delivery vehicles. US6245427 (2001).
- [19] Chancellor, M.B., Fraser, M.O., Chuang, Y-c., De Groat, W.C., Huang, L., Yoshimura, N. Application of lipid vehicles and use for drug delivery. US7063860 (2006).
- [20] Rahman, A. Liposome-encapsulated vinca alkaloids and their use in combatting tumors. US4952408 (1990).
- [21] Graham, R., Barbisin, M. Cationic liposomes and methods of use. US20060159738 (2006).
- [22] Mezei, M., Nugent, F.J. Method of encapsulating biologically active materials in multilamellar lipid vesicles (MLV). US4485054 (1984).
- [23] Kung, V.T., Canova-Davis, E. Liposome immunoassay reagent and method. US4622294 (1986).
- [24] Tournier, H., Schneider, M., Guillot, C. Liposomes with enhanced entrapment capacity and their use in imaging. US5980937 (1999).

- [25] Ho, J-a., Lin, Y-c. Device For Preparation of Liposomes and Method Thereof. US20110163468 (2011).
- [26] Barenholz, Y., Gabizon, A. Liposome/doxorubicin composition and method. US4898735 (1990).
- [27] Rahman, A. Method of administering liposomal encapsulated taxane. US6461637 (2002).
- [28] Rahman, A., Rafaeloff, R., Husain, S.R. Liposome encapsulated taxol and a method of using the same. US5424073 (1995).
- [29] Iga, K., Hamaguchi, N., Ogawa, Y. Liposome composition and production thereof. US5000959 (1991).
- [30] Esuvaranathan, K., Mahendran, R., Lawrence, C. Methods and compositions for delivery of pharmaceutical agents. US7709457 (2010).
- [31] Santana, M.H.A., Rosada, R.S., Castelo, A.A.M.C., Silva, C.L., De La Torre, L.G. Ternary liposomal composition containing a polynucleotide WO2009073941 (2009).
- [32] Stewart BW, Kleihues P. World Cancer Report. IARC Press: Lyon, France 2003.
- [33] (WHO) WHO. Are the number of cancer cases increasing or decreasing in the world? Available at: <http://www.who.int/features/qa/15/en/index.html>. (Accessed on: July 16, 2011).
- [34] Morgan G, Ward R, Barton M. The contribution of cytotoxic chemotherapy to 5-year survival in adult malignancies. Clin Oncol 2004; 16(8): 549-60.
- [35] Pastor F, Kolonias D, Giangrande PH, Gilboa E. Induction of tumour immunity by targeted inhibition of nonsense-mediated mRNA decay. Nature 2010; 465(7295): 227-30.
- [36] Folkman J. Tumor angiogenesis: therapeutic implications. N Engl J Med 1971; 285(21): 1182-6.
- [37] Pang RW, Poon RT. Clinical implications of angiogenesis in cancers. Vasc Health Risk Manag 2006; 2(2): 97-108.
- [38] Bertino JR, Hait W. Princípios do tratamento do câncer. In: Ausiello D, Goldman L, Eds. Cecil, tratado de medicina interna. Rio de Janeiro, Brazil: Elsevier 2005: 1316-30.
- [39] (NCI) NCI. Biological therapy. Available at: <http://www.cancer.gov/cancertopics/treatment/biologicaltherapy>. (Accessed on: August 28, 2011).
- [40] Hanahan D, Weinberg Robert A. Hallmarks of Cancer: The Next Generation. Cell 2011; 144(5): 646-74.
- [41] Coley WB. The Treatment of Inoperable Sarcoma by Bacterial Toxins (the Mixed Toxins of the Streptococcus erysipelas and the Bacillus prodigiosus). Proc R Soc Med 1910; 3: 1-48.
- [42] National Institute of Allergy and Infectious Diseases. Understanding the Immune System - How It Works. In: U.S. Department of Healthy and Human Services National Institutes of Health, Eds. USA: NIH Publication 2007: 1-54.
- [43] Prestwich RJ, Errington F, Hatfield P, Merrick AE, Ilett EJ, Selby PJ, *et al*. The Immune System — is it Relevant to Cancer Development, Progression and Treatment? Clin Oncol 2008; 20(2): 101-12.
- [44] Pulendran B, Banchereau J, Maraskovsky E, Maliszewski C. Modulating the immune response with dendritic cells and their growth factors. Trends Immunol 2001; 22(1): 41-7.
- [45] Markovic SN, Celis E. Antibodies and Vaccines as Novel Cancer Therapeutics. In: Alex AA, John KB, Eds. Novel Anticancer Agents. Burlington: Academic Press 2006: 207-21.
- [46] Scanlan MJ, Gure AO, Jungbluth AA, Old LJ, Chen Y-T. Cancer/testis antigens: an expanding family of targets for cancer immunotherapy. Immunol Rev 2002; 188(1): 22-32.
- [47] Dunn GP, Bruce AT, Ikeda H, Old LJ, Schreiber RD. Cancer immunoediting: from immunosurveillance to tumor escape. Nat Immunol 2002; 3(11): 991-8.
- [48] Steinman RM. Dendritic cells: Understanding immunogenicity. Eur J Immunol 2007; 37(S1): S53-S60.
- [49] Banchereau J, Steinman RM. Dendritic cells and the control of immunity. Nature 1998; 392(6673): 245-52.
- [50] Baleeiro RB, Anselmo LB, Soares FA, Pinto CAL, Ramos O, Gross JL, *et al*. High frequency of immature dendritic cells and altered in situ production of interleukin-4 and tumor necrosis factor- α in lung cancer. Cancer Immunol Immunother 2008; 57(9): 1335-45.
- [51] Sallusto F, Lanzavecchia A. Efficient presentation of soluble antigen by cultured human dendritic cells is maintained by granulocyte/macrophage colony-

- stimulating factor plus interleukin 4 and downregulated by tumor necrosis factor alpha. *J Exp Med* 1994; 179(4): 1109-18.
- [52] Barbuto JAM, Ensina LFC, Neves AR, Bergami-Santos PC, Leite KRM, Marques R, *et al.* Dendritic cell-tumor cell hybrid vaccination for metastatic cancer. *Cancer Immunol Immunother* 2004; 53(12): 1111-8.
- [53] Gilboa E, Vieweg J. Cancer immunotherapy with mRNA-transfected dendritic cells. *Immunol Rev* 2004; 199: 251-63.
- [54] Banchereau J, Briere F, Caux C, Davoust J, Lebecque S, Liu YJ, *et al.* Immunobiology of dendritic cells. *Annu Rev Immunol* 2000; 18: 767-811.
- [55] Ashley DM, Faiola B, Nair S, Hale LP, Bigner DD, Gilboa E. Bone marrow-generated dendritic cells pulsed with tumor extracts or tumor RNA induce antitumor immunity against central nervous system tumors. *J Exp Med* 1997; 186(7): 1177-82.
- [56] Boczkowski D, Nair SK, Nam JH, Lyerly HK, Gilboa E. Induction of tumor immunity and cytotoxic T lymphocyte responses using dendritic cells transfected with messenger RNA amplified from tumor cells. *Cancer Res* 2000; 60(4): 1028-34.
- [57] Boczkowski D, Nair SK, Snyder D, Gilboa E. Dendritic cells pulsed with RNA are potent antigen-presenting cells in vitro and in vivo. *J Exp Med* 1996; 184(2): 465-72.
- [58] Granstein RD, Ding W, Ozawa H. Induction of anti-tumor immunity with epidermal cells pulsed with tumor-derived RNA or intradermal administration of RNA. *J Invest Dermatol* 2000; 114(4): 632-6.
- [59] Koido S, Kashiwaba M, Chen D, Gendler S, Kufe D, Gong J. Induction of antitumor immunity by vaccination of dendritic cells transfected with MUC1 RNA. *J Immunol* 2000; 165(10): 5713-9.
- [60] Nair SK, Heiser A, Boczkowski D, Majumdar A, Naoe M, Lebkowski JS, *et al.* Induction of cytotoxic T cell responses and tumor immunity against unrelated tumors using telomerase reverse transcriptase RNA transfected dendritic cells. *Nat Med* 2000; 6(9): 1011-7.
- [61] Zhang W, He L, Yuan Z, Xie Z, Wang J, Hamada H, *et al.* Enhanced therapeutic efficacy of tumor RNA-pulsed dendritic cells after genetic modification with lymphotactin. *Hum Gene Ther* 1999; 10(7): 1151-61.
- [62] Heiser A, Dahm P, Yancey DR, Maurice MA, Boczkowski D, Nair SK, *et al.* Human dendritic cells transfected with RNA encoding prostate-specific antigen stimulate prostate-specific CTL responses in vitro. *J Immunol* 2000; 164(10): 5508-14.
- [63] Heiser A, Maurice MA, Yancey DR, Coleman DM, Dahm P, Vieweg J. Human dendritic cells transfected with renal tumor RNA stimulate polyclonal T-cell responses against antigens expressed by primary and metastatic tumors. *Cancer Res* 2001; 61(8): 3388-93.
- [64] Heiser A, Maurice MA, Yancey DR, Wu NZ, Dahm P, Pruitt SK, *et al.* Induction of polyclonal prostate cancer-specific CTL using dendritic cells transfected with amplified tumor RNA. *J Immunol* 2001; 166(5): 2953-60.
- [65] Nair SK, Boczkowski D, Morse M, Cumming RI, Lyerly HK, Gilboa E. Induction of primary carcinoembryonic antigen (CEA)-specific cytotoxic T lymphocytes in vitro using human dendritic cells transfected with RNA. *Nat Biotech* 1998; 16(4): 364-9.
- [66] Sæbøe-Larssen S, Fossberg E, Gaudernack G. mRNA-based electrotransfection of human dendritic cells and induction of cytotoxic T lymphocyte responses against the telomerase catalytic subunit (hTERT). *J Immunol Methods* 2002; 259(1-2): 191-203.
- [67] Strobel I, Berchtold S, Götze A, Schulze U, Schuler G, Steinkasserer A. Human dendritic cells transfected with either RNA or DNA encoding influenza matrix protein M1 differ in their ability to stimulate cytotoxic T lymphocytes. *Gene Ther* 2000; 7(23): 2028-35.
- [68] Su Z, Peluso MV, Raffegerst SH, Schendel DJ, Roskrow MA. The generation of LMP2a-specific cytotoxic T lymphocytes for the treatment of patients with Epstein-Barr virus-positive Hodgkin disease. *Eur J Immunol* 2001; 31(3): 947-58.
- [69] Thornburg C, Boczkowski D, Gilboa E, Nair SK. Induction of cytotoxic T lymphocytes with dendritic cells transfected with human papillomavirus E6 and E7 RNA: implications for cervical cancer immunotherapy. *J Immunother* 2000; 23(4): 412-8.

- [70] Van Tendeloo VFI, Ponsaerts P, Lardon F, Nijs G, Lenjou M, Van Broeckhoven C, *et al.* Highly efficient gene delivery by mRNA electroporation in human hematopoietic cells: superiority to lipofection and passive pulsing of mRNA and to electroporation of plasmid cDNA for tumor antigen loading of dendritic cells. *Blood* 2001; 98(1): 49-56.
- [71] Weissman D, Ni H, Scales D, Dude A, Capodici J, McGibney K, *et al.* HIV gag mRNA transfection of dendritic cells (DC) delivers encoded antigen to MHC class I and II molecules, causes DC maturation, and induces a potent human in vitro primary immune response. *J Immunol* 2000; 165(8): 4710-7.
- [72] Heiser A, Coleman D, Dannull J, Yancey D, Maurice MA, Lallas CD, *et al.* Autologous dendritic cells transfected with prostate-specific antigen RNA stimulate CTL responses against metastatic prostate tumors. *J Clin Invest* 2002; 109(3): 409-17.
- [73] Bawa R, Bawa SR, Maebius SB, Flynn T, Wei C. Protecting new ideas and inventions in nanomedicine with patents. *Nanomed Nanotechnol Biol Med* 2005; 1(2): 150-8.
- [74] Moghimi SM, Hunter AC, Murray JC. Nanomedicine: current status and future prospects. *FASEB journal: official publication of the Federation of American Societies for Experimental Biology* 2005; 19(3): 311-30.
- [75] Ferrari M. Cancer nanotechnology: opportunities and challenges. *Nat Rev Cancer* 2005; 5(3): 161-71.
- [76] Ferrari M. Nanovector therapeutics. *Curr Opin Chem Biol* 2005; 9(4): 343-6.
- [77] Fredika R, Mauro F. Introduction and Rationale for Nanotechnology in Cancer Therapy. In: Eds. *Nanotechnology for Cancer Therapy*. CRC Press 2006: 3-10.
- [78] Shigeru K, Mitsuru H, Yuriko H. Pharmacokinetics of Nanocarrier-Mediated Drug and Gene Delivery. In: Amiji MM, Eds. *Nanotechnology for Cancer Therapy*. CRC Press 2006: 43-58.
- [79] Fenart L, Casanova A, Dehouck B, Duhem C, Slupek S, Cecchelli R, *et al.* Evaluation of effect of charge and lipid coating on ability of 60-nm nanoparticles to cross an in vitro model of the blood-brain barrier. *J Pharmacol Exp Ther* 1999; 291(3): 1017-22.
- [80] Furumoto K, Nagayama S, Ogawara K-i, Takakura Y, Hashida M, Higaki K, *et al.* Hepatic uptake of negatively charged particles in rats: possible involvement of serum proteins in recognition by scavenger receptor. *J Controlled Release* 2004; 97(1): 133-41.
- [81] Oberdürster G. Toxicology of ultrafine particles: in vivo studies. *Philosophical Transactions of the Royal Society of London. Series A: Mathematical, Physical and Engineering Sciences* 2000; 358(1775): 2719-40.
- [82] Ogawara K-i, Yoshida M, Higaki K, Toshikuro K, Shiraishi K, Nishikawa M, *et al.* Hepatic uptake of polystyrene microspheres in rats: Effect of particle size on intrahepatic distribution. *J Controlled Release* 1999; 59(1): 15-22.
- [83] Ogawara K-i, Yoshida M, Kubo J-i, Nishikawa M, Takakura Y, Hashida M, *et al.* Mechanisms of hepatic disposition of polystyrene microspheres in rats: Effects of serum depend on the sizes of microspheres. *J Controlled Release* 1999; 61(3): 241-50.
- [84] Hamaguchi T, Matsumura Y, Suzuki M, Shimizu K, Goda R, Nakamura I, *et al.* NK105, a paclitaxel-incorporating micellar nanoparticle formulation, can extend in vivo antitumour activity and reduce the neurotoxicity of paclitaxel. *Br J Cancer* 2005; 92(7): 1240-6.
- [85] Davis ME, Chen Z, Shin DM. Nanoparticle therapeutics: an emerging treatment modality for cancer. *Nature Reviews Drug Discovery* 2008; 7: 771-82.
- [86] Brigger I, Dubernet C, Couvreur P. Nanoparticles in cancer therapy and diagnosis. *Adv Drug Deliv Rev* 2002; 54(5): 631-51.
- [87] Randall M. Active Targeting Strategies in Cancer with a Focus on Potential Nanotechnology Applications. In: Amiji MM, Eds. *Nanotechnology for Cancer Therapy*. CRC Press 2006: 19-42.
- [88] Duncan R. Nanomedicine gets clinical. *Mater Today* 2005; 8(8, Supplement): 16-7.
- [89] Shimab Shahin AK, Shahab Anwar, Peeyush Jain. Nano structure based drug delivery system: An approach to treat cancer *International Journal of Drug Development & Research* 2012; 4(2): 394-407.

- [90] Antunes FE, Marques EF, Miguel MG, Lindman B. Polymer-vesicle association. *Adv Colloid Interface Sci* 2009; 147-148: 18-35.
- [91] Filipe EJM. Quando as moléculas se auto-organizam: micelas e outras estruturas supremoleculares. *Revista de Cultura Científica* 1996; (18): 25-38.
- [92] Park JW, Benz CC, Martin FJ. Future directions of liposome- and immunoliposome-based cancer therapeutics. *Semin Oncol* 2004; 31, Supplement 13: 196-205.
- [93] Evans DF, Wennerström H. *The Colloidal Domain - Where Physics, Chemistry, Biology, and Technology Meet*. 2nd ed. Wiley-vch: USA 1999.
- [94] Israelachvili JN. *Intermolecular and Surface Forces*. 2nd ed. Academic Press: California, USA 1992.
- [95] Lorenz RM, Edgar JS, Jeffries GDM, Zhao Y, McGloin D, Chiu DT. Vortex-Trap-Induced Fusion of Femtoliter-Volume Aqueous Droplets. *Anal. Chem.* 2006; 79(1): 224-8.
- [96] Yagi K. *Medical application of liposomes*. Japan Scientific Societies Press: 1986.
- [97] Hiemenz PC, Rajagopalan R. *Principles of Colloid and Surface Chemistry*, Third Edition, Revised and Expanded. Taylor & Francis: 1997.
- [98] LASIC DD. *Liposomes: From physics to applications*. Elsevier Science Publishers B.V.: Amsterdam 1993.
- [99] Portney N, Ozkan M. Nano-oncology: drug delivery, imaging, and sensing. *Anal Bioanal Chem* 2006; 384(3): 620-30.
- [100] Forssen EA, Tokes ZA. Use of anionic liposomes for the reduction of chronic doxorubicin-induced cardiotoxicity. *Proc Natl Acad Sci USA* 1981; 78(3): 1873-7.
- [101] Robert NJ, Vogel CL, Henderson IC, Sparano JA, Moore MR, Silverman P, *et al*. The role of the liposomal anthracyclines and other systemic therapies in the management of advanced breast cancer. *Semin Oncol* 2004; 31, Supplement 13: 106-46.
- [102] Straubinger RM, Lopez NG, Debs RJ, Hong K, Papahadjopoulos D. Liposome-based therapy of human ovarian cancer: parameters determining potency of negatively charged and antibody-targeted liposomes. *Cancer Res* 1988; 48(18): 5237-45.
- [103] Campbell RB, Balasubramanian SV, Straubinger RM. Influence of cationic lipids on the stability and membrane properties of paclitaxel-containing liposomes. *J Pharm Sci* 2001; 90(8): 1091-105.
- [104] Rowinsky EK, Donehower RC. Paclitaxel (Taxol). *N Engl J Med* 1995; 333(1): 1004-14.
- [105] Dye D, Watkins J. Suspected anaphylactic reaction to Cremophor EL. *Br Med J* 1980; 280(6228): 1353.
- [106] Lorenz W, Reimann HJ, Schmal A, Dormann P, Schwarz B, Neugebauer E, *et al*. Histamine release in dogs by Cremophor E1 and its derivatives: oxethylated oleic acid is the most effective constituent. *Agents Actions* 1977; 7(1): 63-7.
- [107] Yoshizawa Y, Kono Y, Ogawara K-i, Kimura T, Higaki K. PEG liposomalization of paclitaxel improved its in vivo disposition and anti-tumor efficacy. *Int J Pharm* 2011; 412(1-2): 132-41.
- [108] Sapra P, Allen TM. Ligand-targeted liposomal anticancer drugs. *Prog Lipid Res* 2003; 42(5): 439-62.
- [109] Sorgi FL, Huang L. Large scale production of DC-Chol cationic liposomes by microfluidization. *Int J Pharm* 1996; 144(2): 131-9.
- [110] New RRC. *Liposomes: A practical approach*. IRL Press: Oxford University Press 1994.
- [111] Torre LG, Carneiro AL, Rosada RS, Silva CL, Santana MHA. A mathematical model describing the kinetic of cationic liposome production from dried lipid films adsorbed in a multitubular system. *Braz J Chem Eng* 2007; 24: 477-86.
- [112] Barnadas-Rodriguez R, Sabes M. Factors involved in the production of liposomes with a high-pressure homogenizer. *Int J Pharm* 2001; 213(1-2): 175-86.
- [113] Jahn A, Vreeland WN, De Voe DL, Locascio LE, Gaitan M. Microfluidic Directed Formation of Liposomes of Controlled Size. *Langmuir* 2007; 23(11): 6289-93.
- [114] Su Z, Dannull J, Heiser A, Yancey D, Pruitt S, Madden J, *et al*. Immunological and Clinical Responses in Metastatic Renal Cancer Patients Vaccinated with Tumor RNA-transfected Dendritic Cells. *Cancer Res* 2003; 63(9): 2127-33.

- [115] Bonehill A, Van Nuffel AM, Corthals J, Tuyaerts S, Heirman C, Francois V, *et al.* Single-step antigen loading and activation of dendritic cells by mRNA electroporation for the purpose of therapeutic vaccination in melanoma patients. *Clin Cancer Res* 2009; 15(10): 3366-75.
- [116] Grunebach F, Muller MR, Nencioni A, Brossart P. Delivery of tumor-derived RNA for the induction of cytotoxic T-lymphocytes. *Gene Ther* 2003; 10(5): 367-74.
- [117] Milazzo C, Reichardt VL, Müller MR, Grünebach F, Brossart P. Induction of myeloma-specific cytotoxic T cells using dendritic cells transfected with tumor-derived RNA. *Blood* 2003; 101(3): 977-82.
- [118] Müller MR, Grünebach F, Nencioni A, Brossart P. Transfection of dendritic cells with RNA induces CD4- and CD8-mediated T cell immunity against breast carcinomas and reveals the immunodominance of presented T cell epitopes. *J Immunol* 2003; 170(12): 5892-6.
- [119] Nair S, Boczkowski D, Moeller B, Dewhirst M, Vieweg J, Gilboa E. Synergy between tumor immunotherapy and antiangiogenic therapy. *Blood* 2003; 102(3): 964-71.
- [120] Siegel S, Wagner A, Kabelitz D, Marget M, Coggin J, Barsoum A, *et al.* Induction of cytotoxic T-cell responses against the oncofetal antigen-immature laminin receptor for the treatment of hematologic malignancies. *Blood* 2003; 102(13): 4416-23.
- [121] Van Meirvenne S, Straetman L, Heirman C, Dullaers M, De Greef C, Van Tendeloo V, *et al.* Efficient genetic modification of murine dendritic cells by electroporation with mRNA. *Cancer Gene Ther* 2002; 9(9): 787-97.
- [122] Zhao Y, Boczkowski D, Nair SK, Gilboa E. Inhibition of invariant chain expression in dendritic cells presenting endogenous antigens stimulates CD4+ T-cell responses and tumor immunity. *Blood* 2003; 102(12): 4137-42.
- [123] Tavernier G, Andries O, Demeester J, Sanders NN, De Smedt SC, Rejman J. mRNA as gene therapeutic: How to control protein expression. *J Controlled Release* 2011; 150(3): 238-47.
- [124] Xu Y, Szoka FC. Mechanism of DNA Release from Cationic Liposome/DNA Complexes Used in Cell Transfection. *Biochemistry (Mosc)*. 1996; 35(18): 5616-23.
- [125] Bringmann A, Held SAE, Heine A, Brossart P. RNA vaccines in cancer treatment. *J Biomed Biotechnol* 2010; 2010: 1-12.
- [126] De La Torre LG, Rosada RS, Trombone APF, Frantz FG, Coelho-Castelo AAM, Silva CL, *et al.* The synergy between structural stability and DNA-binding controls the antibody production in EPC/DOTAP/DOPE liposomes and DOTAP/DOPE lipoplexes. *Colloids Surf B Biointerfaces* 2009; 73(2): 175-84.
- [127] Rosada RS, De La Torre LG, Frantz FG, Trombone AP, Zarate-Blades CR, Fonseca DM, *et al.* Protection against tuberculosis by a single intranasal administration of DNA-hsp65 vaccine complexed with cationic liposomes. *BMC Immunol* 2008; 9: 38.
- [128] Balbino TA, Gasperini AAM, Oliveira CLP, Azzoni AR, Cavalcanti LP, De La Torre LG. Correlation of the Physicochemical and Structural Properties of pDNA/Cationic Liposome Complexes with Their in Vitro Transfection. *Langmuir* 2012; 28(31): 11535-45.
- [129] Felgner PL, Gadek TR, Holm M, Roman R, Chan HW, Wenz M, *et al.* Lipofection: a highly efficient, lipid-mediated DNA-transfection procedure. *Proc Natl Acad Sci USA* 1987; 84(21): 7413-7.
- [130] Chou LY, Ming K, Chan WC. Strategies for the intracellular delivery of nanoparticles. *Chem Soc Rev* 2011; 40(1): 233-45.
- [131] Zhou X, Huang L. DNA transfection mediated by cationic liposomes containing lipopolylysine: characterization and mechanism of action. *Biochimica et Biophysica Acta (BBA) - Biomembranes* 1994; 1189(2): 195-203.
- [132] Maitani Y, Igarashi S, Sato M, Hattori Y. Cationic liposome (DC-Chol/DOPE = 1:2) and a modified ethanol injection method to prepare liposomes, increased gene expression. *Int J Pharm* 2007; 342(1-2): 33-9.
- [133] Koltover I, Salditt T, Radler JO, Safinya CR. An inverted hexagonal phase of cationic liposome-DNA complexes related to DNA release and delivery. *Sci* 1998; 281(5373): 78-81.
- [134] Gadd JC, Kuyper CL, Fujimoto BS, Allen RW, Chiu DT. Sizing Subcellular Organelles and Nanoparticles Confined

- within Aqueous Droplets. *Anal Chem* 2008; 80(9): 3450-7.
- [135] Caracciolo G, Caminiti R, Digman MA, Gratton E, Sanchez S. Efficient escape from endosomes determines the superior efficiency of multicomponent lipoplexes. *J Phys Chem B* 2009; 113(15): 4995-7.
- [136] Akita H, Kogure K, Moriguchi R, Nakamura Y, Higashi T, Nakamura T, *et al.* Nanoparticles for ex vivo siRNA delivery to dendritic cells for cancer vaccines: Programmed endosomal escape and dissociation. *J Controlled Release* 2010; 143(3): 311-7.
- [137] Oliveira S, van Rooy I, Kranenburg O, Storm G, Schiffelers RM. Fusogenic peptides enhance endosomal escape improving siRNA-induced silencing of oncogenes. *Int J Pharm* 2007; 331(2): 211-4.
- [138] Roy MJ, Wu MS, Barr LJ, Fuller JT, Tussey LG, Speller S, *et al.* Induction of antigen-specific CD8+ T cells, T helper cells, and protective levels of antibody in humans by particle-mediated administration of a hepatitis B virus DNA vaccine. *Vaccine* 2000; 19(7-8): 764-78.
- [139] Ulmer JB, Deck RR, Dewitt CM, Donnelly JJ, Liu MA. Generation of MHC class I-restricted cytotoxic T lymphocytes by expression of a viral protein in muscle cells: antigen presentation by non-muscle cells. *Immunology* 1996; 89(1): 59-67.
- [140] Cheng WF, Hung CF, Chai CY, Hsu KF, He L, Ling M, *et al.* Tumor-specific immunity and antiangiogenesis generated by a DNA vaccine encoding calreticulin linked to a tumor antigen. *J Clin Invest* 2001; 108(5): 669-78.
- [141] Leachman SA, Tigelaar RE, Shlyankevich M, Slade MD, Irwin M, Chang E, *et al.* Granulocyte-macrophage colony-stimulating factor priming plus papillomavirus E6 DNA vaccination: effects on papilloma formation and regression in the cottontail rabbit papillomavirus--rabbit model. *J Virol* 2000; 74(18): 8700-8.
- [142] Roy K, Mao H-Q, Huang SK, Leong KW. Oral gene delivery with chitosan-DNA nanoparticles generates immunologic protection in a murine model of peanut allergy. *Nat Med* 1999; 5(4): 387-91.
- [143] Hattori Y, Kawakami S, Nakamura K, Yamashita F, Hashida M. Efficient gene transfer into macrophages and dendritic cells by in vivo gene delivery with mannosylated lipoplex via the intraperitoneal route. *J Pharmacol Exp Ther* 2006; 318(2): 828-34.
- [144] Ni H, Capodici J, Cannon G, Communi D, Boeynaems J-M, Karikó K, *et al.* Extracellular mRNA induces dendritic cell activation by stimulating tumor necrosis factor-alpha secretion and signaling through a nucleotide receptor. *J Biol Chem* 2002; 277(15):12689-96.
- [145] Scheel B, Aulwurm S, Probst J, Stitz L, Hoerr I, Rammensee H-G, *et al.* Therapeutic anti-tumor immunity triggered by injections of immunostimulating single-stranded RNA. *Eur J Immunol* 2006; 36(10): 2807-16.
- [146] Rejman J, Tavernier G, Bavarsad N, Demeester J, De Smedt SC. mRNA transfection of cervical carcinoma and mesenchymal stem cells mediated by cationic carriers. *J Controlled Release* 2010; 147(3): 385-91.
- [147] Perche F, Benvegna T, Berchel M, Lebegue L, Pichon C, Jaffrès P-A, *et al.* Enhancement of dendritic cells transfection in vivo and of vaccination against B16F10 melanoma with mannosylated histidylated lipopolyplexes loaded with tumor antigen messenger RNA. *Nanomedicine : nanotechnology, biology, and medicine* 2011; 7(4): 445-53.
- [148] Peer D, Karp JM, Hong S, Farokhzad OC, Margalit R, Langer R. Nanocarriers as an emerging platform for cancer therapy. *Nat Nano* 2007; 2(12): 751-60.
- [149] Qiao W, Wang B, Wang Y, Yang L, Zhang Y, Shao P. Cancer Therapy Based on Nanomaterials and Nanocarrier Systems. *Journal of Nanomaterials* 2010; 2010: 1-9.
- [150] Danhier F, Feron O, Preat V. To exploit the tumor microenvironment: Passive and active tumor targeting of nanocarriers for anti-cancer drug delivery. *J Control Release* 2010; 148(2): 135-46.

Capítulo 3 - Dendritic Cells Stimulated by Cationic Liposomes

Micaela Tamara Vitor, BS^a; Patrícia Cruz Bergami-Santos, PhD^b; José Alexandre Marzagão Barbuto, PhD^b; Karen Steponavicius Piedade Cruz, BS^b; Mariana Pereira Pinho, BS^b; Lucimara Gaziola de La Torre, PhD^{a*}

^aSchool of Chemical Engineering, Department of Materials and Bioprocess Engineering, University of Campinas (Unicamp), Av. Albert Einstein, 500, Campinas, SP, 13083-852, Brazil.

^bInstitute of Biomedical Sciences, Department of Immunology, University of São Paulo (USP), Av. Prof. Lineu Prestes, 1730, São Paulo, SP, 05508-000, Brazil.

*Corresponding author:

School of Chemical Engineering, Department of Materials and Bioprocess Engineering, University of Campinas (Unicamp), Av. Albert Einstein, 500, Campinas, SP, 13083-852, Brazil.

Fax number: + 55 19 3521-3910

Telephone number: + 55 19 3521-0397

E-mail address: latorre@feq.unicamp.br

To be submitted to *Nanomedicine: Nanotechnology, Biology, and Medicine*

Abstract

We investigated the effects of cationic liposomes upon dendritic cells (DCs) differentiation/maturation *in vitro* and in T lymphocytes proliferation induced by DCs. The cationic liposomes composed by egg phosphatidylcholine (EPC), 1,2-dioleoyl-3-trimethylammonium propane (DOTAP) and 1,2-dioleoylphosphatidylethanolamine (DOPE) (50/25/25% molar) were prepared by thin film method followed by extrusion (65 ± 9 nm, polydispersity of 0.13) and by the dehydration-rehydration method (95% of the population 107 ± 27 nm, polydispersity of 0.52). The phenotypic analysis of DCs and the analysis of T lymphocytes proliferation were performed by flow cytometry and showed that both cationic liposomes were incorporated and activated DCs, and that DCs which internalized extruded liposomes, provided higher T lymphocytes proliferation. These results demonstrate the ability of cationic liposomes to activate DCs *in vitro* and to increase T lymphocytes proliferation, which could be used as a potential tool in further strategies in cancer immunotherapy and contributes to new strategies in immunotherapy.

Keywords: cationic liposomes, dehydrated-rehydrated vesicles, extruded liposomes, cancer immunotherapy, dendritic cells.

1. Background

Dendritic cells (DCs) are professional antigen-presenting cells in the immune system,¹ responsible to present antigens to T lymphocytes in the secondary lymphoid organs and they are able to detect tissue homeostatic imbalances.² However, tumors create environments that are prone to induce tolerance to their antigens,³ and a solution for this problem can be load DCs with mRNA coding the tumor antigen(s) allowing DCs to present on the surface antigenic peptides recognizable by specific T lymphocytes receptors, thus being able to induce T lymphocytes activation and the consequent immune response.⁴ Therefore, generation of mature DCs *in vitro*⁵ is a promising way to many cancer therapeutic protocols.

DCs can be loaded with tumor antigen(s)^{6, 7} but this process can interfere with antigen presentation by DCs. DCs can be loaded passively by incubation with nucleic acids,⁸ or actively by electroporation⁶ or by nanoparticles that delivery nucleic acids or proteins. Prasad and co-workers⁹ encapsulated tumor-associated antigens from head and neck squamous carcinoma cell lines in polymer nanoparticles to enhance efficiency of antigen delivery for DCs vaccine, leading to a significantly high response of CD8+ T lymphocytes, proving to be an efficient tumor cell elimination method with minimal to no toxicity.

Moreover, cationic liposomes have been used to delivery nucleic acids into DCs, due to their reproducibility, commercial availability and safety of use.¹⁰ Vangasseri *et al.*¹¹ showed that cationic liposomes alone could stimulate DCs leading to the expression of co-stimulatory molecules (CD80 and CD86) in a specific way, as zwitterionic and anionic lipids showed little or no activity. Nakanishi and co-workers¹² corroborate this statement by investigating the relationship between the charge on liposomes' surface and its adjuvant action, indicating that the positive charge on the surface of liposomes represents an important factor for enhancing their immunoadjuvancy in the induction of antigen-specific immune response. They also

reported that cationic liposomes (egg phosphatidylcholine, cholesterol and stearylamine) containing soluble antigens functioned as a potent inducer of antigen-specific T lymphocyte responses and delayed type hypersensitivity responses.¹³ Grunebach and co-workers¹⁴ analyzed the efficiency of tumor antigen transfection into DC using cationic liposomes, and suggested that this technology has the potential to induce antigen-specific cytotoxic T-lymphocytes (CTL).

Nevertheless, cationic lipids can be cytotoxic to cells requiring careful optimization of the transfection protocol, therefore the molar ratio between nucleic acids/cationic lipids and the concentration must be optimized.^{6, 15} Lincopan *et al.*¹⁶ showed toxic effects associated to the synthetic cationic lipid DODAB (dioctadecyldimethylammonium bromide) of amphotericin B. Likewise, Lin *et al.*¹⁷ realized that cationic liposome-PEG-PEI complexed with curcumin had cytotoxic activity fivefold higher than curcumin when tested on curcumin-sensitive cells and 20-fold more active against curcumin-resistant cells. So, cationic lipids must be mixed with others lipids, in order to decrease the cytotoxicity of liposomes to cells. Thus, Perrie, Frederik and Gregoriadis¹⁸ studied cationic liposomes composed by egg phosphatidilcholine (EPC), 1,2-dioleoyl-3-trimethylammonium propane (DOTAP) and 1,2-dioleoylphosphatidylethanolamine (DOPE), for DNA delivery against Hepatitis B, demonstrating the potential of this composition as a non-viral system. Later, our research group¹⁹ studied the cytotoxicity *in vitro* of these liposomes prepared by the dehydration-rehydration method (DRV) upon mice J774 macrophage cell line; observing that the addition of EPC to the cationic liposomes formulation decreased their cytotoxicity. Furthermore, these cationic liposomes demonstrated *in vivo* efficacy for gene vaccination against tuberculosis.^{20, 21} More recently, the cationic liposomes EPC/DOTAP/DOPE (50/25/25% molar) complexed with pDNA in various proportions were studied in their ability to transfect HeLa cells *in vitro*, confirming the low cytotoxic effect.²²

In this context, this study investigated the effects of cationic liposomes composed by EPC/DOTAP/DOPE in their ability to stimulate DCs aiming future applications in new vaccines development. To this end, we investigated the effect of

liposomes obtained by thin film method followed by extrusion (ELs) and by the dehydration-rehydration method (DRVs), which generate liposomes with different physico-chemical properties, besides the same composition and lipid concentration, in order to identify the best condition to stimulate dendritic cells.

2. **Methods**

Egg phosphatidylcholine (EPC) (96% of purity), 1,2-dioleoyl-sn-glycero-3-phosphoethanolamine (DOPE) (99.8% of purity) and 1,2-dioleoyl-3-trimethylammonium-propane (DOTAP) (98% of purity) were purchased from Lipoid Germany and used without further purification, for liposomes production. The fluorescent probe 1,2-dioleoyl-sn-glycero-3-phosphoethanolamine-N-(carboxyfluorescein) (FITC) (Avanti® Polar Lipids, Inc.) was used in cationic liposomes composition to visualize DCs that incorporated the liposomes, in flow cytometry. The specific fluorescent antibodies to CD11c, CD86, HLA-DR, CD4 and CD8 from BD Biosciences used in phenotypic analysis of DCs and analysis of subpopulations of T lymphocytes, in flow cytometry.

2.1. **Liposomes preparation**

The extruded liposomes (EL) were obtained by dried film method,²³ followed by hydration with PBS buffer and then by an extrusion step. Briefly, stock solutions for each of lipids (EPC, DOTAP, DOPE) were prepared in chloroform and stored at -20 °C. Those lipid solutions were added in the required amounts (EPC/DOPE/DOTAP 50/25/25% molar), mixed and dried to a thin film using a rotary evaporator (ART LAB) in a 650 mmHg vacuum for 1 hour. The dried lipid film was hydrated with PBS buffer for 40 minutes to reach a concentration of 16 mM at 30°C, above its phase transition temperature. The liposomes were extruded (Lipex Biomembranes Inc., model T.001) through two stacked polycarbonate membranes (100 nm nominal diameter) 15 times at a nitrogen pressure of 12 kgf/cm². Then, part of the extruded liposomes was submitted to a drying step, such as lyophilization; samples were frozen in liquid nitrogen and lyophilized (Liobrás, model L-101) for 24 hours. Subsequently, the lyophilized particles were controlled rehydrated (DRV liposomes) with PBS buffer to

reach the final lipid concentration of 64 mM, at a temperature above the phase transition of lipids, in this case we used a temperature of 4 °C, and vortexing. This procedure generated DRV liposomes.²⁴ The two methods by which cationic liposomes were prepared are described in Figure 3-1.

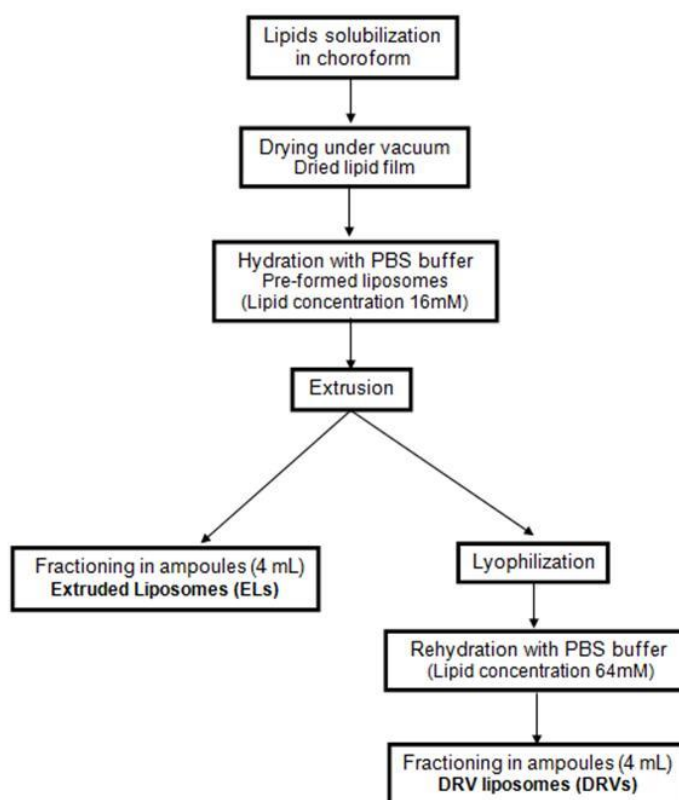


Figure 3-1 - Schematic diagram of processes for cationic liposomes production. Adapted from.²⁵

2.2. Physico-chemical characterization

2.2.1. Average hydrodynamic diameter and zeta potential

The average hydrodynamic diameter and size distribution were determined by dynamic light scattering (Malvern Zetasizer Nano ZS) using a Ne–He laser and measurements at a scattering angle of 173°. The particle's diameter was calculated from the translational diffusion coefficient by using the Stokes–Einstein equation (Equation 3-1).

$$d(H) = \frac{(kT)}{3\pi\eta D} \quad (\text{Equation 3-1})$$

where $d(H)$ is the hydrodynamic diameter; D is the translational diffusion coefficient; k is the Boltzmann's constant, T is the absolute temperature and η is the solvent viscosity. The mean diameter and distribution of particle sizes were estimated by CONTIN algorithm analysis. The intensity-weighted and number-weighted mean diameter and particle distribution were obtained in triplicate.

The zeta potential was measured on the same equipment by diluting cationic liposomes in the appropriate volume of PBS buffer at 25°C. This dilution condition was selected since it is exactly the same condition in which the liposomes were prepared.

Statistical analysis included two-sample t-test for independent samples at 5% significance level, performed with MS Excell 2007.

2.2.2. Morphology

The morphology of the lipid structures were visualized employing transmission electron microscopy (TEM). It was used carbon-coated 200-mesh copper grids with collodion (parloidin with cellulose acetate) film. DRV liposomes were diluted to 0.25 mM total lipids and extruded liposomes were diluted to 0.5 mM total lipids, then they were applied to the carbon grid. After incubation for 5 min at room temperature, the excess was blotted. One drop of uranyl acetate (1% w/v) in water was added to the carbon grid and incubated for 1 min at room temperature before the excess was blotted and air-dried. A Carl Zeiss CEM 902 microscope was operated at 80 kV. The images were acquired using a CCD camera (Proscan) and the platform acquisition was iTem.

2.2.3. Phase transition

The main melting temperature of each lipid structure were obtained through differential scanning calorimetry (DSC) model Q 2000, coupled with software Thermal Advantage. Analyses were performed according to the AOCS method Cj 1-94 (2009).

Aluminum capsules were used, and an empty capsule containing only air was the reference. Lyophilized samples ranged from 8.5 mg to 9.5 mg were heated at a rate of 10°C/min from -20 to 40 °C. Due to the fast heating temperature (10 °C / min) and the broad peaks, which reduce accuracy, the thermograms and melting temperatures given should only be considered for a comparison amongst the samples.

2.3. Biological evaluation of liposomal structures

2.3.1. Differentiation *in vitro* of dendritic cell derived from monocytes

Peripheral blood mononuclear cells (PBMCs) were collected from healthy unrelated volunteers through apheresis performed in a TRIMA ACCEL (Cobe BCT, Denver, CO, USA),²⁶ at the Hospital Alemão Oswaldo Cruz, São Paulo, Brazil, after informed consent of donors. For enrichment of mononuclear cells, the product of apheresis was submitted to a separation with a density gradient (Ficoll-Paque from GE Healthcare Bio-Sciences AB, Upsala, Sweden) for 30 minutes at 900 G, 18 °C. Mononuclear cells were collected and centrifuged at 290 G for 10 minutes, 18 °C for 3 times with RPMI-1640 medium (GIBCO™, Grand Island, NY, EUA). After this process, the mononuclear cells were seeded in 6-well plate (5×10^6 cells/well) in RPMI 1640 culture medium and incubated at 37°C and 5% CO₂ for 2 hours. After this period, non-adherent cells were removed and the RPMI medium was replaced by a R-10 medium (RPMI 1640 culture medium supplemented with 10% fetal bovine serum) supplemented with 50 ng/mL IL-4 and 50 ng/mL GM-CSF (PeproTech, Rocky Hill, NJ, USA). After 5 days in culture, the cells were stimulated by TNF-alpha (50 ng/mL; PeproTech, Rocky Hill, NJ, USA) as a positive control for DCs maturation/activation (mDC - mature DC) or stimulated by extruded liposomes or DRV liposomes (1 mM) labeled with fluorescent probe (FITC-carboxyfluorescein, Avanti-Lipids, USA) to analyze liposomes' internalization by DCs through flow cytometry. And as a negative control group (iDC – immature DC), no stimulus was added to the medium. After 2 days in culture, cells were harvested and labeled with specific fluorescent antibodies for analysis by flow cytometry (BD FACSCanto™).²⁷

2.3.2. Allogeneic T lymphocyte proliferation assay

T lymphocytes were purified from non-adherent cells removed after 2 hours incubation of mononuclear cells for DCs generation using negative selection with immunomagnetic beads (anti-CD14, CD16, CD19, CD36, CD56, CD123, and Glycophorin A) (Pan T Cell Isolation Kit II, Miltenyi Biotec, Bergisch Gladbach, Germany), following the manufacturer's recommendations. For induction of allogeneic T lymphocyte proliferation, purified T lymphocytes (1×10^5 cells/well) were co-cultured with DCs (1×10^4 cells/well), stimulated by TNF-alpha or by extruded liposomes, in U-bottom 96-well microplates. T Lymphocytes were previously stained with 10 μ M of carboxyfluorescein diacetate succinimidyl ester (CellTrace CFSE Cell Proliferation Kit – Invitrogen Dinal AS, Oslo, Norway) to track cell proliferation. After 5 days in culture, cells were harvested, marked and analyzed in the flow cytometry (BD FACSCalibur™).

2.3.3. Flow cytometry

Dendritic cells preparations (2×10^5 cells/well/condition) were labeled with each of the specific fluorescent antibodies: CD11c, CD86 and HLA-DR (BD Biosciences) for phenotypic analysis and to assess the incorporation of liposomes by DCs. These cells were analyzed in the flow cytometry FACSCanto with Diva software. T lymphocytes co-cultured with DCs were labeled with each of the specific fluorescent antibodies: CD4 and CD8 (BD Biosciences) to assess the proliferation of T lymphocytes subpopulations. Then, the labeled cells were analyzed in FACSCalibur with CellQuest software. At least 10,000 events were acquired per antibody analyzed. The data was analyzed by FlowJo 7.6 software (Tree Star Inc., USA).²⁷

3. Results

3.1. Physico-chemical characterization of cationic liposomes production using thin film method followed by extrusion (ELs) and dehydration-rehydration method (DRVs)

Extruded liposomes (EL) and DRV liposomes (DRV) were compared in terms of mean diameter, size distribution, polydispersity and zeta potential, as shown in Table 3-1.

Table 3-1- Physico-chemical properties of cationic liposomes EL and DRV.

Cationic liposomes	Mean diameter (\pm S.D.) nm and distribution (\pm S.D.) %				Polydispersity		Zeta potential	
	Intensity ⁽ⁱ⁾	P-value ^(iv)	Number ⁽ⁱⁱ⁾	P-value ^(iv)	Pdl ⁽ⁱⁱⁱ⁾	P-value ^(iv)	(\pm S.D.) mV	P-value ^(iv)
EL*(1)	97.36 \pm 4.34 (100 \pm 0)		64.93 \pm 9.56 (100 \pm 0)		0.13 \pm 0.02		32.78 \pm 5.38	
DRV**(2)	583.41 \pm 130.80 (79.40 \pm 7.51)	0.00 (1:2)	107.53 \pm 26.82 (94.7 \pm 2.90)	0.01 (1:2)	0.52 \pm 0.08	0.00 (1:2)	38.52 \pm 2.11	0.06 (1:2)
	116.90 \pm 28.15 (20.60 \pm 7.51)		513.24 \pm 145.66 (5.3 \pm 2.90)					

(i) Intensity-weighted average diameter and distribution (I-distribution).

(ii) Number-weighted average diameter and distribution (N-distribution).

(iii) Pdl - Polydispersity of the sample varies in ascending order from 0 to 1.

(iv) P-value > 0.05 indicates that the values compared are not significantly different. The statistical analysis P-value was performed between extruded liposomes and the most abundant population of DRV liposomes.

Results represent means \pm S.D., n = 5

* EL: liposomes produced by dried film method, followed by hydration with PBS buffer and then by an extrusion step.

**DRV: part of extruded liposomes submitted to a lyophilization, for subsequent controlled rehydration with PBS buffer.

For more accurate size characterization, intensity and number-weighted mean diameters and distributions from a dynamic light scattering technique were considered. Although the whole range of diameters is shown in the intensity-weighted distribution (I-distribution), the proportionality to the sixth power of particle diameter (D) ($I \propto D^6$) underestimates the small particles, which are only very weakly weighted.²⁸ The corresponding number-weighted distribution (N-distribution), converted using the Mie theory, is in equivalent proportion to the first power of diameter ($N \propto D$) and determines the actual number of particles that yield the observed intensity in each size class.²⁹⁻³²

Table 3-1 shows that the extruded liposomes (EL) had a single population of 97.36 nm for an intensity-weighted distribution (I-distribution) and 64.93 nm for a number-weighted distribution (N-distribution). Cationic liposomes which have passed

through the same production process but adding the step of dehydration-rehydration (DRV) showed two populations of 583.41 and 116.90 nm for I-distribution and 107.53 and 513.24 nm for N-distribution, in which the predominant population is 107.53 nm with 94.7% of all particles. Additionally, extruded liposomes and DRV liposomes have their corresponding I-distribution in Figure 3-2 A and N-distribution in Figure 3-2 B, showing clearly that DRV structures present a complex size distribution. The statistical analysis (P-value) indicates that extruded liposomes and the most abundant population of DRV liposomes had a significant variation in size in terms of intensity and number-weighted distribution.

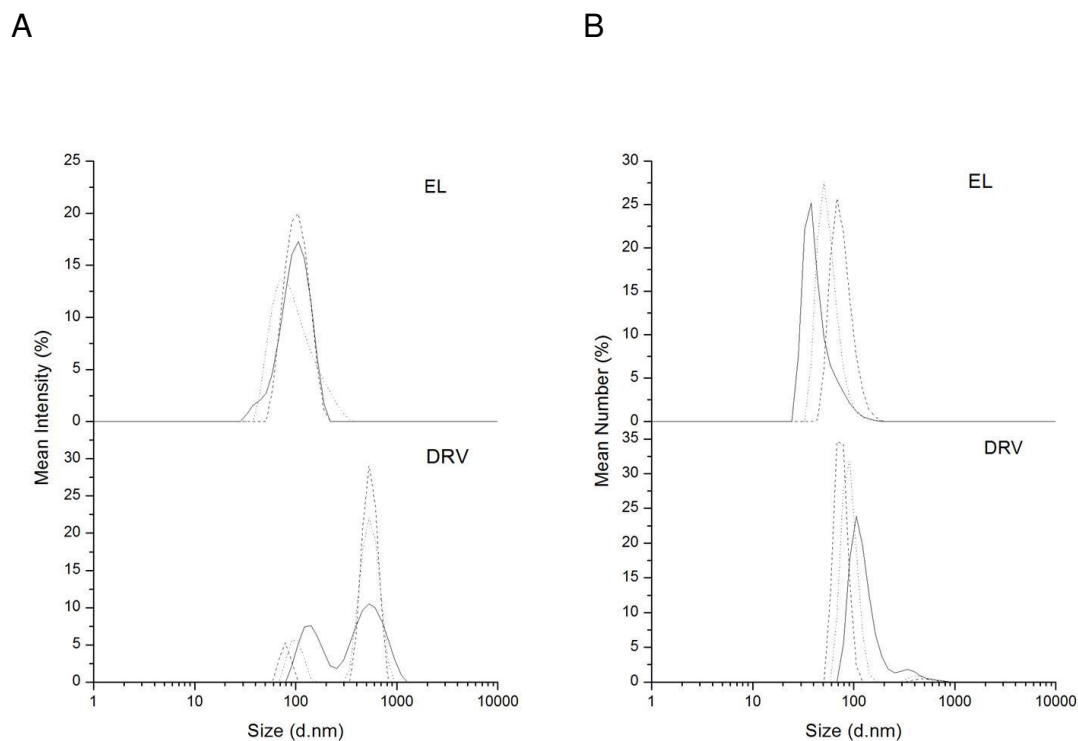


Figure 3-2 - Intensity-weighted distribution (A) and Number-weighted distribution (B) of extruded liposomes and DRV liposomes obtained under different conditions. The dotted, dashed and solid lines in each graph represent one independent size distribution (n=3).

The polydispersity of ELs was 0.13 meanwhile DRV's polydispersity was 0.52, and the statistical analysis (P-value) indicates a significant difference in polydispersity of the two cationic liposomes.

The zeta potential of the liposomes was 32.78 mV for ELs and 38.52 mV for DRVs, showing stable nanostructures, favored by the repulsion due to the predominance of positively charged at their surface. The statistical analysis (P-value) indicates that is no significant difference in zeta potential of the two liposomes.

The liposomes morphology was evaluated using transmission electron microscopy (TEM) and negative staining technique. We evaluated the morphology of EL and DRV liposomes through micrographies presented in Figure 3-3.

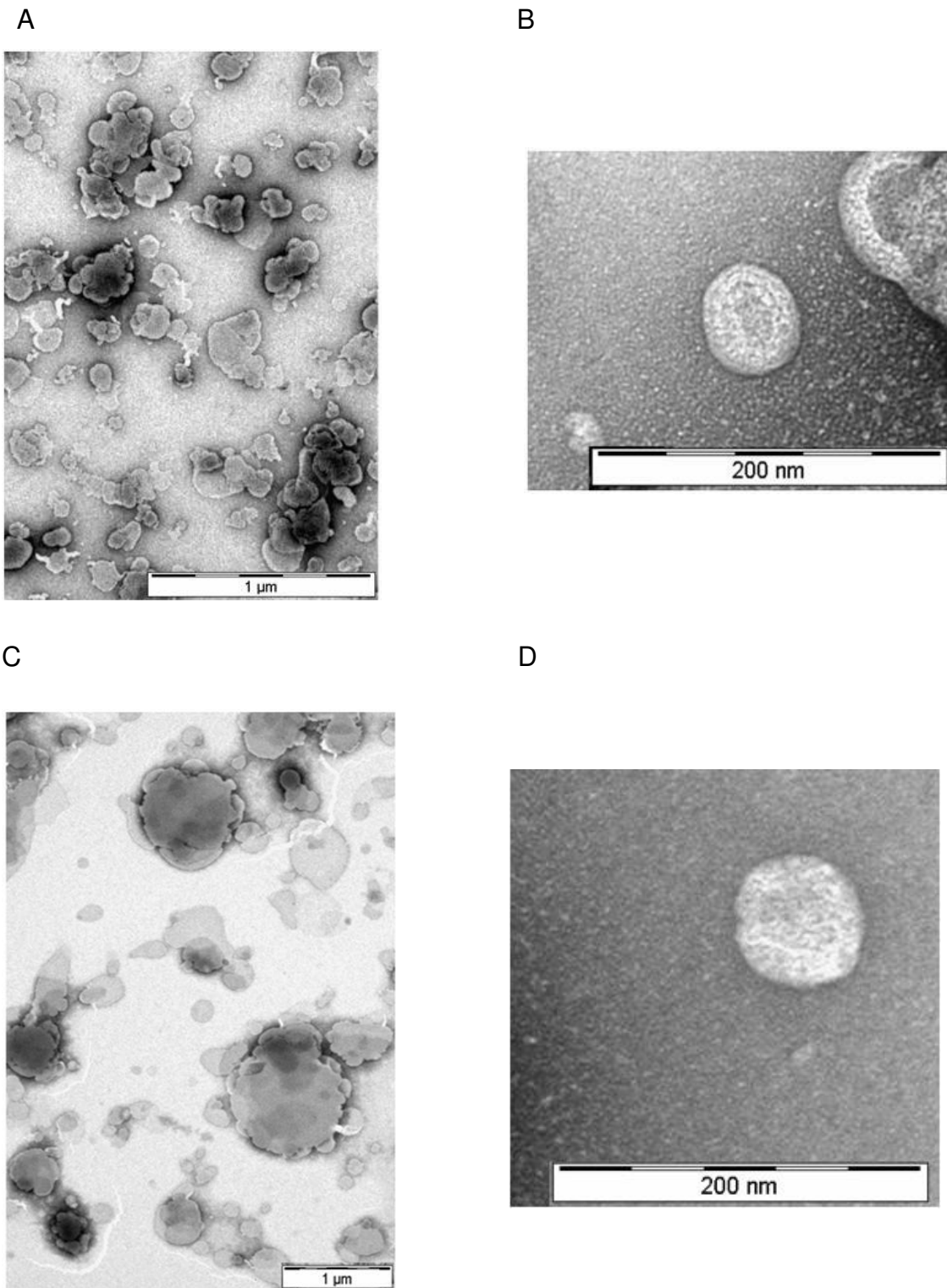


Figure 3-3 – Negative-staining electron micrographs of extruded liposomes (EL) acquired at (A) 1000 nm (B) 200 nm and of DRV liposomes acquired at (C) 1000 nm (D) 200 nm.

Figure 3-3 A e B showed structures approximately spherical and homogeneous, demonstrating low polydispersity in ELs population. Morphology of DRV liposomes also seem to be spherical, but the population is not homogeneous like ELs, demonstrating high polydispersity of DRVs (Figure 3-3 C e D).

The thermal behavior of cationic liposomes was studied by differential scanning calorimetry. The main phase transition (T_m) of EL and DRV were 11.51 °C and 12.48 °C, respectively. The differences in thermograms of ELs at 16 mM and DRVs at 64mM (Figure 3-4) are probably directly related to the total lipid concentration of the process and the different thermal history. The increase in melting temperature for DRV liposomes can be result of an additional processing (dehydration and rehydration) allowing different organization between the lipids.

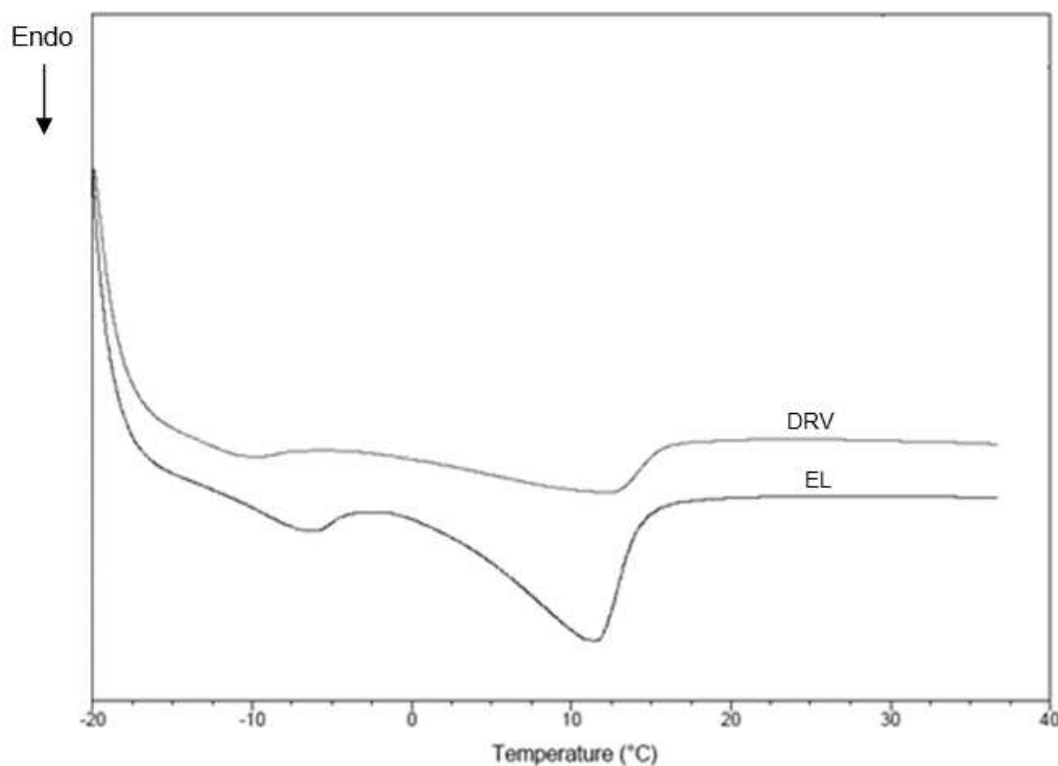


Figure 3-4 – Thermograms of extruded liposomes (EL) at 16 mM and DRV liposomes at 64 mM. Samples were freeze-dried and heated at 10 °C/min. Note: These thermograms and the melting temperatures are for comparison only as the fast heating temperature (10 °C/min) would reduce accuracy.

3.2. Biological evaluation of liposomal structures

3.2.1. *In vitro* evaluation of efficiency and effect of cationic liposomes internalization by dendritic cells

The strategies used for phenotypic analysis of DCs and for analysis of liposomes incorporation are presented in the Supplementary Materials. In order to evaluate the liposomes incorporation by DCs and the DCs activation by liposomes, Table 3-2 present the median of liposomes' probe fluorescence and CD86 fluorescence expressed by dendritic cells stimulated by TNF- α (mDC), or by extruded liposomes or DRV liposomes, and without stimuli (iDC). "Anexo I" presents why we decided to use 0.01% of fluorescent lipid (liposomes' probe) relative to the total lipid concentration.

Table 3-2 – Median of liposomes' probe fluorescence and CD86 fluorescence expressed by dendritic cells stimulated by TNF- α (positive control - mDC), or by extruded liposomes (EL) or DRV liposomes (DRV), and the negative control (iDC).

Population name	Median of liposomes' probe fluorescence (FITC)	Median of CD86 fluorescence (PerCP-Cy5)
iDC	308	2,636
mDC	291	2,613
EL	20,500	4,046
DRV	4,292	2,764

According to the median of liposomes' probe fluorescence (Table 3-2), extruded liposomes and DRV liposomes were incorporated by dendritic cells. However, ELs (20,500) presented more fluorescence intensity than DRVs (4,292), *i.e.* ELs were better incorporated by DCs than DRVs. Investigating the DCs activation, the median of CD86 fluorescence (Table 3-2) shows that both liposomes increased the CD86 expression by DCs, when regarding the median fluorescence of iDC. Also in this case, ELs (4,046) presented more fluorescence intensity than DRVs (2,764), *i.e.* ELs activated better DCs than DRVs. In order to confirm that DCs which internalized liposomes are activated, we presented Dot plot graphics of CD86 versus

liposomes' probe in the Supplementary Materials. Thus, DCs that internalized ELs and DRVs had more co-stimulatory molecules than iDCs.

3.2.2. T lymphocytes proliferation

Aiming to confirm that DCs are able to present antigens to T lymphocytes after internalization of extruded liposomes, allogeneic T lymphocyte were co-cultured with DCs inducing T lymphocytes proliferation. "Anexo II" presents the complementary analyses generate by T lymphocytes proliferation.

Since extruded liposomes demonstrated better incorporation and activation by DCs than DRV liposomes, we analyzed T lymphocytes proliferation only with DCs stimulated by ELs. Therefore, we showed the T lymphocytes proliferation by histograms of CFSE intensity (Figure 3-5) in which the positive control of proliferation assay was compared with the T lymphocytes proliferation co-cultured with DCs stimulated by ELs. The CFSE is a stable cytoplasmic fluorescent dye that is segregated equally between daughter cells after cell division, therefore when T lymphocytes proliferate dilute the amount of CFSE causing a decrease in fluorescence intensity of the dye.

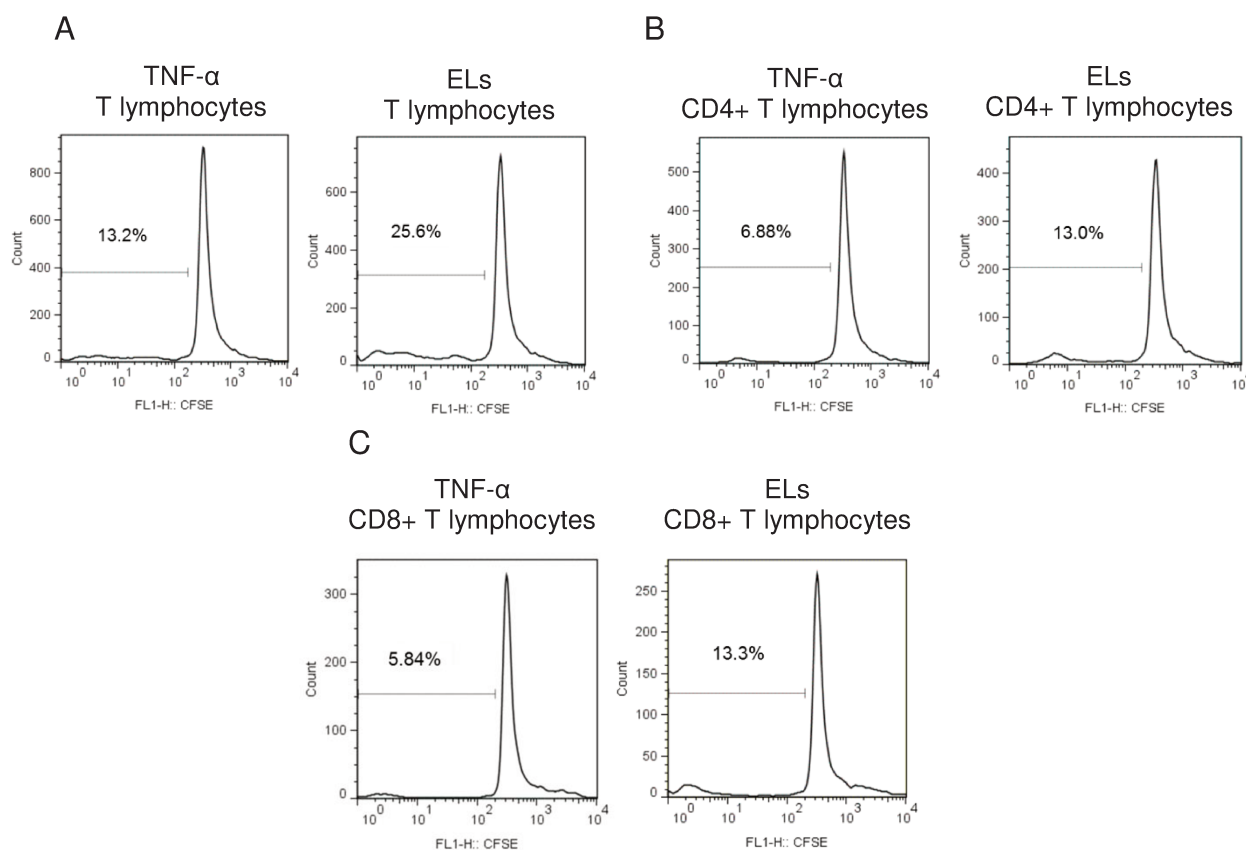


Figure 3-5 - Histograms of CFSE (carboxyfluorescein diacetate succinimidyl ester) dilution representing proliferation of total T lymphocytes (A), CD4⁺ T lymphocytes (B) and CD8⁺ T lymphocytes (C), when co-cultured with allogeneic DCs stimulated by TNF- α (positive control) and when co-cultured with allogeneic DCs stimulated by extruded liposomes (ELs).

Thus, with the aid of histograms of CFSE intensity, we realized that T lymphocytes proliferation were better when T lymphocytes were co-cultured with DCs stimulated by ELs than when stimulated by TNF- α . 13.2% of T Lymphocytes proliferated when TNF- α was involved and 25.6% when ELs was involved (Figure 3-5 A). When considering just CD4⁺ T lymphocytes, 6.88% had CFSE dilution when stimulated with DCs activated with TNF- α compared to 13.0% when stimulated with DCs treated with ELs (Figure 3-5 B). CD8⁺ T lymphocytes proliferation were greater when stimulated with DCs treated with ELs (13.3%) when compared with DCs activated with TNF- α (5.84%) (Figure 3-5 C). Thus, the use of ELs to stimulate DCs increase proliferation of T lymphocytes CD4⁺ and CD8⁺ in approximately 2 times compared with the TNF- α stimulus.

4. **Discussion**

Cationic liposomes EPC/DOTAP/DOPE (50/25/25% molar) prepared by dehydration-rehydration method (DRV), were studied for the first time to entrap pDNA for treatment of hepatitis B.¹⁸ When complexed with DNAhsp65, those liposomes had low cytotoxicity *in vitro*¹⁹ and high efficacy *in vivo* as a genetic vaccine against tuberculosis.^{20, 33} De Paula Rigoletto *et al.*³⁴ found that there was no significant difference in the biological properties if the cationic liposomes were prepared using bulk commercial lipids (96-98% purity) or lipids of analytical grade. In this context, the purpose of this study was to investigate the behavior of cationic liposomes EPC/DOTAP/DOPE (96-98% purity, bulk lipids) extruded (ELs) and DRV *in vitro* upon dendritic cells differentiation/maturation and induction of T lymphocytes proliferation.

The size (number-weighted) of ELs was 64.93 nm, followed dehydration-rehydration step liposomes size increase to 107.53 nm (DRVs) (Table 3-1). Likewise, the polydispersity was lower for ELs (0.13) than the DRVs (0.52) (Table 3-1). The increase in size and polydispersity can probably be result of lipids fusion during dehydration process, since we did not use crioprotector. DRVs and ELs presented statistically different due to their different physico-chemical properties (size and polydispersity). Perrie and Gregoriadis³⁵, Rosada *et al.*²⁰ and de la Torre *et al.*³⁶ also presented dehydrated-rehydrated vesicles with complex size distribution. On the order hand, liposomes that have passed by an extrusion step, whose aims to reduce and homogenize particles size, presented an unimodal distribution. The differences in liposomes size distribution (Figure 3-2) reflect the differences in DCs uptake. It seems that lower average size and polydispersity provide higher uptake by DCs (Table 3-2). Additionally, the higher melting temperature for DRVs (Figure 3-4) indicates higher lipid interactions and probably the difficult for liposome disintegration is higher, leading to a worse DCs activation than ELs (Table 3-2).

We showed that the differences in ELs and DRVs did not produce differences in zeta potential (Table 3-1). Rigoletto and co-workers³⁴ explained that extrusion step, followed by dehydration-rehydration protocol do not produce significant differences in zeta potential, however impurities in bulk lipids decreases zeta potential.

Transmission electron microscopy (Figure 3-3) confirmed the differences in size for ELs and DRVs and showed that extruded and DRV liposomes had a spherical morphology, in the same way as Rosada *et al.*²⁰ and Trevisan *et al.*²⁵ Extruded liposome population is homogeneous; however DRVs presented larger structures that could be generated by aggregation due to the dehydration-rehydration process.²⁰

T_m of DRV liposomes EPC/DOTAP/DOPE with analytical grade lipids were previously published in de la Torre *et al.*¹⁹ EL and DRV differences in the thermograms (Figure 3-4) could be mainly related to differences in crystallinity of liposomes, imparted by the differences in concentrations (16 or 64 mM), since the rehydration process was carried out at higher lipid concentration than ELs.³⁴ Previous studies demonstrated that more amorphous liposome structures were obtained at lower lipid concentration.³⁷

Among the physico-chemical and morphological differences between EL and DRV liposomes, the liposome performance in biological applications, more specifically, in DCs was different. Data presented in Table 3-2 estimated liposomes incorporation by measuring liposomes' probe fluorescence in DCs, deducing that ELs were better incorporated by DCs than DRVs, because ELs showed higher median of lipid fluorescence intensity. This behavior can be explained by analyzing physico-chemical properties of liposomes, more specifically their size and polydispersity, which demonstrated that DRVs were bigger and less homogeneous than ELs. *In vitro* and *in vivo* studies performed by Allen *et al.*³⁸, Papahadjopoulos *et al.*³⁹ and Rejman *et al.*⁴⁰ showed that generally small nanoparticles (range of 100-200 nm) are required in biological applications to facilitate their internalization by cells. Additionally, Kristl *et al.*⁴¹, Licciardi *et al.*⁴² and Muthu *et al.*⁴³ observed that nanoparticles with polydispersity values below 0.2, which evidences a homogenous size distribution, can support *in vitro* internalization by mammalian cells, supposing that cells expend less energy in the capture.

The second aspect of biological application analyzed was the dendritic cells activation by liposomes, showed in Table 3-2 through the median of CD86 fluorescence. ELs, in addition to be more internalized by DCs than DRV liposomes, they up-regulate DC maturation mark CD86, indicating that DCs may enhance the ability to activate T lymphocytes. Cationic liposomes composed by DOPC (1,2-dioleoyl-*sn*-glycero-3-phosphocholine) a neutral lipid and DOTAP (cationic lipid) in various proportions showed that liposomes with a high charge density potently enhanced dendritic cell maturation and antigen uptake. On the other hand, low-charge liposomes failed to activate DCs when internalized even at high concentrations, confirming that the effect of cationic liposomes upon dendritic cells is mostly attributable to their surface charge density.⁴⁴ Our research group²² corroborate the findings, complexing cationic liposomes EPC/DOTAP/DOPE with pDNA in various proportions, showing important differences to transfect HeLa cells *in vitro* when the molar charge ratio was varied. In this work we studied DCs stimulation by empty cationic liposomes, however in future studies we should be attentive with the charge relationship between cationic liposome and nucleic acid so that remains activating DCs and being incorporated by them.

The last but not least aspect of biological application analyzed was T lymphocytes proliferation induced by DCs with ELs incorporated, which was showed in histograms of CFSE intensity (Figure 3-5). The increase in proliferation of T Lymphocytes when co-cultured with DCs stimulated by extruded liposomes is evident (Figure 3-5 A). Moreover, DCs stimulated by extruded liposomes increased CD8+ T Lymphocytes proliferation (Figure 3-5 C), which is the main required in controlling tumor growth.² Hence, ELs are able to activate DCs and these cells were able to induce higher T lymphocytes proliferation *in vitro*, indicating that ELs have a promising future in therapeutic dendritic cell vaccines for cancer patients. A similar study made by Wang and co-workers⁴⁵ incorporated PIC (polyribocytidylic acid, a promising immunopotency for cancer vaccines) into cationic liposome composed by DOTAP, and the results showed that liposome complex was more potent than DOTAP or PIC alone to enhance vaccine-induced tumor-specific cytotoxic T

lymphocyte response and suppressed tumor growth in mice. The researcher group deduced that the superior antitumor effect of liposome complex vaccines could be attributable to enhanced maturation bone-marrow dendritic cells of mouse. Likewise, we can predict a promising future for extruded liposomes EPC/DOTAP/DOPE (50/25/25% molar) in immunotherapy against cancer.

In sum, extruded liposomes are more suitable than DRV liposomes to be used in dendritic cell vaccine aiming immunotherapy against cancer. The physico-chemical properties of extruded and DRV liposomes, more specifically their size and polydispersity, interfere in their incorporation by dendritic cells. We could speculate that size and polydispersity are inversely proportional to internalization by dendritic cells. Therefore, extruded liposomes presented a better incorporation by DCs than DRVs. In addition to incorporation, the extruded liposomes stimulated dendritic cells to increase the CD86 express and dendritic cells that internalized these liposomes induced T lymphocytes proliferation. Then, cationic liposomes EPC/DOTAP/DOPE (50/25/25% molar) composed by bulk commercial lipids are incorporated and able to activate dendritic cells, thus becoming a useful tool to the immunotherapy against cancer based on DCs.

5. **Acknowledgements**

We thanks to Dr. Barbuto's Lab staff to technical support. This work was financial support by Fundação de Amparo à Pesquisa do Estado de São Paulo (FAPESP).

6. **References**

1. Steinman RM. Dendritic cells: Understanding immunogenicity. *Eur J Immunol* 2007;37:S53-S60.
2. Banchereau J, Steinman RM. Dendritic cells and the control of immunity. *Nature* 1998;392:245-52.
3. Baleeiro RB, Anselmo LB, Soares FA, Pinto CAL, Ramos O, Gross JL, *et al.* High frequency of immature dendritic cells and altered in situ production of interleukin-4 and tumor necrosis factor- α in lung cancer. *Cancer Immunol Immunother* 2008;57:1335-45.
4. Vitor MT, Bergami-Santos PC, Barbuto JA, De La Torre LG. Cationic liposomes as non-viral vector for RNA delivery in cancer immunotherapy. *Recent Pat Drug Deliv Formul* 2012 (*in press*).
5. Sallusto F, Lanzavecchia A. Efficient presentation of soluble antigen by cultured

- human dendritic cells is maintained by granulocyte/macrophage colony-stimulating factor plus interleukin 4 and downregulated by tumor necrosis factor alpha. *J Exp Med* 1994;179:1109-18.
6. Gilboa E, Vieweg J. Cancer immunotherapy with mRNA-transfected dendritic cells. *Immunol Rev* 2004;199:251-63.
 7. Rubiolo C, Dendritic Cells. United States Patent US20110097346(2011).
 8. Sullenger BA, Gilboa E. Emerging clinical applications of RNA. *Nature* 2002;418:252-8.
 9. Prasad S, Cody V, Saucier-Sawyer JK, Saltzman WM, Sasaki CT, Edelson RL, *et al.* Polymer nanoparticles containing tumor lysates as antigen delivery vehicles for dendritic cell-based antitumor immunotherapy. *Nanomed Nanotechnol Biol Med* 2011;7:1-10.
 10. Serikawa T, Kikuchi A, Sugaya S, Suzuki N, Kikuchi H, Tanaka K. In vitro and in vivo evaluation of novel cationic liposomes utilized for cancer gene therapy. *J Control Release* 2006;113:255-60.
 11. Vangasseri DP, Cui Z, Chen W, Hokey DA, Falo LD, Huang L. Immunostimulation of dendritic cells by cationic liposomes. *Mol Membr Biol* 2006;23:385-95.
 12. Nakanishi T, Kunisawa J, Hayashi A, Tsutsumi Y, Kubo K, Nakagawa S, *et al.* Positively charged liposome functions as an efficient immunoadjuvant in inducing immune responses to soluble proteins. *Biochem Biophys Res Commun* 1997;240:793-7.
 13. Nakanishi T, Kunisawa J, Hayashi A, Tsutsumi Y, Kubo K, Nakagawa S, *et al.* Positively charged liposome functions as an efficient immunoadjuvant in inducing cell-mediated immune response to soluble proteins. *J Controlled Release* 1999;61:233-40.
 14. Grunebach F, Muller MR, Nencioni A, Brossart P. Delivery of tumor-derived RNA for the induction of cytotoxic T-lymphocytes. *Gene Ther* 2003;10:367-74.
 15. Bringmann A, Held SAE, Heine A, Brossart P. RNA vaccines in cancer treatment. *J Biomed Biotechnol* 2010;2010:1-12.
 16. Lincopan N, Borelli P, Fock R, Mamizuka EM, Carmona-Ribeiro AM. Toxicity of an effective amphotericin B formulation at high cationic lipid to drug molar ratio. *Exp Toxicol Pathol* 2006;58:175-83.
 17. Lin YL, Liu YK, Tsai NM, Hsieh JH, Chen CH, Lin CM, *et al.* A Lipo-PEG-PEI complex for encapsulating curcumin that enhances its antitumor effects on curcumin-sensitive and curcumin-resistance cells. *Nanomedicine-Nanotechnology Biology and Medicine* 2012;8:318-27.
 18. Perrie Y, Frederik PM, Gregoriadis G. Liposome-mediated DNA vaccination: the effect of vesicle composition. *Vaccine* 2001;19:3301-10.
 19. De La Torre LG, Rosada RS, Trombone APF, Frantz FG, Coelho-Castelo AAM, Silva CL, *et al.* The synergy between structural stability and DNA-binding controls the antibody production in EPC/DOTAP/DOPE liposomes and DOTAP/DOPE lipoplexes. *Colloids Surf B Biointerfaces* 2009;73:175-84.
 20. Rosada RS, De La Torre LG, Frantz FG, Trombone AP, Zarate-Blades CR, Fonseca DM, *et al.* Protection against tuberculosis by a single intranasal administration of DNA-hsp65 vaccine complexed with cationic liposomes. *BMC Immunol* 2008;9:38.
 21. Rosada RS, Silva CL, Santana MH, Nakaie CR, De La Torre LG. Effectiveness, against tuberculosis, of pseudo-ternary complexes: peptide-DNA-cationic liposome. *J Colloid Interface Sci* 2012;373:102-9.
 22. Balbino TA, Gasperini AAM, Oliveira CLP, Azzoni AR, Cavalcanti LP, De La Torre LG. Correlation of the Physicochemical and Structural Properties of pDNA/Cationic Liposome Complexes with Their in Vitro Transfection. *Langmuir* 2012;28:11535-45.

- 23 . Bangham AD, Standish MM, Watkins JC. Diffusion of univalent ions across lamellae of swollen phospholipids. *Journal of Molecular Biology* 1965;13:238-&.
- 24 . Kirby C, Gregoriadis G. Dehydration-rehydration vesicles - a simple method for high-yield drug entrapment in liposomes. *Bio-Technology* 1984;2:979-84.
- 25 . Trevisan JE, Cavalcanti LP, Oliveira CLP, De La Torre LG, Santana MHA. Technological aspects of scalable processes for the production of functional liposomes for gene therapy: In: Yuan X-b, editors. *Non-Viral Gene Therapy*. ed.: InTech; 2011, p. 267-92.
- 26 . Neron S, Correa JA, Dajczman E, Kasymjanova G, Kreisman H, Small D. Screening for depressive symptoms in patients with unresectable lung cancer. *Support Care Cancer* 2007;15:1207-12.
- 27 . Barbuto JA, Ensina LF, Neves AR, Bergami-Santos P, Leite KR, Marques R, et al. Dendritic cell-tumor cell hybrid vaccination for metastatic cancer. *Cancer immunology, immunotherapy : CII* 2004;53:1111-8.
- 28 . Egelhaaf SU, Wehrli E, Müller M, Adrian M, Schurtenberger P. Determination of the size distribution of lecithin liposomes: a comparative study using freeze fracture, cryoelectron microscopy and dynamic light scattering. *J Microsc* 1996;184:214-28.
- 29 . Bott S. Particle Size Distribution Assessment and Characterization: In: editors. ed. Washington DC: American Chemical Society; 1987.
- 30 . Hulst HC. Light Scattering by Small Particles: In: editors. ed. New York: Wiley; 1957.
- 31 . Kerker M. The Scattering of Light and Other Electromagnetic Radiation: In: editors. ed. New York: Academic Press; 1969.
- 32 . Meeren PPAV, Vanderdeelen J, Baert L. Particle Size Analysis: In: editors. ed. New York: John Wiley & Sons; 1988.
- 33 . Rosada RS, Silva CL, Andrade Santana MH, Nakaie CR, de la Torre LG. Effectiveness, against tuberculosis, of pseudo-ternary complexes: Peptide-DNA-cationic liposome. *Journal of Colloid and Interface Science* 2012;373:102-09.
- 34 . Rigoletto TP, Silva CL, Santana MH, Rosada RS, De La Torre LG. Effects of extrusion, lipid concentration and purity on physico-chemical and biological properties of cationic liposomes for gene vaccine applications. *J Microencapsul* 2012;29:759-69.
- 35 . Perrie Y, Gregoriadis G. Liposome-entrapped plasmid DNA: characterisation studies. *Biochim Biophys Acta* 2000;1475:125-32.
- 36 . de la Torre LG, Rosada RS, Favaro Trombone AP, Frantz FG, Coelho-Castelo AAM, Silva CL, et al. The synergy between structural stability and DNA-binding controls the antibody production in EPC/DOTAP/DOPE liposomes and DOTAP/DOPE lipoplexes. *Colloids and Surfaces B-Biointerfaces* 2009;73:175-84.
- 37 . Alves GP, Santana MHA. Phospholipid dry powders produced by spray drying processing: structural, thermodynamic and physical properties. *Powder Technol* 2004;145:139-48.
- 38 . Allen TM, Austin GA, Chonn A, Lin L, Lee KC. Uptake of liposomes by cultured mouse bone marrow macrophages: influence of liposome composition and size. *Biochim Biophys Acta* 1991;1061:56-64.
- 39 . Papahadjopoulos D, Allen TM, Gabizon A, Mayhew E, Matthey K, Huang SK, et al. Sterically stabilized liposomes: improvements in pharmacokinetics and antitumor therapeutic efficacy. *Proc Natl Acad Sci U S A* 1991;88:11460-4.
- 40 . Rejman J, Oberle V, Zuhorn IS, Hoekstra D. Size-dependent internalization of particles via the pathways of clathrin- and caveolae-mediated endocytosis. *Biochem J* 2004;377:159-69.

-
- 41 . Kristl J, Teskac K, Caddeo C, Abramovic Z, Sentjurc M. Improvements of cellular stress response on resveratrol in liposomes. *Eur J Pharm Biopharm* 2009;73:253-9.
- 42 . Licciardi M, Paolino D, Celia C, Giammona G, Cavallaro G, Fresta M. Folate-targeted supramolecular vesicular aggregates based on polyaspartyl-hydrazide copolymers for the selective delivery of antitumoral drugs. *Biomaterials* 2010;31:7340-54.
- 43 . Muthu MS, Kulkarni SA, Raju A, Feng SS. Theranostic liposomes of TPGS coating for targeted co-delivery of docetaxel and quantum dots. *Biomaterials* 2012;33:3494-501.
- 44 . Ma Y, Zhuang Y, Xie X, Wang C, Wang F, Zhou D, *et al.* The role of surface charge density in cationic liposome-promoted dendritic cell maturation and vaccine-induced immune responses. *Nanoscale* 2011;3:2307-14.
- 45 . Wang C, Zhuang Y, Zhang Y, Luo Z, Gao N, Li P, *et al.* Toll-like receptor 3 agonist complexed with cationic liposome augments vaccine-elicited antitumor immunity by enhancing TLR3-IRF3 signaling and type I interferons in dendritic cells. *Vaccine* 2012;30:4790-9.

7. Supplementary materials

7.1. Strategy of dendritic cells analysis

For phenotypic characterization and evaluation of liposomes incorporation, we delimited gate with cell size and granularity compatible with the DCs, by analysis "side scatter" (SSC) - granularity (internal structure and complexity) and the "forward scatter" (FSC) - relative size of the cells (Figure 3-6 A). Considering the analyzed region bounded by the gate, cells were analyzed through the expression of myeloid cells and antigen presenting cells markers, respectively CD11c and HLA-DR. Furthermore, when we analyzed the expression of co-stimulatory molecules within this population HLA-DR⁺CD11c⁺, called Gate R1 (Figure 3-6 B), we observed that cells also showed expression of CD86 (described below). This procedure was performed for all samples presenting dendritic cells marked, such as dendritic cells stimulated by TNF- α (positive control - mDC), or by extruded liposomes (EL) or DRV liposomes (DRV).

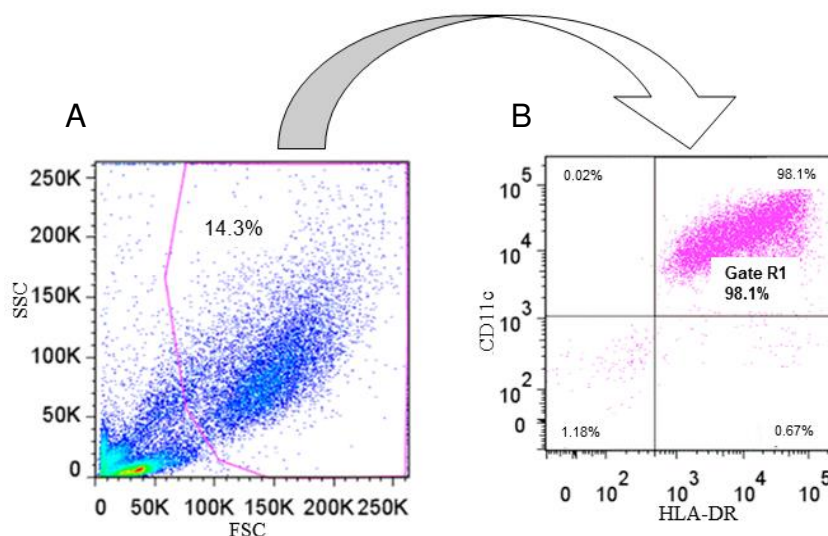


Figure 3-6 – Strategy of dendritic cells analysis. (A) Dot Plot graph of SSC (side scatter) by FSC (forward scatter) to delimit DCs gate. (B) Graph of CD11c versus HLA-DR to delimit Gate R1, corresponding to cells double-positive.

7.2. Dendritic cells activation by liposomes

In order to evaluate the dendritic cells activation by liposomes, it was plotted graphics of CD86 versus liposomes' probe (Figure 3-7) of dendritic cells stimulated by TNF- α (positive control - mDC), or by EL or DRV liposomes. They showed that 73.20% of DCs had internalized ELs and presented CD86, while 43.00% of DCs had internalized DRV liposomes and presented CD86.

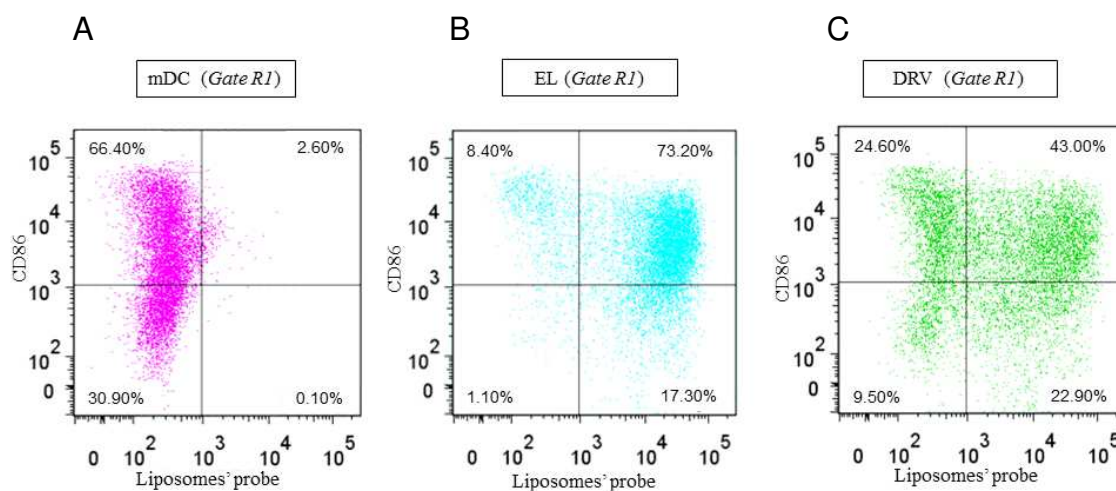


Figure 3-7 - Graphics CD86 versus liposomes' probe of dendritic cells (A) stimulated by TNF- α (positive control - mDC), or by (B) extruded liposomes (EL) or (C) DRV liposomes (DRV).

Capítulo 4 - Cationic Liposomes Produced *via* the Ethanol Injection Method Internalized by Dendritic Cells

Micaela Tamara Vitor

School of Chemical Engineering, Department of Materials and Bioprocess Engineering, University of Campinas (Unicamp), Av. Albert Einstein, 500, Campinas, SP, 13083-852, Brazil.

E-mail address: micaelatamaravitor@gmail.com

Patrícia Cruz Bergami-Santos

Institute of Biomedical Sciences, Department of Immunology, University of São Paulo (USP), Av. Prof. Lineu Prestes, 1730, São Paulo, SP, 05508-000, Brazil.

E-mail address: patriciabergami@yahoo.com.br

José Alexandre Marzagão Barbuto

Institute of Biomedical Sciences, Department of Immunology, University of São Paulo (USP), Av. Prof. Lineu Prestes, 1730, São Paulo, SP, 05508-000, Brazil.

E-mail address: jbarbuto@icb.usp.br

Rafael Henrique Freitas Zômpero

School of Chemical Engineering, Department of Materials and Bioprocess Engineering, University of Campinas (Unicamp), Av. Albert Einstein, 500, Campinas, SP, 13083-852, Brazil.

E-mail address: rzompero@gmail.com

Karen Steponavicius Piedade Cruz

Institute of Biomedical Sciences, Department of Immunology, University of São Paulo (USP), Av. Prof. Lineu Prestes, 1730, São Paulo, SP, 05508-000, Brazil.

E-mail address: kstepon@hotmail.com

Mariana Pereira Pinho

Institute of Biomedical Sciences, Department of Immunology, University of São Paulo (USP), Av. Prof. Lineu Prestes, 1730, São Paulo, SP, 05508-000, Brazil.

E-mail address: marianappinho@gmail.com

Lucimara Gaziola De La Torre*

*Corresponding author:

School of Chemical Engineering, Department of Materials and Bioprocess Engineering, University of Campinas (Unicamp), Av. Albert Einstein, 500, Campinas, SP, 13083-852, Brazil.

E-mail address: latorre@feq.unicamp.br

Telephone number: + 55 19 3521-0397

Fax number: + 55 19 3521-3910

To be submitted to *Journal of Colloid and Interface Science*

Abstract

Cationic liposomes are gene delivery systems that, when obtained at the laboratory scale, have controlled size and polydispersity, characteristics required for internalization by dendritic cells (DCs, antigen-presenting cells). However, the control of liposomes' characteristics in industrial processes remains a challenge. The aim of this study was to investigate the development of a scalable process for the production

of liposomes with physico-chemical properties similar to those produced using a conventional method based on the hydration of a dried film followed by extrusion. Toward this end, cationic liposomes composed of egg phosphatidylcholine (EPC), 1,2-dioleoyl-3-trimethylammonium propane (DOTAP) and 1,2-dioleoylphosphatidylethanolamine (DOPE) were produced via the ethanol injection method, which involves dispersion in an Ultra-Turrax (ST-liposomes) or dispersion in an Ultra-Turrax followed by microfluidization (SM-liposomes). The method was optimized via experimental design, through which the ST-liposomes size was decreased from 290 nm to 110 nm, and the polydispersity was decreased from 0.54 to 0.17; the SM-liposomes size was decreased from 128 nm to 107 nm, and the polydispersity was decreased from 0.40 to 0.18. Then, we demonstrate the ability of these cationic liposomes obtained using a scalable technique optimized, to be internalized and to activate DCs *in vitro* and to induce T lymphocytes proliferation.

Keywords: ethanol injection method, cationic liposomes, microfluidization, experimental design, dendritic cells.

1. Introduction

The human genome sequencing project and the elucidation of genetic codes of microorganisms has allowed the medical community to understand the genetic basis of diseases and has consequently resulted in the development of gene therapy [1, 2]. In brief, the concept of gene therapy is to introduce a piece of genetic material into target cells to cure a disease or slowdown the disease's progression [3]. The delivery of a therapeutic gene or nucleic acid to the site of disease is accomplished by viral or non-viral vectors [4]. Viral vectors can be immunogenic, cytopathic or recombinogenic [5]. Among non-viral vectors, cationic liposomes show particular promise for the delivery of therapeutic nucleic acid to patients [6].

Liposomes are colloidal structures that are biodegradable, nontoxic and typically of spherical shape. These structures are produced from the self-assembly of phospholipids to form bilayer structures (similar to biological membranes) that

aggregate in vesicles in the presence of excess water [7-9]. Cationic liposomes are able to complex electrostatically with nucleic acid and efficiently delivery it into cells.

Cationic liposomes, which are typically composed of the cationic lipids DOTMA (*N*-[1-(2,3-dioleoyloxy)propyl]-*N,N,N*-trimethylammonium chloride), DOPE (1,2-dioleoylphosphatidylethanolamine) and DOTAP (1,2-dioleoyl-3-trimethylammonium propane) in different proportions and mixed with other lipids to reduce cytotoxicity, have been produced and used for the delivery of nucleic acid into cells in culture, in animals and in patients enrolled in phase I and phase II clinical trials [10]. Compared to viral vectors, cationic liposomes are superior in terms of reproducibility, simplicity and safety of use [11]. The major limitation of cationic liposomes in culture cells and in animals was the degree of toxicity [12].

Commercial liposomes used as non-viral vectors in gene therapy include Lipofectamine® [13][14]; DOTAP/Boehringer Mannheim [15]; Lipofectin® [16][17]; FuGENE® HD [18]; Transfast™ [19]; ProFection® [20]; CLONfectin™ [21]; and LipofectAce™ [22]. The cationic liposome that contains the lipids EPC (egg phosphatidylcholine), DOTAP and DOPE was first studied by Perrie, *et al.* [23], and the potentiality of this composition was demonstrated as non-viral system for DNA delivery against Hepatitis B. Later, our research group [24, 25] presented these cationic liposomes as a new prospective agent for use in vaccine gene delivery against tuberculosis. In addition, this vaccine showed low cytotoxicity *in vitro* on the mice J774 macrophage cell line and the potential to be utilised in gene vaccination by the intranasal route [26]. More recently, these cationic liposomes complexed with pDNA in various proportions have been investigated for their ability to transfect HeLa cells *in vitro* and showed important differences when the molar charge ratio was varied [27].

Despite the potential of cationic liposomes EPC/DOTAP/DOPE, the search for a scalable process to produce them is still a challenge. Many methods are available for liposomes production, but most of them tend to be variable or unsuitable for large

scale production, representing the major obstacle in commercialization of liposomes [28]. In addition, the technological processes must be scalable and it must guarantee the reproducibility of the formulation when more liposomes have to be produced for pre-clinical and clinical assays before industrial production [29]. Therefore, researchers have increased the interest in developing industrial scale processes for liposomal production, which reproduce the physico-chemical and biological properties of the previously prepared liposomes on a laboratory scale [29]. Scalable processes for liposomal production include ether/ethanol injection [30, 31], multitubular systems [32, 33], spray-drying processing [34], microfluidic systems [35-37] and high-pressure homogenisation–extrusion (HPHE), which can be used for downsizing large lipid vesicles and covers a full range of processing capacities from laboratory to large-scale continuous production [38].

In this context, our research group [29], aiming to produce gene vaccine composed of EPC/DOTAP/DOPE liposomes complexed with DNA in commercial scale, used the ethanol injection method to obtain the nanoparticles achieving promising results. Conventional ethanol injection consists on the controlled addition of an ethanol/lipid solution to a batch reactor that contains a buffer or water under controlled stirring [29]. The advantages of this method are its simplicity and the use of ethanol, which is less harmful compared to other organic solvents (e.g., chloroform and methanol) [30]. Moreover, according to Kremer and co-workers [39], depending on the lipid concentration and injection flow, post-treatment size reduction may not be necessary. The disadvantages are the low lipid concentration in ethanol (i.e., the size of the liposomes increase with the lipid concentration, which requires post-treatment for size reduction), the difficulty in achieving reproducibility and the necessity to remove the ethanol in an additional step [30, 37]. To minimise these disadvantages, the ethanol injection method can be modified using a high lipid concentration in the alcohol phase, which consequently minimises the concentration of ethanol in the liposome formulation and increases the final lipid concentration to 50 mM [29]. However, depending on application, liposomes with a low final lipid concentration can

be used, and these liposomes undeniably contain a small amount of residual ethanol; thus, such liposomes do not require modification in the ethanol injection method. Maitani, *et al.* [40] compared cationic liposomes composed of 3β -[N-(N',N'-dimethylaminoethane)-carbonyl] cholesterol and DOPE prepared via a dry film method and via a modified ethanol injection method. They reported a greater DNA transfection in HeLa cells when the modified ethanol injection method was used to prepare liposomes than the dry film method [40].

De Haes, *et al.* [41] transfected mRNA encoding HIV Gag protein in dendritic cells (DCs), professional antigen-presenting cells, using Lipofectamine as nanovector. The results showed that DCs stimulated HIV-specific T lymphocytes responses and that mRNA lipoplex internalization by DC proceeded preferentially by macropinocytosis and/or phagocytosis [41]. Cationic liposomes can be also used to transfect mRNA-encoding (tumor) antigens in dendritic cells focusing on immunotherapy strategies against cancer [42]. DCs have an important role as initiators of the immune response and as inducers of central and peripheral tolerance. So, besides being used in therapies against HIV and cancer, dendritic cells loaded with nucleic acids carried by liposomes, may be also used against other diseases such as influenza [43], prolong allograft survival or inhibit autoimmune diseases [44], etc. However, generally, liposomes, to be internalized by cells, require special physico-chemical properties, like small size [45-47] and polydispersity [48-50], which are more common in liposomes produced via laboratory methods.

Thus, our aim in this study is to investigate process parameters that influence both the ethanol injection method and the subsequent high-pressure microfluidization method with respect to the production of EPC/DOTAP/DOPE liposomes. Then, we demonstrated, through biological assays *in vitro*, the viability of the ethanol injection method to produce liposomes with physico-chemical properties that allow their use as nonviral vector to transfect cells, like DCs. Thereby, our results contribute to the development of scalable methods to produce non-viral vectors for nucleic acid delivery.

2. Materials and methods

2.1. Materials

Egg phosphatidylcholine (EPC) (96% of purity), 1,2-dioleoyl-sn-glycero-3-phosphoethanolamine (DOPE) (99.8% of purity) and 1,2-dioleoyl-3-trimethylammonium-propane (DOTAP) (98% of purity) were purchased from Lipid Germany and used without further purification, for liposomes production. The fluorescent probe 1,2-dioleoyl-sn-glycero-3-phosphoethanolamine-N-(carboxyfluorescein) (FITC) (Avanti® Polar Lipids, Inc.) was used in cationic liposomes composition to visualize DCs that incorporated the liposomes, in flow cytometry. The fluorescent antibodies specific to CD11c, CD86, HLA-DR, CD4 and CD8 from BD Biosciences were used in phenotypic analysis of DCs and analysis of subpopulations of T lymphocytes, in flow cytometry.

2.2. Liposomes preparation using ethanol injection method, followed by high-pressure microfluidization

The liposomes were prepared using a scalable ethanol injection method (ST-liposomes) and followed by high-pressure microfluidization (SM-liposomes) (Figure 4-1). Briefly, the ethanol/lipid suspension composed of a mixture of the lipids EPC/DOPE/DOTAP (50/25/25% molar) with ethanol in a glass syringe (1) was fed at a previously defined injection flow through a syringe pump (2) into the bottom of a 150 mL reactor with four baffles and that contained PBS buffer (3). A continuous mechanical stirring rate was provided by an Ultra-Turrax® (4). The final lipid concentration varied from 2 mM to 16 mM. After the feeding was complete, stirring was maintained for an additional 15 min, and the sample subsequently stored in a refrigerator at 8 °C. The colloidal dispersion was dispersed by being stirred in the Ultra-Turrax® at a stirring rate of 6,000 to 24,000 rpm; the injection flow was 20.1 to 57.6 mL/min [29].

The cationic liposomes obtained via the ethanol injection method (ST-liposomes) were stored at 8 °C for at least 2 hours. Then, the size reduction and homogenisation of the liposomes were performed in a Microfluidics® M-110P (Newton, Massachusetts, USA) high-pressure homogeniser at 850 bar; the cycles passage ranged from 1 to 10 (SM-liposomes) [29].

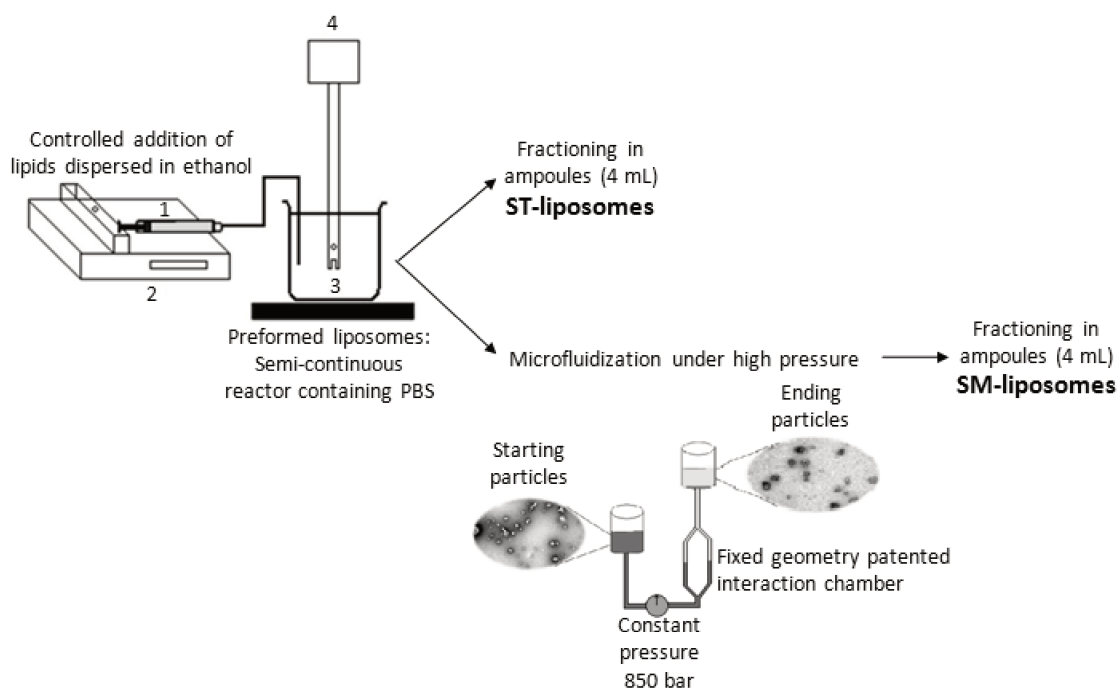


Figure 4-1 – Schematic process diagram of the investigated scalable processes for cationic liposome production. Note: the experimental setup used for liposome preparation using Ultra-Turrax®: 1) Glass syringe (Tomopal - Japan) with a 20 ml capacity containing the lipid dispersion in ethanol; 2) the syringe pump (KDScientific, model KDS-200 - Holliston, Massachusetts, USA) with a capacity for two syringes; 3) the reactor with four fins containing 150 mL of PBS buffer; 4) the Ultra-Turrax® Homogenizer (Ika Works, model IKA T25 digital – Staufen, Germany) with a S25N-10G small impeller (Wilmington, North Carolina, USA). Adapted from Trevisan, Cavalcanti, Oliveira, De La Torre and Santana [29].

2.3. Experimental design

A central composite design (CCD) was used for process optimization to decrease the polydispersity and size of liposomes. The investigated parameters were the final lipid concentration of the liposomal dispersions, the stirring rate and the

injection flow of lipid/ethanol dispersion in the reactor. We designed a full CCD design for 3 factors that consisted of 14 combinations plus the replicates at centre points (8 factorial points, 6 star points and 3 replicates at the centre point) using the software STATISTICA 8.0 for Windows (StatSoft - Tulsa, Oklahoma, USA). The coded levels and real values for the studied factors are shown in Table 4-1.

Table 4-1– CCD matrix with the coded and real values for the factors (stirring rate, final lipid concentration, and injection flow) tested and the responses (particle size and polydispersity (Pdl)) obtained from the experimental design for liposome production using the ethanol injection method.

Factors	-1.68	-1	0	1	1.68
1: Stirring rate (rpm*1000)	6.0	9.6	15.0	20.4	24.0
2: Final lipid concentration (mM)	2.0	4.8	9.0	13.2	16.0
3: Injection flow (mL/min)	20.1	27.7	38.8	50.0	57.6
Factor Experiment	Factor			Response	
	1	2	3	Particle size* (nm)	Pdl
1	-1	-1	-1	489.90	0.42
2	1	-1	-1	336.40	0.54
3	-1	1	-1	1413.33	0.96
4	1	1	-1	593.67	0.66
5	-1	-1	1	160.70	0.19
6	1	-1	1	296.83	0.43
7	-1	1	1	391.80	0.55
8	1	1	1	236.00	0.30
9	-1.68	0	0	372.70	0.52
10	1.68	0	0	188.30	0.23
11	0	-1.68	0	114.35	0.23
12	0	1.68	0	295.13	0.38
13	0	0	-1.68	212.30	0.23
14	0	0	1.68	245.43	0.35
15	0	0	0	204.90	0.23
16	0	0	0	199.10	0.28
17	0	0	0	209.40	0.29

*Particle size is presented in terms of Z-average.

The final lipid concentration ranged such that the ethanol residue from the liposomes were kept constant at 2.43% w/w in all experiments. This amount of ethanol residue was the same as that within ST-liposome at 16 mM, produced before optimization from a 400 mM stock solution (mixture of lipids in ethanol). This aspect is an important consideration because the ethanol residue may represent an obstacle to

the application of the scalable ethanol injection method for the production of liposomes that would be used in cells.

2.4. Physico-chemical characterisation

2.4.1. Average hydrodynamic diameter and zeta potential

The average hydrodynamic diameter and size distribution were determined by dynamic light scattering (Malvern Zetasizer Nano Series, model ZEN3600 - Worcestershire, United Kingdom) using a Ne–He laser; measurements were performed at a scattering angle of 173°. The particle's diameter was calculated from the translational diffusion coefficient using the Stokes–Einstein equation (Equation 4-1).

$$d(H) = \frac{(kT)}{3\pi\eta D} \quad (\text{Equation 4-1})$$

where $d(H)$ is the hydrodynamic diameter; D is the translational diffusion coefficient; k is Boltzmann's constant; T is the absolute temperature; and η is the solvent viscosity. The mean diameter and distribution of particle sizes were estimated by CONTIN algorithm analysis. The intensity-weighted and number-weighted mean diameter and particle distribution were obtained in triplicate.

The zeta potential was measured on the same equipment after the cationic liposomes were diluted in the appropriate volume of PBS buffer at 25 °C. These dilution conditions were selected because they were the same conditions in which the liposomes were prepared.

2.4.2. Morphology

The morphology of the liposomes produced using different scalable processes were visualised with a negative staining technique using transmission electron microscopy (TEM). Carbon-coated 200-mesh copper grids with collodion (parloidin with cellulose acetate) films were used. Each liposome preparation was diluted to 0.5

mM total lipids and then applied to the carbon grid. After incubation for 5 min at room temperature, the excess was blotted. One drop of uranyl acetate (1% w/v) in water was added to the carbon grid and incubated for 1 min at room temperature before the excess was blotted and the grid was air-dried. A Carl Zeiss CEM 902 (Germany) microscope was operated at 80 kV. The images were acquired using a CCD camera (Proscan), and the platform acquisition was iTem.

2.4.3. Phase transition

The main melting temperature of each scalable process (ST-liposomes and SM-liposomes) was obtained through differential scanning calorimetry (DSC) on a TA Instruments model Q 2000 (New Castle, Delaware, USA) coupled with the Thermal Advantage software package. Analyses were performed according to the AOCS method Cj 1-94 (2009). Aluminium capsules were used; an empty capsule that contained only air was the reference. Lyophilised samples with masses that ranged from 8.5 mg to 9.5 mg were heated at a rate of 10 °C/min from -20 to 40 °C. Because of the fast heating temperature (10 °C/min) and the occurrence of broad peaks, which reduce accuracy, the thermograms and melting temperatures should only be considered for purposes of comparisons among the samples.

2.5. Biological evaluation of liposomal structures

2.5.1. Differentiation *in vitro* of dendritic cell derived from monocytes

Peripheral blood mononuclear cells (PBMCs) were collected from healthy unrelated volunteers through apheresis performed in a TRIMA ACCEL (Cobe BCT, Denver, CO, USA) [51], at the Hospital Alemão Oswaldo Cruz, São Paulo, Brazil, after informed consent of donors. For enrichment of mononuclear cells, the product of apheresis was submitted to a separation with a density gradient (Ficoll-Paque from GE Healthcare Bio-Sciences AB, Upsala, Sweden) for 30 minutes at 900 G, 18 °C. Mononuclear cells were collected and centrifuged at 290 G for 10 minutes, 18 °C for 3 times with RPMI-1640 medium (GIBCO™, Grand Island, NY, EUA). After this process, the mononuclear cells were seeded in 6-well plate (5×10^6 cells/well) in RPMI

1640 culture medium and incubated at 37 °C and 5% CO₂ for 2 hours. After this period, non-adherent cells were removed and the RPMI medium was replaced by a R-10 medium (RPMI 1640 culture medium supplemented with 10% fetal bovine serum) supplemented with 50 ng/mL IL-4 and 50 ng/mL GM-CSF (PeproTech, Rocky Hill, NJ, USA). After 5 days in culture, the cells were stimulated with TNF-alpha (50 ng/mL; PeproTech, Rocky Hill, NJ, USA) as a positive control for DCs maturation/activation (mDC - mature DC) or stimulated by ST-liposomes or SM-liposomes after optimization (1 mM) labeled with fluorescent probe (FITC-carboxyfluorescein, Avanti-Lipids, USA) to analyze liposomes' internalization by DCs through flow cytometry. As a negative control group (iDC – immature DC), no stimulus was added to the medium. After 2 days in culture, cells were harvested and labeled with specific fluorescent antibodies for analysis by flow cytometry (BD FACSCalibur™) [52].

2.5.2. Allogeneic T lymphocyte proliferation assay

T lymphocytes were purified from non-adherent cells removed after 2 hours incubation of mononuclear cells for DCs generation using negative selection with immunomagnetic beads (anti-CD14, CD16, CD19, CD36, CD56, CD123, and Glycophorin A) (Pan T Cell Isolation Kit II, Miltenyi Biotec, Bergisch Gladbach, Germany), following the manufacturer's recommendations. For induction of allogeneic T lymphocyte proliferation, purified T lymphocytes (1×10^5 cells/well) were co-cultured with DCs (1×10^4 cells/well), stimulated by TNF-alpha or by ST-liposomes or SM-liposomes after optimization, in U-bottom 96-well microplates. T Lymphocytes were previously stained with 10 μM of carboxyfluorescein diacetate succinimidyl ester (CellTrace CFSE Cell Proliferation Kit – Invitrogen Dinal AS, Oslo, Norway) to track cell proliferation. After 5 days in culture, cells were harvested, marked and analyzed in the flow cytometry (BD FACSCalibur™).

2.5.3. Flow cytometry

Dendritic cells preparations (2×10^5 cells/well/condition) were labeled with each of the specific fluorescent antibodies: CD11c, CD86 and HLA-DR (BD Biosciences) for phenotypic analysis and to assess the incorporation of liposomes by DCs. T lymphocyte co-cultured with DCs were labeled with the specific fluorescent antibodies CD4 and CD8 (BD Biosciences) to assess the proliferation of T lymphocytes subpopulations. Then, the labeled cells were analyzed by flow cytometry in FACSCallibur with CellQuest software. At least 10,000 events were acquired per antibody analyzed. The data was analyzed by FlowJo 7.6 software (Tree Star Inc., USA) [52].

3. Results and discussion

3.1. Preliminary investigation of cationic liposome production using the ethanol injection method and high-pressure microfluidization

The cationic liposomes were initially prepared via the scalable ethanol injection method with a final lipid concentration of 16 mM based on the previous work of Trevisan, Cavalcanti, Oliveira, De La Torre and Santana [29], who developed this method (ethanol injection method + high-pressure microfluidization) using only EPC in the liposome composition. The lipid dispersion in ethanol was injected at 57.6 mL/min into a reactor that contained PBS under stirring (Ultra-Turrax® at 24,000 rpm), which resulted in ST-liposomes. These liposomes were then microfluidized at 850 bar and 1 cycle passage to produce SM-liposomes (combined Ultra-Turrax® + Microfluidizer® processes). The physico-chemical properties of the ST- and SM-liposomes (before optimization) were characterised by determination of their average hydrodynamic diameter, their polydispersity and their zeta potential (Table 4-2).

Table 4-2 - Physico-chemical properties of liposomes produced by the ethanol injection method (ST-liposomes) followed by microfluidization (SM-liposomes) before and after optimization.

Liposome process production	Z-Average		Polydispersity		Zeta potential	
	(±SD) nm	P-value*	Pdl**	P-value*	(±SD) mV	P-value*
Before optimization						
ST-liposomes (1)	290.22 ± 87.25		0.54 ± 0.16		30.81 ± 2.16	
SM-liposomes (2)	128.97 ± 67.30		0.40 ± 0.16		29.93 ± 1.18	
After Optimization						
ST-liposomes (3)	110.86 ± 3.67	0.067 (1:3)	0.17 ± 0.02	0.014 (1:3)	20.87 ± 1.62	0.046 (1:3)
SM-liposomes (4)	107.27 ± 3.62	0.548 (2:4)	0.18 ± 0.01	0.161 (2:4)	13.63 ± 1.07	0.002 (2:4)

Results represent means of independent experiments ± S.D., n=3.

ST process parameters before optimization: final lipid concentration of 16 mM, stirring rate of 24,000 rpm and injection flow of 57.6 mL/min. SM process parameters: 850 bar and 1 cycle passage.

ST process parameters after optimization: final lipid concentration of 2 mM, stirring rate of 11,000 rpm and injection flow of 44.4 mL/min. SM process parameters: 850 bar and 1 cycle passage.

* P-value > 0.05 indicates that the values compared are not significantly different. The P-value calculation was performed for ST-liposomes before and after optimization and for SM-liposomes before and after optimization.

** Pdl - Polydispersity of the sample varies in ascending order from 0 to 1.

The average hydrodynamic diameter of the ST- and SM-liposomes (before optimization) were 290.22 and 128.97 nm, respectively. The microfluidization resulted in a size reduction of approximately 55%. However, the polydispersity initially at 0.54 (ST-liposomes) was reduced to only 0.40 after microfluidization. The processes exhibited similar zeta potentials, which were approximately 30 mV.

Because the ST- and SM-liposomes exhibited high polydispersity and two populations, we directed our efforts to search for operating conditions that would allow the generation of liposomes with lower polydispersity and with diameters near 100 nm. Our decision to use this approach was supported by previous study of Kremer and co-workers [39], who postulated that lipid concentration in the ethanol injection method primarily influences liposome size and that *in vitro* and *in vivo* applications generally require small nanoparticles (i.e., in the size range of 100-200 nm) to facilitate internalisation [45-47]. In addition, the high polydispersity can be adverse for *in vitro* applications of nanoparticles with mammalian cells because they, in most of cases, internalise a greater number of particles with a single and homogeneous population to expend less energy during the capture [48-50].

3.2. Experimental design of cationic liposome production by the ethanol injection method

Because the high polydispersity and size values obtained for the ST- and SM-liposomes under the preliminary conditions used (Table 4-2) may be a drawback for *in vivo* and *in vitro* transfection in mammalian cells, our focus was the optimization of the previously discussed process. Because the size and polydispersity of liposomes obtained using the ethanol injection method depends on several factors, such as the lipid concentration, the stirring rate, the injection flow and the choice of lipids [37], we designed a central composite design (CCD) to determine the best process conditions for each variable. We investigated the influence of the final lipid concentration in the liposome colloidal dispersion, the stirring rate and the ethanol injection flow (factors) as functions of the average hydrodynamic diameter and the polydispersity (response parameters). The results are shown in Table 4-1.

As evident from the results in Table 4-1, the fifth experiment (i.e., a stirring rate of 9,600 rpm, a final lipid concentration of 4.8 mM and an injection flow of 50 mL/min) produced cationic liposomes with the smallest polydispersity and a Z-average of 0.19 and 160.70 nm, respectively. These values are lower than those of the ST-liposomes before optimization (Table 4-2). In contrast, the third experiment (i.e., a stirring rate of 9,600, a final lipid concentration of 13.2 mM and an injection flow of 27.7 mL/min) resulted in the worst results in terms of size (1413.33 nm) and polydispersity (0.96).

Analysis of variance (ANOVA) was used to analyse the statistical significance of the factors in the polydispersity and size responses (Table 4-3). The result of the Fisher F-test was greater than the listed value for a 75% confidence level for the polydispersity and the size of liposomes; therefore, all factors significantly influenced the resulting particle size and polydispersity (Table 4-3 and Figure 4-2). However, the correlation coefficient (R^2) was 0.62 for liposome size in terms of the Z-average and 0.47 for liposome polydispersity, which indicated that the obtained mathematical model cannot be used to describe the surface response.

Table 4-3 - Analysis of variance and regression analyses for the response of the 2³ central composite design.

Source of variation	Sum of square		Degrees of freedom		Mean square		F-test	
	Particle size*	Pdl**	Particle size	Pdl	Particle size	Pdl	Particle size	Pdl
Regression	890,574	0.304	6	4	148,429.0	0.076	2.69 ^a	2.71 ^b
Residual	551,325	0.338	10	12	55,132.5	0.028		
Lack of Fit	551,272	0.336	8	10	68,909.0	0.034		
Pure Error	53	0.002	2	2	26.5	0.001		
Total	1,441,899	0.642	16	16				

*Particle size is presented in terms of Z-average.

**Pdl: abbreviation of polydispersity.

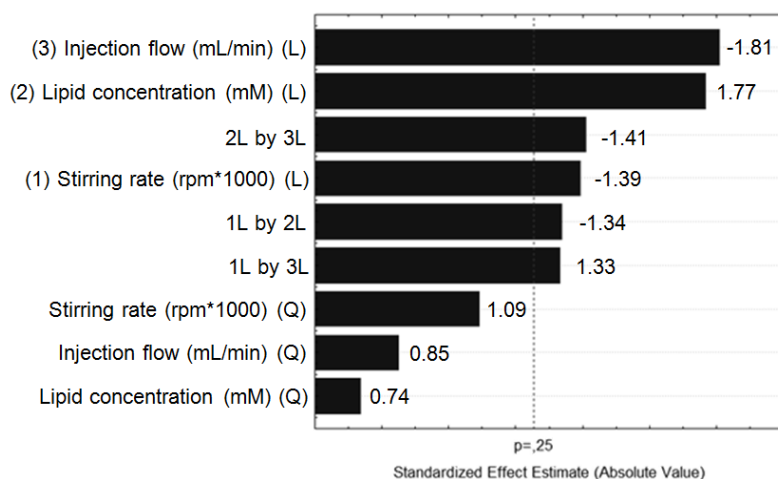
Regression coefficient: Particle size $R^2 = 0.62$; Pdl $R^2 = 0.47$

^a $F_{6; 10; 0.25} = 1.58$

^b $F_{4; 12; 0.25} = 1.55$

The effects of the variables and their interactions on particle size (Figure 4-2 A) show that the injection flow, the final lipid concentration, the interaction between the final lipid concentration and injection flow, the stirring rate, the interaction between the stirring rate and final lipid concentration and the interaction between the stirring rate and injection flow were statistically significant at a 75% confidence level. In addition, for polydispersity (Figure 4-2 B), the interaction between the stirring rate and final lipid concentration, the final lipid concentration, the quadratic stirring rate and the injection flow were statistically significant. Because the intrinsic variability of the process is high, the results were analysed at a 75% confidence level after elimination of the statically insignificant terms ($p > 0.25$).

A



B

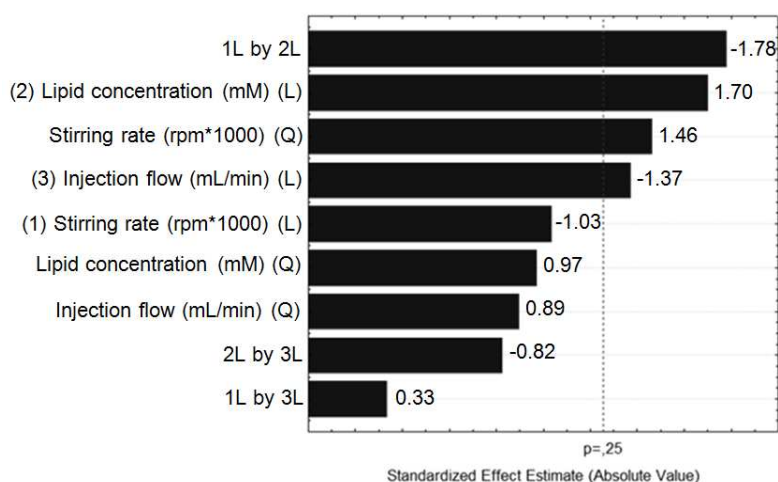


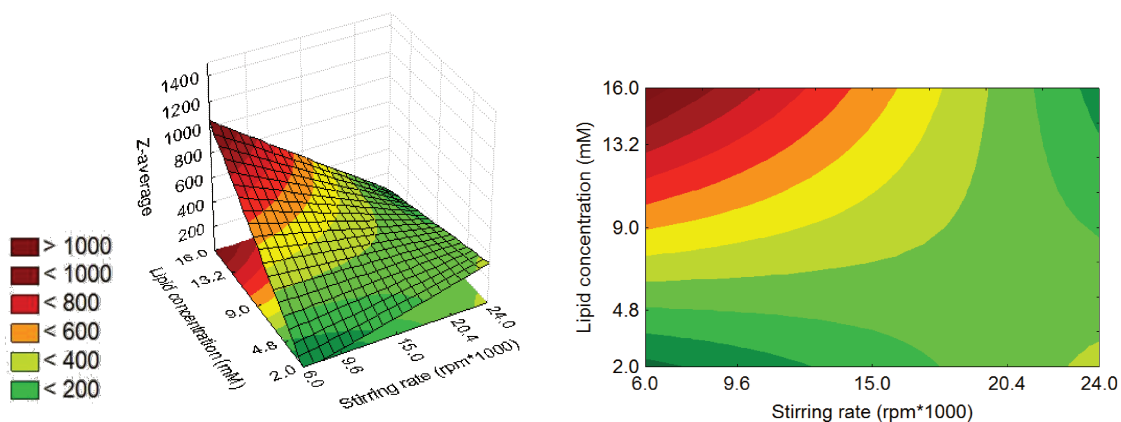
Figure 4-2 – Pareto's graphics of the t value calculated for each variable, which represents the importance of variables on estimating particle size (A) and polydispersity (B).

Despite the experimental design not providing an appropriate statistical model, we were able to produce liposomes in an acceptable range with respect to size and polydispersity (experiment 5, Table 4-1). Given that our main goal was not the determination of a mathematical model but rather the identification of process parameters, we investigated the surface response tendency to select the best process conditions for further validation. These conditions must be chosen in order to

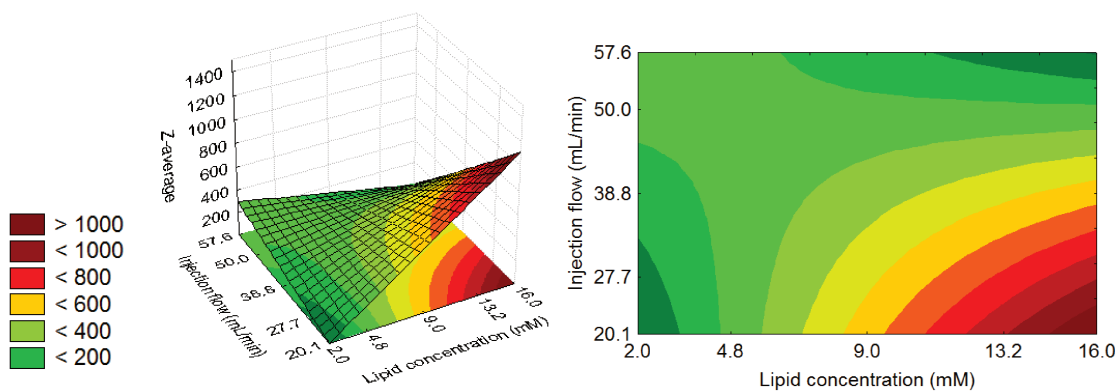
produce cationic liposomes with physico-chemical properties close to liposomes produced by traditional methods, such as lipid film hydration and extrusion (i.e., a size of approximately to 100 nm and a polydispersity 0.20) [27].

The response surfaces and contour plots (Figures 4-3 A, 4-3 B and 4-3 C) were chosen among the possible combinations to visualise the simultaneous effects of stirring rate, lipid concentration and injection flow on the Z-average of the obtained cationic liposomes.

A



B



C

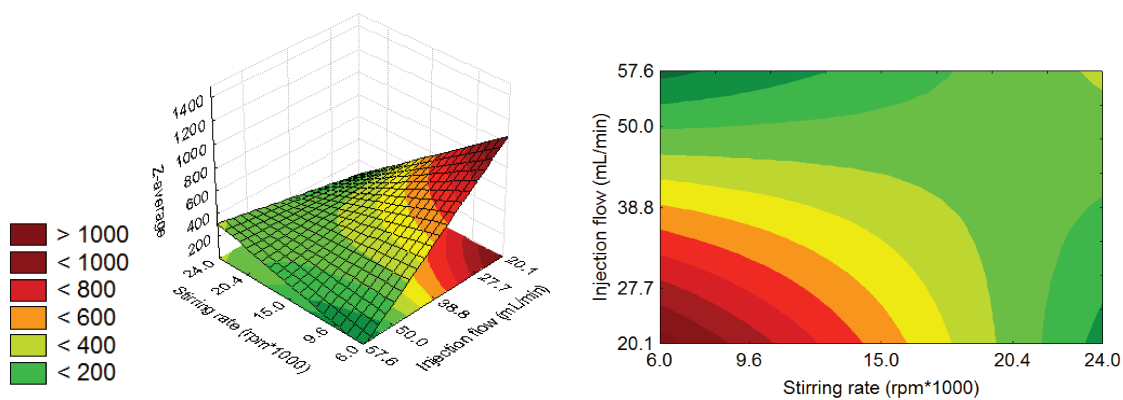


Figure 4-3 – Response surface and contour curve for the Z-average as a function of (A) the stirring rate versus the lipid concentration, (B) the lipid concentration versus the injection flow and (C) the stirring rate versus the injection flow.

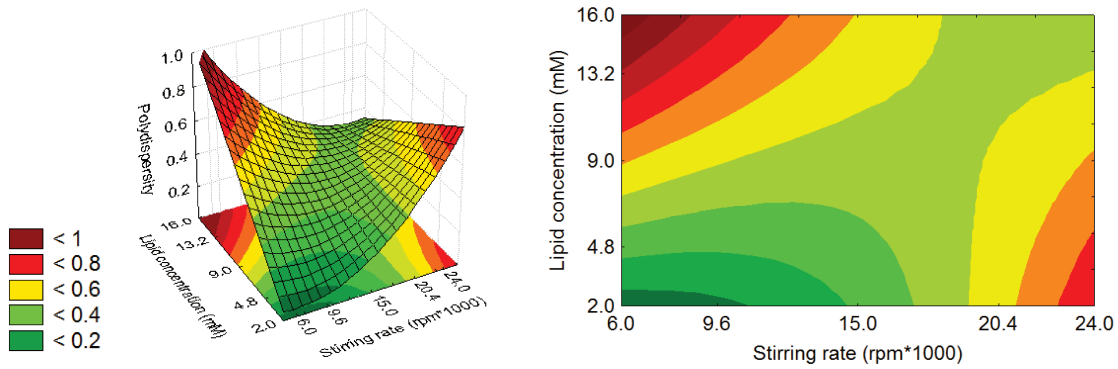
The size of liposomes decreases with a low final concentration and low stirring rate or with a high lipid concentration and a high stirring rate (Figure 4-3 A). The Z-average is not so affected by injection flow when the final lipid concentration is low; however, if the final lipid concentration is high, the injection flow must also be high to decrease the size (Figure 4-3 B). Similarly, with a slow stirring rate and a fast injection flow or with a high stirring rate and a low injection flow, the size of cationic liposomes decreases (Figure 4-3 C).

The response surfaces and contour plots obtained as a result of the experimental design with respect to size, specifically the Z-average (cumulative mean hydrodynamic diameter) (Figure 4-3), indicate that a high lipid concentration increases the size of the liposomes. The first research group that studied the variables that influences vesicles prepared by the ethanol injection method was Kremer and co-workers [39], who, in the same way as us, postulated that the size of liposomes is directly proportional to the lipid concentration. More recently, Gentine and co-workers [53] characterised a method based on the same principle as ethanol injection but used another water-soluble solvent, isopropanol. They showed that the particle size increased (78 to 95 nm) with increasing lipid concentration (0.94 to 15 mM); they comparatively tested the ethanol injection process for the same concentrations, and their results showed a significant increase in the vesicle size (107 to 163 nm) with increasing lipid concentration. These results demonstrate that the size of liposomes increases with high lipid concentrations; however, isopropanol allowed a better control of vesicle diameter compared with ethanol. For biological applications of these liposomes, isopropanol could be harmful for cells and therefore require an additional step, such as dialysis, to eliminate the organic solvent residue. To better control the mixing conditions, the alcohol injection method was recently adapted for use in a microfluidic device [36, 54]; thus, we can make an analogy between the two methods. Recently, our research group [55] showed that a microfluidic system produces smaller particles using lower lipid concentrations in ethanol dispersions.

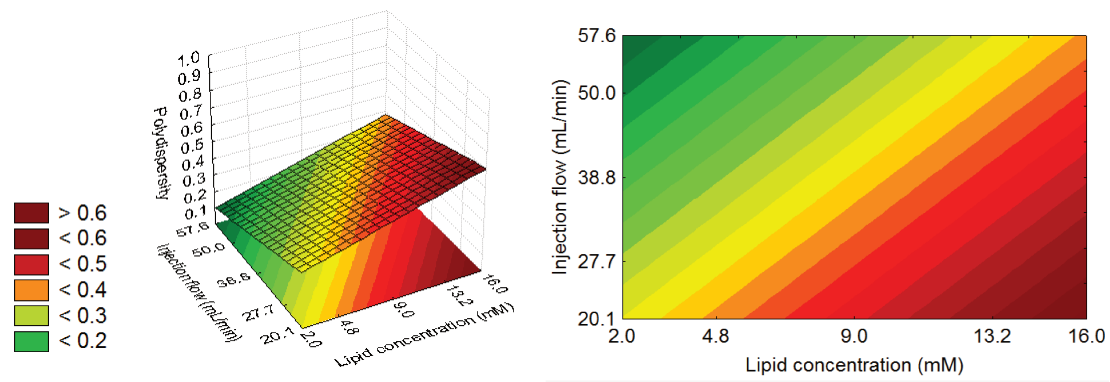
Concerning the analyses of the response surfaces and contour plots obtained as results of the experimental design with respect to size (Figure 4-3), the liposomes' size decreased with the stirring rate was decreased, and the liposomes' size decreased when the injection rate was increased. Gentine and co-workers [53] have reported that decreasing (400 to 100 rpm) or increasing (400 to 1000 rpm) the stirring rate increased the size of the vesicles, but not significantly. However, in addition to using isopropanol, which exhibits a molecular diffusivity in water that is 51.7% lower than that of ethanol in water, those authors tested a range of stirring rate tested (100-1000 rpm) that was significantly lower than that used in this work (6,000 rpm-24,000 rpm) [53]. They also showed that the influence of the injection flow rate on vesicle size was not significant; however, the range of tested injection flow rates (100-1.800 μ l/min) was also significantly smaller than that used in this work (20.1-57.6 mL/min) [53].

The simultaneous effects of the stirring rate, the lipid concentration and the injection flow on the polydispersity of cationic liposomes are shown by the response surfaces and contour plots (Figures 4-4 A, 4-4 B and 4-4 C).

A



B



C

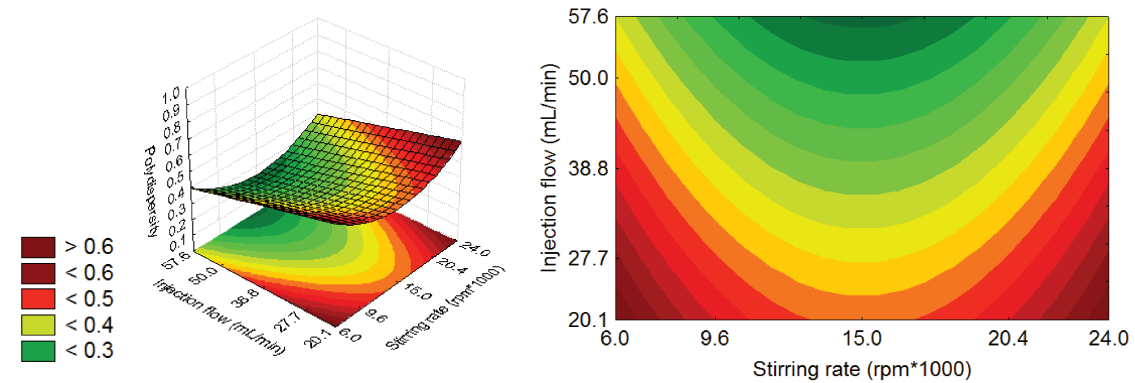


Figure 4-4 – Response surface and contour curve for polydispersity as a function (A) the stirring rate versus the lipid concentration, (B) the lipid concentration versus the injection flow and (C) the stirring rate versus the injection flow.

The polydispersity of the liposome populations decreases with a low final concentration and a low stirring rate or with a high lipid concentration and a high stirring rate (Figure 4-4 A). Likewise, when the final lipid concentration is low and the injection flow is high, polydispersity decreases (Figure 4-4 B). The polydispersity of cationic liposomes decreases with a slow stirring rate and a fast injection flow or with a high stirring rate and a high injection flow (Figure 4-4 C).

The response surfaces and contour plots obtained as results of the experimental design with respect to polydispersity (Figure 4-4) indicate that a high lipid concentration, a fast stirring rate and a low injection flow increase both the liposomes' size and their polydispersity. However, based on the results in Figure 4-4 A, we concluded that the negative effect of a high lipid concentration on the polydispersity can be minimised through the use of a fast stirring rate, which agrees with results of Kremer and co-workers [39]. Trevisan, Cavalcanti, Oliveira, De La Torre and Santana [29] have shown that liposomes with relatively low polydispersity (approximately 0.3) can be obtained using ethanol injection parameters of a final lipid concentration of 50 mM, a stirring rate of 24,000 rpm and an injection flow of 57.6 mL/min. With respect to the *in vitro* and *in vivo* applications, the minimisation of residual ethanol in liposomes is desirable, which is a disadvantage of this scalable process. Thus, it is better to obtain liposomes with a low final lipid concentration when a low concentration is suitable for biological applications. According to Gentine, Bubel, Crucifix, Bourel-Bonnet and Frisch [53], a decrease (400 to 100 rpm) or increase (400 to 1000 rpm) in the stirring rate increases the polydispersity of the vesicles, but not significantly, which is consistent with our results with respect to size. Gentine, Bubel, Crucifix, Bourel-Bonnet and Frisch [53] also showed that the influence of the injection flow rate on the vesicle polydispersity is not significant and that the polydispersity remained unchanged (0.140–0.230) when the lipid concentration varied, except when the concentration was 0.94 mM, in which case it was approximately 0.300. The lack of agreement between our results and those of Gentine, Bubel, Crucifix, Bourel-Bonnet and Frisch [53] is most likely because they

used isopropanol, which exhibits a molecular diffusivity in water that is significantly lower than that of ethanol in water and the fact that the ranges of stirring and injection flow tested by them were significantly smaller than those used in this study.

Based on our findings, we here propose a mechanism for the formation of EPC/DOTAP/DOPE liposomes using the ethanol injection method. We based this mechanism on that previously described by Zook and Vreeland [56] in the case of the microfluidic process, where a central stream (isopropanol and lipids) is hydrodynamically compressed by two aqueous streams. According to these authors, because the channel dimensions in the microfluidic device are on the order of microns, the flow pattern is laminar and the diffusion and convection (advection) contributions primarily occur in different coordinates [56]. In this case, the alcohol diffusion into the aqueous streams generates an ethanol gradient that favours the formation of phospholipid bilayer fragments (PBFs) that are stabilised by the presence of ethanol in water [56]. Because the alcohol concentration is diminished, the bilayer auto-aggregation is favoured because regions of lower polarity diminish the lipid solubility, which facilitates their self-assembly into PBFs [56]. Our research group [55] investigated the formation of EPC/DOTAP/DOPE liposomes in microfluidic devices using ethanol as the organic solvent. Because the diffusion coefficients of ethanol and isopropanol are different (ethanol diffuses 7 times faster than isopropanol), the hydrodynamic behaviour is different; consequently, the final liposomes exhibit different physico-chemical properties when the use of these solvents is compared under the same process conditions. Similarly, in our case, the mixture tank allows diffusion and convection; however, these mass transfer contributions occur in all directions. In addition to the differences in direction and the differences between the ethanol injection method and the microfluidic approach investigated by Zook and Vreeland [56], the mechanism for liposome formation is most likely the same, and the alcohol diffusion most likely plays a major role in the final characteristics of the liposomes, as shown in Figure 4-5.

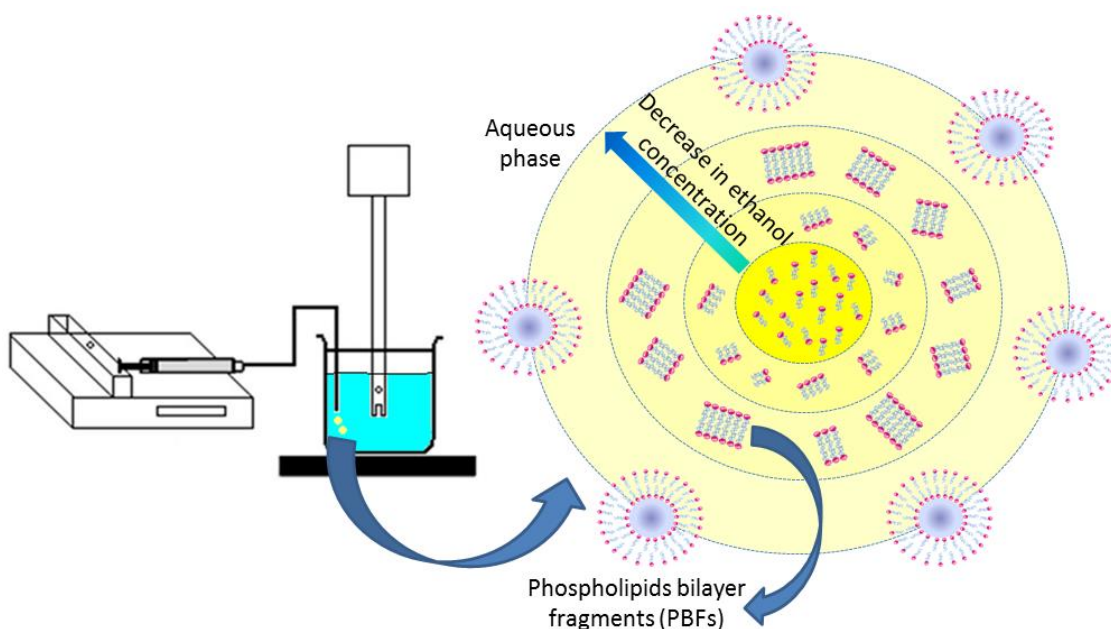


Figure 4-5 - Schematic diagram of the hypothesised mechanism for liposome formation using the ethanol injection method. The droplets injected into the tank mixture are composed of the lipid dispersion in ethanol. The Ultra-Turrax® mixes the droplets in the aqueous phase to form phospholipid bilayer fragments (PBF) that grow into vesicles to stabilise their hydrophobic PBF edges. The decrease in ethanol concentration destabilises the PBFs, which causes them to close into vesicles and thus form liposomes.

The proposed mechanism for liposome formation using the ethanol injection method (Figure 4-5) is based on mass transfer contributions and intermolecular forces between phospholipids to form phospholipid bilayer fragments, which are the precursors of liposomes. Initially, we analysed the system by varying the stirring rate and the injection flow but maintained the same final lipid concentration. Notably, an optimum balance exists between the injection flow rate and the stirring rate with respect to size and polydispersity. In this case, a high stirring rate and a high injection flow rate increase the mass transfer of ethanol from the lipid/ethanol phase to the aqueous phase. This result indicates that no ethanol gradients will exist in the tank in less time, which will influence the proper formation of PBFs. Thus, with a high injection flow rate, insufficient time is allowed for lipids to aggregate to form large PBFs, so the liposome size decreases. Higher stirring rates result in small liposomes because less time is available for the aggregation of lipids and for PBFs to form; however, the high stirring rate disturbs the formation of PBFs and increases the

liposome polydispersity. Low stirring rates and low injection flow rates also compromise the ethanol/water mass transfer and the PBF formation, which leads to the formation of larger liposomes.

In addition, we analysed the system by varying the total lipid concentration while maintaining the same stirring and injection flow rates. When the lipid concentration is high, more interaction forces are present between phospholipids; however, the same time is allowed for PBF formation with respect to the diffusion of ethanol into water. In this case, an increase in the number of molecules of lipids per unit volume was observed, and this increase facilitated the formation of larger PBFs and, as consequence, larger liposomes. Furthermore, an increase in the lipid concentration disorganises the aggregation process among lipids over time, which leads to a high polydispersity. This behaviour is consistent with that reported for the microfluidic device described by Balbino, Aoki, Gasperini, Oliveira, Cavalcati, Azzoni and De La Torre [55], who observed that an increase in the lipid concentration in the final liposome dispersion reflects a decrease in the proportion between the ethanol and lipids, which the authors observed to compromise the formation of the PBFs and to lead to an increased size of the final liposomes.

Balbino and co-workers [55] produced cationic EPC/DOTAP/DOPE liposomes in single-hydrodynamic-focusing microfluidic devices using a flow rate ratio of 10, a flow velocity of 165 mm/s and a lipid concentration of the dispersion in ethanol of 25 mM. Their method resulted in nanoparticles with a size of 124.9 ± 8.9 and a polydispersity of 0.31 ± 0.05 [55]. They also produced the same liposomes in double-hydrodynamic-focusing microfluidic devices using conditions of a flow rate ratio of 10, a flow velocity of 285 mm/s and a lipid concentration of the dispersion in ethanol of 25 mM, which resulted in a nanoparticles size of 101.9 ± 1.6 and a polydispersity of 0.34 ± 0.02 [55]. A comparison of the liposomes prepared via the ethanol injection method with liposomes prepared via microfluidic devices indicates that the liposomes have the same physico-chemical properties, but the advantage for ethanol injection method over the midrofluidic system is the possibility of massive production.

Gentine, Bubel, Crucifix, Bourel-Bonnet and Frisch [53] has affirmed that their results achieved with isopropanol injection, which resulted in a particle size that changed from 78 to 95 nm and a polydispersity that was practically unchanged between 0.140 and 0.230 when the lipid concentration used in the process was varied, allows better control of the vesicle diameter than does the ethanol injection method as a function of the lipid concentration. However, through optimization of the ethanol injection method, we obtained liposomes with sizes slightly larger than those obtained by Gentine, Bubel, Crucifix, Bourel-Bonnet and Frisch [53] and with the same polydispersity. In addition, the ST-liposomes exhibited similar diameters as liposomes produced using hydration of the dried film followed by extrusion to an acceptable size for *in vitro* transfection [27]. The final lipid concentration is also not limiting for *in vitro* applications that require a low lipid concentration.

As a result of the tendencies exhibited in the analysed contour curve and response surface, we selected the process parameters of a final lipid concentration of 2 mM, a stirring rate of 11,000 rpm and an injection flow of 44.4 mL/min and produced the cationic liposomes in triplicate for validation of the observed tendencies. The liposomes produced using these process parameters were named ST-liposomes after the process was optimized, and they exhibited a Z-average of 110.86 ± 3.67 nm and a polydispersity of 0.17 ± 0.02 (Table 4-2). The comparison between ST-liposomes before and after optimization indicated no significant variation in their size (Table 4-2). However, the polydispersity exhibited a significant difference caused by the optimization (Table 4-2). Thus, these process conditions were used in subsequent studies of liposome microfluidization under high pressures.

3.3. Microfluidization for uniformity of size and polydispersity

The ST-liposomes produced under the previously determined optimized conditions were subsequently submitted to high-pressure microfluidization, which resulted in SM-liposomes. The microfluidization process parameters were based on the previous work of Trevisan, Cavalcanti, Oliveira, De La Torre and Santana [29] for

EPC at 850 bar. We investigated the influence of an increase in the number of cycles passage (one, two, three, five, seven and ten) on the polydispersity and the Z-average. The physico-chemical properties of the SM-liposomes are presented in Figure 4-6 in terms of their size (Z-average) and their polydispersity as functions of the number of cycles.

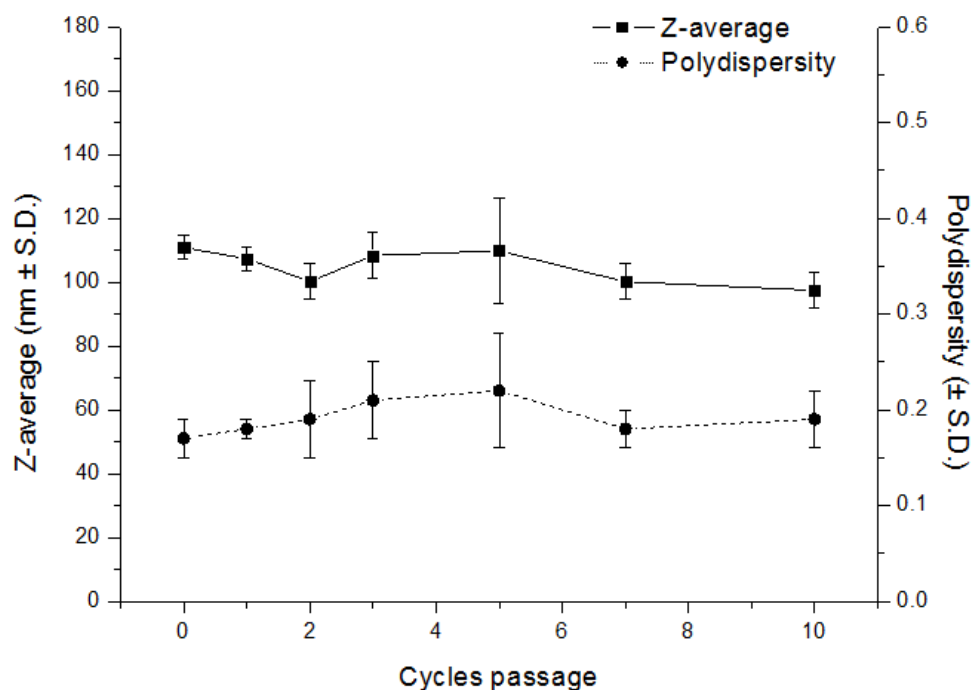


Figure 4-6 – Z-average and polydispersity profiles of SM-liposomes obtained after microfluidization at 850 bar as functions of the number of cycles. The lines are for visual reference only.

The polydispersity and size of SM-liposomes tend to be constant after the third cycle passage in the microfluidizer when the standard deviations are considered (Figure 4-6), which is in agreement with the results of Trevisan and co-workers [29]. Therefore, we analysed the properties of the liposomes after one to three cycles. In this context, SM-liposomes that passed only one time through the equipment are preferred because, with a Z-average of 107.27 nm and a polydispersity of 0.18, they are suitable for biological applications; these conditions therefore make the process more profitable than when several cycles are used. Notwithstanding, SM-liposomes before and after optimization did not exhibit a significant variation in size and

polydispersity based on the results of a t-test performed at a level of 5%. However, the zeta potential decreased from 20.87 mV to 13.63 mV after one cycle of microfluidization (Table 4-2). The applied shear in the colloidal liposome dispersion imposed by the microfluidization process can modify the lamellar phase organisation [57], which reflects the differences in zeta potentials and also the increase in melting temperatures.

According to Barnadas-Rodriguez and Sabes [58], the mean liposome diameter decreases as the number of microfluidizer cycles increases; however, this relationship was observed when the pressure was maintained constant at 2.4 bar, *i.e.*, the conditions were studied at a pressure 2.82 times greater than that used in this study. In addition, Gregoriadis and co-workers[59] studied the effect of the number of cycles through a microfluidizer operated at 60 psi with respect to dehydration–rehydration liposomes (DRVs) and observed no considerable change in liposome size after 5.2 cycles (*i.e.*, after 5.2 cycles, the size was 168.1 nm; after 7.1 cycles, the size was 159.5 nm; and after 10.6 cycles, the size was 155.7 nm); they also observed that the polydispersity indexes changed only slightly with the number of cycles (*i.e.*, the polydispersity ranged from 0.503 to 0.653). These results are similar to ours; however, here, the liposome size and polydispersity did not change after 3 cycles, which may be due to the lower lipid concentration used in this study.

3.4. Physico-chemical characterisation of cationic liposomes produced using the ethanol injection method and high-pressure homogenisation

The ST- and SM-liposomes before and after optimization were compared in terms of their size distribution (Figure 4-7). For the ST-liposomes, the experimental design resulted in a decrease of the liposome size and an increase in the homogeneity of the population (Figure 4-7 A). For SM-liposomes, the experimental design resulted in an increase in the homogeneity of the population; however, the size of the liposomes remained almost unchanged (Figure 4-7 B). The size distribution of the ST-liposomes after optimization confirms the previous analysis in

terms of the Z-average and indicates that microfluidization is not necessary to achieve a reduction of the liposomes' size and polydispersity.

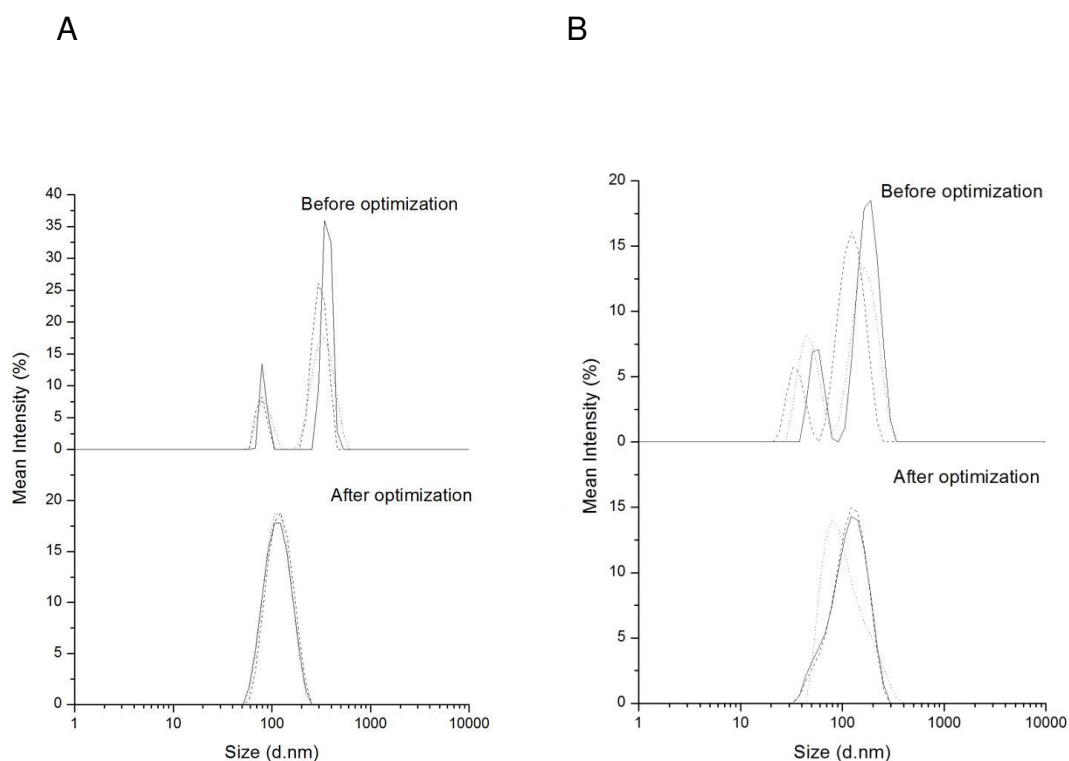


Figure 4-7 – Intensity-weighted and number-weighted size distributions of (A) ST-liposomes and (B) SM-liposomes before and after optimization. The dotted, dashed and solid lines in each graph represent one independent size distribution (n =3).

The morphology of the liposomes was evaluated using transmission electron microscopy (TEM) and a negative staining technique. We evaluated the morphology of ST-liposomes prepared under two sets of conditions: (i) those obtained from the fifth experiment of the CCD, which produced liposomes with a diameter of approximately 100 nm and a polydispersity of 0.20 (Table 4-1; final lipid concentration of 4.8 mM, dispersed using the Ultra-Turrax® at 9,600 rpm and an injection flow of 50.0 mL/min) (Figure 4-8); and (ii) those obtained under the optimized conditions (final lipid concentration of 2.0 mM, dispersed using the Ultra-Turrax® at 11,000 rpm and an injection flow of 44.4 mL/min) (Figure 4-9).

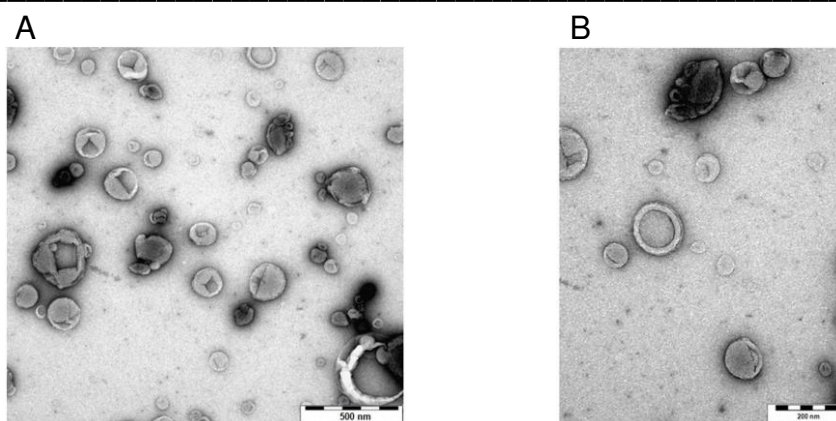


Figure 4-8 – Micrographs of ST-liposomes produced at 4.8 mM, 9,600 rpm and 50.0 mL/min (trial 5, Table 4-1) obtained via the negative staining technique using transmission electron microscopy. Bars indicate (A) 500 nm and (B) 200 nm.

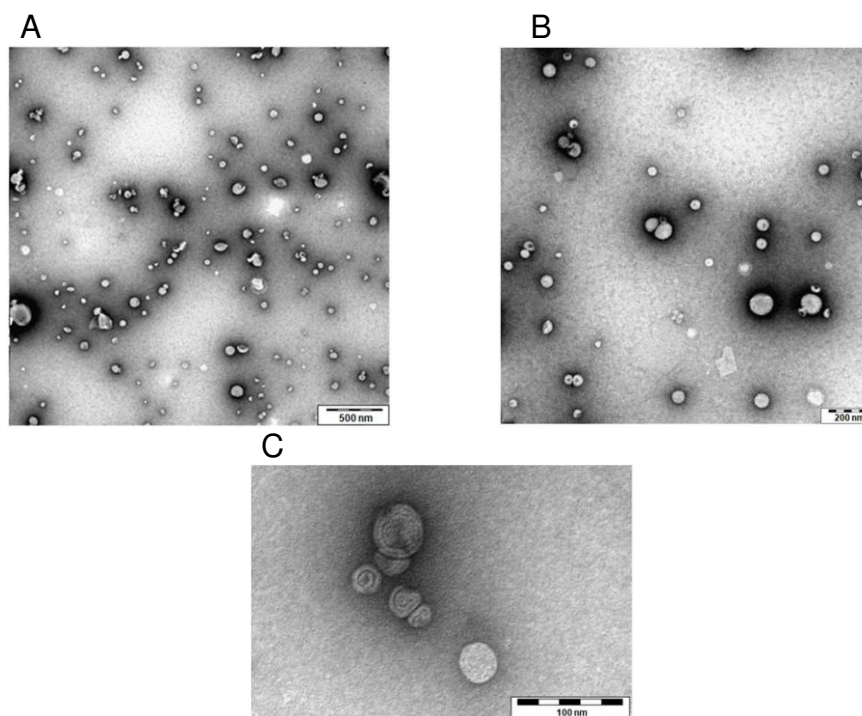


Figure 4-9 - Micrographs of ST-liposomes after optimization produced at 2.0 mM, 11,000 rpm and 44.4 mL/min (Table 4-2) obtained via the negative staining technique using transmission electron microscopy. Bars indicate: (A) 500 nm, (B) 200 nm and (C) 100 nm.

The ST-liposomes obtained under two different sets of conditions (fifth experiment and after optimization) exhibited spherical morphology. The ST-liposomes obtained from the fifth experiment exhibited a diameter of approximately 150 nm (Figure 4-8 B), which agrees with the Z-average of 160.70 nm presented in Table 4-1.

However, the ST-liposomes obtained after optimization exhibited a diameter of approximately 50 nm (Figure 4-9 C), which does not correspond to the Z-average of 110.86 nm presented in Table 4-2. This discrepancy may have occurred because only the part of population with small nanoparticles was observed in the micrographs. We did not observe evidence of aggregation and/or fusion. The micrographs of the ST-liposomes obtained from the fifth experiment (Figure 4-8) and those obtained after optimization (Figure 4-9) show that the liposomes are all homogeneous, which indicates their low polydispersity and confirms the physico-properties of the ST-liposomes presented in Table 4-1 (ST-liposomes obtained from the fifth experiment) and Table 4-2 (ST-liposomes obtained after optimization).

The morphology of the SM-liposomes after optimization (Table 4-2) is presented in Figure 4-10. As evident from Figure 4-10, after microfluidization, even with only one cycle, cylindrical structures (indicated with arrows) observed, which were most likely formed because of the high pressure that is characteristic of this type of equipment. Although the presence of cylindrical structures was evident, neither fused nor aggregated structures were observed. However, the number of cycles influenced the morphological characteristics of the SM-liposomes [29], which were not as spherical as ST-liposomes (Figure 4-10), because of the high shearing to which the SM-liposomes were subjected. These morphological differences are most likely the reason for the decrease in the zeta potential from 20.87 for ST-liposomes to 13.63 mV for SM-liposomes (Table 4-2).

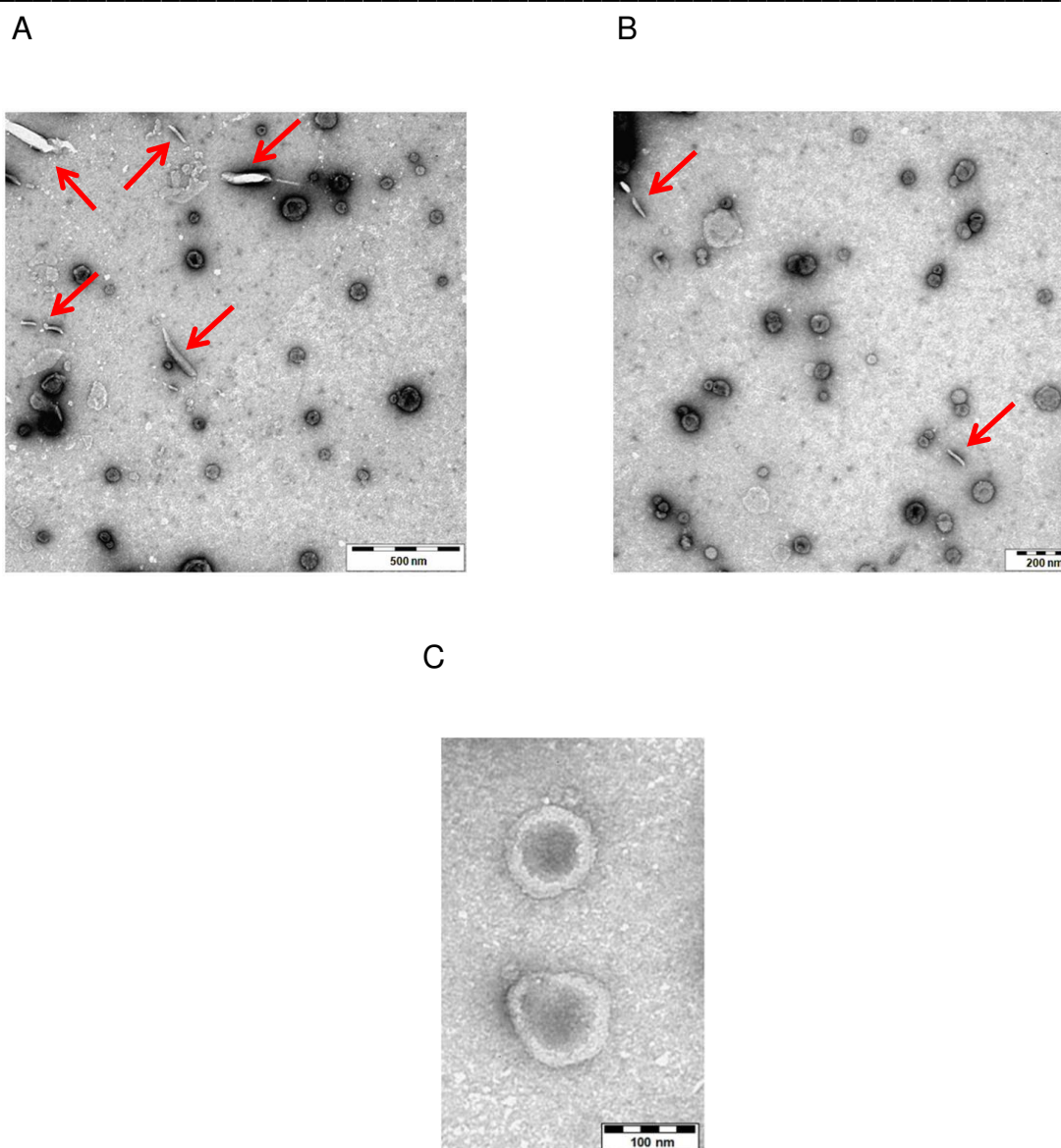


Figure 4-10 - Micrographs of SM-liposomes after optimization produced at 2.0 mM, 11,000 rpm and 44.4 mL/min; these liposomes were later microfluidized at 850 bar for 1 cycle (Table 4-2) and were observed using the negative staining technique in conjunction with transmission electron microscopy. The presence of cylindrical structures, which are most likely formed due to the high pressure that is characteristic of this type of equipment, are indicated with arrows. Bars indicate (A) 500 nm, (B) 200 nm and (C) 100 nm.

The thermal behaviour of the ST- and SM-liposomes (before and after optimization) was studied using differential scanning calorimetry (DSC). The main phase transition and the thermograms are presented in Table 4-4 and Figure 4-11, respectively. The main melting temperatures of the ST-liposomes obtained before

optimization increased by 1.08 °C when they were microfluidized (SM-liposomes) (Table 4-4). The main melting temperature of the ST-liposomes obtained after optimization increased by 1.37 °C after they were microfluidized (SM-liposomes) (Table 4-4). The differences in the thermograms of the ST- and SM-liposomes (Figure 4-11) are most likely a consequence of the smaller interlamellar distance of the ST-liposomes submitted to the microfluidizer (SM-liposomes) [29]. In addition, the differences in the thermograms of liposomes before and after optimization (Figure 4-11) are directly related to the total lipid concentration of each process and to the size of the liposomes.

Table 4-4 - Melting temperature of the liposomes produced via the ethanol injection method (ST-liposomes) and that of the liposomes subsequently subjected to microfluidization (SM-liposomes) before and after optimization. Samples were freeze-dried and heated at 10 °C/min.

Cationic liposomes process	T _m
Before optimization	
ST-liposomes	12.20 °C
SM-liposomes	13.28 °C
After optimization	
ST-liposomes	12.93 °C
SM-liposomes	14.30 °C

Note: These thermograms and the melting temperatures are for comparison only as the fast heating temperature (10°C/min) would reduce accuracy.

ST process parameters before optimization: final lipid concentration of 16 mM, stirring rate of 24,000 rpm and injection flow of 57.6 mL/min. SM process parameters: 850 bar and 1 cycle passage.

ST process parameters after optimization: final lipid concentration of 2 mM, stirring rate of 11,000 rpm and injection flow of 44.4 mL/min. SM process parameters: 850 bar and 1 cycle passage.

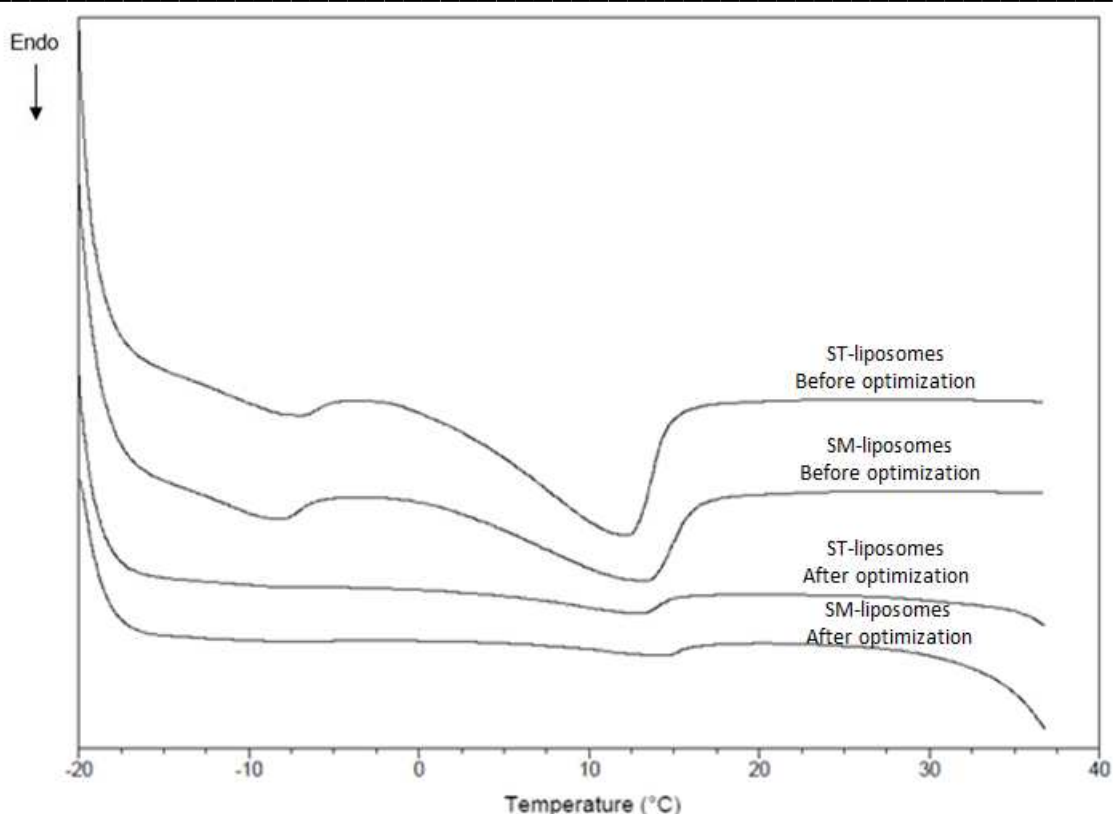


Figure 4-11 - Thermogram of the liposomes produced via the ethanol injection method (ST-liposomes) and that of the liposomes subsequently subjected to microfluidization (SM-liposomes) before and after optimization. Samples were freeze-dried and heated at 10 °C/min. Note: These thermograms and the melting temperatures are for comparison only because the fast heating temperature (10 °C/min) reduced their accuracy.

Differential scanning calorimetry experiments were used to investigate the effect of scalable processes optimization on the main melting temperatures of liposomes (Table 4-4) and on their thermograms (Figure 4-11). Liposome self-assembly is result of a balance between attractive forces from the hydrophobic tails (van der Waals interactions) and repulsive forces from the polar head groups [60]. Modifications of these forces caused by differences in the liposome production processes can modify the cooperative melting interactions, which is reflected in the variation in the T_m values shown in Table 4-4. Nevertheless, the T_m values presented in Table 4-4 are similar to the main melting temperatures of cationic liposomes composed of analytical-grade EPC/DOTAP/DOPE (12.97 °C) published by De La Torre, Rosada, Trombone, Frantz, Coelho-Castelo, Silva and Santana [26]. The differences in the thermograms before and after optimization (Figure 4-10) may be

related to differences in the crystallinity of the liposomes imparted by the differences in concentrations (2 or 16 mM) [61]. Previous studies have demonstrated that more-amorphous liposome structures were obtained at lower lipid concentrations [34]. Furthermore, Trevisan, Cavalcanti, Oliveira, De La Torre and Santana [29] have demonstrated using small-angle X-ray scattering (SAXS) that SM-liposomes have shorter interlamellar distances than ST-liposomes, *i.e.*, the interlamellar distances are shorter because the microfluidizer decreases the amount of water in the interlamellar space of the liposomes.

3.5. Biological evaluation of liposomal structures

3.5.1. *In vitro* evaluation of efficiency and effect of cationic liposomes internalization by dendritic cells

The strategies used for phenotypic analysis of DCs and for analysis of liposomes incorporation are presented in the Supplementary Data. In order to evaluate the liposomes incorporation by DCs and the DCs activation by liposomes, Table 4-5 present the median of liposomes' probe fluorescence and CD86 fluorescence expressed by dendritic cells stimulated by TNF- α (mDC), or by ST-liposomes or SM-liposomes after optimization, and without stimuli (iDC).

Table 4-5 – Mean and median of liposomes' probe fluorescence and CD86 fluorescence expressed by dendritic cells stimulated by TNF- α (positive control - mDC), or by ST-liposomes after optimization (final lipid concentration of 2 mM, stirring rate of 11,000 rpm and injection flow of 44.4 mL/min), or SM-liposomes after optimization (850 bar and 1 cycle passage) and the negative control (iDC).

Population name	Median of liposomes' probe fluorescence (FITC)	Median of CD86 fluorescence (PerCP-Cy5)
iDC	4.14	14.70
mDC	4.19	7.71
ST-liposomes After optimization	32.30	40.90
SM-liposomes After optimization	16.80	35.20

According to the median of liposomes' probe fluorescence (Table 4-5), ST- and SM-liposomes were incorporated by dendritic cells. However, ST-liposomes (32.30) presented more fluorescence intensity than SM-liposomes (16.80), *i.e.* ST-liposomes were better incorporated by DCs than SM-liposomes. This behaviour can be explained by analysing morphological properties of liposomes, since their physico-chemical properties (size and polydispersity) (Table 4-2) are very similar. SM-liposomes present cylindrical structures formed because of the high pressure that they were submitted in the Microfluidizer (Figure 4-10). On the other hand, ST-liposomes present only spherical structures (Figure 4-9) that facilitates their internalization by DCs. This hypothesis is based in others works that demonstrate the importance of homogenous size distribution [48-50] and small nanoparticles [45-47] in the internalization process by cells, supposing that cells expend less energy in the capture of the nanoparticles with these characteristics.

Investigating the DCs activation, the median of CD86 fluorescence (Table 4-5) shows that both liposomes increased the CD86 expression by DCs, when regarding the median fluorescence of iDC. Also in this case, ST-liposomes (40.90) presented more fluorescence intensity than SM-liposomes (35.20), *i.e.* ST-liposomes activated better DCs than SM-liposomes, probably because they were better internalized. In order to confirm that DCs which internalized liposomes are activated, we presented Dot plot graphics of CD86 versus liposomes' probe in the Supplementary Data. Thus, DCs that internalized ST-liposomes and SM-liposomes had more co-stimulatory molecules than iDCs. In the same way as us, Ma, *et al.* [62] showed that cationic liposomes with a high positive charge density potently enhanced dendritic cell maturation and antigen uptake. Additionally, Korsholm, *et al.* [63] showed that cationic liposomes composed by dimethyldioctadecylammonium (DDA) and ovalbumin (OVA) were effective on maturation of murine bone marrow- derived dendritic cells (BM-DCs) related to the expression of surface molecules of major histocompatibility complex (MHC) class II, CD40, CD80 and CD86.

3.5.2. T lymphocytes proliferation

Aiming to confirm that DCs are able to present antigens to T lymphocytes after internalization of ST- and SM-liposomes after optimization, allogeneic T lymphocyte were co-cultured with DCs inducing T lymphocytes proliferation. “Anexo II” presents the complementary analyses generate by T lymphocytes proliferation.

We showed the T lymphocytes proliferation by histograms of CFSE intensity (Figure 4-12) in which the positive control of proliferation assay was compared with the T lymphocytes proliferation co-cultured with DCs stimulated by ST-liposomes or SM-liposomes after optimization. The CFSE is a stable cytoplasmic fluorescent dye that is segregated equally between daughter cells after cell division, therefore when T lymphocytes proliferate dilute the amount of CFSE causing a decrease in fluorescence intensity of the dye.

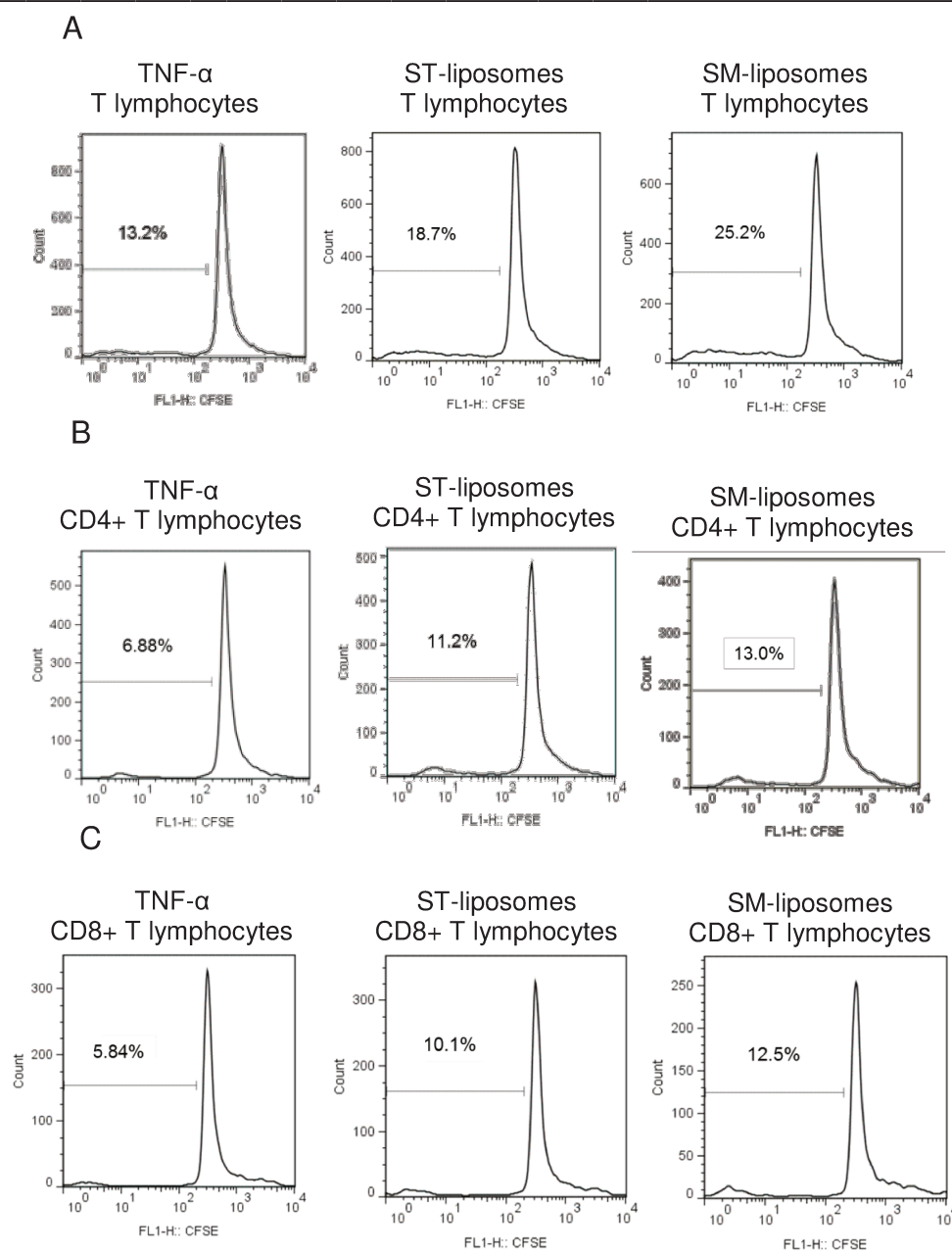


Figure 4-12 - Histograms of CFSE (carboxyfluorescein diacetate succinimidyl ester) dilution representing proliferation of total T lymphocytes (A), CD4⁺ T lymphocytes (B) and CD8⁺ T lymphocytes (C), when co-cultured with allogeneic DCs stimulated by TNF- α (positive control) and when co-cultured with allogeneic DCs stimulated by ST-liposomes after optimization (final lipid concentration of 2 mM, stirring rate of 11,000 rpm and injection flow of 44.4 mL/min) or by SM-liposomes after optimization (850 bar and 1 cycle passage).

Thus, with the aid of histograms of CFSE intensity, we realized that T lymphocytes proliferation were better when T lymphocytes were co-cultured with DCs

stimulated by ST-liposomes or SM-liposomes than when T lymphocytes were co-cultured with DCs stimulated by TNF- α . 13.2% of T Lymphocytes proliferated when TNF- α was involved, 18.7% when ST-liposomes was involved and 25.2% when SM-liposomes was involved (Figure 4-12 A). When considering just CD4⁺ T lymphocytes, 6.88% had CFSE dilution when stimulated with DCs activated with TNF- α compared to 11.2% when stimulated with DCs treated with ST-liposomes and to 13.0% when stimulated with DCs treated with SM-liposomes (Figure 4-12 B). CD8⁺ T lymphocytes proliferation were greater when stimulated with DCs treated with ST-liposomes (10.1%) and SM-liposomes (12.5%) when compared with DCs activated with TNF- α (5.84%) (Figure 4-12 C).

Thus, the use of ST-liposomes to stimulate DCs increase proliferation of CD4⁺ and CD8⁺ T Lymphocytes in approximately 1.5 times compared with the TNF- α stimulus. And the use of SM-liposomes to stimulate DCs increase proliferation of CD4⁺ and CD8⁺ T Lymphocytes in approximately 2 times compared with the TNF- α stimulus. These results indicate that ST- and SM-liposomes after optimization have a promising future as gene delivery systems for cells, like dendritic cells.

4. **Conclusion**

The results presented here demonstrate the feasibility of the production of EPC/DOTAP/DOPE by the scalable ethanol injection method for *in vitro* applications of gene therapy. The effects of ethanol mass transfer and interaction forces between phospholipids imposed for the production of liposomes by the ethanol injection method influence the formation of the liposomes' phospholipid bilayer fragments (*i.e.*, the precursors of liposomes). At the same lipid concentration, greater stirring rates decrease the size of liposomes and increase their polydispersity, whereas greater injection flow rates decrease the size of liposomes size and their polydispersity. Furthermore, for an ethanol injection system with the same stirring and injection flow rates, the size and polydispersity of liposomes increase at high lipid concentrations.

Furthermore, biological assays showed that ST-liposomes after optimization (final lipid concentration of 2 mM, stirring rate of 11,000 rpm and injection flow of 44.4 mL/min) and SM-liposomes after optimization (850 bar and 1 cycle passage) were able to stimulate and activate DCs, and DCs which internalized the liposomes induced higher T lymphocytes proliferation. Therefore, demonstrating that ST- and SM-liposomes after optimization have a promising future as gene delivery systems for cells that internalized nanoparticles in the same way as dendritic cells.

The insights gained from these results will contribute to a better understanding of the formation mechanisms of cationic liposomes produced by the scalable method of ethanol injection. In addition, these results demonstrate that the physico-chemical and morphological properties of these scalable liposomes render them suitable for *in vitro* applications.

5. **Acknowledgements**

We thanks to Dr. Barbuto's Lab staff to technical support. We are grateful for ideas and encouragement of Dr. Maria Helena A. Santana to explore the ethanol injection method. The study was financially supported by the Fundação de Amparo à Pesquisa do Estado de São Paulo (FAPESP).

6. **References**

- | | |
|--|---|
| [1] S. Das, L. Yu, C. Gaitatzes, R. Rogers, J. Freeman, J. Bienkowska, R.M. Adams, T.F. Smith, J. Lindelien, <i>Nature</i> 385 (1997) 29-30. | [7] F.E. Antunes, E.F. Marques, M.G. Miguel, B. Lindman, <i>Adv. Colloid Interface Sci.</i> 147-148 (2009) 18-35. |
| [2] T. Friedmann, <i>Nat. Med.</i> 2 (1996) 144-147. | [8] E.J.M. Filipe, <i>Revista de Cultura Científica</i> (1996) 25-38. |
| [3] I.M. Verma, M.D. Weitzman, <i>Annu Rev Biochem</i> 74 (2005) 711-738. | [9] J.W. Park, C.C. Benz, F.J. Martin, <i>Seminars in oncology</i> 31 (2004) 196-205. |
| [4] A.D. Miller, <i>IDrugs</i> 1 (1998) 574-583. | [10] C.R. Dass, P.F. Choong, <i>J Control Release</i> 113 (2006) 155-163. |
| [5] F.D. Ledley, <i>Hum. Gene Ther.</i> 6 (1995) 1129-1144. | [11] T. Serikawa, A. Kikuchi, S. Sugaya, N. Suzuki, H. Kikuchi, K. Tanaka, <i>J Control Release</i> 113 (2006) 255-260. |
| [6] X. Gao, L. Huang, <i>Gene Ther.</i> 2 (1995) 710-722. | |

- [12] C.R. Dass, *Int. J. Pharm.* 241 (2002) 1-25.
- [13] L. TECHNOLOGIES, Which Lipofectamine® Transfection Reagent is Right for You? . <http://www.invitrogen.com/site/us/en/home/brands/Product-Brand/lipofectamine.html> [accessed July 15 2012].
- [14] C. Magin-Lachmann, G. Kotzamanis, L. D'Aiuto, H. Cooke, C. Huxley, E. Wagner, *The Journal of Gene Medicine* 6 (2004) 195-209.
- [15] D.J. Porteous, J.R. Dorin, G. McLachlan, H. Davidson-Smith, H. Davidson, B.J. Stevenson, A.D. Carothers, W.A. Wallace, S. Moralee, C. Hoenes, G. Kallmeyer, U. Michaelis, K. Naujoks, L.P. Ho, J.M. Samways, M. Imrie, A.P. Greening, J.A. Innes, *Gene Ther.* 4 (1997) 210-218.
- [16] L. TECHNOLOGIES, Lipofectin® Transfection Reagent. <http://products.invitrogen.com/ivgn/product/18292037> [accessed July 15 2012].
- [17] V. Niborski, Y. Li, F. Brennan, M. Lane, A.M. Torché, M. Remond, M. Bonneau, S. Riffault, C. Stirling, G. Hutchings, H. Takamatsu, P. Barnett, B. Charley, I. Schwartz-Cornil, *Vaccine* 24 (2006) 7204-7213.
- [18] Y. Kang, X.-Y. Zhang, W. Jiang, C.-Q. Wu, C.-M. Chen, J.-R. Gu, Y.-F. Zheng, C.-J. Xu, *Cell Biol. Int.* 33 (2009) 509-515.
- [19] D.S. Conti, B. Bharatwaj, D. Brewer, S.R.P. da Rocha, *J. Controlled Release* 157 (2012) 406-417.
- [20] N. Nukumi, K. Ikeda, M. Osawa, T. Iwamori, K. Naito, H. Tojo, *Dev. Biol.* 274 (2004) 31-44.
- [21] M. Chaudhri, M. Scarabel, A. Aitken, *Biochem. Biophys. Res. Commun.* 300 (2003) 679-685.
- [22] D.L. McKenzie, K.Y. Kwok, K.G. Rice, *J Biol Chem* 275 (2000) 9970-9977.
- [23] Y. Perrie, P.M. Frederik, G. Gregoriadis, *Vaccine* 19 (2001) 3301-3310.
- [24] R.S. Rosada, L.G. De La Torre, F.G. Frantz, A.P. Trombone, C.R. Zarate-Blades, D.M. Fonseca, P.R. Souza, I.T. Brandao, A.P. Masson, E.G. Soares, S.G. Ramos, L.H. Faccioli, C.L. Silva, M.H. Santana, A.A. Coelho-Castelo, *BMC Immunol* 9 (2008) 38.
- [25] R.S. Rosada, C.L. Silva, M.H. Santana, C.R. Nakaie, L.G. De La Torre, *J. Colloid Interface Sci.* 373 (2012) 102-109.
- [26] L.G. De La Torre, R.S. Rosada, A.P.F. Trombone, F.G. Frantz, A.A.M. Coelho-Castelo, C.L. Silva, M.H.A. Santana, *Colloids Surf. B. Biointerfaces* 73 (2009) 175-184.
- [27] T.A. Balbino, A.A.M. Gasperini, C.L.P. Oliveira, A.R. Azzoni, L.P. Cavalcanti, L.G. De La Torre, *Langmuir* 28 (2012) 11535-11545.
- [28] F.L. Sorgi, L. Huang, *Int. J. Pharm.* 144 (1996) 131-139.
- [29] J.E. Trevisan, L.P. Cavalcanti, C.L.P. Oliveira, L.G. De La Torre, M.H.A. Santana, in: X.-b. Yuan, *Non-Viral Gene Therapy*; InTech, 2011, p 267-292.
- [30] D.D. LASIC, *Liposomes: From physics to applications*. Elsevier Science Publishers B.V. , Amsterdam, 1993.
- [31] R.R.C. New, *Liposomes: A practical approach*. IRL Press, Oxford University Press, 1994.
- [32] L.G. Torre, A.L. Carneiro, R.S. Rosada, C.L. Silva, M.H.A. Santana, *Brazilian Journal of Chemical Engineering* 24 (2007) 477-486.
- [33] H. Tournier, M. Schneider, C. Guillot, *Liposomes with enhanced entrapment capacity and their use in imaging Patent US5980937(1999)*.
- [34] G.P. Alves, M.H.A. Santana, *Powder Technol.* 145 (2004) 139-148.
- [35] A. Jahn, W.N. Vreeland, D.L. DeVoe, L.E. Locascio, M. Gaitan, *Langmuir : the ACS*

- journal of surfaces and colloids 23 (2007) 6289-6293.
- [36] A. Jahn, W.N. Vreeland, M. Gaitan, L.E. Locascio, *J. Am. Chem. Soc.* 126 (2004) 2674-2675.
- [37] A. Wagner, K. Vorauer-Uhl, G. Kreismayr, H. Katinger, *J Liposome Res* 12 (2002) 259-270.
- [38] E. Pupo, A. Padron, E. Santana, J. Sotolongo, D. Quintana, S. Duenas, C. Duarte, M.C. de la Rosa, E. Hardy, *J Control Release* 104 (2005) 379-396.
- [39] J.M.H. Kremer, M.W. Van der Esker, C. Pathmamanoharan, P.H. Wiersema, *Biochemistry (Mosc)*. 16 (1977) 3932-3935.
- [40] Y. Maitani, S. Igarashi, M. Sato, Y. Hattori, *Int. J. Pharm.* 342 (2007) 33-39.
- [41] W. De Haes, G. Van Mol, C. Merlin, S.C. De Smedt, G. Vanham, J. Rejman, *Mol Pharm* 9 (2012) 2942-2949.
- [42] M.T. Vitor, P.C. Bergami-Santos, J.A. Barbuto, L.G. De La Torre, *Recent Pat Drug Deliv Formul* (2012 (*in press*)).
- [43] I. Strobel, S. Berchtold, A. Götze, U. Schulze, G. Schuler, A. Steinkasserer, *Gene Ther.* 7 (2000) 2028-2035.
- [44] P. Morel, M. FEILI-HARIRI, P. Coates, A.W. Thomson, *Clin. Exp. Immunol.* 133 (2003) 1-10.
- [45] T.M. Allen, G.A. Austin, A. Chonn, L. Lin, K.C. Lee, *Biochim Biophys Acta* 1061 (1991) 56-64.
- [46] D. Papahadjopoulos, T.M. Allen, A. Gabizon, E. Mayhew, K. Matthay, S.K. Huang, K.D. Lee, M.C. Woodle, D.D. Lasic, C. Redemann, et al., *Proc Natl Acad Sci U S A* 88 (1991) 11460-11464.
- [47] J. Rejman, V. Oberle, I.S. Zuhorn, D. Hoekstra, *Biochem J* 377 (2004) 159-169.
- [48] J. Kristl, K. Teskac, C. Caddeo, Z. Abramovic, M. Sentjurc, *Eur. J. Pharm. Biopharm.* 73 (2009) 253-259.
- [49] M. Licciardi, D. Paolino, C. Celia, G. Giammona, G. Cavallaro, M. Fresta, *Biomaterials* 31 (2010) 7340-7354.
- [50] M.S. Muthu, S.A. Kulkarni, A. Raju, S.S. Feng, *Biomaterials* 33 (2012) 3494-3501.
- [51] S. Neron, J.A. Correa, E. Dajczman, G. Kasymjanova, H. Kreisman, D. Small, *Support. Care Cancer* 15 (2007) 1207-1212.
- [52] J.A. Barbuto, L.F. Ensina, A.R. Neves, P. Bergami-Santos, K.R. Leite, R. Marques, F. Costa, S.C. Martins, L.H. Camara-Lopes, A.C. Buzaid, *Cancer immunology, immunotherapy* : CII 53 (2004) 1111-1118.
- [53] P. Gentine, A. Bubel, C. Crucifix, L. Bourel-Bonnet, B. Frisch, *J Liposome Res* 22 (2012) 18-30.
- [54] A. Jahn, W.N. Vreeland, D.L. De Voe, L.E. Locascio, M. Gaitan, *Langmuir* 23 (2007) 6289-6293.
- [55] T.A. Balbino, N.T. Aoki, A. Gasperini, C.L.P. Oliveira, L.P. Cavalcati, A.R. Azzoni, L.G. De La Torre, (submitted 2012).
- [56] J.M. Zook, W.N. Vreeland, *Soft Matter* 6 (2010) 1352-1360.
- [57] O. Diat, D. Roux, F. Nallet, *Journal De Physique II* 3 (1993) 1427-1452.
- [58] R. Barnadas-Rodriguez, M. Sabes, *Int. J. Pharm.* 213 (2001) 175-186.
- [59] G. Gregoriadis, H. da Silva, A.T. Florence, *Int. J. Pharm.* 65 (1990) 235-242.
- [60] D.F. Evans, H. Wennerström, *The Colloidal Domain - Where Physics, Chemistry, Biology, and Technology Meet.* 2nd ed., Wiley-vch, USA, 1999.
- [61] T.P. Rigoletto, C.L. Silva, M.H. Santana, R.S. Rosada, L.G. De La Torre, *J. Microencapsul.* 29 (2012) 759-769.
- [62] Y. Ma, Y. Zhuang, X. Xie, C. Wang, F. Wang, D. Zhou, J. Zeng, L. Cai, *Nanoscale* 3 (2011) 2307-2314.

- [63] K.S. Korsholm, E.M. Agger, C. Foged, D. Christensen, J. Dietrich, C.S. Andersen, C. Geisler, P. Andersen, Immunology 121(2007)216-226.

7. Supplementary data

7.1. Strategy of dendritic cells analysis

For phenotypic characterization and evaluation of the liposomes incorporation, we delimited gate with cell size and granularity compatible with the DCs, by analysis "side scatter" (SSC) - granularity (internal structure and complexity) and the "forward scatter" (FSC) - relative size of the cells (Figure 4-13 A). Considering the analyzed region bounded by the gate, cells were analyzed through the expression of myeloid cells and antigen presenting cells markers, respectively CD11c and HLA-DR. Furthermore, when we analyzed the expression of co-stimulatory molecules within this population HLA-DR⁺CD11c⁺, called Gate R1 (Figure 4-13 B), we observed that cells also showed expression of CD86 (described below). This procedure was performed for all samples presenting dendritic cells marked, such as dendritic cells stimulated by TNF- α (positive control - mDC), or by ST-liposomes after optimization or by SM-liposomes after optimization.

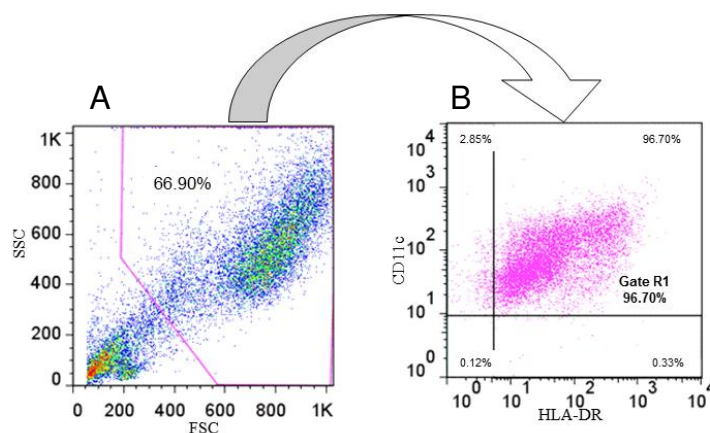


Figure 4-13 – Strategy of dendritic cells analysis. (A) Dot Plot graph of SSC (side scatter) by FSC (forward scatter) to delimit DCs gate. (B) Graph of CD11c versus HLA-DR to delimit Gate R1, corresponding to cells double-positive.

7.2. Dendritic cells activation by liposomes

In order to evaluate the dendritic cells activation by liposomes, it was plotted graphics of CD86 versus liposomes' probe (Figure 4-14) of dendritic cells stimulated

by TNF- α (positive control - mDC) or by ST-liposomes or SM-liposomes. They showed that 48.1% of DCs had internalized ST-liposomes and presented CD86, while 41.2% of DCs had internalized SM-liposomes and presented CD86.

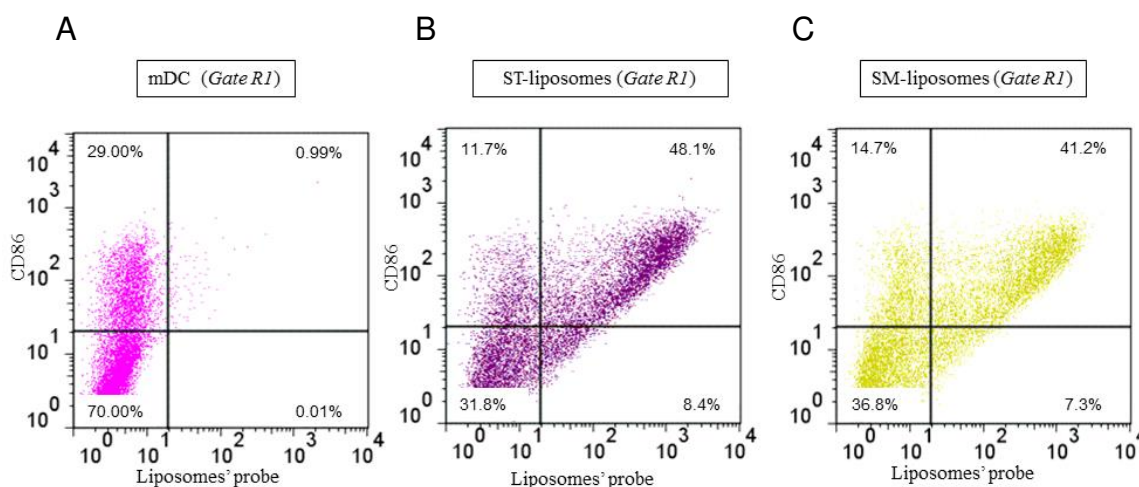


Figure 4-14 - Graphics CD86 versus liposomes' probe of dendritic cells (A) stimulated by TNF- α (positive control - mDC), or by (B) ST-liposomes after optimization (final lipid concentration of 2 mM, stirring rate of 11,000 rpm and injection flow of 44.4 mL/min) or (C) SM-liposomes after optimization (850 bar and 1 cycle passage).

Capítulo 5 - Cationic Liposomes incorporated with RNA from Human Breast Carcinoma (SK-BR-3) Internalized by Dendritic Cells

Micaela Tamara Vitor, BS^a; Patrícia Cruz Bergami-Santos, PhD^b; José Alexandre Marzagão Barbuto, PhD^b; Karen Steponavicius Piedade Cruz, BS^b; Mariana Pereira Pinho, BS^b; Lucimara Gaziola de La Torre, PhD^{a*}

^aSchool of Chemical Engineering, Department of Materials and Bioprocess Engineering, University of Campinas (Unicamp), Av. Albert Einstein, 500, Campinas, SP, 13083-852, Brazil.

^bInstitute of Biomedical Sciences, Department of Immunology, University of São Paulo (USP), Av. Prof. Lineu Prestes, 1730, São Paulo, SP, 05508-000, Brazil.

*Corresponding author:

School of Chemical Engineering, Department of Materials and Bioprocess Engineering, University of Campinas (Unicamp), Av. Albert Einstein, 500, Campinas, SP, 13083-852, Brazil.

Fax number: + 55 19 3521-3910

Telephone number: + 55 19 3521-0397

E-mail address: latorre@feq.unicamp.br

To be submitted to *Nanomedicine: Nanotechnology, Biology, and Medicine*

Abstract

We investigated the effects of cationic liposomes incorporated with RNA from SK-BR-3 upon dendritic cells (DCs) differentiation/maturation *in vitro*, RNA transfection and in T lymphocytes proliferation induced by DCs. The cationic liposomes composed by egg phosphatidylcholine (EPC), 1,2-dioleoyl-3-trimethylammonium propane (DOTAP) and 1,2-dioleoylphosphatidylethanolamine (DOPE) (50/25/25% molar) were prepared *via* thin film method followed by extrusion (ELs) and *via* the ethanol injection method (ST-liposomes). Total RNA from SK-BR-3 cell line, derived from a human breast carcinoma overexpressing HER-2/*neu*, were incorporated into ELs and ST-liposomes at cationic lipid/RNA anionic molar charge ratio 15 (119.2 nm, polydispersity of 0.18; and 123.6 nm, polydispersity of 0.32). The phenotypic analysis of DCs and the analysis of T lymphocytes proliferation showed that both cationic liposomes complexes were incorporated by DCs, and that DCs which internalized

complexes, provided T lymphocytes proliferation. These RNA/cationic liposomes complexes could contribute to new strategies in cancer immunotherapy.

Keywords: cationic liposomes, ethanol injection method, dendritic cells, RNA, human breast carcinoma.

1. **Background**

Gene therapy is a promising strategy for the treatment of human diseases, however vectors are necessary to transport or deliver the therapeutic gene or nucleic acid inside the proper cells. Vectors for gene therapy are divided in two categories, viral and nonviral, in which viral vectors have potential hazards and need to be replaced by an efficient nonviral gene delivery system for successful gene-based therapies and nucleic acid delivery to cells.^{1, 2} Nonviral vectors have several advantages over viral vectors particularly from the viewpoints of safety and commercial production.³ Within nonviral vectors, cationic liposomes are able to form complexes with nucleic acids (DNA or RNA), helping them to cross the cellular membranes and delivering them into cells. Liposomes are colloidal systems formed from the self-assembly of phospholipids, generating bilayer structures (similar to biological membranes) that in excess of water aggregates in vesicles. The interesting property of cationic liposomes opens several applications in gene delivery and vaccines, particularly in cancer immunotherapy.⁴

Currently, various efforts in scientific research are being conducted to establish different procedures to combat and treat cancer.⁵⁻⁸ Cancer immunotherapy emerges as a promising strategy to improve efficiency over the conventional treatments, which goals are the enhancement of patient's immune response,⁹ to contain the growth of tumors.¹⁰ However, generally, tumors create environments that are prone to induce tolerance to tumor antigens, thus avoiding the involvement of the immune system in their control.¹¹ In this context, dendritic cells (DCs), antigen-presenting cells,¹² have an important role, since they are able to present the antigens therein to T lymphocytes in the secondary lymphoid organs,¹³ recruiting the immune system to

fight against the tumor cells.¹⁴ Therefore, the generation of mature DCs *in vitro*¹⁵ loaded with RNA coding the tumor antigen(s) allow DCs to present antigenic peptides on their surface which are recognizable by specific T lymphocytes receptors, thus being able to induce T lymphocytes activation and the consequent immune response against tumor.¹⁶

Nevertheless, the loading of DCs with the tumor antigen(s) is a crucial step^{17, 18} which can interfere with antigen presentation by DCs. This process can occur by incubating DCs with RNA but it showed low efficiency of RNA transfer (measured by gene expression), and no doubt reflects the sensitivity of the immune system to recognize minute amounts of antigens not detectable by conventional means.¹⁹ Another method to introduce RNA into DCs was described using electroporation which does not require additional reagents and is compatible with clinical use, even though DCs subjected to electroporation become fragile and need special care to be recovered.¹⁷ In addition, cationic liposomes have been used to delivery nucleic acids into DCs, due to their reproducibility, commercial availability and safety of use.²⁰ In the first study, using mRNA-transfected DCs to stimulate immune responses in mice, RNA was transfected into murine DCs with the use of the cationic lipid 1,2-dioleoyloxy-3-trimethylammonium propane (DOTAP).²¹ Afterward, cationic liposomes composed by DOTAP lipid were used to deliver tumor extracts into dendritic cells,²² to pulse DCs with tumor mRNA²³ and to transfect DCs with MUC1 RNA and IL-12 for vaccination.²⁴ Grunebach and co-workers²⁵ analyzed the efficiency of tumor RNA transfection into DC using cationic liposomes (Unifectin), and suggested that this technology has the potential to induce cytotoxic T lymphocytes.

Nucleic acids-cationic liposomes complexes are spontaneously formed due to the electrostatic association between positive charges of cationic lipids and the negative charges of nucleic acids, even so the final liquid charge of complex is positive, allowing their interaction with the negatively charged cells surface.²⁶ Nakanishi and co-workers²⁷ investigated the relationship between the charge on liposomes' surface and its adjuvant action, and the results indicated that the positive

charge on the surface of liposomes represents an important factor for enhancing their immunoadjuvancy in the induction of antigen-specific immune response. They also reported that positively charged liposomes containing soluble antigens functioned as a more potent inducer of antigen-specific T lymphocyte responses and delayed-type hypersensitivity responses than anionic and neutral liposomes containing the same concentration of antigens.²⁸

However, the cationic characteristic of lipids is well known as cytotoxic to cells requiring careful optimization of the transfection protocol, therefore the molar ratio between nucleic acids/cationic lipids and the used concentration must be optimized.^{17, 29} Perrie, Frederik and Gregoriadis³⁰ studied a strategy to overcome this cytotoxicity by incorporating egg phosphatidylcholine (EPC) in the liposomes composed by the cationic lipid 1,2-dioleoyl-3-trimethylammonium propane (DOTAP) and 1,2-dioleoylphosphatidylethanolamine (DOPE); the results demonstrated the potential of this composition as non-viral system for DNA delivery against Hepatitis B. Later, our research group^{31, 32} demonstrated the *in vivo* efficacy of the cationic liposomes EPC/DOTAP/DOPE (50/25/25% molar) for gene vaccination against tuberculosis. Additionally, this vaccine showed low cytotoxicity *in vitro* on mice J774-macrophage cell line and potential utilization in gene vaccination by the intranasal route.³³ More recently, these cationic liposomes complexed with pDNA in various proportions were studied in their ability to transfect HeLa cells *in vitro*, showing important differences when the molar charge ratio was varied.³⁴

Despite the potentiality of cationic liposomes EPC/DOTAP/DOPE, it must be taken into account that the scalable process to produce them is still a challenge. The scalable methods for liposomes production tend to be variable, which is a drawback for pre-clinical and clinical assays, since the reproducibility of the formulation is a primordial necessity.^{35, 36} Process modifications and purity of lipids may alter the final liposomes physico-chemical properties³⁷ and as consequence, the cellular uptake. Therefore, the interest in developing scale processes, which reproduce the physico-chemical and biological properties of the previously liposomes prepared on a

laboratory scale, is increasing.³⁶ In this context, the ethanol injection method has emerged as a potential technique for the scale-up of EPC/DOTAP/DOPE cationic liposomes. Conventional ethanol injection consists on the controlled addition of an ethanol/lipid solution to a batch reactor that contains a buffer or water under controlled stirring³⁶. Maitani *et al.*³⁸ showed that cationic liposomes composed by 3 β -[N-(N',N'-dimethylaminoethane)-carbonyl] cholesterol (DC-Chol) and DOPE prepared *via* modified ethanol injection method were better to transfect DNA in HeLa cells than liposomes prepared *via* a dry film method (laboratory process).

Thus, our aim in this study was to investigate the effects of these cationic liposomes EPC/DOTAP/DOPE (50/25/25% molar) obtained *via* thin film method followed by extrusion (ELs) and *via* ethanol injection method (ST-liposomes) incorporated with RNA of SK-BR-3 upon dendritic cells differentiation/maturation *in vitro* and RNA transfection. The main goal is the comparison between the effect of laboratory method (thin film/extrusion process) and scalable process (ethanol injection method) on RNA incorporation in liposomes and their uptake by DCs aiming at the development of new alternatives for the cancer immunotherapy. We selected SK-BR-3 cell line delivered from human breast cancers that overexpress the proto-oncogene *Her-2/neu* to obtain total RNA since this tumor antigen is presented in a variety of human carcinomas, including ovarian and breast cancer.³⁹ In addition, Kaufman *et al.*⁴⁰ observed that more than 50% of cases of relapsed metastatic disease present this tumor antigen. Thus, *Her-2/neu* is an attractive therapeutic target, since its overexpression appears to be stable over time and researches suggest that its overexpression at the primary site of disease correlates strongly with at metastatic sites.⁴¹ For this purpose, liposomes incorporated with RNA were characterized in their physico-chemical properties, such as mean hydrodynamic size distribution, zeta potential and morphology. And then, they were *in vitro* evaluated for their ability to be internalized and to stimulate dendritic cells differentiation/maturation, to transfect RNA in DCs and to induce T lymphocyte proliferation by DCs.

2. **Methods**

Egg phosphatidylcholine (EPC) (96% of purity), 1,2-dioleoyl-sn-glycero-3-phosphoethanolamine (DOPE) (99.8% of purity) and 1,2-dioleoyl-3-trimethylammonium-propane (DOTAP) (98% of purity) were purchased from Lipoid Germany and used without further purification, for liposomes production.³⁷ The lipid fluorescent probe 1,2-dioleoyl-sn-glycero-3-phosphoethanolamine-N-(carboxyfluorescein) (FITC) (Avanti® Polar Lipids, Inc.) was used in cationic liposomes composition to visualize DCs that incorporated the liposomes, in flow cytometry. The specific fluorescent antibodies to Her-2/*neu*, CD11c, CD80, CD86, CD274, CD40, HLA-DR, CD4 and CD8 from BD Biosciences used in phenotypic analysis of DCs and analysis of subpopulations of T lymphocytes, in flow cytometry.

2.1. **Liposomes preparation**

2.1.1. **Liposomes preparation using thin film method followed by extrusion**

The extruded liposomes (ELs) were obtained *via* thin film method,⁴² followed by hydration with PBS buffer and then by an extrusion step. Briefly, stock solutions for each of lipids (EPC, DOTAP, DOPE) were prepared in chloroform and stored at -20 °C. Those lipid solutions were added in the required amounts (EPC/DOPE/DOTAP 50/25/25% molar), mixed and dried to a thin film using a rotary evaporator (ART LAB) in a 650 mmHg vacuum for 1 hour. The dried lipid film was hydrated with PBS buffer for 40 minutes to reach a concentration of 16 mM at 30°C, above its phase transition temperature. The liposomes were extruded (Lipex Biomembranes Inc., model T.001) through two stacked polycarbonate membranes (100 nm nominal diameter) 15 times at a nitrogen pressure of 12 kgf/cm². The cationic liposomes obtained *via* the thin film method followed by extrusion (ELs) were stored at 8 °C for at least 2 hours before physico-chemical characterization.

2.1.2. Liposomes preparation using ethanol injection method

The ST-liposomes were obtained *via* scalable ethanol injection method. Briefly, the ethanol/lipid suspension at 62.5 mM composed of a mixture of the lipids EPC/DOPE/DOTAP (50/25/25% molar) with ethanol in a glass syringe was fed at a previously defined injection flow through a syringe pump into the bottom of a 150 mL reactor with four baffles and that contained PBS buffer. A continuous mechanical stirring rate was provided by an Ultra-Turrax®. The colloidal dispersion was dispersed by being stirred in the Ultra-Turrax® at a stirring rate of 11,000 rpm; the injection flow was 44.4 mL/min, and the obtained final lipid concentration was 2 mM.³⁶ After the feeding was complete, stirring was maintained for an additional 15 min. The cationic liposomes obtained *via* the ethanol injection method (ST-liposomes) were stored at 8 °C for at least 2 hours before physico-chemical characterization.

2.2. SK-BR-3 cell line cultivation, isolation of RNA from SK-BR-3 and preparation of RNA/cationic liposomes complexes

The HER-2/*neu* overexpressing SK-BR-3 cell line, derived from a human breast carcinoma was maintained cryopreserved in liquid nitrogen. The cells were cultured in medium R-10, which consisted of RPMI 1640 culture medium (GIBCO™, Grand Island, NY, EUA) supplemented with 10% fetal bovine serum and 1% of antibiotic-antimycotic solution. Then, cells were seeded in 75 cm² flasks and incubated at 37 °C with 5% CO₂ to form a monolayer and used in subsequent experiments. The total RNA was isolated from the samples using TRIzol® Reagent (Invitrogen, California, USA), as described in manufacturer's protocol. After that, RNA samples were their concentration quantified and qualified on the Nanodrop ND-1000, and RNA samples were stored on ice or – 80 °C to minimize degradation. RNA/cationic liposomes complexes were obtained by adding the appropriate amount of RNA to cationic liposome, in an ice bath under intense vortexing at 4 °C for at least 40 seconds, forming RNA/ELs and RNA/ST-liposomes.^{31, 33} RNA/cationic liposomes complexes were prepared at different cationic lipid:RNA molar charge ratios

($R_{+/-}$ = 5,7,10 and 15).⁴³ The molar charge ratio was defined by the number cationic-charge moles, in this case DOTAP moles, divided by the number of negative charge moles from the DNA, which can be used analogously to RNA.⁴³

2.3. Physico-chemical characterization of RNA/cationic liposomes complexes

2.3.1. Average hydrodynamic diameter and zeta potential

The average hydrodynamic diameter and size distribution were determined by dynamic light scattering (Malvern Zetasizer Nano ZS) using a Ne–He laser and measurements at a scattering angle of 173°. The particle's diameter was calculated from the translational diffusion coefficient by using the Stokes–Einstein equation (Equation 5-1).

$$d(H) = \frac{(kT)}{3\pi\eta D} \quad (\text{Equation 5-1})$$

where $d(H)$ is the hydrodynamic diameter; D is the translational diffusion coefficient; k is the Boltzmann's constant, T is the absolute temperature and η is the solvent viscosity. The mean diameter and distribution of particle sizes were estimated by CONTIN algorithm analysis. The intensity-weighted and number-weighted mean diameter and particle distribution were obtained in triplicate. The zeta potential was measured on the same equipment by diluting cationic liposomes in the appropriate volume of water at 25 °C.

2.3.2. Morphology

The morphology of the ST-liposomes and ELs incorporated with RNA were visualised with a negative staining technique using transmission electron microscopy (TEM). Carbon-coated 200-mesh copper grids with collodion (parloidin with cellulose acetate) films were used. Each liposome preparation was diluted to 0.5 mM total lipids and then applied to the carbon grid. After incubation for 5 min at room temperature, the excess was blotted. One drop of uranyl acetate (1% w/v) in water was added to the carbon grid and incubated for 1 min at room temperature before the

excess was blotted and the grid was air-dried. A Carl Zeiss CEM 902 (Germany) microscope was operated at 80 kV. The images were acquired using a CCD camera (Proscan), and the platform acquisition was iTem.

2.4. Biological evaluation of liposomal structures incorporated with RNA

2.4.1. Differentiation *in vitro* of dendritic cell derived from monocytes

Peripheral blood mononuclear cells (PBMCs) were collected from healthy unrelated volunteers through apheresis performed in a TRIMA ACCEL (Cobe BCT, Denver, CO, USA),⁴⁴ at the Hospital Alemão Oswaldo Cruz, São Paulo, Brazil, after informed consent of donors. For enrichment of mononuclear cells, the product of apheresis was submitted to a separation with a density gradient (Ficoll-Paque from GE Healthcare Bio-Sciences AB, Upsala, Sweden) for 30 minutes at 900 G, 18 °C. Mononuclear cells were collected and centrifuged at 290 G for 10 minutes, 18 °C for 3 times with RPMI-1640 medium. After this process, the mononuclear cells were seeded in 6-well plate (5×10^6 cells/well) in RPMI 1640 culture medium and incubated at 37 °C and 5% CO₂ for 2 hours. After this period, non-adherent cells were removed and the RPMI medium was replaced by a R-10 medium supplemented with 50 ng/mL IL-4 and 50 ng/mL GM-CSF (PeproTech, Rocky Hill, NJ, USA). After 5 days in culture, the cells were stimulated with TNF-alpha (50 ng/mL; PeproTech, Rocky Hill, NJ, USA) as a positive control for DCs maturation/activation (mDC - mature DC) or stimulated by cationic liposomes (ELs or ST-liposomes) or by RNA/cationic liposomes complexes (ELs or ST-liposomes incorporated with RNA (1 mM, $R_{+/-}=15$)), all labeled with fluorescent probe (FITC-carboxyfluorescein, Avanti-Lipids, USA) to analyze liposomes' internalization by DCs through flow cytometry. As a negative control group (iDC – immature DC), no stimulus was added to the medium. After 2 days in culture, *i.e.* the transfection time was two days, cells were harvested and labeled with specific fluorescent antibodies for analysis by flow cytometry (BD FACSCalibur™).¹⁴

2.4.2. Allogeneic T lymphocyte proliferation assay

T lymphocytes were purified from non-adherent cells removed after 2 hours incubation of mononuclear cells for DCs generation using negative selection with immunomagnetic beads (CD14, CD16, CD19, CD36, CD56, CD123, and Glycophorin A) (Pan T Cell Isolation Kit II, Miltenyi Biotec, Bergisch Gladbach, Germany), following the manufacturer's recommendations. For induction of allogeneic T lymphocyte proliferation, purified T lymphocytes (1×10^5 cells/well) were co-cultured with DCs (1×10^4 cells/well), stimulated by TNF-alpha or by ELs and ST-liposomes incorporated with RNA (1 mM, $R_{+/-}=15$), in U-bottom 96-well microplates. T Lymphocytes were previously stained with 10 μ M of carboxyfluorescein diacetate succinimidyl ester (CellTrace CFSE Cell Proliferation Kit – Invitrogen Dinal AS, Oslo, Norway) to track cell proliferation. After 5 days in culture, cells were harvested, stained with CD4 and CD8 antibodies, and analyzed in the flow cytometry (BD FACSCalibur™).

2.4.3. Flow cytometry and florescence images

Dendritic cells preparations (2×10^5 cells/well/condition) were labeled with each of the specific fluorescent antibodies: Her-2/*neu*, CD11c, CD80, CD86, CD274, CD40 and HLA-DR (BD Biosciences) for phenotypic analysis and to assess the incorporation of liposomes by DCs. T lymphocyte co-cultured with DCs were labeled with the specific fluorescent antibodies CD4 and CD8 (BD Biosciences) to assess the proliferation of T lymphocytes subpopulations. Then, the labeled cells were analyzed by flow cytometry in FACSCallibur with CellQuest software. At least 10,000 events were acquired per antibody analyzed. The data was analyzed by FlowJo 7.6 software (Tree Star Inc., USA).¹⁴

Then, dendritic cells stimulated with cationic liposomes (ELs and ST-liposomes) and RNA/cationic liposomes complexes (RNA/ELs and RNA/ST-liposomes complexes), all labeled with fluorescent probe, had their fluorescence

images taken at different positions using the fluorescence microscope Nikon Eclipse Ti-S (Nikon, Melville, NY, USA) with NIS-Elements AR software (Nikon).

3. Results

3.1. Physico-chemical characterization of RNA/cationic liposomes complexes

The physico-chemical properties of the RNA/cationic liposomes complexes obtained at different molar charge ratios ($R_{+/-}$) were characterized by determination of their number-weighted mean diameter, polydispersity index and zeta potential as a function of $R_{+/-}$ (Table 5-1).

Table 5-1 - Physico-chemical properties of RNA/ELs complexes and RNA/ST-liposomes complexes at different molar charge ratios ($R_{+/-}$).

Molar Charge Ratio ($R_{+/-}$)	Number-weighted mean ⁽ⁱ⁾ (\pm SD) nm	Polydispersity	Zeta potential (\pm SD) mV
ELs	76.0 \pm 30.5	0.12 \pm 0.08	49.83 \pm 2.10
R $_{+/-}$ = 15	119.2 \pm 18.8	0.18 \pm 0.00	41.17 \pm 0.67
R $_{+/-}$ = 10	113.0 \pm 18.9	0.35 \pm 0.13	41.97 \pm 2.91
R $_{+/-}$ = 7	132.9 \pm 20.3	0.38 \pm 0.05	39.10 \pm 2.23
R $_{+/-}$ = 5	150.5 \pm 31.2	0.48 \pm 0.02	39.47 \pm 2.45
ST-liposomes	64.5 \pm 3.6	0.17 \pm 0.01	43.47 \pm 2.90
R $_{+/-}$ = 15	123.6 \pm 13.4	0.32 \pm 0.05	33.33 \pm 5.06
R $_{+/-}$ = 10	832.8 \pm 27.3	0.42 \pm 0.07	37.05 \pm 1.77
R $_{+/-}$ = 7	842.4 \pm 99.7	0.53 \pm 0.14	36.10 \pm 1.08
R $_{+/-}$ = 5	770.4 \pm 111.9	0.60 \pm 0.15	- 33.15 \pm 3.61

(i) Number-weighted hydrodynamic mean diameter, called also Number Mean.

The number-weighted mean diameter and polydispersity index of RNA/ELs complexes and RNA/ST-liposomes complexes increase with addition of RNA (Table 5-1). For RNA/ELs complexes the major size (150.5 nm) and polydispersity (0.48) was when the molar charge ratio was 5, and the minor size (119.2 nm) and polydispersity (0.18) was obtained when the $R_{+/-}$ was 15 (Table 5-1). For RNA/ST-liposomes complexes the major size (770.4 nm) and polydispersity (0.60) was when the molar charge ratio was 5, and the minor size (123.6 nm) and polydispersity (0.32) was obtained when the $R_{+/-}$ was 15 (Table 5-1). Thus, with increasing $R_{+/-}$ values (decreasing the proportion of RNA and increasing the lipid content), the complexes

size and polydispersity decrease until the liposome properties are achieved (diameter approximately of 100 nm and a polydispersity of 0.1-0.2). The zeta potential decreases while adding RNA in RNA/cationic liposomes complexes (Table 5-1). In the case of RNA/ELs complexes the zeta potential decrease from 41.17 mV to 39.47 mV, and the zeta potential of RNA/ST-liposomes complexes decrease from 33.33 mV in to - 33.15 mV (Table 5-1). This large difference in the decrease of zeta potential occurs probably due to different liposome structures, which permit more or less RNA encapsulated inside them. Another important side that must be showed is that liposomes obtained by ethanol injection method have always ethanol residue, which may represent an obstacle to the application of this method for the production of liposomes that would be used in cells. However, in this case, ST-liposomes at 2 mM have the ethanol residue at 2.43% w/w in terms of lipid concentration, and we verified (data did not shown) that this ethanol residue was not harmful to DCs.

For more accurate size characterization, both intensity and number-weighted size distributions were evaluated together as a function of $R_{+/-}$ values. Although the whole range of diameters is shown in the intensity-weighted distribution, the proportionality to the sixth power of particle diameter (D) ($I \propto D^6$) underestimates the small particles, which are only very weakly weighted.⁴⁵ The corresponding number-weighted distribution, converted using the Mie theory, is in equivalent proportion to the first power of diameter ($N \propto D$) and determines the relevant number of particles that yield the observed intensity in each size class.⁴⁶⁻⁴⁹

The size distribution (intensity and number-weighted) of RNA/ELs complexes and RNA/ST-liposomes complexes as a function of four different $R_{+/-}$ values (5, 7, 10 and 15) are presented in Figures 5-1 A and B, respectively.

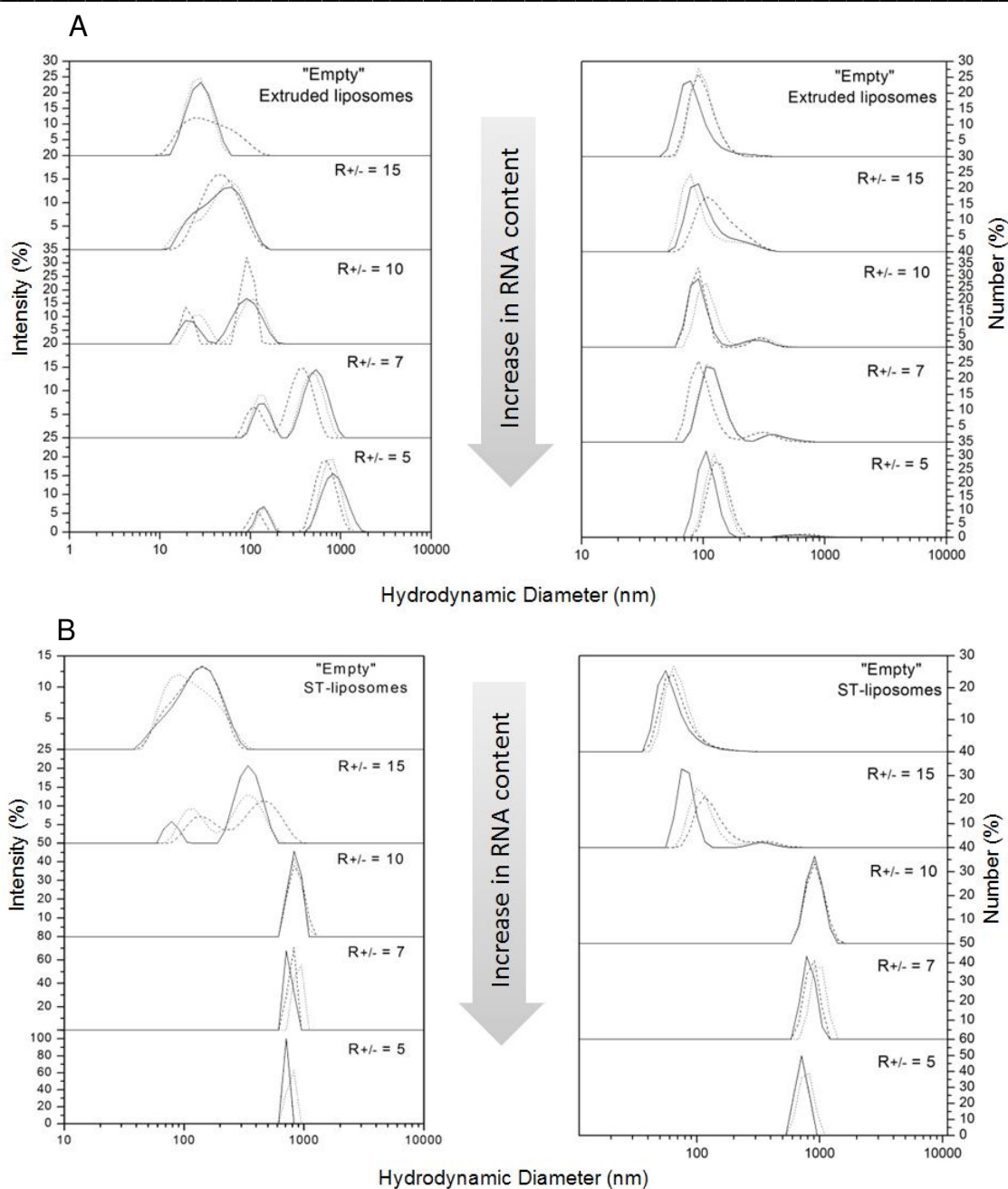


Figure 5-1 - Intensity and number-weighted size distribution of RNA/ELs complexes (A) and RNA/ST-liposomes complexes (B) at molar charge ratios (R \pm) of 5, 7, 10 and 15. "Empty" cationic liposomes are presented for comparison. The lines in each size distribution represent the profile of three independent RNA/cationic liposome complexes.

Extruded liposomes (Figure 5-1 A) and ST-liposomes (Figure 5-1 B) without RNA ("empty") showed in intensity and in number a small width of the size distribution, that increase with RNA incorporation; agreeing with the increase in

polydispersity with RNA addition in liposomes showed in Table 5-1. RNA/ELs complexes in $R_{+/-}$ 15 presented a single population of 190.67 nm for an intensity-weighted distribution and 119.23 nm for a number-weighted distribution (Figure 5-1 A). However, adding RNA to the ELs ($R_{+/-}$ = 10, 7 and 5) the nanoparticles started to have two populations, showing clearly that these complexes present a complex size distribution, in agreement with the increase in ELs polydispersity when adding RNA showed in Table 5-1. In the case of RNA/ST-liposomes complexes in $R_{+/-}$ 15, they had two populations of 375.27 nm (72.2%) and 155.23 nm (27.8%) for an intensity-weighted distribution and 316.77 nm (26.33%) and 138.12 nm (73.67%) for a number-weighted distribution (Figure 5-1 B). On the other hand, adding RNA to the ST-liposomes ($R_{+/-}$ = 10, 7 and 5) the nanoparticles arise abruptly the size and started to present one population with almost 1000 nm.

Thus, considering the lowest polydispersity and diameter are the best conditions for in vitro studies with cells, we selected the molar charge ratio ($R_{+/-}$) 15 for RNA/ELs complexes and to RNA/ST-liposomes. In addition, at $R_{+/-}$ 15, the RNA/liposome complexes presented properties similar cationic liposomes. These properties of nanoparticles are necessary since others works demonstrate the importance of homogenous size distribution⁵⁰⁻⁵² and small nanoparticles⁵³⁻⁵⁵ in the internalization process by cells, supposing that cells expend less energy in the capture of the nanoparticles with these characteristics. Furthermore, in $R_{+/-}$ = 15 RNA/cationic liposomes complexes have a positive zeta potential, which is the minimal condition for transfection experiments in the absence of any specific mechanism for transfection.⁵⁶

The morphology of RNA/ELs complexes and of RNA/ST-liposomes complexes at a molar charge ratio of $R_{+/-}$ =15 were evaluated by transmission electron microscopy (TEM) using a negative staining technique (Figure 5-2).

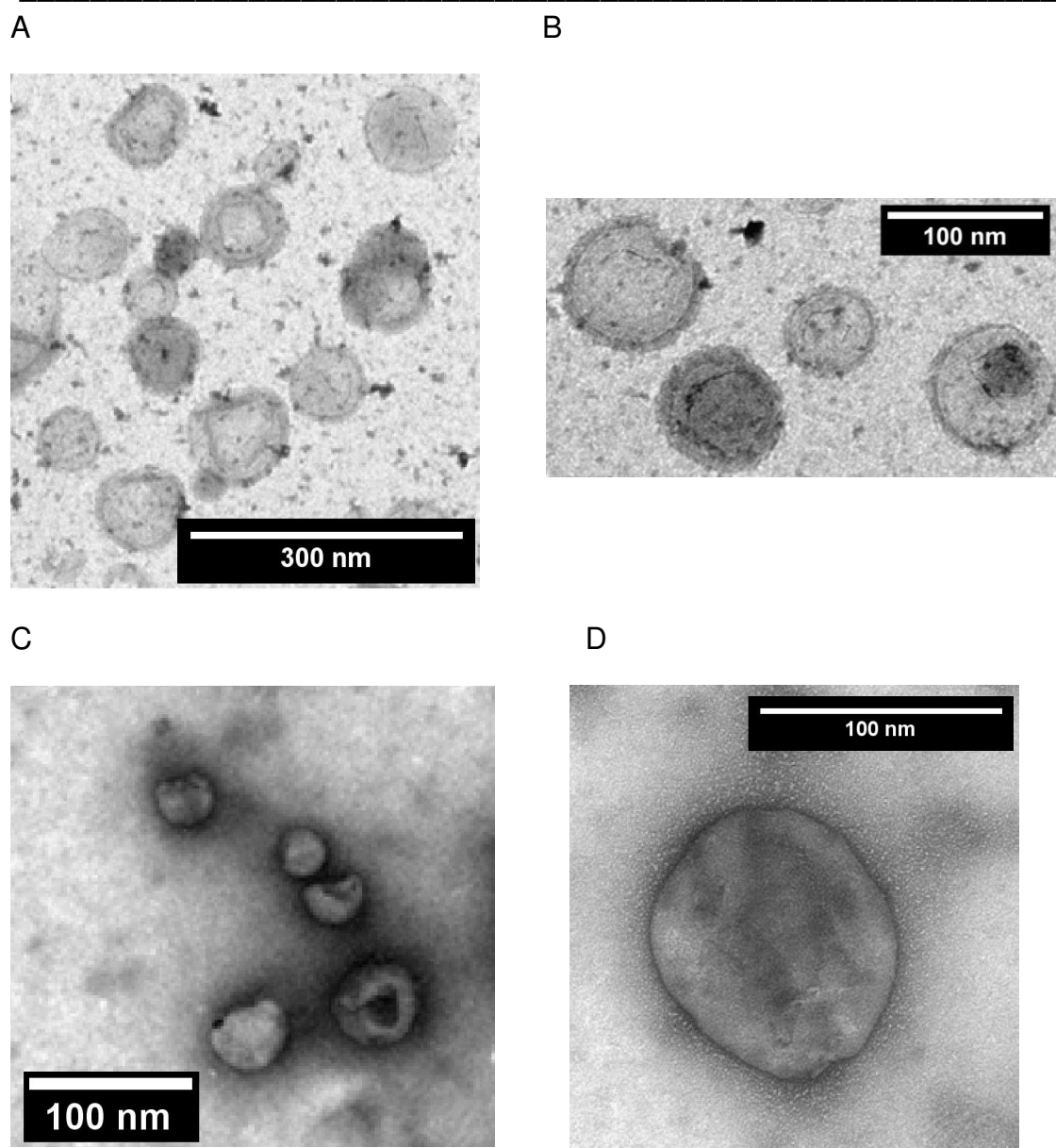


Figure 5-2 - Negative staining electron micrographs (TEM) of RNA/ELs complexes at a molar charge ratio of $R_{+/-}=15$ (A and B) and RNA/ST-liposomes complexes at a molar charge ratio of $R_{+/-}=15$ (C and D). Scale bars indicate 300 nm in (A) and 100 nm in (B, C and D).

RNA/ELs (Figure 5-2 A and B) and RNA/ST-liposomes complexes (Figure 5-2 C and D) at a molar charge ratio of $R_{+/-}=15$ present structures approximately spherical and homogeneous, demonstrating low polydispersity in population. By MET images, RNA/ELs complexes exhibited a diameter of approximately 130 nm ($n=14$), which agrees with the average hydrodynamic size of 119.23 nm presented in Table 5-1.

However, by MET images, RNA/ST-liposomes complexes exhibited a diameter of approximately 75 nm (n=5), which is minor than the average hydrodynamic size of 123.60 nm presented in Table 5-1. This discrepancy may have occurred because only the part of population with small nanoparticles was observed in the micrographs.

3.2. Biological evaluation of liposomal structures

3.2.1. *In vitro* evaluation of efficiency and effect of cationic liposomes internalization by dendritic cells

The strategy used for phenotypic analysis of dendritic cells is presented in the Supplementary Data. In order to evaluate the liposomes incorporation by DCs, Table 5-2 present the median of liposomes' probe fluorescence and SSC expressed by dendritic cells stimulated by TNF- α (mDC), or by extruded liposomes (ELs), or RNA/extruded liposomes complexes at a molar charge ratio of $R_{+/-}=15$, or ST-liposomes, or RNA/ST-liposomes complexes at a molar charge ratio of $R_{+/-}=15$.

Table 5-2 – Median of liposomes' probe fluorescence and SSC expressed by dendritic cells stimulated by TNF- α (positive control - mDC) or by extruded liposomes (ELs), RNA/ELs complexes at a molar charge ratio of $R_{+/-}=15$, ST-liposomes, RNA/ST-liposomes complexes at a molar charge ratio ($R_{+/-}$) of 15.

Population name	Median of liposomes' probe fluorescence (FITC)	Median of SSC ⁽ⁱ⁾ (cells granularity)
mDC	3.22	299
ELs	105.00	415
RNA/ELs	87.30	330
ST-liposomes	211.00	358
RNA/ST-liposomes	86.70	276

(i) SSC is "side scatter" - granularity (internal structure and complexity) of dendritic cells.

According to the median of liposomes' probe fluorescence (Table 5-2), ELs, RNA/ELs complexes, ST-liposomes, RNA/ST-liposomes complexes were incorporated by dendritic cells. However, cationic liposomes without adding RNA, ELs (105.00) and ST-liposomes (211.00), presented more fluorescence intensity than cationic liposomes with RNA in $R_{+/-} = 15$, RNA/ELs complexes (87.30) and RNA/ST-liposomes complexes (86.70), *i.e.* cationic liposomes were better incorporated by DCs than RNA/cationic liposomes complexes.

Otherwise, besides the fluorescent probe, the internalization of cationic liposome and complexes by DCs can also be indicated by the change in cells morphology when incorporate liposomes. Therefore, the median of side scatter (SSC) of dendritic cells (Table 5-2) showed almost the same granularity of DCs stimulated by TNF- α (299) or by cationic liposomes with RNA in $R_{+/-} = 15$, RNA/ELs complexes (330) and RNA/ST-liposomes complexes (276). On the other hand, DCs stimulated by cationic liposomes without adding of RNA showed a small increase in the granularity of DCs, presenting SSC values of 415 and 358 for ELs and ST-liposomes, respectively (Table 5-2). Consequently, a greater change in cells granularity indicates a greater uptake of these complexes by DCs.

Fluorescence images of dendritic cells stimulated by TNF- α , or by both complexes (RNA/ST and RNA/EL, $R_{+/-}=15$) or by “empty” liposomes (all nanoparticles labeled with lipid fluorescent probe, FITC) are presented in Figure 5-3.

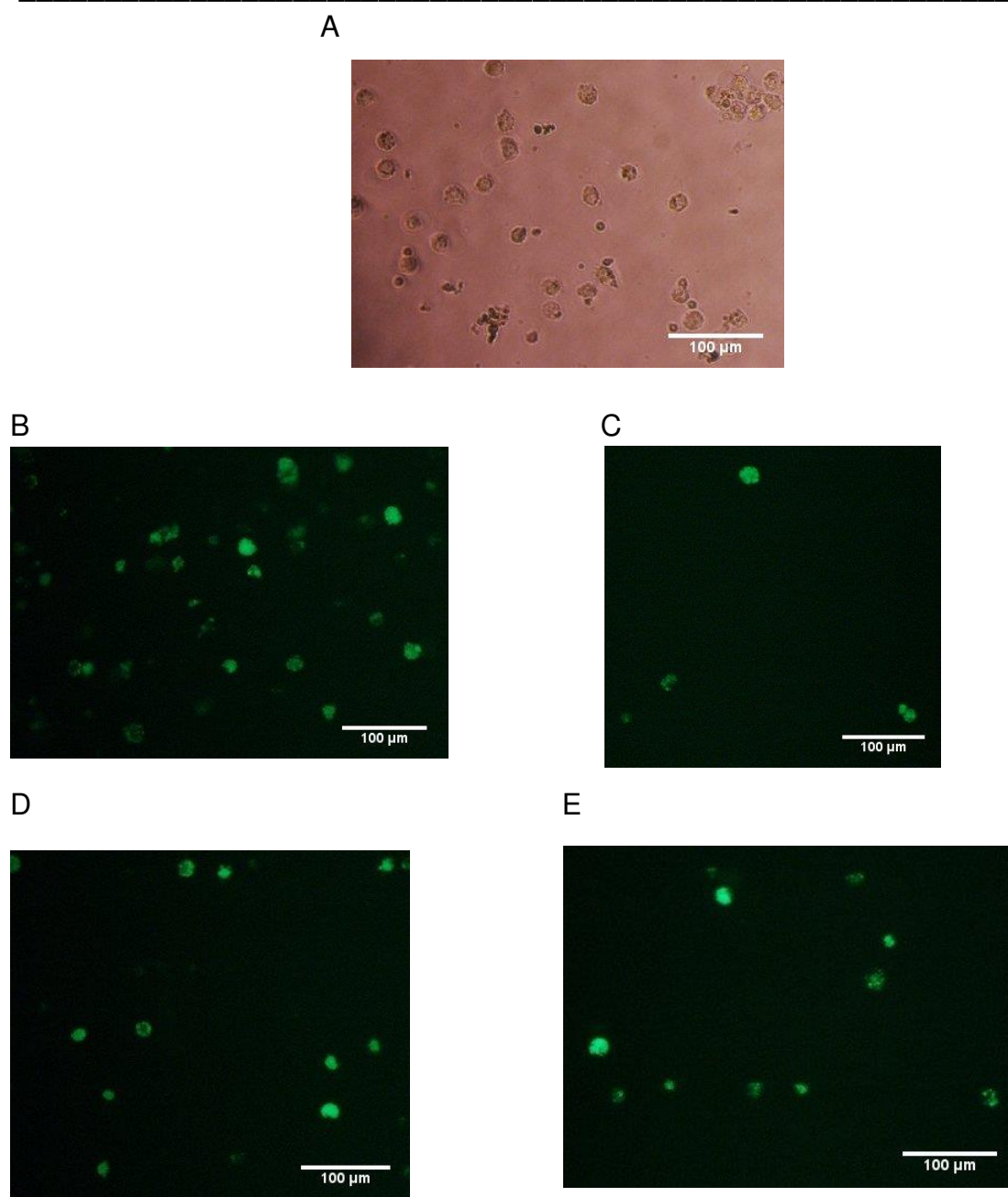


Figure 5-3 – Fluorescence images of dendritic cells stimulated by TNF- α (A), extruded liposomes (B), RNA/extruded liposomes complexes at a molar charge ratio of $R_{+/-}=15$ (C), ST-liposomes (D), RNA/ST-liposomes complexes at a molar charge ratio of $R_{+/-}=15$ (E); all cationic liposomes were labeled with lipid fluorescent probe (FITC). Scale bars indicate 100 μm .

We observed for all DCs stimulated by liposomes and complexes that the fluorescence images presented green points inside DCs in contrast with DCs stimulated by only TNF- α , confirming that liposomes were internalized by DCs (Figure

5-3). We also observed that cationic liposomes and complexes can be localized on the DC membrane or throughout the cytoplasm of DCs (Figure 5-3).

The dendritic cells molecule expression was evaluated through flow cytometry, as shown in Figure 5-4. Nevertheless, the lipid fluorescent probe (FL1, FITC - fluorescein) presented in cationic liposomes and complexes were well internalized by DCs and interfered a lot in the fluorescence detector FL2 and FL3. Thus, we used a different strategy to analyze the results, according to showed in the Supplementary Materials.

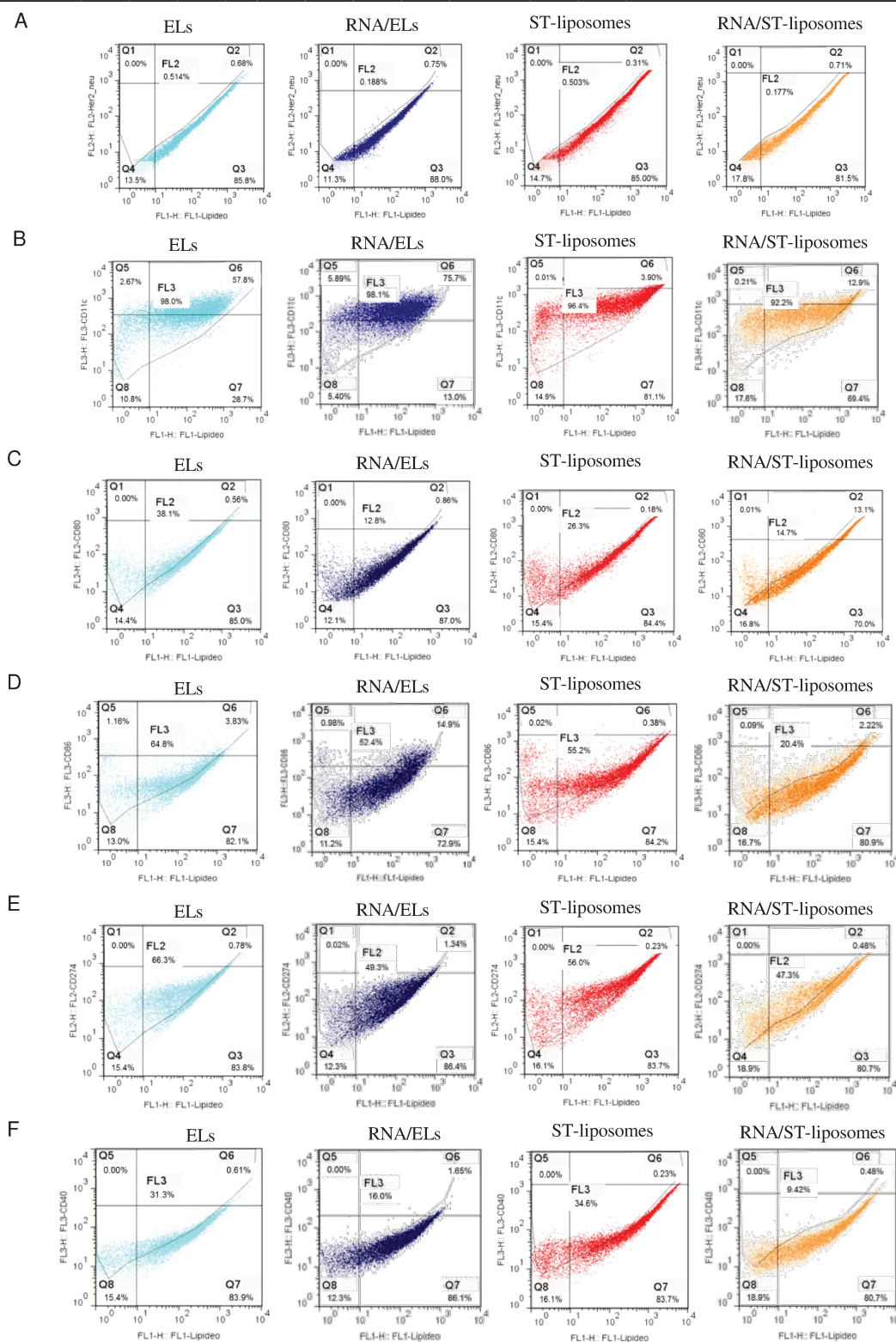


Figure 5-4 – Dot plot of Her-2/neu (A), CD11c (B), CD80 (C), CD86 (D), CD274 (E) and CD40 (F) versus liposomes' probe of Gate R1 dendritic cells stimulated by extruded liposomes (ELs), RNA/ELs complexes at a molar charge ratio of $R_{+/-}=15$, ST-liposomes and RNA/ST-liposomes complexes at a molar charge ratio of $R_{+/-}=15$.

Figure 5-4 A showed that Her-2/*neu* was almost not expressed by DCs, since 0.514%, 0.188%, 0.503% and 0.177% of DCs stimulated by ELs, RNA/ELs, ST-liposomes or RNA/ST-liposomes, respectively, had internalized the nanoparticles and presented Her-2/*neu*. The Dot Plot of CD11c (Figure 5-4 B) showed that CD11c was expressed by all DCs; 98.0% of DCs stimulated by ELs, 98.1% of DCs stimulated by RNA/ELs complexes, 96.4% of DCs stimulated by ST-liposomes and 92.2% of DCs stimulated by RNA/ST-liposomes complexes. The CD80 molecule was more expressed by DCs stimulated by cationic liposomes without RNA adding (Figure 5-4 C); 38.1% of DCs stimulated by ELs, 12.8% of DCs stimulated by RNA/ELs complexes, 26.3% of DCs stimulated by ST-liposomes and 14.7% of DCs stimulated by RNA/ST-liposomes complexes. However, CD86 molecule was more expressed by DCs stimulated by cationic liposomes without RNA adding and also by DCs stimulated by RNA/ELs complexes (Figure 5-4 D); 64.8% of DCs stimulated by ELs, 52.4% of DCs stimulated by RNA/ELs complexes, 55.2% of DCs stimulated by ST-liposomes and 20.4% of DCs stimulated by RNA/ST-liposomes complexes. The expression of immunosuppressive protein CD274 by DCs was 66.3% when stimulated by ELs, 49.3% when stimulated by RNA/ELs complexes, 56.0% when stimulated by ST-liposomes and 47.3% when stimulated by RNA/ST-liposomes complexes (Figure 5-4 E). And finally, the CD40 molecule was also more expressed by DCs stimulated by cationic liposomes without RNA adding (Figure 5-4 F); 31.3% of DCs stimulated by ELs, 16.0% of DCs stimulated by RNA/ELs complexes, 34.6% of DCs stimulated by ST-liposomes and 9.42% of DCs stimulated by RNA/ST-liposomes complexes.

3.2.2. T lymphocytes proliferation

Aiming to confirm that DCs are able to present antigens to T lymphocytes after internalization of cationic liposomes and their complexes, allogeneic T lymphocyte were co-cultured with DCs inducing T lymphocytes proliferation. “Anexo II” presents the complementary analyses generate by T lymphocytes proliferation. Figure 5-5 showed the T lymphocytes proliferation by histograms of CFSE intensity, in which the

positive control of proliferation assay was compared with the T lymphocytes proliferation co-cultured with DCs stimulated by RNA/ELs complexes or by RNA/ST-liposomes complexes. The CFSE is a stable cytoplasmic fluorescent dye that is segregated equally between daughter cells after cell division, therefore when T lymphocytes proliferate dilute the amount of CFSE causing a decrease in fluorescence intensity of the dye.

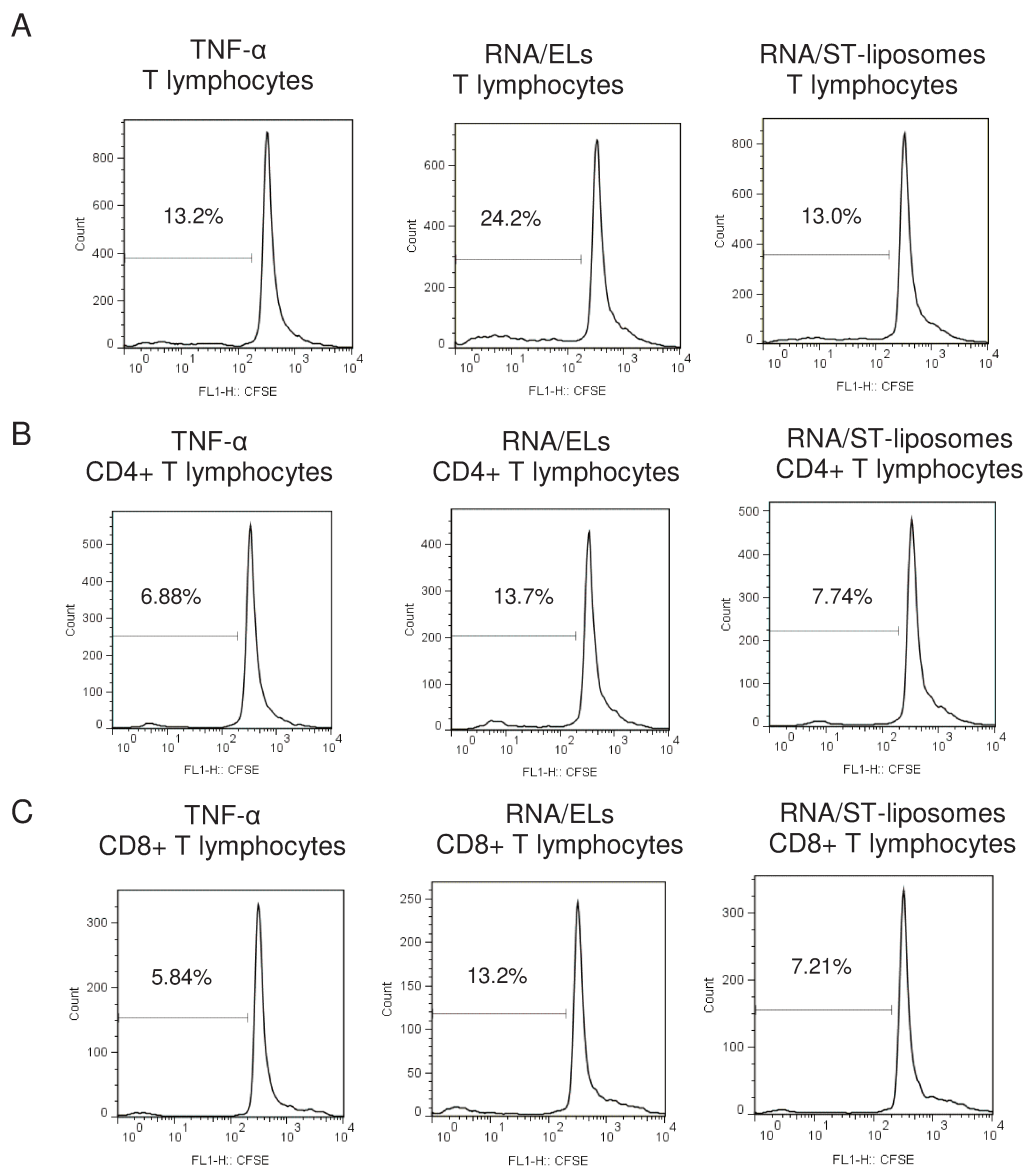


Figure 5-5 - Histograms of CFSE (carboxyfluorescein diacetate succinimidyl ester) intensity representing proliferation of total T lymphocytes (A), CD4+ T lymphocytes (B) and CD8+ T lymphocytes (C), when co-cultured with allogeneic DCs stimulated by TNF- α (positive control) and when co-cultured with allogeneic DCs stimulated by RNA/extruded liposomes complexes at a molar charge ratio of $R_{+/-}=15$ and RNA/ST-liposomes complexes at a molar charge ratio of $R_{+/-}=15$.

Thus, with the aid of histograms of CFSE intensity, we noticed that T lymphocytes proliferation was the same or better when T lymphocytes were co-cultured with DCs stimulated by RNA/ELs complexes or by RNA/ST-liposomes complexes than when T lymphocytes were co-cultured with DCs stimulated by TNF- α . 13.2% of T Lymphocytes proliferated when TNF- α was involved, 24.2% when RNA/ELs complexes was involved and 13.0% when RNA/ST-liposomes complexes was involved (Figure 5-5 A). When considering just CD4⁺ T lymphocytes, 6.88% had CFSE dilution when stimulated with DCs activated with TNF- α , compared to 13.7% when stimulated with DCs treated with RNA/ELs complexes, compared to 7.74% when stimulated with DCs treated with RNA/ST-liposomes complexes (Figure 5-5 B). CD8⁺ T lymphocytes proliferation were greater when stimulated with DCs treated with RNA/ELs complexes (13.3%) and when stimulated with DCs treated with RNA/ST-liposomes complexes (7.21%), compared with DCs activated with TNF- α (5.84%) (Figure 5-5 C). Thus, the use of RNA/ELs complexes to stimulate DCs increase proliferation of T Lymphocytes CD4⁺ and CD8⁺ in approximately 2 times compared with the TNF- α stimulus. And the use of RNA/ST-liposomes complexes to stimulate DCs resulted in nearly the same proliferation of T Lymphocytes CD4⁺ and CD8⁺ presented when DCs were stimulated by TNF- α .

4. **Discussion**

Dendritic cells when loaded with tumor antigen(s) could present them therein to T lymphocytes,¹³ recruiting the immune system to fight against the tumor cells.¹⁴ However, the loading of DCs with the tumor antigen(s) is a crucial step^{17, 18} which can interfere with antigen presentation by DCs. In this context, cationic liposomes are non-viral vectors which can do this role safely. Cationic liposomes EPC/DOTAP/DOPE (50/25/25% molar) were studied for the first time to entrap pDNA for treatment of hepatitis B.³⁰ When complexed with DNAhsp65, those liposomes had low cytotoxicity *in vitro*³³ and high efficacy *in vivo* as a genetic vaccine against tuberculosis.^{31, 57} Given the promising results in *in vitro* and *in vivo* studies, which involved the application of EPC/DOTAP/DOPE liposomes, the search for new

approaches for the development of scalable processes to produce these aggregates is still a challenge in the field of chemical engineering, because to reproduce the physico-chemical and biological properties of the previously liposomes prepared on a laboratory scale is not easy.³⁶ Moreover, tumor antigen can be represented by Her-2/*neu*, which is a molecule overexpressed in SK-BR-3, cell line derived from human breast cancer; and consequently codified in the total RNA of SK-BR-3.³⁹ Thus, the purpose of this study was to investigate *in vitro* the effects of cationic liposomes EPC/DOTAP/DOPE obtained *via* laboratorial method (ELs) and obtained *via* scalable method (ST-liposomes) incorporated with RNA of SK-BR-3 to stimulate dendritic cells and to initiate T lymphocytes proliferation by DCs.

The initial step in the investigation of the RNA/cationic liposome complexes focused on conventional physico-chemical characterization, aimed at identification of the proper conditions for *in vitro* internalization by DCs. For this, we evaluated the number-weighted mean diameter, polydispersity and zeta potential as a function of the cationic/anionic molar charge ratio between cationic lipids and RNA ($R_{+/-}$) (Table 5-1); and also the size distribution of RNA/ELs complexes (Figure 5-1 A) and RNA/ST-liposomes complexes (Figure 5-1 B) as a function of molar charge ratio 5, 7, 10 and 15 in terms of intensity-weighted distribution and number-weighted distribution.

It was observed that RNA/ELs complexes and RNA/ST-liposomes complexes at a molar charge ratio of $R_{+/-}=15$ represent the ideal proportional between RNA and cationic liposome for *in vitro* investigation. There is because RNA/ELs complexes in this condition showed a single population with average diameter of 119.2 nm and polydispersity of 0.18 (Table 5-1 and Figure 5-1 A) and RNA/ST-liposomes complexes showed two populations with average diameter of 123.6 nm and polydispersity of 0.32 (Table 5-1 and Figure 5-1 B). RNA/ST-liposomes had a higher polydispersity and size than RNA/ELs, because ST-liposomes had higher polydispersity than ELs (Table 5-1) and when incorporating RNA the heterogeneity of population tends to generate complexes with higher size and polydispersity. The size

of the RNA/liposomes complexes is usually larger than the liposomes due to lipid structural rearrangement involved in RNA encapsulation.^{58, 59} Even so, Desigaux *et al.*⁶⁰ showed that the smaller irregular structures of siRNA/cationic liposomes complexes (cationic liposomes composed by cationic lipidic aminoglycoside derivatives) are more efficacious in transfecting d2GFP, HeLa and HEK293 cells when compared to larger structures. Confirming this increase in size complex while adding nucleic acids to cationic liposomes, Balbino *et al.*⁶¹ incorporated pDNA in EPC/DOTAP/DOPE liposomes prepared *via* thin film method followed by extrusion varying size from 500 to 100 nm and polydispersity from 0.5 to 0.1 while increasing pDNA incorporation. And also, Maitani *et al.*³⁸ showed that DC-Chol (3 β -[N-(N',N'-dimethylaminoethane)-carbamoyl] cholesterol)/DOPE liposomes prepared by modified ethanol injection method (in the first step was made a lipid film, which is after dissolved in ethanol and this ethanolic lipid solution is injected in a aqueous solution) and by the dry-film method, increased their size as incorporating DNA to the complexes.

Besides the minor size and polydispersity of the complexes, RNA/ELs complexes and RNA/ST-liposomes complexes at a molar charge ratio ($R_{+/-}$) of 15 assumed positive values of zeta potential (Table 5-1). The positive particle zeta potential provide a long-term colloidal stability of lipoplexes, and is also helpful in the nanoparticles internalization by cells, as they can interact with the negatively charged cell membranes (due to heparin sulfate proteoglycans and integrins).⁶² In order to show the benefits of positive charge of lipoplexes, Zhang *et al.*⁶³ prepared siRNA/DC-chol lipoplexes at different $R_{+/-}$ to vary potential zeta from (-30 mV) to (+50 mV) and obtained an increase in transfection efficiency from 50 to almost 90% as the potential zeta increase. In a similar way as us, Taetz *et al.*⁶⁴ prepared liposomes DOTAP/DOPE *via* modified ethanol injection method, whose size was 110 nm and zeta potential rage of +50 to +60 mV. While adding siRNA, at charge ratios from 1 to 8, the resulted lipoplexes increase size next to 200 nm and zeta potential decrease achieving negative valor at $R_{+/-}$ 1.⁶¹

Then, RNA/ELs complexes and RNA/ST-liposomes complexes at a molar charge ratio of $R_{+/-}=15$ were morphological characterized by MET images (Figure 5-2), to help in understanding the relative structures, orientation of RNA molecules and assembly of the complexes, which can influence in the stability of the complex *in vitro*.⁶⁵ Figure 5-2 showed that both RNA/cationic liposomes complexes present structures approximately spherical and homogeneous, although our research group had characterized the liposomal structures by small angle X-ray scattering (SAXS) concluding that these ELs are unilamellar vesicles⁶¹ and that these ST-liposomes multilamellar liposomes.³⁶ Thus, RNA could be inserted between liposomes layers in the ST-liposomes, allowing more RNA incorporation than inside ELs structures; and this major incorporation of RNA caused the negative potential value in RNA/ST-liposomes at $R_{+/-} 5$ (-33.15 mV) and RNA/ELs in the same quantity of RNA added remained with positive zeta potential (39.47 mV). Desigaux *et al.*⁶⁰ showed by Cryo transmission electron microscopy that siRNA entrapped in small multilamellar liposomes exhibit lamellar microdomains, which correspond to siRNA molecules sandwiched between the lipid bilayers. In contrast to this, DNA could be arranged inside cationic liposomes as meatballs, in which DNA is localized between the lipid layers in multilayered structures^{66, 67}, or as spaghetti, in which fibrils are formed as a result of DNA being sandwiched between the lipid layers on each side, when large quantity of DNA is encapsulated.^{33, 68} Even so, the structures formed by cationic liposomes with RNA and DNA are effective in cells internalization. Spaghetti structures have been shown to be efficacious due to effective interaction of high curvature structure with the cell membrane thereby enabling better penetration,⁶⁸ like obtained by our research group³³ which complexed DOTAP/DOPE (50:50% molar) with DNA-hsp65 at $R_{+/-}10$ focusing on the tuberculosis therapy and vaccination. Moreover, RNA lipoplexes structures have been shown to be efficacious due to the smaller irregular structures formed, which facilitates the endocytic uptake and the endosomal destabilization,⁶⁰ as presented in Figure 5-2.

The second step in the investigation of the RNA/cationic liposomes complexes focused on *in vitro* biological assays stimulating DCs and inducing T lymphocytes proliferation by DCs. The incorporation of extruded liposomes (ELs), RNA/ELs complexes at a molar charge ratio of $R_{+/-}=15$, ST-liposomes, RNA/ST-liposomes complexes at a molar charge ratio of $R_{+/-}=15$ by DCs were estimated measuring the median of liposomes' probe fluorescence and of SSC expressed by DCs (Table 5-2). The FITC median fluorescence and SSC showed that all cationic liposomes and RNA/cationic liposomes complexes were incorporated by DCs; however, cationic liposomes were better incorporated by DCs than RNA/cationic liposomes complexes (Table 5-2). This behavior can be explained by the little higher size and polydispersity of complexes than cationic liposomes, although we have chosen the RNA/cationic liposomes complexes with physico-chemical characteristics more similar to the cationic liposomes without adding RNA ($R_{+/-}=15$). *In vitro* and *in vivo* studies performed by Allen *et al.*,⁵³ Papahadjopoulos *et al.*⁵⁴ and Rejman *et al.*⁵⁵ showed that generally small nanoparticles (range of 100-200 nm) are required in biological applications to facilitate their internalization by cells. Additionally, Kristl *et al.*⁵⁰, Licciardi *et al.*⁶⁹ and Muthu *et al.*⁵² observed that nanoparticles with polydispersity values below 0.2, which evidences a homogenous size distribution, can support *in vitro* internalization by mammalian cells, supposing that cells expend less energy in the capture. Furthermore, Taetz *et al.*⁶⁴ proved that the liposomes DOTAP/DOPE obtained *via* modified ethanol injection method with siRNA at $R_{+/-}$ 2 and 8 (size below 200 nm and polydispersity smaller than 0.25) were better internalized by A549 cells than the commercial liposomes Lipofectamine 2000.

The fluorescence images confirmed that all cationic liposomes and RNA/cationic liposomes complexes, were internalized by DCs (Figure 5-3). The nanoparticles were identified as green granules inside DCs (Figure 5-3) and consequently, these structures increase the granularity of DCs (Table 5-2). Hence, the internalization of nanoparticles by DCs can be indicated by the change in cells morphology, increase in dendritic cells SSC, besides fluorescent probe in nanoparticles.

The efficiency transfection of RNA from SK-BR-3 using ELs and ST-liposomes as non-viral vectors was determinate by DCs expression Her-2/*neu*, and the data showed that Her-2/*neu* was almost not expressed by DCs (Figure 5-4 A). These result do not necessarily mean that ELs and ST-liposomes are not good vectors to transfect RNA to DCs, because others transfection parameters must be optimized, such as transfection time²⁶ and transport of nanoparticles/nucleic acid to the cell, which occurs in stagnant flow in wells.⁷⁰ Meer van der *et al.*⁷⁰ showed that human endothelial cells transfected with siRNA by liposomes increase the transfection efficiency when using shear stress to transport complexes to cells. Penacho *et al.*⁷¹ showed that cationic liposomes DOTAP:Chol (cholesterol) liposomes prepared *via* modified ethanol injection method complexed with DNA pre-condensed with low molar weight polyethylenimine resulted in a better β -galactosidase gene expression in HeLa cells than cationic liposomes prepared *via* thin film method followed by extrusion. Likewise, Maitani *et al.*³⁸ conclude that DC-Chol/DOPE liposomes prepared by modified ethanol injection method complexed with DNA at 0.5 molar ratio achieved more efficient transfection in HeLa cells than liposomes prepared by than the dry-film. This better performance of *in vitro* transfection could be explained by the residue of ethanol in the transfection medium, which can fluidize the biomembranes^{72,73} when present at low concentrations and can enhance the role of DOPE in destabilization of the plasma membrane and/or endosome,³⁸ thus facilitating the entry of the complexes into cells.⁷⁴

Dendritic cells stimulated by ELs, RNA/ELs complexes, ST-liposomes and RNA/ST-liposomes complexes were analyzed in terms of co-stimulatory and immunosuppressive molecules expression, such as CD11c (Figure 5-4 B), CD80 (Figure 5-4 C), CD86 (Figure 5-4 D), CD274 (Figure 5-4 E) and CD40 (Figure 5-4 F). The molecule CD11c was expressed by DCs stimulated with all treatments (Figure 5-4 B), because CD11c is myeloid dendritic cells marker, *i.e.* myeloid DCs are CD11c positive. The molecule CD80, CD86 and CD40 were, in general, more expressed by DCs stimulated by cationic liposomes without RNA adding (Figure 5-4 C, D and F), however DCs treated with cationic liposome complexes also had higher expression of

those molecules. Thus, it is necessary to compare molecules expressed by DCs stimulated by cationic liposomes with iDC molecule expression to conclude about DC activation; which is not possible in this work due to the interference of FITC in FL2 and FL3 detectors. In contrast to this, the immunosuppressive protein CD274 was more expressed by DCs stimulated by cationic liposomes without RNA adding; demonstrating that complexes (minor DCs CD274 expression) are more suitable to be used in DCs vaccine for cancer immunotherapy. CD274 or PDL-1 is important in regulating lymphocytes activation in both lymphoid and peripheral sites.⁷⁵ Activation of T lymphocytes is dependent upon DCs antigen processing and presentation on the surface through class I and class II major histocompatibility complex (MHC), together with a second signal (co-stimulation). Thus, T lymphocytes activation requires a first signal provided by the interaction of antigenic peptide/MHC with the T lymphocytes receptor and a second, antigen-independent, co-stimulatory signal.^{76, 77} Therefore, while CD40, CD80 and CD86 molecules are positive co-stimulation that may generate a positive activation of the immune system, CD274 is a negative co-stimulation molecule that leads to suppression the immune response; thus it is necessary to investigate all these molecules expression by DCs for cancer immunotherapy strategies.

The last but not least aspect of biological application analyzed was T lymphocytes proliferation stimulated by RNA/ELs complexes and by RNA/ST-liposomes complexes, which was showed in histograms of CFSE intensity (Figure 5-5). The increase in proliferation of T Lymphocytes when co-cultured with DCs stimulated by RNA/ELs complexes is evident, and DCs stimulated by RNA/ST-liposomes complexes proliferated T Lymphocytes in a similar way as DCs stimulated by TNF- α . Hence, RNA/cationic liposomes complexes stimulate DCs and these cells were able to induce T lymphocytes proliferation *in vitro*, indicating that RNA/cationic liposomes complexes have a promising future in therapeutic dendritic cell vaccines for cancer patients.

In sum, we can predict a promising future for RNA/ELs complexes at a molar charge ratio of $R_{+/-}=15$ and RNA/ST-liposomes complexes at a molar charge ratio of $R_{+/-}=15$ in immunotherapy against cancer. However, further experiments are necessary to optimize transfection conditions and not use fluorescent lipid to analyze the nanoparticles internalization by DCs, only use the increase in DCs granularity for this purpose.

5. Acknowledgements

We thanks to Dr. Barbuto's Lab staff to technical support. This work was financial support by Fundação de Amparo à Pesquisa do Estado de São Paulo (FAPESP).

6. References

1. Gao X, Huang L. Cationic liposome-mediated gene transfer. *Gene Ther* 1995;2:710-22.
2. Miller AD. Cationic liposome systems in gene therapy. *IDrugs* 1998;1:574-83.
3. Akita H, Hatakeyama H, Khalil IA, Yamada Y, Harashima H. 4.425 - Delivery of Nucleic Acids and Gene Delivery: In: Editor-in-Chief: Paul D, editors. *Comprehensive Biomaterials*. ed. Oxford: Elsevier; 2011, p. 411-44.
4. Cao A, Briane D, Coudert R. Chapter 5: Cationic Liposomes as Transmembrane Carriers of Nucleic Acids: In: Liu AL, editors. *Advances in Planar Lipid Bilayers and Liposomes*. Volume 4 Volume 4, ed.: Academic Press; 2006, p. 135-90.
5. Bertino JR, Hait W. Princípios do tratamento do câncer: In: Ausiello D, Goldman L, editors. *Cecil, tratado de medicina interna*. 22 ed. Rio de Janeiro, Brazil: Elsevier; 2005, p. 1316-30.
6. (NCI) NCI, *Biological therapy*. <http://www.cancer.gov/cancertopics/treatment/biologicaltherapy> [accessed August 28 2011].
7. Folkman J. Tumor angiogenesis: therapeutic implications. *N Engl J Med* 1971;285:1182-86.
8. Pang RW, Poon RT. Clinical implications of angiogenesis in cancers. *Vasc Health Risk Manag* 2006;2:97-108.
9. Prestwich RJ, Errington F, Hatfield P, Merrick AE, Ilett EJ, Selby PJ, *et al*. The Immune System — is it Relevant to Cancer Development, Progression and Treatment? *Clin Oncol* 2008;20:101-12.
10. Hanahan D, Weinberg Robert A. Hallmarks of Cancer: The Next Generation. *Cell* 2011;144:646-74.
11. Dunn GP, Bruce AT, Ikeda H, Old LJ, Schreiber RD. Cancer immunoediting: from immunosurveillance to tumor escape. *Nat Immunol* 2002;3:991-98.
12. Steinman RM. Dendritic cells: Understanding immunogenicity. *Eur J Immunol* 2007;37:S53-S60.
13. Banchereau J, Steinman RM. Dendritic cells and the control of immunity. *Nature* 1998;392:245-52.

14. Barbuto JA, Ensina LF, Neves AR, Bergami-Santos P, Leite KR, Marques R, et al. Dendritic cell-tumor cell hybrid vaccination for metastatic cancer. *Cancer immunology, immunotherapy : CII* 2004;53:1111-8.
15. Sallusto F, Lanzavecchia A. Efficient presentation of soluble antigen by cultured human dendritic cells is maintained by granulocyte/macrophage colony-stimulating factor plus interleukin 4 and downregulated by tumor necrosis factor alpha. *J Exp Med* 1994;179:1109-18.
16. Vitor MT, Bergami-Santos PC, Barbuto JA, De La Torre LG. Cationic liposomes as non-viral vector for RNA delivery in cancer immunotherapy. *Recent Pat Drug Deliv Formul* 2012 (in press).
17. Gilboa E, Vieweg J. Cancer immunotherapy with mRNA-transfected dendritic cells. *Immunol Rev* 2004;199:251-63.
18. Rubiolo C, Dendritic Cells. United States Patent US20110097346(2011).
19. Sullenger BA, Gilboa E. Emerging clinical applications of RNA. *Nature* 2002;418:252-8.
20. Serikawa T, Kikuchi A, Sugaya S, Suzuki N, Kikuchi H, Tanaka K. In vitro and in vivo evaluation of novel cationic liposomes utilized for cancer gene therapy. *J Control Release* 2006;113:255-60.
21. Boczkowski D, Nair SK, Snyder D, Gilboa E. Dendritic cells pulsed with RNA are potent antigen-presenting cells in vitro and in vivo. *J Exp Med* 1996;184:465-72.
22. Ashley DM, Faiola B, Nair S, Hale LP, Bigner DD, Gilboa E. Bone marrow-generated dendritic cells pulsed with tumor extracts or tumor RNA induce antitumor immunity against central nervous system tumors. *J Exp Med* 1997;186:1177-82.
23. Zhang W, He L, Yuan Z, Xie Z, Wang J, Hamada H, et al. Enhanced therapeutic efficacy of tumor RNA-pulsed dendritic cells after genetic modification with lymphotactin. *Hum Gene Ther* 1999;10:1151-61.
24. Koido S, Kashiwaba M, Chen D, Gendler S, Kufe D, Gong J. Induction of antitumor immunity by vaccination of dendritic cells transfected with MUC1 RNA. *J Immunol* 2000;165:5713-9.
25. Grunebach F, Muller MR, Nencioni A, Brossart P. Delivery of tumor-derived RNA for the induction of cytotoxic T-lymphocytes. *Gene Ther* 2003;10:367-74.
26. Felgner PL, Gadek TR, Holm M, Roman R, Chan HW, Wenz M, et al. Lipofection: a highly efficient, lipid-mediated DNA-transfection procedure. *Proc Natl Acad Sci U S A* 1987;84:7413-7.
27. Nakanishi T, Kunisawa J, Hayashi A, Tsutsumi Y, Kubo K, Nakagawa S, et al. Positively charged liposome functions as an efficient immunoadjuvant in inducing immune responses to soluble proteins. *Biochem Biophys Res Commun* 1997;240:793-7.
28. Nakanishi T, Kunisawa J, Hayashi A, Tsutsumi Y, Kubo K, Nakagawa S, et al. Positively charged liposome functions as an efficient immunoadjuvant in inducing cell-mediated immune response to soluble proteins. *J Controlled Release* 1999;61:233-40.
29. Bringmann A, Held SAE, Heine A, Brossart P. RNA vaccines in cancer treatment. *J Biomed Biotechnol* 2010;2010:1-12.
30. Perrie Y, Frederik PM, Gregoriadis G. Liposome-mediated DNA vaccination: the effect of vesicle composition. *Vaccine* 2001;19:3301-10.
31. Rosada RS, De La Torre LG, Frantz FG, Trombone AP, Zarate-Blades CR, Fonseca DM, et al. Protection against tuberculosis by a single intranasal administration of DNA-hsp65 vaccine complexed with cationic liposomes. *BMC Immunol* 2008;9:38.
32. Rosada RS, Silva CL, Santana MH, Nakaie CR, De La Torre LG. Effectiveness, against

- tuberculosis, of pseudo-ternary complexes: peptide-DNA-cationic liposome. *J Colloid Interface Sci* 2012;373:102-9.
- 33 . De La Torre LG, Rosada RS, Trombone APF, Frantz FG, Coelho-Castelo AAM, Silva CL, *et al.* The synergy between structural stability and DNA-binding controls the antibody production in EPC/DOTAP/DOPE liposomes and DOTAP/DOPE lipoplexes. *Colloids Surf B Biointerfaces* 2009;73:175-84.
 - 34 . Tiago A. Balbino AG, Cristiano L. P. Oliveira, Adriano R. Azzoni, Leide P. Cavalcanti, Lucimara G. de La Torre. Correlation of the physico-chemical and structural properties of pDNA/Cationic liposome complexes with their in vitro transfection. *Langmuir : the ACS journal of surfaces and colloids* 2012:submitted
 - 35 . Sorgi FL, Huang L. Large scale production of DC-Chol cationic liposomes by microfluidization. *Int J Pharm* 1996;144:131-39.
 - 36 . Trevisan JE, Cavalcanti LP, Oliveira CLP, De La Torre LG, Santana MHA. Technological aspects of scalable processes for the production of functional liposomes for gene therapy: In: Yuan X-b, editors. *Non-Viral Gene Therapy*. ed.: InTech; 2011, p. 267-92.
 - 37 . Rigoletto TP, Silva CL, Santana MH, Rosada RS, De La Torre LG. Effects of extrusion, lipid concentration and purity on physico-chemical and biological properties of cationic liposomes for gene vaccine applications. *J Microencapsul* 2012;29:759-69.
 - 38 . Maitani Y, Igarashi S, Sato M, Hattori Y. Cationic liposome (DC-Chol/DOPE = 1:2) and a modified ethanol injection method to prepare liposomes, increased gene expression. *Int J Pharm* 2007;342:33-39.
 - 39 . Wallace PK, Kaufman PA, Lewis LD, Keler T, Givan AL, Fisher JL, *et al.* Bispecific antibody-targeted phagocytosis of HER-2/neu expressing tumor cells by myeloid cells activated in vivo. *J Immunol Methods* 2001;248:167-82.
 - 40 . Kaufman PA, Guyre PM, Lewis LD, Valone FH, Memoli V, Wells WAA, *et al.* Her-2/neu targeted immunotherapy: a pilot study of multi-dose MDX-210 in patients with breast or ovarian cancers that overexpress HER-2/neu and a report of an increased incidence of HER-2/neu overexpression in metastatic breast cancer. *Tumor Target* 1996;2:17-28.
 - 41 . Niehans GA, Singleton TP, Dykoski D, Kiang DT. Stability of Her-2/Neu expression over time and at multiple metastatic sites. *J Natl Cancer Inst* 1993;85:1230-35.
 - 42 . Bangham AD, Standish MM, Watkins JC. Diffusion of univalent ions across lamellae of swollen phospholipids. *Journal of Molecular Biology* 1965;13:238-&.
 - 43 . Radler JO, Koltover I, Jamieson A, Salditt T, Safinya CR. Structure and interfacial aspects of self-assembled cationic lipid-DNA gene carrier complexes. *Langmuir* 1998;14:4272-83.
 - 44 . Neron S, Correa JA, Dajczman E, Kasymjanova G, Kreisman H, Small D. Screening for depressive symptoms in patients with unresectable lung cancer. *Support Care Cancer* 2007;15:1207-12.
 - 45 . Egelhaaf SU, Wehrli E, Müller M, Adrian M, Schurtenberger P. Determination of the size distribution of lecithin liposomes: a comparative study using freeze fracture, cryoelectron microscopy and dynamic light scattering. *J Microsc* 1996;184:214-28.
 - 46 . BOTT S. Particle Size Distribution Assessment and Characterization: In: editors. ed. Washington DC: American Chemical Society; 1987, p.
 - 47 . HULST HC. Light Scattering by Small Particles: In: editors. ed. New York: Wiley; 1957, p.
 - 48 . KERKER M. The Scattering of Light and Other Electromagnetic Radiation: In:

- editors. ed. New York: Academic Press; 1969, p.
- 49 . Meeren PPAV, Vanderdeelen J, Baert L. Particle Size Analysis: In: editors. ed. New York: John Wiley & Sons; 1988, p.
 - 50 . Kristl J, Teskac K, Caddeo C, Abramovic Z, Sentjurc M. Improvements of cellular stress response on resveratrol in liposomes. *Eur J Pharm Biopharm* 2009;73:253-9.
 - 51 . Licciardi M, Paolino D, Celia C, Giammona G, Cavallaro G, Fresta M. Folate-targeted supramolecular vesicular aggregates based on polyaspartyl-hydrazide copolymers for the selective delivery of antitumoral drugs. *Biomaterials* 2010;31:7340-54.
 - 52 . Muthu MS, Kulkarni SA, Raju A, Feng SS. Theranostic liposomes of TPGS coating for targeted co-delivery of docetaxel and quantum dots. *Biomaterials* 2012;33:3494-501.
 - 53 . Allen TM, Austin GA, Chonn A, Lin L, Lee KC. Uptake of liposomes by cultured mouse bone marrow macrophages: influence of liposome composition and size. *Biochim Biophys Acta* 1991;1061:56-64.
 - 54 . Papahadjopoulos D, Allen TM, Gabizon A, Mayhew E, Matthay K, Huang SK, *et al.* Sterically stabilized liposomes: improvements in pharmacokinetics and antitumor therapeutic efficacy. *Proc Natl Acad Sci U S A* 1991;88:11460-4.
 - 55 . Rejman J, Oberle V, Zuhorn IS, Hoekstra D. Size-dependent internalization of particles via the pathways of clathrin- and caveolae-mediated endocytosis. *Biochem J* 2004;377:159-69.
 - 56 . Chesnoy S, Huang L. Structure and function of lipid-DNA complexes for gene delivery. *Annual Review of Biophysics and Biomolecular Structure* 2000;29:27-47.
 - 57 . Rosada RS, Silva CL, Andrade Santana MH, Nakaie CR, de la Torre LG. Effectiveness, against tuberculosis, of pseudo-ternary complexes: Peptide-DNA-cationic liposome. *Journal of Colloid and Interface Science* 2012;373:102-09.
 - 58 . Santel A, Aleku M, Keil O, Endruschat J, Esche V, Fisch G, *et al.* A novel siRNA-lipoplex technology for RNA interference in the mouse vascular endothelium. *Gene Ther* 2006;13:1222-34.
 - 59 . Suh MS, Shim G, Lee HY, Han S-E, Yu Y-H, Choi Y, *et al.* Anionic amino acid-derived cationic lipid for siRNA delivery. *J Controlled Release* 2009;140:268-76.
 - 60 . Desigaux L, Sainlos M, Lambert O, Chevre R, Letrou-Bonneval E, Vigneron J-P, *et al.* Self-assembled lamellar complexes of siRNA with lipidic aminoglycoside derivatives promote efficient siRNA delivery and interference. *Proceedings of the National Academy of Sciences* 2007;104:16534-39.
 - 61 . Balbino TA, Gasperini AAM, Oliveira CLP, Azzoni AR, Cavalcanti LP, De La Torre LG. Correlation of the Physicochemical and Structural Properties of pDNA/Cationic Liposome Complexes with Their in Vitro Transfection. *Langmuir* 2012;28:11535-45.
 - 62 . Wiese G, Healy T. Effect of particle size on colloid stability. *Trans Faraday Soc* 1970;66:490-99.
 - 63 . Zhang Y, Li H, Sun J, Gao J, Liu W, Li B, *et al.* DC-Chol/DOPE cationic liposomes: a comparative study of the influence factors on plasmid pDNA and siRNA gene delivery. *Int J Pharm* 2010;390:198-207.
 - 64 . Taetz S, Bochot A, Surace C, Arpicco S, Renoir J-M, Schaefer UF, *et al.* Hyaluronic acid-modified DOTAP/DOPE liposomes for the targeted delivery of anti-telomerase siRNA to CD44-expressing lung cancer cells. *Oligonucleotides* 2009;19:103-16.
 - 65 . Kapoor M, Burgess DJ, Patil SD. Physicochemical characterization techniques for lipid based delivery systems for siRNA. *Int J Pharm* 2012;427:35-57.
 - 66 . Lasic DD, Strey H, Stuart MC, Podgornik R, Frederik PM. The structure of DNA-

- liposome complexes. *J Am Chem Soc* 1997;119:832-33.
67. Rädler JO, Koltover I, Salditt T, Safinya CR. Structure of DNA-cationic liposome complexes: DNA intercalation in multilamellar membranes in distinct interhelical packing regimes. *Sci* 1997;275:810-14.
68. Sternberg B, Sorgi FL, Huang L. New structures in complex formation between DNA and cationic liposomes visualized by freeze—fracture electron microscopy. *FEBS Lett* 1994;356:361-66.
69. Licciardi M, Paolino D, Celia C, Giammona G, Cavallaro G, Fresta M. Folate-targeted supramolecular vesicular aggregates based on polyaspartyl-hydrazide copolymers for the selective delivery of antitumoral drugs. *Biomaterials* 2010;31:7340-54.
70. Meer van der AD, Kamphuis MMJ, Poot AA, Feijen J, Vermes I. A microfluidic device for monitoring siRNA delivery under fluid flow. *J Controlled Release* 2008;132:e42-e44.
71. Penacho N, Simões S, de Lima MCP. Polyethylenimine of various molecular weights as adjuvant for transfection mediated by cationic liposomes. *Mol Membr Biol* 2009;26:249-63.
72. Bailey AL, Sullivan SM. Efficient encapsulation of DNA plasmids in small neutral liposomes induced by ethanol and calcium. *Biochimica et Biophysica Acta (BBA)-Biomembranes* 2000;1468:239-52.
73. Chin J, Goldstein D. Effects of low concentrations of ethanol on the fluidity of spin-labeled erythrocyte and brain membranes. *Mol Pharmacol* 1977;13:435-41.
74. Anji A, Shaik KA, Kumari M. Effect of Ethanol on Lipid-Mediated Transfection of Primary Cortical Neurons. *Ann N Y Acad Sci* 2003;993:95-102.
75. Greenwald RJ, Freeman GJ, Sharpe AH. The B7 family revisited. *Annu Rev Immunol* 2005;23:515-48.
76. Lafferty KJ, Andrus L, Prowse SJ. Role of lymphokine and antigen in the control of specific T cell responses. *Immunol Rev* 1980;51:279-314.
77. Saresella M, Rainone V, M Al-Daghri N, Clerici M, Trabattoni D. The PD-1/PD-L1 pathway in human pathology. *Curr Mol Med* 2012;12:259-67.

7. Supplementary materials

7.1 Strategy of dendritic cells analysis

For phenotypic characterization and evaluation of the liposomes incorporation, we delimited gate with cell size and granularity compatible with the DCs, by analysis "side scatter" (SSC) - granularity (internal structure and complexity) and the "forward scatter" (FSC) - relative size of the cells (Figure 5-6 A). Considering the analyzed region bounded by the gate, cells were analyzed through the expression of antigen presenting cells marker, HLA-DR (Figure 5-6 B). Furthermore, we analyzed the expression of co-stimulatory and immunosuppressive molecules within this population

HLA-DR⁺, called Gate R1 (described below). This procedure was performed for all samples presenting dendritic cells marked, such as dendritic cells stimulated by TNF- α (positive control - mDC), or by extruded liposomes (ELs), or RNA/ELs complexes at a molar charge ratio of $R_{+/-}=15$ (ELs + RNA), or ST-liposomes or RNA/ST-liposomes complexes at a molar charge ratio of $R_{+/-}=15$ (ST-liposomes + RNA).

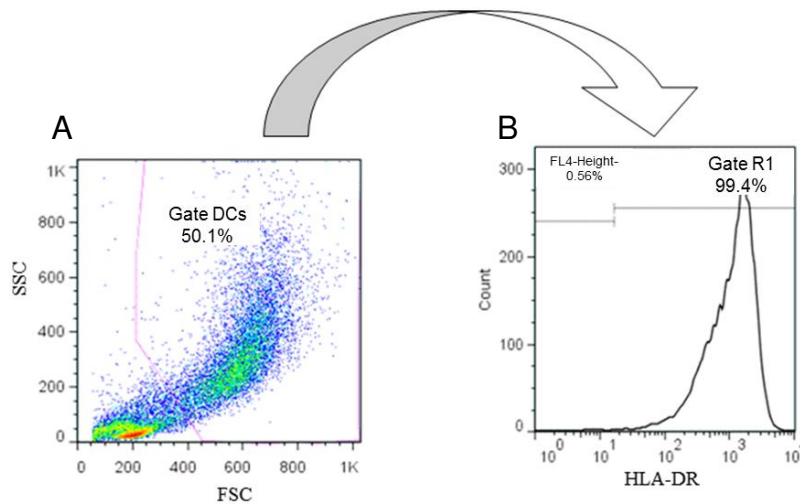


Figure 5-6 – Strategy of dendritic cells analysis. (A) Dot Plot graph of SSC (side scatter) by FSC (forward scatter) to delimit DCs gate. (B) Histogram of HLA-DR fluorescence to delimit Gate R1, corresponding to cells presented in the fluorescent positive part of the histogram.

7.2. Strategy of dendritic cells molecule expression analysis

Flow cytometers use separate fluorescence (FL-) channels to detect light emitted, such as fluorescent molecules, and the specificity of detection is controlled by optical filters, which block certain wavelengths while transmitting (passing) others. Cationic liposomes labeled with lipid fluorescent probe (FL1, FITC - fluorescein) were good internalized by DCs, and because of that, the fluorescein interfered a lot in the fluorescent detector FL2 and FL3, causing a disturb in the analysis of DCs molecules expression presented in these two detectors. Thus, the increase in FL2 or FL3 molecule expressing could be due to a better liposome internalization by DCs or could be due to an overexpression of the referred molecule by DCs.

Therefore, the analysis of surface molecule expression by DCs was performed in two steps. In the first step we plotted the graph Dot Plot of unlabeled DCs, FL1

(lipid fluorescent probe) by FL2 or FL3 (detectors in which FL1 interfered) (Figure 5-7 A). In there, we delimited the gate of DCs that expressed molecules whose fluorescence intensity was higher than the interference of FITC, thus ensuring that the fluorescence is due to expression of the molecule and not to the FITC interference. Then, in the second step, we plotted the graph Dot Plot of labeled DCs, FITC (lipid fluorescent probe) by Her-2/neu or CD11c or CD80 or CD86 or CD274 or CD40 (fluorescent molecules present in FL2 or FL3) (Figure 5-7 B) and put the same gate determinate before. Thus, it was possible to appoint, in each treatment (dendritic cells stimulated by extruded liposomes (ELs), RNA/ELs complexes at $R_{+/-}$ 15 (ELs + RNA), ST-liposomes and RNA/ST-liposomes complexes at $R_{+/-}$ 15 (ST-liposomes + RNA), the DCs population which express double-positive fluorescent molecules.

However, it was not possible to conclude about DCs activation, since iDCs (immature DCs) molecules expressing could not be compared with DCs stimulated by liposomes. The only possible analysis to do was to compare the DCs molecule expression between treatments with liposomes.

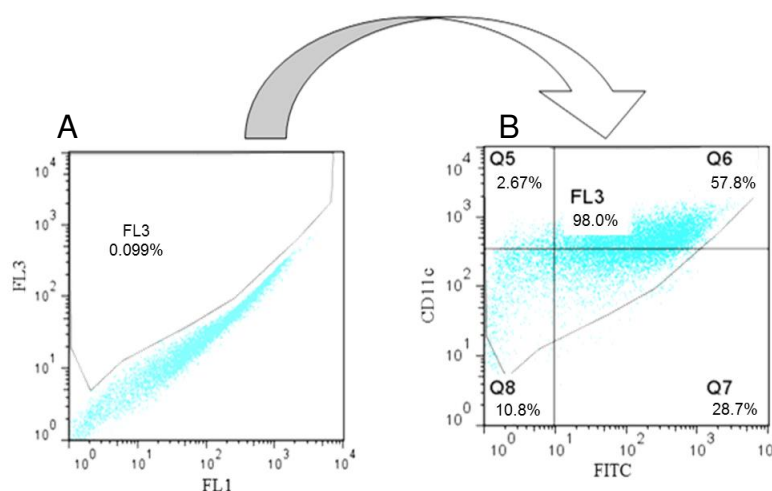


Figure 5-7 – Strategy of dendritic cells molecule expression analysis. (A) Dot Plot graph of FL1 (lipid fluorescent probe) by FL2 or FL3 (detectors in which FL1 interfered) to delimit the gate of DCs that expressed molecules whose fluorescence intensity is higher than the interference of FITC (B) Dot Plot graph of FITC (lipid fluorescent probe) by Her-2/neu or CD11c or CD80 or CD86 or CD274 or CD40 (molecules present in FL2 or FL3) to analyze the DCs expressing double-positive fluorescent molecules.

Capítulo 6 – Conclusões Finais

Com este trabalho que vislumbra prioritariamente, o desenvolvimento de nanoestrutura lipossomal capaz de veicular RNA tumoral total para células dendríticas *in vitro*, visando a imunoterapia do câncer, pôde-se concluir que:

- Os lipossomas EPC/DOTAP/DOPE (50/25/25% molar) preparados pelo método do filme seco seguido por extrusão são melhor internalizados pelas DCs que os lipossomas produzidos pelo método da desidratação-reidratação (DRV).
- As propriedades físico-químicas dos lipossomas interferem na sua incorporação por células dendríticas. Pode-se concluir que o tamanho e a polidispersidade são inversamente proporcionais à internalização por células dendríticas.
- Os lipossomas preparados pelo método do filme seco seguido por extrusão estimularam as células dendríticas a expressar CD86 e as células dendríticas que haviam internalizado estes lipossomas induziram a proliferação de linfócitos T.
- Os lipossomas catiônicos produzidos pelo método escalonável de injeção de etanol otimizado foram internalizados pelas DCs, estimularam as células dendríticas a aumentarem expressão da molécula co-estimuladora CD86 e as DCs que haviam internalizado estes lipossomas induziram a proliferação de linfócitos T, indicando que estes lipossomas são viáveis para aplicações biológicas, como a terapia gênica, *in vitro* e *in vivo*.
- Estudando o fenômeno da formação de lipossomas catiônicos produzidos pelo método escalonável de injeção de etanol, percebe-se a influência dos efeitos de transferência de massa dentro do reator e da interação entre os fosfolipídios sobre as propriedades físico-químicas dos lipossomas.
- A concentração elevada de lipídeo, a alta velocidade de agitação na fase aquosa e a baixa taxa de injeção da solução de lipídeo-etanol aumentam

o tamanho e a polidispersidade dos lipossomas catiônicos obtidos pelo método de injeção de etanol. Por outro lado, o efeito negativo da concentração de lipídeo pode ser minimizado através da utilização de alta velocidade de agitação, o que diminuirá a polidispersidade dos lipossomas.

- Lipossomas catiônicos preparados pelo método de injeção de etanol otimizado e os lipossomas preparados pelo método laboratorial do filme seco incorporados com RNA (RNA/ST-liposomes e RNA/ELs, respectivamente) possuem menor tamanho e polidispersidade quando estão na $R_{+/-} 15$, sendo mais adequados para veicular ácidos nucleicos para DCs.
- Os complexos RNA/ST-liposomes e RNA/ELs na $R_{+/-} 15$, foram incorporados pelas DCs, estimulando-as a expressarem moléculas co-estimuladoras (CD80, CD86 e CD40) e reguladoras (CD274) e a induzirem a proliferação de linfócitos T.
- A baixa expressão de Her-2/*neu* pelas DCs demonstra baixa eficiência de transfecção com os complexos RNA/ST-liposomes e RNA/ELs ($R_{+/-} 15$), indicando que parâmetros da transfecção devem ser otimizados.

De uma forma geral, os lipossomas catiônicos EPC/DOTAP/DOPE (50/25/25% molar) produzidos pelo método escalonável de injeção de etanol demonstraram ser uma ferramenta útil para a imunoterapia do câncer baseado em vacina de DCs. Além disso, este estudo irá contribuir para uma melhor compreensão dos mecanismos de formação de lipossomas catiônicos produzidos pelo método escalonável de injeção de etanol.

Capítulo 7 - Sugestões para trabalhos futuros

Para a continuação de pesquisas futuras no que tange ao desenvolvimento de nanoestruturas lipossomais capazes de veicular RNA para células dendríticas *in vitro* destinadas à imunoterapia do câncer, as seguintes sugestões são citadas:

- Reavaliar os complexos RNA/ST-liposomes e RNA/ELs na razão molar de cargas 15 quanto à estimulação/maturação e transfecção nas DCs, sem que os lipossomas estejam marcados com lipídio fluorescente para que não haja interferência da fluorescência em outros detectores. A incorporação neste caso será medida pelo aumento da granulosidade das DCs.
- Estudar a cinética de transfecção *in vitro* dos lipossomas catiônicos constituídos pelos lipídeos EPC, DOTAP e DOPE incorporados com RNA nas células dendríticas; de forma a determinar condições ótimas de transfecção, bem como a influência dos parâmetros tempo e taxa de cisalhamento na eficiência de transfecção.
- Avaliar a potencialidade da incorporação de RNA em lipossomas catiônicos através de outras técnicas que não a da agitação, como por exemplo em dispositivos microfluídicos, de forma a estudar a influência da razão molar de cargas na eficiência de transfecção pelas células dendríticas.
- Desenvolver ensaios biológicos no sentido de viabilizar a utilização dos lipossomas catiônicos EPC/DOTAP/DOPE (50/25/25% molar) obtidos pelo método de injeção de etanol na produção de vacina de células dendríticas para serem utilizadas em tratamentos de pacientes com câncer.

ANEXO I – Determinação da proporção apropriada de marcador fluorescente para os lipossomas

Um conjunto de experimentos foi delineado a fim de se identificar a melhor quantidade (% m/m) de lipídeo fluorescente (FITC) a ser incorporado nos lipossomas catiônicos durante o processo de produção em escala laboratorial extrudado (ELs) e DRVs laboratorial extrudado (DRVs). Esta determinação foi realizada através de citometria de fluxo e é importante para observação da resposta das células dendríticas ao estímulo dos lipossomas. Para isso, lipossomas contendo 0,1%, 0,01% e 0,001% de FITC em relação à concentração total de lipídios foram produzidos em método laboratorial (extrudado e DRV).

Seguindo o procedimento apresentado nos Capítulos 3, no quinto dia de cultivo, as células foram estimuladas com TNF-alfa (mDC - células dendríticas maduras) como controle positivo, com os lipossomas laboratorial extrudado e os DRVs laboratorial extrudado com as diversas proporções de sonda fluorescente apresentadas anteriormente e algumas células não foram estimuladas (iDC - células dendríticas imaturas) representando o controle negativo. A Tabela 1 apresenta a nomenclatura utilizada para cada proporção.

Tabela 1– Nomenclatura utilizada para cada lipossomas com diferentes proporções de lipídio fluorescente.

NOMENCLATURA	DESCRIÇÃO
EL 0,001%	Lipossomas laboratorial extrudado com 0,001% de sonda fluorescente
EL 0,01%	Lipossomas laboratorial extrudado com 0,01% de sonda fluorescente
EL 0,1%	Lipossomas laboratorial extrudado com 0,1% de sonda fluorescente
DRV 0,001%	DRVs laboratorial extrudado com 0,001% de sonda fluorescente
DRV 0,01%	DRVs laboratorial extrudado com 0,01% de sonda fluorescente
DRV 0,1%	DRVs laboratorial extrudado com 0,1% de sonda fluorescente
mDC	Células dendríticas maduras
iDC	Células dendríticas imaturas

No sétimo dia de cultivo, adicionaram-se às DCs estimuladas com os lipossomas (EL ou DRV, produzidos nas diversas concentrações de lipídeo fluorescente – Tabela 1) os marcadores apropriados para caracterização das células através de citometria de fluxo (marcação das células), conforme esquema apresentado na Figura 1. A caracterização visa à determinação do fenótipo de membrana das DCs.

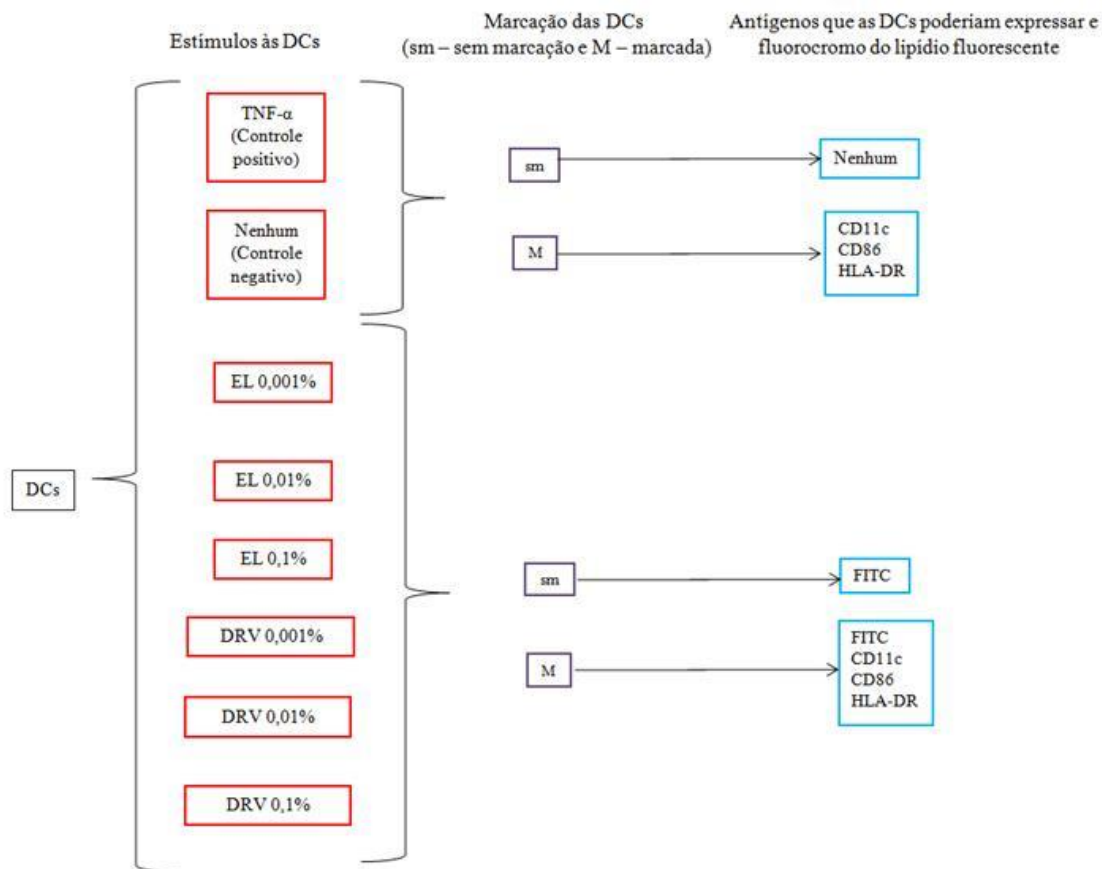


Figura 1 – Esquema de marcação das células dendríticas estimuladas por lipossomas laboratoriais e TNF- α analisadas no citômetro de fluxo.

A influência da proporção de lipídeo fluorescente nos lipossomas catiônicos pode ser avaliada de forma comparativa para os ELs e DRVs a partir dos histogramas apresentados na Figura 2.

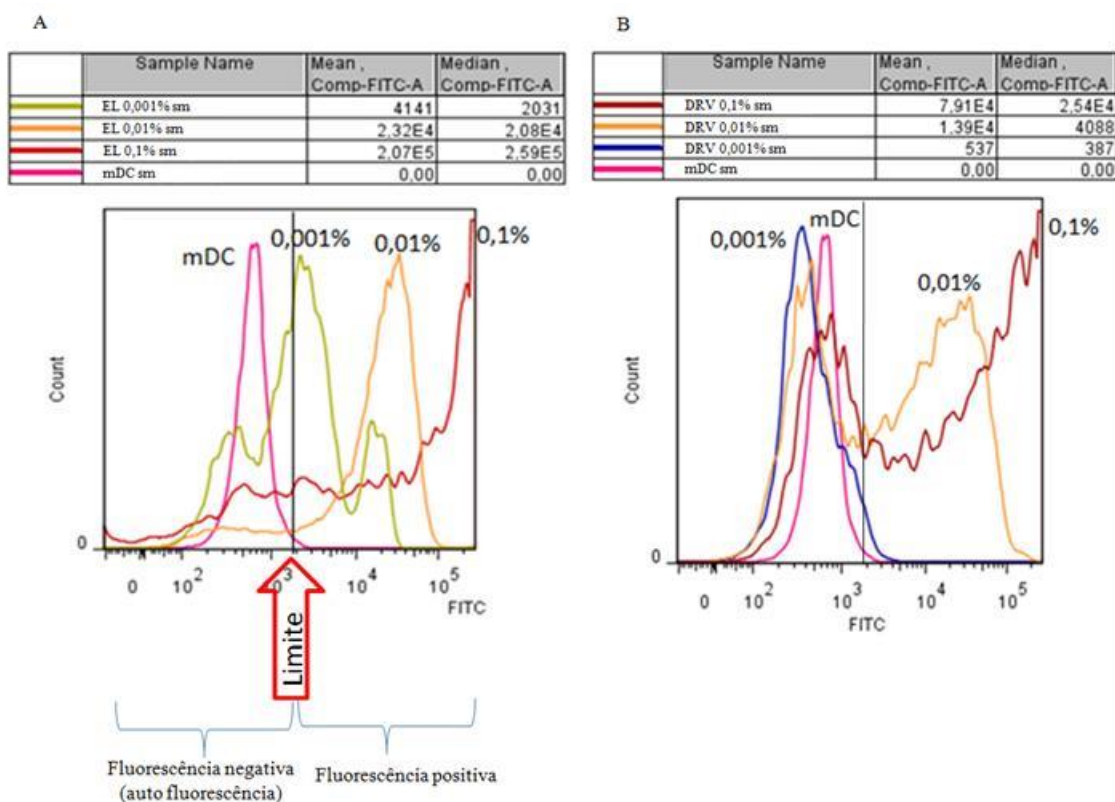


Figura 2 – Histogramas do fluorocromo FITC em função do número de DCs estimuladas com (A) lipossomas LE e (B) com DRV-LE contendo 0,1%, 0,01% e 0,001% de lipídio fluorescente.

A partir dos histogramas é possível avaliar o número de células (*Count*) em relação a um determinado parâmetro, neste caso a fluorescência da sonda que marca os lipossomas. As células possuem uma auto-fluorescência, sendo necessário fazer uma correção da leitura excluindo a população que apresentar uma fluorescência negativa do marcador analisado. A determinação desta população foi feita traçando-se um limite no qual aproximadamente 99% da população das mDC sm (células dendríticas estimuladas por TNF- α –controle positivo- sem marcação) está à esquerda do histograma, pois como elas não estão marcadas logo a fluorescência por elas emitida corresponde à auto fluorescência das células. Após traçar este limite, as populações que se encontram à direita são positivas para o parâmetro analisado, ou seja, células que tem o fluorocromo ligado à membrana ou internalizado nas células. Um alto pico no histograma significa que uma numerosa população de células emite fluorescência numa determinada intensidade.

Nas tabelas acima dos gráficos é apresentado o *Mean* e o *Median* do FITC, eles significam a média da fluorescência por quantidade de células e a mediana da fluorescência por quantidade de células. Quanto maior a média maior é a fluorescência, neste caso maior número de lipossomas em cada célula dendrítica.

Seguindo esta estratégia é possível observar que quando se utiliza lipídeo fluorescente em proporção a 0,001% tem-se uma parte que é FITC negativo, devido à concentração de fluorocromo ser baixa e não detectável pelo citômetro. Já as DCs estimuladas com lipossomas contendo 0,1% de lipídio fluorescente extrapolam o histograma, demonstrando que a concentração de fluorocromo utilizada é muito alta. Quando as DCs são estimuladas com lipossomas contendo 0,01% de lipídio fluorescente, uma população numerosa é FITC positivo, devido à concentração de fluorocromo utilizada ser detecta pelo citômetro, mas sem extrapolar o histograma. Esta concentração de 0,01% é a que se apresenta mais apropriada para os próximos estudos.

ANEXO II – Avaliação *in vitro* da proliferação de linfócitos T

A avaliação *in vitro* da proliferação de linfócitos T quando colocados em co-cultura com células dendríticas (DCs) estimuladas por TNF- α e lipossomas laboratoriais extrudados foi realizada através de análise no citômetro de fluxo FACSCalibur™. As células obtidas das culturas foram marcadas com anticorpos monoclonais comerciais CD4, CD8 e CD25, para possibilitar a análise através do citômetro de fluxo. Metodologias apresentadas nos Capítulos 3, 4 e 5.

Quanto à apresentação de molécula CD25, os linfócitos T colocados em co-cultura com DCs estimuladas por TNF- α , conclui-se que 13,5% eram linfócitos T CD25+ (Figura 3 A), 19,2% eram linfócitos T CD25+ induzidos por DCs estimuladas por ELs (Figura 3 B), 16,1% eram linfócitos T CD25+ induzidos por DCs estimuladas por ST-liposomes (Figura 3 C), 19,0% eram linfócitos T CD25+ induzidos por DCs estimuladas por SM-liposomes (Figura 3 D), 18,0% eram linfócitos T CD25+ induzidos por DCs estimuladas por RNA/ELs (Figura 3 E) e 15,3% eram linfócitos T CD25+ induzidos por DCs estimuladas por RNA/ST-liposomes (Figura 3 F).

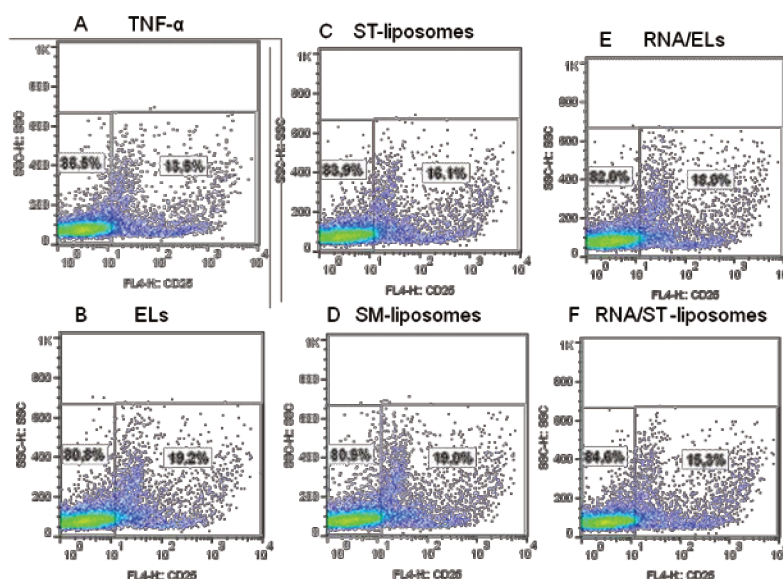


Figura 3 – Gráficos dot plot de CD25 versus SSC, para análise da molécula CD25 apresentada por linfócitos T quando colocados em co-cultura com DCs estimuladas por TNF- α (A), extruded liposomes (ELs) (B), ST-liposomes depois da otimização (C), SM-liposomes depois da otimização (D), complexos RNA/ELs (E) e complexos RNA/ST-liposomas (F).

A apresentação da molécula CD25 pelos linfócitos T CD4⁺ foi de 13,0% quando colocados em co-cultura com DCs estimuladas por TNF- α (Figura 4 A), 14,6% eram linfócitos T CD4⁺ CD25⁺ induzidos por DCs estimuladas por ELs (Figura 4 B), 12,8% eram linfócitos T CD4⁺ CD25⁺ induzidos por DCs estimuladas por ST-liposomes (Figura 4 C), 13,6% eram linfócitos T CD4⁺ CD25⁺ induzidos por DCs estimuladas por SM-liposomes (Figura 4 D), 14,5% eram linfócitos T CD4⁺ CD25⁺ induzidos por DCs estimuladas por RNA/ELs (Figura 4 E) e 13,7% eram linfócitos T CD4⁺ CD25⁺ induzidos por DCs estimuladas por RNA/ST-liposomes (Figura 4 F).

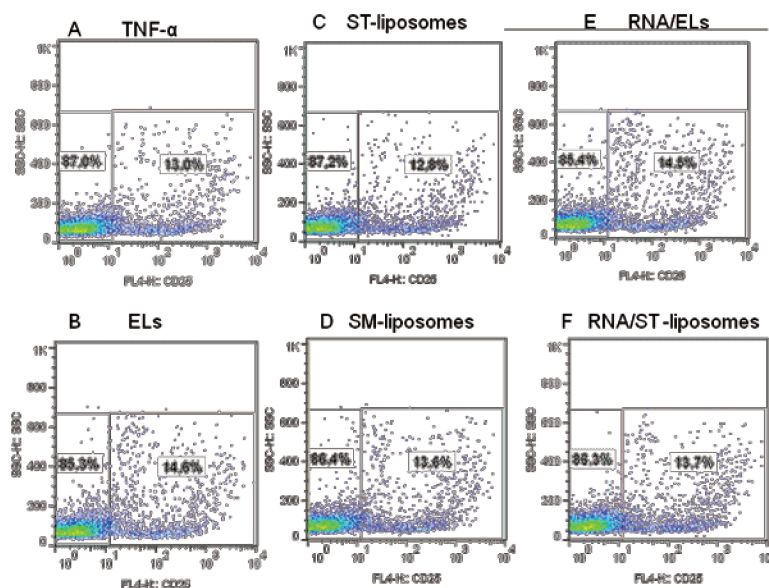


Figura 4 – Gráficos dot plot de CD25 versus SSC, para análise da molécula CD25 apresentada por linfócitos T CD4⁺ quando colocados em co-cultura com DCs estimuladas por TNF- α (A), extruded liposomes (ELs) (B), ST-liposomes depois da otimização (C), SM-liposomes depois da otimização (D), complexos RNA/ELs (E) e complexos RNA/ST-liposomas (F).

A apresentação da molécula CD25 pelos linfócitos T CD8⁺ foi de 6,51% quando colocados em co-cultura com DCs estimuladas por TNF- α (Figura 5 A), 10,5% eram linfócitos T CD4⁺ CD25⁺ induzidos por DCs estimuladas por ELs (Figura 5 B), 11,1% eram linfócitos T CD4⁺ CD25⁺ induzidos por DCs estimuladas por ST-liposomes (Figura 5 C), 9,74% eram linfócitos T CD4⁺ CD25⁺ induzidos por DCs estimuladas por SM-liposomes (Figura 5 D), 10,3% eram linfócitos T CD4⁺ CD25⁺ induzidos por DCs estimuladas por RNA/ELs (Figura 5 E) e 11,3% eram linfócitos T CD4⁺ CD25⁺ induzidos por DCs estimuladas por RNA/ST-liposomes (Figura 5 F).

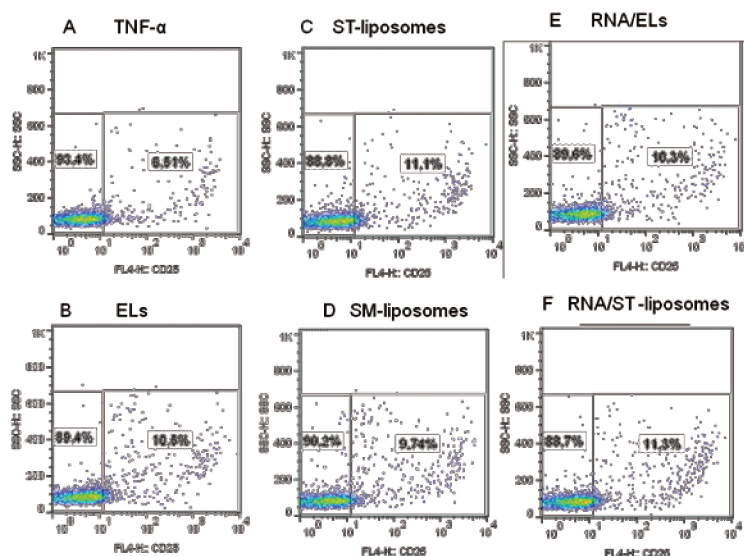


Figura 5 - Gráficos dot plot de CD25 versus SSC, para análise da molécula CD25 apresentada por linfócitos T CD8⁺ quando colocados em co-cultura com DCs estimuladas por TNF- α (A), extruded liposomes (ELs) (B), ST-liposomes depois da otimização (C), SM-liposomes depois da otimização (D), complexos RNA/ELs (E) e complexos RNA/ST-liposomes (F).

Dessa forma, os lipossomas extrudados, ST-liposomes depois da otimização, SM-liposomes depois da otimização, os complexos RNA/ELs e RNA/ST-liposomes demonstraram potencial para serem utilizados como ferramenta na imunoterapia do câncer, mas que também são necessários experimentos *in vivo* para verificar se os linfócitos T supressores de resposta imune podem prevalecer sobre os ativadores e os citotóxicos, diminuindo a resposta imune do indivíduo contra o câncer.

ANEXO III – Curriculum Vitae e Histórico Escolar

CURRICULUM VITAE

Nome: Micaela Tamara Vitor

1) Formação

Ano	Título
08/2010 – previsão 04/2013	MESTRADO EM ENGENHARIA QUÍMICA, na Universidade Estadual de Campinas (Unicamp), em Campinas-SP
03/2005 - 07/2010	GRADUAÇÃO EM ENGENHARIA DE ALIMENTOS, na Universidade Federal de Viçosa (UFV), em Viçosa-MG

2) Atividade profissional

- Estagiária, DOMAINE DU BOLLENBERG, na França, 2009-2010.
- Estagiária, LABORATÓRIO DE MICROBIOLOGIA, na Universidade Federal de Viçosa, Minas Gerais, Brasil, 2007-2009.
- Estagiária, FRIGORÍFICO INDUSTRIAL VALE DO PIRANGA S.A., em Oratórios, Minas Gerais, Brasil, 2009-2009.
- Estagiária, ALIMENTOS JÚNIOR, na Universidade Federal de Viçosa, Minas Gerais, Brasil, 2008-2008.
- Estagiária, INDÚSTRIA FAVO DE MEL LTDA, em Belo Horizonte, Minas Gerais, Brasil, 2008-2008.

3) Publicações

▪ **Artigos aceitos para publicação:**

- VITOR, M. T.; BERGAMI-SANTOS, P. C.; BARBUTO, J. A. M.; DE LA TORRE, L. G. Cationic Liposomes as Non-viral Vector for RNA Delivery in Cancer Immunotherapy. *Recent Patents on Drug Delivery & Formulation*, 2013, *in press*.

▪ **Resumos expandidos publicados em anais de congressos:**

- VITOR, M. T.; BERGAMI-SANTOS, P. C.; BARBUTO, J. A. M.; DE LA TORRE, L. G. Processo escalonável de produção de lipossomas para veiculação de RNA para aplicações *in vitro*. XIX Congresso Brasileiro de Engenharia Química. Búzios, Rio de Janeiro, 09 a 12 de setembro de 2012.
- HÚNGARO, H. M.; MENDONÇA, R. C. S.; VITOR, M. T.; TETTE, P. A. S.; RESENDE, A. C. V. Isolamento de bacteriófagos com potencial para utilização em biocontrole. V Congresso Brasileiro de Ciência e Tecnologia de Carnes. Campinas, SP, Brasil, 25 a 27 de agosto de 2009.

▪ **Resumos publicados em anais de congressos:**

- VITOR, M. T.; BERGAMI-SANTOS, P. C.; BARBUTO, J. A. M.; SIPOLI, C. C.; DE LA TORRE, L. G. Dendritic cells stimulated by cationic liposomes. Colloids and Nanomedicine 2012. NH Grand Krasnapolsky, Amsterdam, Netherlands, 15 a 17 de julho de 2012.
- VITOR, M. T.; BERGAMI-SANTOS, P. C.; BARBUTO, J. A. M.; DE LA TORRE, L. G. Scalable process for the production of liposomes as nucleic acids carriers for *in vitro* applications. South-American Symposium on Microencapsulation. Limeira, São Paulo, Brasil, 30 de abril a 02 de maio de 2012.
- MAGALHÃES, D. R.; MENDONÇA, R. C. S.; CIOLFI, F. C.; VITOR, M. T.; SOUZA, E. C.; PINHEIRO, F. G. Avaliação do efeito inibitório de diferentes frações de extratos vegetais e óleos essenciais sobre *Campylobacter jejuni* isolados de frangos de corte. XVIII Simpósio de Iniciação Científica – SIC, VIII Mostra Científica da Pós-Graduação - SIMPÓS, VI Simpósio de Extensão Universitária – SEU e II Simpósio de Ensino - SEN. Campus da Universidade Federal de Viçosa, 22 a 25 de outubro de 2008.
- CIOLFI, F. C.; MENDONÇA, R. C. S.; MAGALHÃES, D. R.; VITOR, M. T.; SOUZA, E. C.; PINHEIRO, F. G. Avaliação do efeito inibitório de diferentes extratos e óleos essenciais de vegetais sobre *Campylobacter jejuni* isolados de frangos de corte. XXI Congresso Brasileiro de Ciência e Tecnologia de Alimentos e XV Seminário Latino Americano e do Caribe de Ciência e Tecnologia de Alimentos. Belo Horizonte, Minas Gerais, 06 a 09 de outubro de 2008.
- CIOLFI, F. C.; MENDONÇA, R. C. S.; MAGALHÃES, D. R.; VITOR, M. T.; OLIVEIRA, K. A. M. Avaliação do efeito inibitório de diferentes extratos alcoólicos e óleos essenciais de vegetais sobre *Campylobacter jejuni* isolados de frangos de corte. III Simpósio Mineiro de Microbiologia de Alimentos e III Fórum de Debates Sobre Vigilância Sanitária. Campus da Universidade Federal de Viçosa, 14 a 18 de abril de 2008.

4) **Iniciação científica**

Uso de bacteriófagos para controle de *Salmonella enteritidis* em carcaça de frangos de corte. Orientadora: Profa. Dra. Regina Célia Santos Mendonça, Universidade Federal de Viçosa. Bolsista FAPEMIG (Fundação de Amparo à Pesquisa do Estado de Minas Gerais).

5) **Bolsa de mestrado**

Veiculação de mRNA de células tumorais em lipossomas catiônicos para imunoterapia do câncer. Orientadora: Profa. Dra. Lucimara Gaziola de la Torre, Universidade Estadual de Campinas. Bolsista FAPESP (Fundação de Amparo à Pesquisa do Estado de São Paulo), processo 2010/13818-3.

6) **Participação em eventos científicos durante o mestrado**

- Curso de Escrita Científica em Inglês para as Áreas de Exatas e Tecnológicas, na Unicamp – Carga horária de 16h – no período de 17 a 18 de setembro de 2012.
- Curso de Propriedade Intelectual, Patentes e Transferência de Tecnologia, na Unicamp – Carga horária de 3h – no período de 27 de abril de 2012.
- Curso de Citometria de Fluxo, na Unicamp – Carga horária de 24h – no período de 29 de março a 06 de abril de 2011.

- Curso de Capacitação em Pesquisa Bibliográfica, na Unicamp – Carga horária de 2h – no período de 26 de agosto de 2010.
- Curso de Normalização Bibliográfica - Referências, na Unicamp - Carga horária de 2h – no período de 21 de outubro de 2010.

7) **Idiomas**

- Certificado de proficiência na língua inglesa TEAP (Test of English for Academic Purposes) na área de Exatas/Tecnológicas.
- Certificado de proficiência na língua francesa DELF B1 e BELF B2.



UNIVERSIDADE ESTADUAL DE CAMPINAS

Diretoria Acadêmica



Histórico Escolar

Nome		Registro Acadêmico	
Micaela Tamara Vitor		108996	
Documento de Identidade	CPF	Nascimento	Sexo
MG10872291-MG	076.323.896-10	24/03/1987	Feminino
Naturalidade		Nacionalidade	
Belo Horizonte - MG		Brasileira	

Dados do Ingresso		Nível	
Curso: 9 - Mestrado em Engenharia Química		Mestrado	
Área de Concentração			
AF - Desenvolvimento de Processos Biotecnológicos Reconhecido pela Portaria MEC nº 1077 de 31/08/2012			
Forma de Ingresso		Mês/Ano de Ingresso	
Exame Seleção Pós-Graduação		08/2010	
Escola Anterior		Mês/Ano da Conclusão	
Universidade Federal de Viçosa - UFV		07/2010	

Situação no Curso		Ano de Catálogo	Ano da Turma
Curso em andamento		2010	2010
Prazo para Integralização		Coeficiente de Rendimento (0 a 4)	
07/2013		4.0	
Aptidão em Língua Estrangeira		Data	Resultado
Inglês		03/06/2011	Aprovado
Exame de Qualificação		Data	Resultado
Geral		22/08/2012	Aprovado
Tema da Banca			
Veiculação de mRNA de Células Tumorais em Lipossomas Cati-ônicos para Imunoterapia do Câncer			
Comissão Examinadora - Exame de Qualificação			
Profa Doutora Lucimara Gaziola de La Torre			
Prof José Alexandre Marzagão Barbuto			
Prof Nelson Eduardo Durán Caballero			
Orientador (es)			
Profa Doutora Lucimara Gaziola de La Torre			

CÓDIGO DE AUTENTICIDADE

Verifique a autenticidade deste documento na página <http://www.daconline.unicamp.br/ActionConsultaDiploma.asp>
 Código: 99a1e5f60c6ec9b4231ca5e31de0e5932846f1e7

UNICAMP – Universidade Estadual de Campinas
 DAC – Diretoria Acadêmica
 Diretoria de Registro e Gerenciamento Acadêmico
 Rua Sérgio Buarque de Holanda, 251 - Cidade Universitária - Barão Geraldo - Campinas/SP - 13063-970
www.dac.unicamp.br



UNIVERSIDADE ESTADUAL DE CAMPINAS

Diretoria Acadêmica



Histórico Escolar

Nome	Registro Acadêmico
Micaela Tamara Vitor	108996

Disciplinas Cursadas

Observações

Nas disciplinas com situação 'Aprovado', o aluno obteve frequência igual ou superior a 75% da Carga Horária. Este documento contém todas as disciplinas cursadas pelo aluno.

- Disciplinas cursadas na condição de Estudante Especial - aproveitadas na integralização do curso.

* - Carga Horária segundo catálogo seguido pelo aluno. (Informação CCPG Nº 4/2008)

! - Disciplinas cursadas como Estudante Especial / não válidas para o programa.

2º Semestre de 2010 - 01/08/2010 até 31/12/2010

Código	Nome da Disciplina	Conc.	CH	Crd	Situação
IQ030	Metodologia de Redação Científica e Utilização de Recursos	A	15	1	Aprovado por Conceito e Frequência
IQ042	Seminários de Mestrado	A	15	1	Aprovado por Conceito e Frequência
IQ053	Recuperação e Purificação de Bioprodutos: "Downstream Processing"	A	30	2	Aprovado por Conceito e Frequência
IQ063	Obtenção de Bioprodutos pelo Cultivo de Células Animais	A	30	2	Aprovado por Conceito e Frequência
IQ064	Encapsulação de Agentes Bioativos	A	30	2	Aprovado por Conceito e Frequência
IQ066	Métodos Matemáticos Aplicados a Bioprocessos	A	30	2	Aprovado por Conceito e Frequência

1º Semestre de 2011 - 01/03/2011 até 30/06/2011

Código	Nome da Disciplina	Conc.	CH	Crd	Situação
AA001	Dissertação de Mestrado	P	--	-	Tese em Andamento
IQ061	Cinética e Biorreatores Homogêneos	A	60	4	Aprovado por Conceito e Frequência
IQ475	Tópicos em Sistemas Químicos	---	-	-	Desistência de Matrícula
QP434	Tópicos Especiais em Físico-Química II	A	30	2	Aprovado por Conceito e Frequência

2º Semestre de 2011 - 01/08/2011 até 31/12/2011

Código	Nome da Disciplina	Conc.	CH	Crd	Situação
AA001	Dissertação de Mestrado	P	--	-	Tese em Andamento
IQ263	Tópicos em Engenharia Química II	A	45	3	Aprovado por Conceito e Frequência
IQ475	Tópicos em Sistemas Químicos	A	30	2	Aprovado por Conceito e Frequência

CÓDIGO DE AUTENTICIDADE

Verifique a autenticidade deste documento na página <http://www.daonline.unicamp.br/ActionConsultaDiploma.asp>
Código: 99a1e5f60c6ec9b4231ca5e31de0e5932846f1e7

UNICAMP – Universidade Estadual de Campinas
DAC – Diretoria Acadêmica
Diretoria de Registro e Gerenciamento Acadêmico
Rua Sérgio Buarque de Holanda, 251 - Cidade Universitária - Barão Geraldo - Campinas/SP - 13063-970
www.dac.unicamp.br

Emissão: 21-12-2012

Pag.: 2 de 3



UNIVERSIDADE ESTADUAL DE CAMPINAS

Diretoria Acadêmica



Histórico Escolar

Nome	Registro Acadêmico
Micaela Tamara Vitor	108996

1º Semestre de 2012 - 01/03/2012 até 30/06/2012					
Código	Nome da Disciplina	Conc.	CH	Crd	Situação
AA001	Dissertação de Mestrado	P	--	-	Tese em Andamento

2º Semestre de 2012 - 01/08/2012 até 31/12/2012					
Código	Nome da Disciplina	Conc.	CH	Crd	Situação
AA001	Dissertação de Mestrado	P	--	-	Tese em Andamento

Carga Horária		
Total da Carga Horária Completada	Total da Carga Horária Supervisionada	Total de Créditos
315	315	21

CÓDIGO DE AUTENTICIDADE

Verifique a autenticidade deste documento na página <http://www.daconline.unicamp.br/ActionConsultaDiploma.asp>
 Código: 99a1e5f60c6ec9b4231ca5e31de0e5932846f1e7

UNICAMP – Universidade Estadual de Campinas
 DAC – Diretoria Acadêmica
 Diretoria de Registro e Gerenciamento Acadêmico
 Rua Sérgio Buarque de Holanda, 251 - Cidade Universitária - Barão Geraldo - Campinas/SP - 13065-970
www.dac.unicamp.br

ANEXO IV – Artigo apresentado no Capítulo 2 aceito para publicação na Recent Patents on Drug Delivery and Formulation

NCBI Resources How To

PubMed.gov
US National Library of Medicine
National Institutes of Health

PubMed

Display Settings: Abstract

Send to:

[Recent Pat Drug Deliv Formul.](#) 2012 Dec 31. [Epub ahead of print]

Cationic liposomes as non-viral vector for RNA delivery in cancer immunotherapy.

[Vitor MT](#), [Berqami-Santos PC](#), [Barbuto JA](#), [De La Torre LG](#).

School of Chemical Engineering, Department of Materials and Bioprocess Engineering, University of Campinas (Unicamp) Current address: Av. Albert Einstein, 500, Campinas, SP, 13083-852, Brazil. latorre@feq.unicamp.br.

Abstract

This review presents the current status in the use of liposomes as non-viral vector for nucleic acid delivery in cancer immunotherapy. Currently, cancer treatment uses surgery, radiotherapy and/or chemotherapy. The search for new strategies to improve the efficiency of conventional treatments is a challenge, and biological therapy has emerged as a promising technique. Immunotherapy is a branch of biological therapy that uses the body's immune system to detect and destroy cancer cells. One immunotherapy approach is the activation of T lymphocytes from cancer patients by dendritic cells (DCs) loaded with tumor antigens. Among different antigens, mRNA coding the tumor antigens is advantageous due to its capability to be amplified from small amounts of tumor tissue, its safety because it is easily degraded without integrating into the host genome, and it does not need to cross the nuclear barrier to exert its biological activity. Nanotechnology is an approach to deliver tumor antigens into DCs. Specially, we review the use of nanoliposomes in the field of cancer therapy because cationic liposomes can be used as non-viral vectors for mRNA delivery. Aside from the promise of liposomes, the development of scalable processes and facilities to the use this individualized therapy is still a challenge. Thus, we also present the recent techniques used for liposome production. In this context, the integration between technological knowledge in the production of cationic liposomes and immunotherapy using mRNA may contribute to the development of new strategies for cancer therapy.

PMID: 23286512 [PubMed - as supplied by publisher]